

**Membrane attack and therapy in autoimmune
disease: modulating pathology whilst
retaining physiology**

By

Marieta Milkova Ruseva

**A thesis submitted to
Cardiff University
in Candidature for the Degree of Doctor of Philosophy.**

**Department of Infection, Immunity and Biochemistry,
School of Medicine,
Cardiff University,
Cardiff
Wales, United Kingdom**

December 2010

UMI Number: U564300

All rights reserved

INFORMATION TO ALL USERS

The quality of this reproduction is dependent upon the quality of the copy submitted.

In the unlikely event that the author did not send a complete manuscript and there are missing pages, these will be noted. Also, if material had to be removed, a note will indicate the deletion.



UMI U564300

Published by ProQuest LLC 2013. Copyright in the Dissertation held by the Author.
Microform Edition © ProQuest LLC.

All rights reserved. This work is protected against
unauthorized copying under Title 17, United States Code.



ProQuest LLC
789 East Eisenhower Parkway
P.O. Box 1346
Ann Arbor, MI 48106-1346

DECLARATION

This work has not previously been accepted in substance for any degree and is not concurrently submitted in candidature for any degree.

Signed  Date 28.03.2011

STATEMENT 1

This thesis is being submitted in partial fulfillment of the requirements for the degree of PhD.

Signed  Date 28.03.2011

STATEMENT 2

This thesis is the result of my own independent work/investigation, except where otherwise stated.

Other sources are acknowledged by explicit references.

Signed  Date 28.03.2011

STATEMENT 3

I hereby give consent for my thesis, if accepted, to be available for photocopying and for inter-library loan, and for the title and summary to be made available to outside organisations.

Signed Date

STATEMENT 4: PREVIOUSLY APPROVED BAR ON ACCESS

I hereby give consent for my thesis, if accepted, to be available for photocopying and for inter-library loans **after expiry of a bar on access previously approved by the Graduate Development Committee.**

Signed Date

Acknowledgments

This thesis would not have been possible without the guidance and the help of several individuals who in one way or another contributed and extended their valuable assistance in the preparation and completion of this study. First and foremost, my utmost gratitude to my supervisor, Dr. Claire Harris, whose sincerity and encouragement I will never forget. Her truly scientist intuition and passion of science exceptionally inspire and enrich my growth as a researcher and scientist. I am heartily thankful to Professor Paul Morgan, whose guidance and support from the initial to the final level enabled me to develop an understanding of the Complement.

I offer my regards and blessings to all of those who supported me in any respect during the completion of the project. My special thanks go to Danielle Paixao-Cavalcante, Meike Heurich, Ruth Lewis and James Hindley for their friendship and help.

I convey special acknowledgement to Dr. Tim Hughes for his help with the model of atherosclerosis.

Words fail me to express my appreciation to Martin for his dedication, love and persistent confidence in me. I dedicate this thesis to you, Martin!

Where would I be without my family? My Mum, Dad and Ivo deserve special mention for their inseparable support.

Finally, I would like to thank everybody who was important to the successful realization of this thesis, as well as expressing my apology that I could not mention personally one by one.

Summary

The complement system is implicated in a number of diseases where it exacerbates or triggers pathology. The majority of the anti-complement agents inhibit systemically, risking infection and immune complex disease with long-term use in humans. Many of these have a short half-life *in vivo*, necessitating repetitive administration. To overcome these limitations, two types of reagents were generated. Both target late stages of complement activation, preventing membrane attack complex (MAC) formation, which is implicated in many diseases.

The saliva of the soft tick, *Ornithodoros moubata*, contains a powerful complement inhibitor (OmCI) which has been developed by others for therapy. Recombinant OmCI rapidly binds circulating C5 when given to animals, completely inhibiting complement. However, excess agent is excreted within minutes, making long-term therapy with this agent problematic. To overcome this, I fused OmCI to the Fc domain of murine IgG2a, generating OmCI-Fc, an anti-complement therapeutic with extended *in vivo* half-life. OmCI-Fc efficiently inhibited the terminal pathway *in vitro* and, by binding C5 following resynthesis, also provided prolonged inhibition *in vivo*.

A second group of agents comprised CD59, a powerful MAC inhibitor, and the murine complement receptor of the immunoglobulin superfamily (CRIg). CRIg binds complement activation fragments, thus has potential to deliver therapy directly to tissues attacked by complement. An antibody hinge domain was engineered between the two moieties in CD59-CRIg to promote dimerisation and increase avidity for target tissue. The dimeric agent localised efficiently to the surface of complement-attacked cells *in vitro* and specifically targeted diseased tissue *ex vivo*.

I have created novel anti-complement reagents designed to deliver effective therapy locally, or where inhibition is long-term, to target only the terminal stages of complement. These agents have exciting potential to effectively treat complement-mediated diseases and to retain other crucial biological functions of complement such as opsonisation and immune complex solubilisation.

Abbreviations

Ab:	Antibody
AChR:	Acetylcholine receptor
ADEAE:	Antibody-dependent experimental autoimmune encephalomyelitis
ADP:	Adenosine-5'-diphosphate
aHUS:	Atypical haemolytic uremic syndrome
AIA:	Antigen-induced arthritis
AMD:	Age-related macular degeneration
AP:	Alternative pathway
ApoE:	Apolipoprotein E (main apoprotein of the chylomicron)
ATP:	Adenosine-5'-triphosphate
BBB:	Blood brain barrier
BSA:	Bovine serum albumin
C4bp:	C4b-binding protein
CAIA:	Anti-collagen type II Ab transfer
cDNA:	Complementary deoxyribonucleic acid
CDRs:	Complementarity determining regions
CFA:	Complete Freund's adjuvant
CFD:	Complement fixation diluent
CHO:	Chinese hamster ovary cells
CIA:	Collagen type II-induced arthritis
CNS:	Central nervous system
CNV:	Choroidal neovascularisation
CPB:	Cardiopulmonary bypass
CP:	Classical pathway
CR:	Complement receptor
CR1g:	Complement receptor of the immunoglobulin superfamily
CRP:	C-reactive protein
Crry:	Complement receptor 1-related/gene protein y
CSF:	Cerebrospinal fluid
CVF:	Cobra venom factor
DAF:	Decay accelerating factor

DAPI:	Diamidino-2-phenylindole
DDD:	Dense deposit disease
DMSO:	Dimethylsulphoxide
DNA:	Deoxyribonucleic acid
dNTP:	Deoxynucleotidetriphosphates
DTT:	Dithiothreitol
EAE:	Experimental autoimmune encephalomyelitis
EArb:	Antibody-sensitised rabbit erythrocytes
EAsh:	Antibody-sensitised sheep erythrocytes
EDTA:	Ethylene diamine tetraacetic acid
EGTA:	Ethylene glycol tetraacetic acid
ELISA:	Enzyme-linked immunosorbent assay
Epo:	Erythropoetin
Fc:	Fragment crystallisable
FcR:	Fc receptor
FCS:	Foetal calf serum
FDC:	Follicular dendritic cells
fH:	Factor H
fHL:	Factor H-like protein
fHR:	Factor H-related protein
GPE:	Guinea pig erythrocytes
GPI:	Glycosylphosphatidylinositol
HAT:	Hypoxanthine, aminopterin and thymidine
HEPES:	4-(2-hydroxyethyl)-1-piperazineethanesulfonic acid
HRPO:	Horseradish peroxidase
HRV:	Human rhinovirus
HT:	Hypoxanthine and thymidine
<i>i.n.</i> :	Intranasal
IC:	Immune complex
IFA:	Incomplete Freund's adjuvant
<i>ip</i> :	Intraperitoneal
IR:	Ischaemia reperfusion
<i>iv</i> :	Intravenous
K _D :	Equilibrium dissociation constant

LB:	Lauria-Bertani
LDL:	Low-density lipoprotein
LHR:	Long homologous repeats
LP:	Lectin pathway
LPS:	Lipopolysaccharide
mAb:	Monoclonal antibody
MAC:	Membrane attack complex
MASPs:	Mannan binding lectin-associated serine proteases
MBL:	Mannan binding lectin
MCP:	Membrane cofactor protein
MPGN:	Membranoproliferative glomerulonephritis
MS:	Multiple sclerosis
OCT:	Optimum cutting temperature compound
OmCI:	Ornithodores moubata Complement Inhibitor
OPD:	O-Phenylenediamine dihydrochloride
pAb:	Polyclonal antibody
PBS:	Phosphate buffered saline
PCR:	Polymerase chain reaction
PEG:	Polyethylene glycol
PE:	Phycoerythrin
PNH:	Paroxysmal nocturnal haemoglobinuria
PS:	Protein S
PTEC:	Proximal tubule epithelial cells
RA:	Rheumatoid arthritis
RCA:	Regulators of complement activation
rMOG:	Recombinant myelin oligodendrocyte glycoprotein
RNA:	Ribonucleic acid
RPMI-1640:	Roswell Park Memorial Institute 1640
RU:	Resonance unit
SAP:	Serum amyloid protein
SAP:	Shrimp alkaline phosphatase
SCR:	Short consensus repeat
sCR1:	Soluble complement receptor 1
sc:	Subcutaneous

SDS PAGE: Sodium dodecyl sulphate polyacrylamide gel electrophoresis
SDS: Sodium dodecyl sulphate
Serpin: Serine protease inhibitor
SLE: Systemic lupus erythematosus
SPR: Surface plasmon resonance
TBS: Tris buffered saline
TfR: Transferrin receptor 1
THP: Tris (hydroxypropyl) phosphine
v/v: Volume to volume
VSIG4: V-set and Ig domain-containing 4
w/v: Weight to volume

Table of contents

Chapter 1. Introduction	15
1.1. The Complement system	15
1.1.1. Activation pathways	17
1.1.1.1. Classical pathway (CP)	17
1.1.1.2. Lectin pathway (LP).....	18
1.1.1.3. Alternative pathway (AP).....	18
1.1.2. Terminal pathway.....	20
1.1.3. Physiological role of the complement system in health	22
1.1.3.1. Host defence against infection	22
1.1.3.1.1. Opsonisation.....	22
1.1.3.1.2. Chemotaxis and activation of leukocytes	23
1.1.3.1.3. Lysis of bacteria and cells	24
1.1.3.2. Disposal of waste.....	24
1.1.3.2.1. Clearance of immune complexes from tissues	24
1.1.3.2.2. Clearance of apoptotic cells	24
1.1.3.3. Link between innate and adaptive immunity	25
1.2. Complement regulation and regulators	26
1.2.1. Factor I	29
1.2.2. Regulators of complement activation (RCA) gene cluster.....	29
1.2.2.1. Factor H family	31
1.2.2.2. Membrane cofactor protein (MCP, CD46).....	33
1.2.2.3. Decay accelerating factor (DAF, CD55).....	34
1.2.2.4. C4b-binding protein	34
1.2.2.5. Complement receptor 1-related/gene protein y (Crry).....	35
1.2.3. C1-inhibitor	35
1.2.4. CD59	35
1.3. Complement receptors.....	36
1.3.1. Receptors encoded by the RCA gene cluster	36
1.3.1.1. Complement receptor type 1 (CR1)	36
1.3.1.2. Complement receptor type 2 (CR2)	37
1.3.1.3. Murine complement receptor type 1 and complement receptor type 2.....	38
1.3.2. β_2 -Integrin family.....	38
1.3.3. Type 1 transmembrane Ig superfamily.....	38
1.4. Complement and diseases/pathology	39
1.4.1. Infectious disease and pathogen evasion of complement.....	40
1.4.2. Complement dysregulation and disease	41
1.4.2.1. Acute conditions.....	41
1.4.2.2. Autoimmune diseases.....	42
1.4.2.2.1. Rheumatoid arthritis	46
1.4.2.2.2. Multiple sclerosis	47
1.4.2.3. Cardiovascular disease	48
1.4.2.4. Disease with genetically defined mutations of complement inhibitors and/or complement proteins	49
1.4.2.4.1. Membranoproliferative glomerulonephritis type II.....	50
1.4.2.4.2. Atypical haemolytic uraemic syndrome.....	50
1.4.2.4.3. Paroxysmal nocturnal haemoglobinuria.....	51
1.5. Anti-complement therapeutics	51

1.5.1. Cobra Venom Factor	51
1.5.2. Polyanionic agents.....	52
1.5.3. Small molecule inhibitors.....	52
1.5.4. Peptide inhibitors.....	53
1.5.5. Recombinant complement receptor 1	54
1.5.6. Complement regulator-Fc fusion proteins.....	62
1.5.6.1. Crry-Fc	62
1.5.6.2. CR1g-Fc.....	63
1.5.6.3. DAF-Fc.....	63
1.5.6.4. CD59-Fc	63
1.5.7. Complement regulator-complement receptor fusion proteins.....	64
1.5.7.1. CR2-DAF	64
1.5.7.2. CR2-CD59.....	64
1.5.7.3. CR2-Crry	65
1.5.7.4. CR2-fH.....	65
1.5.8. Antibody targeting.....	66
1.5.8.1. IgG-CD59	66
1.5.8.2. IgG-DAF	66
1.5.8.3. IgG-Crry	67
1.5.9. Blocking antibodies.....	67
1.5.9.1. Anti-C5	68
1.5.10. Recombinant CD59	70
1.5.11. Recombinant OmCI.....	70
1.5.12. Optimal target for complement inhibition.....	71
1.6. Project Aims	72
Chapter 2. Materials and methods.....	76
2.1. Preparation of plasmids encoding the anti-complement therapeutics-molecular biology.....	76
2.1.1. Solutions.....	76
2.1.2. RNA preparation	76
2.1.3. Reverse transcriptase PCR (RT PCR).....	77
2.1.4. PCR	77
2.1.5. Screening PCR (see also Bacterial screening)	79
2.1.6. Agarose Gel electrophoresis.....	79
2.1.7. Purification of PCR products	79
2.1.8. Restriction digests	80
2.1.9. Ligation	80
2.1.10. Transformation	81
2.1.11. Bacterial colony screening	81
2.1.12. Plasmid isolation	82
2.1.13. DNA sequencing	82
2.1.14. Plasmid dephosphorylation	83
2.2. Mammalian cell expression.....	83
2.2.1. Media.....	84
2.2.2. CHO cells	84
2.2.3. Transfection of CHO cells.....	84
2.2.4. Cloning by limiting dilution	85
2.2.5. Storage of CHO cells.....	85
2.2.6. High-density expression systems	86
2.2.6.1. Two-compartment bioreactor CELLine AD1000 for CHO cell culture	86

2.2.6.2. HYPER <i>Flask</i> for CHO cell culture	87
2.3. Protein purification	87
2.3.1. Buffers and solutions	87
2.3.2. Clarification of supernatant	87
2.3.3. Protein A and G chromatography	88
2.3.4. IgM purification	89
2.3.5. Gel filtration	89
2.3.6. Affinity chromatography	90
2.3.6.1. Generation of affinity columns	90
2.3.6.2. Protein purification using affinity columns	90
2.3.7. Purification of mouse C3	91
2.3.8. Dialysis of proteins	91
2.4. Characterisation of purified proteins	92
2.4.1. Buffers	92
2.4.2. Protein concentration	92
2.4.3. SDS-PAGE analysis	93
2.4.3.1. Coomassie Blue staining	94
2.4.3.2. Silver staining	95
2.4.4. Western blot analysis	95
2.4.5. Dot blot	97
2.4.6. ELISA	97
2.4.7. Estimation of protein molecular weight	98
2.4.7.1. Mobility in SDS PAGE	98
2.4.7.2. Mobility in Superdex 200	99
2.5. Generation of monoclonal antibodies (mAbs)	99
2.5.1. Medium	99
2.5.2. Immunisation protocol	100
2.5.3. Droplet test	101
2.5.4. Preparation of splenocytes	101
2.5.5. Preparation of myeloma cells	101
2.5.6. Preparation of macrophage	101
2.5.7. Cell fusion	102
2.5.8. CELLLine CL1000	102
2.5.9. Isotyping of mAbs	103
2.5.9.1. Isotyping of mouse mAbs	103
2.5.9.2. Isotyping of rat mAbs	103
2.6. Protein manipulations	103
2.6.1. Labelling with horseradish peroxidase (HRPO)	103
2.6.2. Chemical cross-linking of CR1g-3-CD59 and CD59-3-CR1g	104
2.6.3. Papan digest	105
2.6.4. 3C rhinovirus protease digest	105
2.6.5. Labelling of CD59-2a-CR1g	105
2.7. Functional analysis	106
2.7.1. Buffers and reagents	106
2.7.2. Classical pathway haemolysis assay	107
2.7.2.1 Preparation of erythrocytes	107
2.7.2.2. Titration of serum for inhibition assays	107
2.7.2.3. Function of OmCI and OmCI-Fc	108
2.7.2.4. Functional analysis of mouse C5	108
2.7.2.5. Assay for identification of C3-containing fractions	108

2.7.3. Alternative pathway haemolysis	109
2.7.3.1. Titration of rat serum.....	109
2.7.3.2. Function of CRiG-CD59 fusion proteins	109
2.7.4. Terminal pathway assay	110
2.7.4.1. Generation of C5b-7 sites on GPE using C8 depleted human serum.....	110
2.7.4.2. Generation of C5b-7 sites on GPE using purified C5b-6 and C7 human proteins	110
2.7.4.3. Titration of mouse serum	110
2.7.4.4. Function of CRiG-CD59 fusion proteins	111
2.7.5. Binding OmCI-Fc and pOmCI to C5	112
2.7.5.1. Preparation of pOmCI and OmCI-Fc surface.....	112
2.7.5.2. Binding of OmCI-Fc and pOmCI to human and mouse C5. Affinity analysis	112
2.7.6. MBI-Om1-OmCI binding interaction	113
2.7.7. Binding CRiG-CD59 proteins to mouse C3b and iC3b.....	113
2.7.7.1. Preparation of C3b surface	114
2.7.7.2. Preparation of iC3b surface.....	114
2.7.7.3. Binding of CRiG-CD59 proteins to C3b and iC3b. Affinity analysis	115
2.7.8. Binding of CRiG-2a-CD59 to C3b-opsonised red blood cells-flow cytometry..	115
2.7.9. Binding of anti-CD59 mAb (mCD59a-7) to mouse -flow cytometry	116
2.8. <i>In vivo</i> and <i>ex vivo</i> analysis	116
2.8.1. Animals	116
2.8.2. <i>In vivo</i> clearance of OmCI-Fc and pOmCI in DBA2 mice	117
2.8.3. <i>In vivo</i> half-life of OmCI-Fc and pOmCI in C57Bl/6 mice	117
2.8.4. <i>In vivo</i> complement inhibitory activity of OmCI-Fc and pOmCI	118
2.8.4.1. Complement activity	118
2.8.4.2. C5 activity	119
2.8.5. Induction of antibody-dependent experimental autoimmune encephalomyelitis (ADEAE).....	119
2.8.6. Induction of atherosclerosis.....	120
2.8.7. Immunohistochemical analysis	121
Chapter 3. Cloning and expression of anti-terminal pathway therapeutics.....	123
3.1. Design of anti-complement therapeutics	125
3.2. Generation of OmCI-Fc.....	127
3.2.1. Cloning strategy	129
3.2.1.1. Cloning of DNA encoding mouse IgG2a Fc	131
3.2.1.2. Cloning of DNA encoding OmCI	133
3.2.2. Transfection.....	136
3.2.3. Large-scale protein expression.....	137
3.2.3.1. Integra CELLline AD1000flasks.....	137
3.2.3.2. HYPER <i>Flask</i> vessel	139
3.3. Generation of fusion proteins consisting of CRiG and CD59	142
3.3.1. Construction of expression plasmids.....	142
3.3.1.1. CRiG-CD59, CRiG-3-CD59 and CRiG-2a-CD59	142
3.3.1.2. CD59-CRiG, CD59-3-CRiG and CD59-2a-CRiG	147
3.3.1.3. Generation of cleavable CD59-CRiG	148
3.3.2. Transfection.....	149
3.3.3. Large-scale expression of CRiG-CD59 fusion proteins	152
3.4. Discussion	153

Chapter 4. Production of monoclonal antibodies against OmCI, mouse CRIG and mouse CD59	156
4.1 Introduction	156
4.2 Anti-OmCI monoclonal antibodies	158
4.2.1 Generation of hybridomas secreting anti-OmCI antibodies	158
4.2.2. ELISA for screening hybridoma cells secreting anti-OmCI mAbs.....	159
4.2.3. Large-scale production of Anti-OmCI antibodies.....	161
4.2.4. Purification of Anti-OmCI antibodies.....	161
4.2.4.1. Purification of anti-OmCI mAbs of IgG isotype (MBI-Om1 and MBI-Om3)	
.....	161
4.2.4.2. Purification of MBI-Om2 (IgM)	162
4.2.5. Characterisation of anti-OmCI mAbs.....	165
4.2.5.1. Characterisation of MBI-Om1 (IgG1).....	165
4.2.5.1.1. Western blot analysis.....	165
4.2.5.1.2. Capture ELISA.....	165
4.2.5.1.3. Surface Plasmon Resonance (SPR).....	166
4.2.5.2. Characterisation of MBI-Om3 (IgG2b).....	168
4.3. Rat anti-mouse CRIG and rat anti-mouse CD59a monoclonal antibodies.....	170
4.3.1. Generation of rat anti-mouse CRIG and rat anti-mouse CD59a monoclonal antibodies.....	170
4.3.2. Screening ELISA.....	171
4.3.3. Purification of rat anti-mouse CRIG and rat anti-mouse CD59a monoclonal antibodies.....	172
4.3.4. Characterisation of rat anti-mouse CRIG and rat anti-mouse CD59a monoclonal antibodies.....	172
4.3.4.1. Characterisation of anti-CD59 mAb.....	173
4.3.4.2. Characterisation of anti-CRIG mAb	174
4.4. Discussion	177
Chapter 5. Purification and biochemical characterisation of anti-complement therapeutics	180
5.1. OmCI-Fc.....	180
5.1.1. Purification of OmCI-Fc	180
5.1.1.1. Purifying via the Fc portion.....	180
5.1.1.2. Purifying via the OmCI domain	181
5.1.1.2.1. Polyclonal anti-OmCI affinity chromatography.....	181
5.1.1.2.2. Monoclonal anti-OmCI affinity chromatography	182
5.1.2. Biochemical characterisation of OmCI-Fc.....	183
5.1.2.1. SDS-PAGE characterisation of OmCI-Fc.....	183
5.1.2.2. Gel filtration of OmCI-Fc.....	184
5.2. CRIG-CD59 fusion proteins.....	188
5.2.1. Purification of CRIG-CD59 fusion proteins	189
5.2.2. Biochemical characterisation of CRIG-CD59 fusion proteins.....	191
5.2.2.1. SDS-PAGE analysis of CRIG-CD59 fusion proteins	191
5.2.2.2. Gel filtration analysis of CRIG-CD59 fusion proteins.....	193
5.2.3. Generation of soluble CD59 and soluble CRIG.....	195
5.3. Purification of ligands for anti-complement reagents	200
5.3.1. Purification of mouse C5.....	200
5.3.2. Purification of mouse C3.....	202
5.4. Discussion	205
Chapter 6. <i>In vitro</i> functional analysis of OmCI-Fc and CD59-CRIG fusion proteins	207

6.1. <i>In vitro</i> characterisation of OmCI-Fc	207
6.1.1. Binding of OmCI-Fc and pOmCI to C5; affinity analysis.	207
6.1.2. Complement inhibitory activity of OmCI-Fc	210
6.2. <i>In vitro</i> characterisation of CD59-CRIg fusion proteins	213
6.2.1. SPR analysis	213
6.2.1.1. Preparation of the C3b surface	213
6.2.1.2. Preparation of iC3b surface	215
6.2.1.3. Interaction of CRIg-CD59, CD59-CRIg, CRIg-3-CD59 and CD59-3-CRIg with C3b	216
6.2.1.4. Interaction of chemically cross-linked (XL) CD59-3-CRIg with C3b.....	218
6.2.1.5. Interaction of monomeric and dimeric forms of CD59-2a-CRIg with C3b	219
6.2.1.6. Interaction of CRIg-3-CD59 with iC3b.....	221
6.2.2. Binding to C3b-opsonised target cells as analysed by flow cytometry.....	221
6.2.3. Complement Inhibition.....	222
6.2.3.1. Alternative pathway haemolysis assay.....	224
6.2.3.2. Terminal pathway haemolysis assays.....	227
6.2.3.2.1. CD59-CRIg function on cells bearing C5b-7 sites in absence of C3b.	227
6.2.3.2.2. CRIg-CD59 function on cells bearing C5b-7 sites in presence of C3b	228
6.3. Discussion	234
Chapter 7. <i>In vivo</i> and <i>ex vivo</i> functional analysis of OmCI-Fc and CD59-CRIg fusion proteins	239
7.1. OmCI-Fc.....	239
7.1.1. Clearance of OmCI-Fc in mice	239
7.1.1.1. OmCI-Fc elimination in the absence of C5	239
7.1.1.2. Half-life OmCI-Fc in the presence of C5	241
7.1.2. <i>In vivo</i> inhibitory activity	244
7.1.2.1. pOmCI and OmCI-Fc- individual effect on complement inhibition.....	244
7.1.2.2. pOmCI and OmCI-Fc-cooperative effect on complement inhibition	246
7.1.2.3. Routes of administration: subcutaneous versus intravenous	249
7.2. Targeting of CD59-CRIg <i>in vivo</i> and <i>ex vivo</i>	251
7.2.1. ADEAE	251
7.2.1.1. Identification of ligands for CRIg, C3b and iC3b, in diseased tissue	252
7.2.1.2. <i>Ex vivo</i> and <i>in vivo</i> targeting of reagents to demyelinating lesion	253
7.2.2. Atherosclerosis	255
7.2.2.1. Identification of ligands for CRIg, C3b and iC3b, in diseased tissue	255
7.2.2.2. <i>Ex vivo</i> targeting of reagents to atherosclerotic plaques	256
7.2.2.3. Plasma levels of CD59-2a-CRIg in treated atherosclerotic mice and <i>in vivo</i> targeting of reagent to atherosclerotic plaques.....	256
7.3 Discussion	259
Chapter 8. Final Discussion	267
8.1. OmCI therapy	267
8.1.1. pOmCI: a powerful C5 inhibitor for treatment of acute disease and conditions	267
8.1.2. OmCI-Fc: an excellent long-lived reagent for treatment of chronic disease	268
8.1.3. OmCI: Prospects for therapy	271
8.2. CD59-CRIg therapy	277
8.2.1. CD59-2a-CRIg: a unique targeted anti-complement drug	277
8.2.2. CD59-2a-CRIg: Prospects for therapy	281
8.3. Final thoughts	283
References	284

Chapter 1. Introduction

In this chapter I will present a general overview of the literature relating to complement suppression in the context of disease. The chapter starts by describing the complement system and its physiological role in health. I will provide detailed information about complement regulatory molecules and give an overview of clinical conditions in which pathology is triggered by altered complement regulation. The focus is then moved to anti-complement therapy where previously generated complement blocking drugs are comprehensively discussed. Finally, this chapter introduces the objectives of the current study.

1.1. The Complement system

Complement is a part of innate immunity with a crucial role in promoting inflammation, facilitating elimination of pathogens and maintaining homeostasis. Complement also has a role in modulation of adaptive immunity. The complement system consists of at least 30 proteins. Some of the proteins circulate in a proenzymatic form and are only activated after proteolytic cleavage by earlier components in the cascade. Normal host tissues are protected from complement attack by complement control proteins; therefore failure in complement control mechanisms may result in damage to host cells. Complement activation occurs through three pathways: the classical (CP), lectin (LP) and alternative pathway (AP). This is illustrated in fig 1.1.

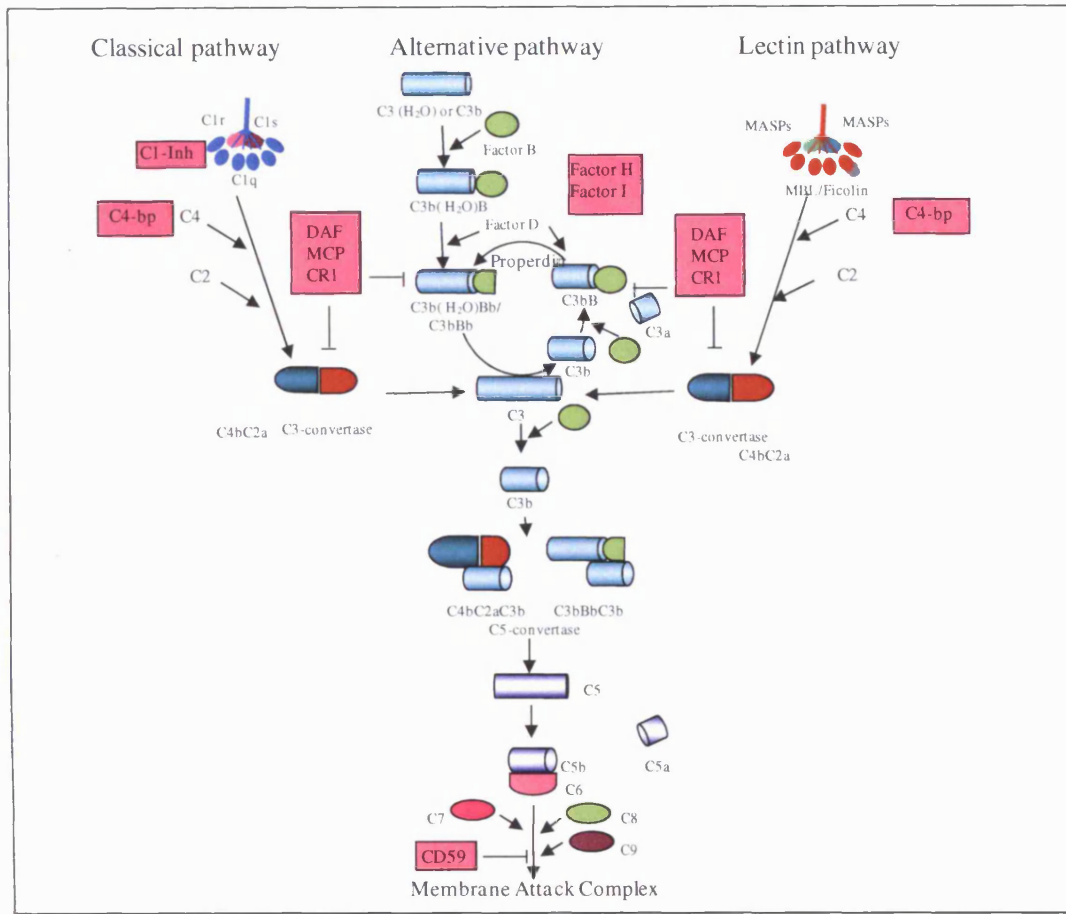


Fig.1.1 Complement system. The CP is initiated by the binding of the C1 complex to antibodies bound to antigens. C1s first cleaves C4, which binds covalently to the bacterial surface, and then cleaves C2. C4b and C2a forms C3-convertase (C4b2a) of the CP. The LP is initiated by binding of the complex of mannose-binding lectin or ficolins and the serine proteases mannose-binding lectin-associated proteases 1 and 2 (MASP1 and MASP2) to sugars on the pathogen surfaces. MASP2 acts in a fashion similar to that of C1s to lead to the formation of the C3 convertase. MASP1 may be able to cleave C3 directly. The AP is initiated by the covalent binding of a small amount of C3b to hydroxyl groups on cell-surface carbohydrates and proteins and is activated by low-grade cleavage of C3 in plasma. C3b binds factor B and forms a C3bB complex. Factor D cleaves factor B bound to C3b to form the AP C3-convertase (C3bBb). The binding of properdin stabilizes this enzyme. The C3-convertases cleave C3 to C3b, which bind covalently around the site of complement activation. Some of this C3b binds to the C4b and C3b in the convertase enzymes of the CP and AP, respectively, forming C5-convertase. These enzymes cleave C5 to C5a and C5b, which initiates the formation of the membrane-attack complex (MAC). MAC is assembled of C5b, C6, C7, C8 and multiple C9 molecules.

1.1.1. Activation pathways

1.1.1.1. Classical pathway (CP)

The CP is initiated by binding of C1 to antibodies produced during the humoral response (IgG and IgM), to natural antibodies, and other molecules generated as a result of an inflammatory reaction such as C-reactive protein (CRP) or serum amyloid protein (SAP), as well as pathogen-associated molecular patterns, such as lipopolysaccharide (LPS). C1 is a multi-molecular complex comprising C1q and serine proteases C1r and C1s (C1qC1r2C1s2) [1]. The activation of the pathway occurs when C1q within the C1 complex binds one of the above mentioned target molecules. Ligands for C1q are listed in table 1.1.

Ligands for C1q:

Immunoglobulins	Fc domain of IgM and IgG (IgG3, IgG1 and IgG2)
Gram-negative bacteria	Lipid A of LPS, Porins
Gram-positive bacteris	Lipoteichoic acid
Viruses	Moloney virus, Vesicular stomatitis virus, DNA polyoma virus, HIV-1
Polyanions	Heparin, Chondroitin-4-sulphate Polynucleotides, Single stranded and double stranded DNA, Cardiolipin and other anionic polyanions in vesicles or on apoptotic cells
Other proteins	Ligand bound pentraxins: CRP and SAP (bound to bacterial and host cell breakdown products such as chromatin)

Table 1.1 C1q ligands

The complex then binds C4 and activated C1s cleaves it to C4b. Surface attached C4b

interacts with C2. C2 is then cleaved by the activated C1s into C2a and C2b. C4b and C2a fragments form the C3 convertase that cleaves the third component of complement, C3. Activation of C3 results in generation of C3a and C3b fragments. As seen in Fig.1.1, C3b forms a complex with C4b and C2a to generate the C5 convertase that will cleave C5 to C5a and C5b [1]. C3a and C5a are anaphylatoxins that mediate multiple reactions in the acute inflammatory response, such as smooth muscle contraction, changes in vascular permeability, histamine release from mast cells, neutrophil chemotaxis, platelet activation and aggregation. C5a is the most potent, followed by C3a and C4a.

1.1.1.2. Lectin pathway (LP)

The LP has features in common with the CP but is evolutionarily much older [2, 3]. Activation of the LP occurs through recognition of oligosaccharide-based or actetyl-based pathogen-associated molecular patterns by either mannan binding lectin (MBL) or ficolins in associations with MBL-associated serine proteases (MASPs). MBL and ficolins are plasma proteins that recognise carbohydrate motifs found on bacteria, viruses, fungi or altered self-molecules (Table. 1.2) [4]. In humans there are three MASPs (MASP-1, -2 and 3) and an alternative splicing fragment of MASP-2 called Map19 [5]. These enzymes are very similar to C1r and C1s of the CP. Upon binding to the target, the MASPs are activated and can cleave C4 and C2, this allows the generation of the CP C3 convertase (C4bC2a).

1.1.1.3. Alternative pathway (AP)

In contrast to the CP and LP, AP has no recognition proteins similar in structure to C1q, MBL or ficolins. However a low level of C3 activation (1% of total C3 per hour) takes place in the blood. A spontaneous hydrolysis of thioester bond in C3 occurs resulting in the generation of C3(H₂O), a molecule with similar properties to C3b. C3(H₂O) is capable of binding to factor B (fB).

Target Pathogens for MBL and ficulins

Bacteria	<i>E.coli</i> <i>Salmonella sp.</i> <i>Pseudomonas aruginosa</i> <i>Haemophilus influenzae</i> <i>Neisseria meningitidei</i> and <i>N. gonorrhoea</i>
Viruses	Herpes simplex virus HIV-1 and HIV-2 Influenza A Virus
Fungi	<i>Candida albicans</i> <i>Saccharomyces cerevisiae</i> <i>Aspergillus fumigatus</i>
Endogenous ligands	Dying cells Ischemic tissue Transformed cells Nucleic acids Phospholipids

Table 1.2. Pathogens recognised by MBL and ficulins

Upon the binding fB changes conformation and can be then cleaved by serum protease factor D (fD) into Ba and Bb. The Bb fragment remains associated with the complex to form “initiation” C3-convertase (C3(H₂O)Bb) and through its own serine protease domain cleaves additional C3 molecules into small fragment C3a and large fragment, nascent C3b. This process leads to conformational changes and exposure of an internal thioester bond, which following nucleophilic attack by a surface group, allows covalent association of C3b with pathogen surfaces. C3b associates with fB to generate C3-convertase of the AP (C3bBb). This process is known as the tickover mechanism of the alternative pathway as it constantly generates low levels of activated C3b-like molecules capable of forming a convertase. The C3 convertase is stabilized by the binding of an oligomeric protein known as properdin [6, 7]. Cleavage of C3 and binding of this additional C3b to the convertase (forming a C3b ‘dimer’) gives rise to the C5 convertase of the alternative pathway. This enzyme activates C5.

Another mechanism of activation of the alternative pathway has been recently proposed. Spitzer and colleagues have shown that properdin can directly bind to some target surfaces such as yeast cell wall and *Neisseria gonorrhoeae* and recruit fluid-phase C3b to the surface [8]. Properdin-bound C3b associates with fB in a similar fashion as the nascent C3b.

The alternative pathway also serves as an “amplification loop” for CP and LP [9, 10]. The C3b molecules, generated by the activation of CP or LP, bind fB. Similarly to the tickover process, fB is then cleaved and activated by fD.

1.1.2. Terminal pathway

All three pathways of complement activation converge at the level of C3. Activation of C3 followed by C5 activation triggers the terminal pathway of the complement system. The terminal pathway and the assembly of the Membrane Attack Complex (MAC) are illustrated in figure 1.2. The terminal pathway starts when C5 is split into the chemo-attractant, C5a, and C5b by the C5 convertase. C5a is a potent anaphylatoxin that mediates inflammatory responses at the site of injury by stimulating neutrophils, eosinophils, phagocytes and endothelial cells [11]. C5b forms a complex with C6 and the subsequent binding of C5b6 to C7 induces a hydrophilic to amphipilic transition that allows C5b7complex to bind the target lipid bilayer membranes. Incorporation of C8 and multiple C9 molecules allows the complex to penetrate the lipid bilayers creating complete transmembrane channels resulting in osmotic lysis of the cell.

C5b-7 is cytolytically inactive and does not form a pore in the cell membrane, whereas C5b-8 and C5b-9 are pore-forming complexes. C5b-8 pores range from 0.4 to 3nm in diameter and a large number is required to lyse erythrocytes and nucleated cells [12]. The diameter of C5b-9 pores can range from 1 to 11 nm [13, 14].

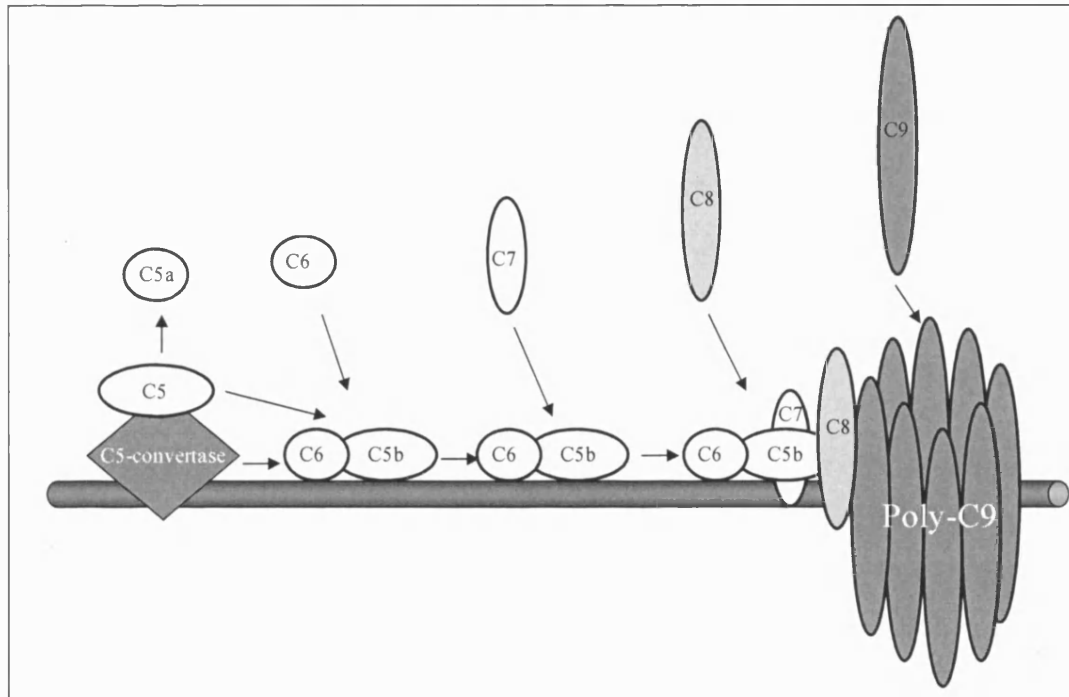


Fig. 1.2 Schematic diagram of terminal complement pathway and MAC formation. C5 convertase binds and cleaves C5 into C5b and C5a. C5a (anaphylatoxin) is released in the fluid phase. C5b binds C6. Upon the binding C6 undergoes conformational changes that allows binding to the lipid bilayer. C7 and then C8 sequentially bind to C5b and insert into the lipid bilayer, forming C5b-7 and C5b-8 complexes, respectively. One molecule of C9 binds to C8, which is followed by polymerisation of multiple C9 molecules, forming the C5b-9 complex.

Papadimitriou and colleagues have demonstrated that MAC lytic activity is characterized by a rapid increase in intracellular Ca^{2+} , followed by loss of mitochondrial polarity and adenine nucleotide pools (ADP and ATP) [15]. Multiple C5b-9 complexes are required to kill nucleated cells, resistance to MAC-mediated killing being dependent on the ability of the cells to eliminate C5b-9 complexes and repair the cellular membranes. Insufficient numbers of C5b-9 complexes form short-lived channels that can easily be eliminated through endocytosis and exocytosis without causing any cell lysis. This sublytic dose of C5b-9 can induce cell-cycle progression by activating signal transduction pathways, transcription factors and various components of the cell-cycle machinery [16-19].

1.1.3. Physiological role of the complement system in health

Complement participates in different steps of inflammatory reactions to protect the host against infection and from chemical or physical injury.

1.1.3.1. Host defence against infection

Complement is a major component of innate immunity that takes part in host defense against foreign pathogens. Activation of complement results in opsonisation, chemotaxis and activation of leukocytes and cytolysis of pathogens by MAC, all processes are responsible for pathogen removal.

1.1. 3.1.1. Opsonisation

Activation of the CP, LP and the AP converge at the level of C3 cleavage. Proteolytic cleavage of C3 into C3a and C3b results in conformational changes exposing the internal thioester bond and allowing covalent association of C3b with pathogen surfaces (bacterial, viral and protozoal) or circulating immune complexes. Further proteolysis of C3b results in formation of opsonins iC3b and C3dg and these can be recognized by different receptors on phagocytes promoting uptake of microbes coated with opsonins [20]. This process is known as opsonisation.

Complement receptors (CR) on leukocytes form an important link to the complement system. The receptors are discussed in section 1.5. Briefly, Complement Receptor type 1 (CR1, CD35) binds the opsonin fragments C3b and C4b and promotes phagocytosis and clearance of antigen-antibody complexes [21]. Complement Receptor type 2 (CR2, CD21) binds iC3b and C3dg. This receptor is part of the B cell receptor (BCR) complex; binding of antigen-complement complexes to CR2 increases the sensitivity of the B cell to antigen by up to a thousand fold. Complement Receptor type 3 (CR3, CD11b/CD18, MAC-1) and Complement Receptor type 4 (CR4, CD11c/CD18, p150.95) are integrin molecules that bind iC3b, β -glucan, intercellular adhesion molecule-1 (ICAM-1), and fibrinogen. These

molecules serve as complement receptors, adhesion molecules and transmembrane signalling adapters. As complement receptors, CR4 and CR3 bind iC3b opsonised pathogens and trigger phagocytosis and degranulation of the effector cells [22, 23]. CR3 is the primary receptor responsible for phagocytosis of opsonised bacteria by neutrophils [24]. In addition to its complement-related function, CR3 binding to ICAM-1 expressed by stimulated endothelium allows monocytes, macrophages, neutrophils, NK and dendritic cells to adhere to blood vessel walls and move into the tissues at the site of inflammation [25, 26].

CR1g (Complement receptor of the immunoglobulin superfamily) is another complement receptor that recognizes C3 cleavage products. It binds opsonins C3b and iC3b and facilitates the clearance of pathogens. Although the Kupffer cells express CR3, CR1g is the main complement phagocytic receptor in liver. CR3 does not participate in immediate recognition of iC3b-coated pathogens, but contributes to the clearance indirectly by recruitment of neutrophils through interaction with ICAM-1 on neutrophils [27]. Moreover CR3 only binds iC3b, while CR1g can recognise also C3b, the first C3 cleavage product and thus ensures immediate pathogen recognition.

1.1.3.1.2. Chemotaxis and activation of leukocytes

Upon complement activation, small molecules C3a, C4a and C5a (~9kDa; 74-77 residues), known as anaphylatoxins are released. The anaphylatoxins exhibit important proinflammatory activities such as increase in vascular permeability, smooth muscle contraction, leukocyte recruitment and promoting production and release of other inflammatory mediators such as histamine [28]. C5a has been shown to be the most potent and C4a to be the weakest [29]. The functional response of the anaphylatoxins are mediated through interaction with seven-transmembrane G-protein-coupled receptors (C3aR for C3a, C5aR and C5L2 for C5a) expressed on the effector cells such as granulocytes, mast cells, monocytes and macrophages. It has been demonstrated that together with C3a and bacterial formylated peptides, C5a attracts phagocytes to the site of infection [30]. It can modulate the activity of a number of cell types such as eosinophils, basophils, neutrophils, monocytes and macrophages [31-35]. C5a, upon interaction with the C5a receptor (C5aR, CD88), can

stimulate oxidative burst (release of reactive oxygen species) in neutrophils and enhances phagocytosis and release of granule enzymes [36, 37].

1.1.3.1.3. Lysis of bacteria and cells

Activation of the complement cascade results in formation of the membrane attack complex, which can disrupt the integrity of the bacterial cell wall, especially in Gram-negative bacteria (*Neisseria meningitidis*), which have an outer lipid membrane. However, Gram-positive bacteria resist this attack by the fact that their cell membrane is shielded by a thick cell wall [38] which prevents the C5b-9 complex from penetrating the thick peptidoglycan layer. The elimination of Gram-positive bacteria occurs via phagocytosis.

1.1.3.2. Disposal of waste

1.1.3.2.1. Clearance of immune complexes from tissues

Complement plays a role in maintaining homeostasis and removing antigen-antibody complexes generated during the adaptive immune response. This prevents immune complex (IC) deposition within the tissues and subsequent inflammatory reactions induced by these complexes. In humans and other primates, erythrocytes express CR1 organized in clusters on the cell surface, which bind C3b and/or C4b opsonised IC. The red blood cells transport these IC to the spleen and liver where they are cleared by macrophages [39, 40]. In autoimmune disease such as SLE (systemic lupus erythematosus) the number of CR1 on erythrocytes is reduced [41, 42]. This leads to failure in IC disposal and their deposition in the glomeruli and small vessels, which can trigger inflammation.

1.1.3.2.2. Clearance of apoptotic cells

Apoptosis is a genetically-controlled programmed cell death, which plays a crucial role in maintaining tissue homeostasis and eliminating aberrant cells. This process is associated

with morphological changes such as shrinkage, plasma membrane blebbing, chromatin condensation followed by cellular fragmentation and formation of apoptotic bodies. Self-derived dead cells are a source of autoantigens therefore the apoptotic cells need to be rapidly cleared from the body. The apoptotic cells have the ability to activate the complement system and this facilitates the clearance of the cells through phagocytosis. Binding of C1q to apoptotic cells and apoptotic debris induces complement activation and C3b and iC3b deposition followed by clearance of the dying cells by macrophages through binding to specific receptors immune [43-46]. CRP also binds apoptotic cells and can activate the complement cascade resulting in opsonisation [47].

1.1.3.3. Link between innate and adaptive immunity

Complement provides a link between innate and adaptive immunity. It is involved in regulation of the humoral and T cell response.

Complement modulates humoral immunity by augmentation of the antibody response and enhancement of immunological memory. *In vitro* and *in vivo* studies have demonstrated that deficiency in C3, C4 or CR1/2 (CR1 and CR2 are product of a single gene in mice, explained in section 1.5.2.1) results in a less efficient humoral response to T-independent and T-dependent antigens [48-51]. B cells express complement receptors CR1 and CR2. Complement receptor CR2 on B-cells forms a co-receptor together with CD19 and CD81. Co-ligation of the co-receptor with the BCR through C3dg-coated antigens has been found to enhance downstream signaling and the amount of antigen required to activate B cells and to induce antibody response *in vitro* and *in vivo* [52-55]; thus the complement system acts as an adjuvant.

Follicular dendritic cells (FDC) are involved in modulation of the humoral response. FDC are stromal cells which produce B lymphocyte chemoattractant chemokines and participate in organisation of germinal centers in the B cell follicles [56]. They also express complement receptors CR1 and CR2 and are involved in modulation of the humoral memory by binding and harboring C3-tagged antigens and immune complexes over the long term to be presented to the antigen specific B cell [57-60]. This event is important for clonal

selection of B cells within the germinal center and efficient maintenance of long-term antibody responses and memory. Complement also plays a role in immunoglobulin class-switching by modulating cytokine production. For example, C1q deficiency in mice resulted in a blocking of class-switching to IgG2a and IgG3 due to reduction of IFN- γ production [61, 62].

Complement participates in regulation of T cells. For example, C3 deficient mice demonstrated reduced anti-influenza CD4⁺ and CD8⁺ T-cell responses in the context of viral infection [63]. Furthermore complement has been found to play a role in development of induced regulatory T cells. Crosslinking of membrane cofactor protein with CD3 on CD4⁺ T cell induces regulatory T-cell phenotype with Il-10 production [64].

1.2. Complement regulation and regulators

Complement is a powerful component of the innate immune system and modulator of the adaptive response. However it also has a potential to damage host tissues. For this reason, control of complement activation is crucial. Distinguishing self and non-self or altered self is the first point of control. For example the CP is initiated by antibody recognition of a microbial target and the LP recognizes patterns specific for pathogen surfaces. Once activated, complement is controlled by a number of membrane-bound (Table 1.3) and soluble (Table 1.4) complement regulators described below. The regulators inactivate complement at different stages of the cascade, mainly at the level of the convertases and at MAC-assembly.

Regulator	Genes/ alternative splicing	Membrane attachment	Molecular size and structure	Expression	Ligands	Complement inhibitory function and mode of action
CR1 Human	1 gene/ no	TM	23-37 SCRs; 180-280kDa;	Peripheral blood cells and FDC, astocytes, podocyte	C4b, C3b, iC3b	Decay accelerating activity; Co-factor I activity; Clearance of IC, stimulate phagocytosis;
Mouse	1 gene/ yes CR2	TM	21 SCRs-CR1 15 SCRs-CR2	B cells, FDC		
Crry (rodents only) Mouse	1 gene/ no	TM	5 SCRs; 65kDa	Broad	C4b, C3b	Decay accelerating activity; Co-factor I activity;
MCP Human	1 gene/yes	TM	4SCRs; 58-68kDa with STP 48-56kDa no STP	Broad (Except erythrocytes)	C4b, C3b	Co-factor I activity;
Mouse	1 gene/yes	TM	4SCRs; 60kDa	In the testis		
DAF Human	1 gene/no	GPI-, secreted	4 SCRs; 70kDa (membrane associated)	Broad	C4b, C3b	Decay accelerating activity;
Mouse	2 genes/yes	GPI-, secreted, transmembrane	4 SCRs; 70kDa (membrane associated)	Broad for GPI-DAF1 Testis for TM-DAF2		
CD59 Human	1 gene/yes	GPI	20kDa	Broad	C5b-8 complex	Prevents insertion of C9 molecules into the cell membrane and inhibits MAC formation;
Mouse	2 genes/no	GPI	20kDa	CD59a-broad CD59b-testis		

Table 1.3. Membrane bound complement regulators in human and mouse. GPI, glycosphosphatidyl inositol anchored; TM, transmembrane; STP, region enriched in serines, threonine and prolines;

Regulator	Molecular size and structure	Ligands	Function
Factor H	150kDa; 20 SCRs	C3b	Accelerates the decay of AP convertases and acts as a cofactor for the factor I-mediated cleavage of C3b.
C4bp	500kDa Human: 8 SCRs in α -chain, seven α -chains, 3 SCRs in β -chain, one β -chain; Mouse-: no β -chain	C4b Non-complement ligands: heparin, serum amyloid P component and protein S;	Cofactor for factor I-mediated cleavage for C4b; Link complement and coagulation system;
C1 inhibitor	Human 104kDa/Mouse 96 kDa	C1 and MBL-MASP complexes Non-complement ligands: factor XII and kalikrein, factor XI and thrombin tissue, plasminogen activator and plasmin;	Dissociates C1r and C1s from the C1 and MASPs from the MBL-MASPs complex. Non-complement function-Blocks contact system, coagulation system and fibrinolytic system;
Factor I	Serine protease, 88kDa	C3b, C4b, Factor H, C4bp, MCP, CR1	Cleaves C4b and C3b (in cooperation with essential cofactors)

Table 1.4 Soluble complement regulators

Two different regulatory mechanisms have evolved to control the complement convertases. The first one prevents the formation of active convertase by catabolism of C3b and C4b via factor I cleavage (Fig.1.3). Factor I requires cofactors such as membrane cofactor protein (MCP), CR1 and factor H (fH) and the rodent specific regulator Complement receptor 1-related/gene protein y (Crry), for its proteolytic activity and thus this regulatory mechanism is known as “cofactor activity”. The second mechanism of regulation is the dissociation of inappropriately formed convertase (Fig.1.4). There are several complement inhibitors that exhibit a decay accelerating activity. These are the decay accelerating factor (DAF), CR1, fH, C4-binding protein (C4bp) and Crry.

1.2.1. Factor I

Factor I consists of noncatalytic heavy chain linked by a disulfide bond to a catalytic chain. It is a soluble complement regulatory serine protease that cleaves three peptide bonds in α -chain of C3b and two bonds in the α -chain of C4b and inactivates these proteins in presence of cofactors such as factor H, MCP, C4bp and CR1 [65]. C3b is cleaved into iC3b and C3f [66]. Further C3 degradation to C3c and C3dg is observed in presence of CR1 as a co-factor of factor I [67]. C4b is cleaved to C4c and C4d in presence of C4bp, MCP and CR1 [68, 69].

1.2.2. Regulators of complement activation (RCA) gene cluster

Many of the complement regulators are encoded by a cluster of genes located on the long arm of chromosome 1 (1q32), this region is known as Regulators of Complement Activation (RCA) gene cluster [70, 71]. In humans these are proteins from the factor H family, C4bp, DAF, MCP and CR1. Another member of this family is CR2.

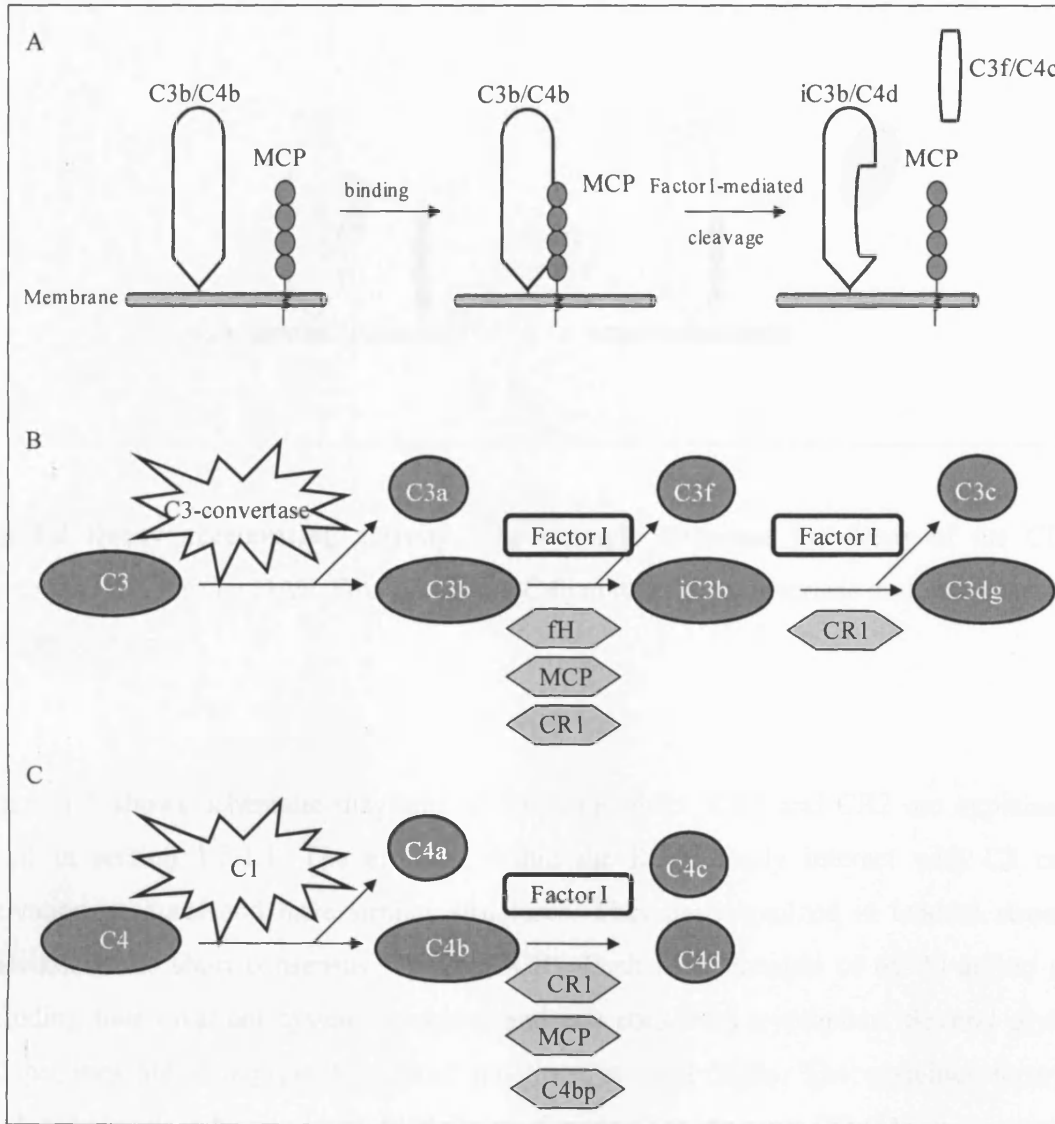


Fig. 1.3 Schematic diagram of factor I mediated cleavage and generation of C3 and C4 fragments. A. Factor I cleaves and inactivates C3b and C4b in presence of cofactor activity. This includes MCP, fH, CR1 and C4bp. MCP is illustrated as an example. B. Cleavage of C3 and generation of C3 fragments. C3 is activated by the C3 convertase to generate C3a and C3b. C3b is inactivated by cleavage with factor I into inactive iC3b and C3dg. Co-factors for factor I cleavage are shown below the arrows. C. Cleavage of and generation of C4 fragments. C4 is activated by the C1 complex to generate C4a and C4b. C4b is inactivated by cleavage with factor I to generate C4d and C4c. Co-factors for factor I cleavage are shown below the arrows.

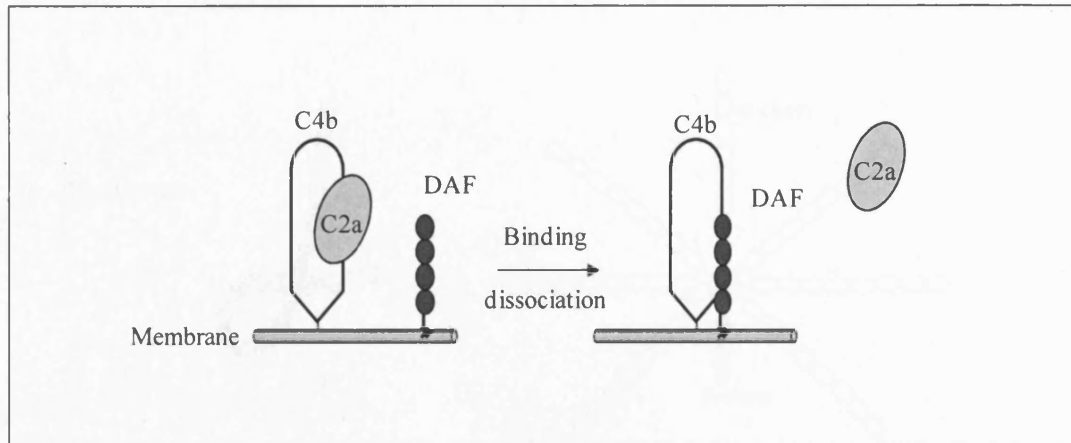


Fig. 1.4 Decay accelerating activity. The example illustrates the decay of the CP C3 convertase (C4b2a) by DAF. DAF binds the C4b units of the convertase and dissociates C2a from the enzyme.

Figure 1.5 shows schematic diagrams of RCA members. CR1 and CR2 are explained in detail in section 1.5.1.1. The proteins within the RCA family interact with C3 or C4 activation products and have similar structures. They are organized in tandem structural units known as short consensus repeats (SCR). Each SCR consists of 60-70 amino acids including four invariant cysteine residues and one conserved tryptophan. Several glycines and prolines are also present in fixed positions in most SCRs. The cysteines form two disulphide bonds, which hold the SCRs in rigid triple-loop structure [72, 73].

1.2.2.1. Factor H family

Factor H family includes Factor H (fH), factor H-like 1 (fHL1) and five factor H-related proteins (fHR1 to 5). Factor H is a 150 kDa fluid phase regulatory protein that binds C3b of the alternative pathway C3 convertase (C3bBb) accelerates its decay and acts as co-factor for the factor I-mediated proteolytic inactivation of C3b [74, 75]. fH can act in fluid phase and on the cellular surface. It is of particular importance for the protection of cells that lack surface-bound regulators. Self and non-self discrimination depends on the composition of the surface to which C3b is bound [76-78].

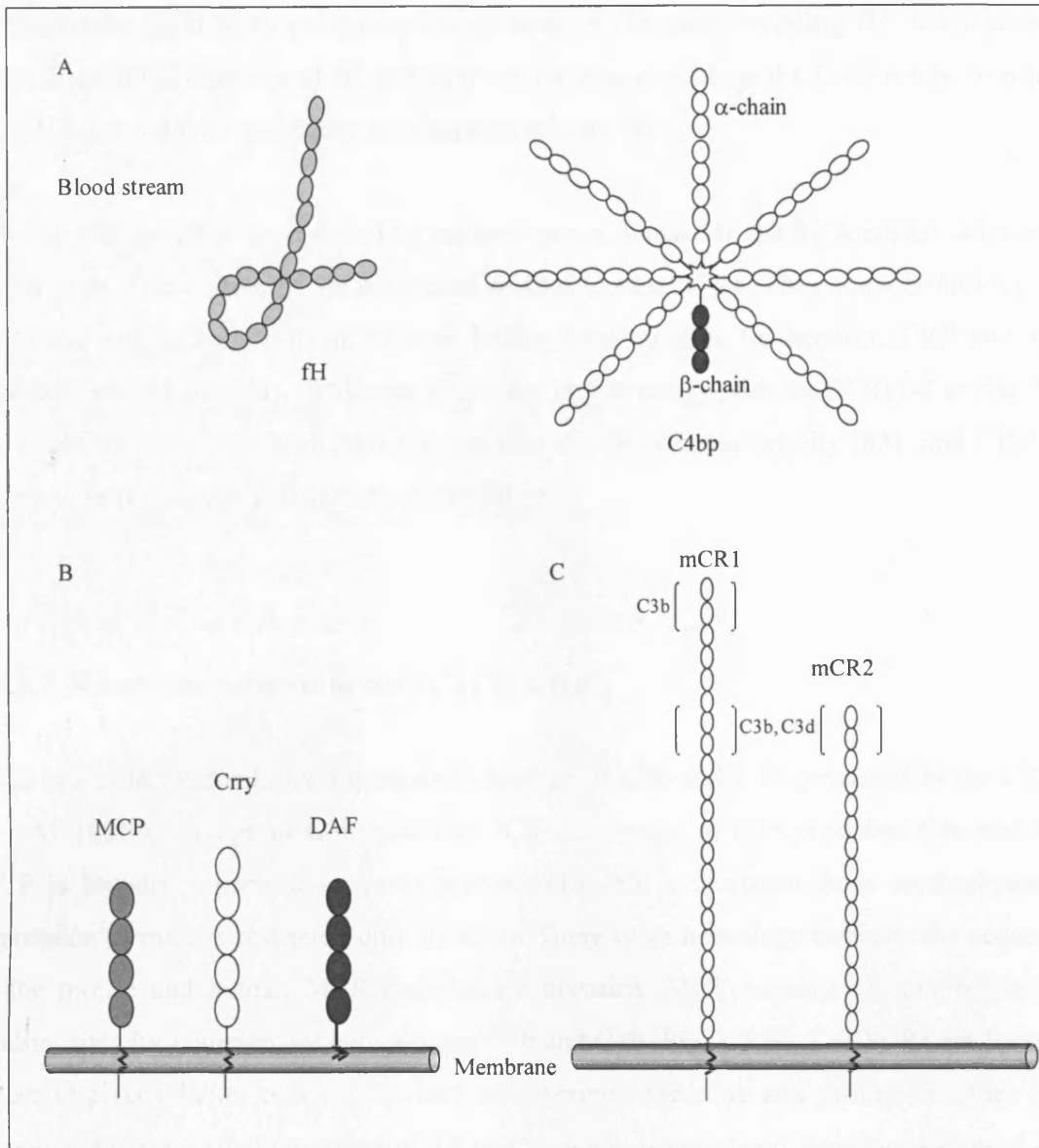


Fig.1.5 Schematic diagram of membrane bound and soluble members of RCA

A. Soluble members: fH and C4bp. B. Membrane bound members: MCP, Crry and DAF. C. Mouse CR1 and CR2. C3 binding sites are indicated.

fH attaches to the surface through binding with glycosaminoglycans on the host cells. fH is composed of 20 SCR [79] (Fig.1.5A). It has three C3b binding sites. The binding site in SCR1-4 is essential for the factor I co-factor activity of factor H [80-83].

fHL1 protein (42kDa) is an alternative splicing of the gene encoding fH. It contains the seven N-terminal domains of fH and four unique amino acids at the C-terminus. Similar to fH, fHL1 has cofactor and decay accelerating activity [84]

The five fHR proteins are encoded by separate genes, located in the RCA cluster, adjacent to the *fH* gene. These proteins are composed of four to nine SCRs. They show homology with SCRs 6-9 and SCRs 19-20 of fH thus having binding sites for heparin, CRP and some microbial surface proteins. Although they have no homology with the SCRs1-4 of fH, fHR3 and fHR4 proteins have been found to enhance the fH cofactor activity [85] and fHR5 has shown a weak cofactor and decay activity [86, 87].

1.2.2.2. Membrane cofactor protein (MCP, CD46)

MCP is a cofactor for factor I-mediated cleavage of C3b and C4b generated in the CP, LP and AP [88]. Cleavage of C3b generates iC3b. Cleavage of C4b produces C4c and C4d. MCP is broadly expressed on most human cells, but it is absent from erythrocytes. Its expression in mice is restricted only to testis. There is no homology between the sequences of the mouse and human MCP cytoplasmic domains. MCP consists of four SCRs with binding sites for complement components C3b and C4b (Fig. 1.5 B). The SCRs are followed by an O-glycosylation region, enriched with serine, threonine and proline residues (STP domain). Next are small segment of 12 amino acids of undefined function, followed by a transmembrane domain, cytoplasmic anchor and one of two non-homologous cytoplasmic tails. The tails contain signalling motifs and drive differential processing of isoforms [89]. MCP is most effective in regulation of the amplification loop of the AP [88, 90]. As a cofactor for the factor I-mediated cleavage, it prevents C3b deposition on the host cells [88, 90]. In addition to its complement inhibitory activity, MCP is also a receptor for some pathogens including measles virus, human herpes virus 6, group A Streptococci, group B and D adenoviruses, *Neisseria gonorrhoeae* and *Neisseria meningitidis* [91-96]. Infection with these pathogens leads to down-regulation of MCP expression and this enhances complement activity [97]. As demonstrated by Schnorr and co-workers, cells infected with measles virus had enhanced sensitivity to complement-mediated killing due to the down regulation of MCP. This molecule also plays an important role in cell signalling.

Crosslinking of MCP leads to cell activation and regulation of T-cell immune function [64, 98-102].

1.2.2.3. Decay accelerating factor (DAF, CD55)

DAF is composed of four SCRs followed by glycosylated stalk and a glycosyl phosphatidyl inositol (GPI) anchor [103-105] (Fig.1.5 B). DAF accelerates decay of Bb from the AP convertase and C2a from the CP enzyme (Fig.1.4). Together with MCP, DAF protects host cells from opsonisation and complement-mediated damage by inactivating the convertases [106, 107]. It is expressed on tissue and peripheral blood cells: erythrocytes, granulocytes, T-cells, B-cells, monocytes and platelets, it is also found on bone marrow mononuclear cells and erythroid progenitors [108-110]. A secreted form of DAF has been found in plasma, tears, saliva, urine, synovial and cerebrospinal fluids [111]. This soluble DAF is likely to be a product from alternative splicing of the *DAF* gene [104]. In the mouse there are two forms of DAF encoded by different genes: GPI-anchored and a transmembrane form. Whilst the mouse GPI-anchored DAF is broadly expressed [112], expression of the transmembrane form is restricted to mouse testis [113]. An additional soluble form of DAF was also described [114]. Like MCP, DAF is a ligand for pathogens such as enteroviruses, some picornaviruses (Coxsackieviruses) and uropathogenic *E. coli* [115, 116].

1.2.2.4. C4b-binding protein

C4b-binding protein is a 500-kDa glycoprotein, composed of seven identical α -chains and a β -chain linked together by a central core (Fig.1.5 A). The α -chains contain eight and the β -chain contains three SCRs [117, 118]. It inhibits the CP by acting as a cofactor to the serine proteinase factor I in the proteolytic inactivation of C4b [117], preventing the assembly of the classical and lectin C3-convertase (C4b2a) and accelerating the natural decay of the complex [119]. It has been suggested that C4bp also acts as factor I cofactor in the cleavage of C3b in the fluid phase thereby inhibiting to some extent the AP of complement but it is not as efficient as fH. C4bp interacts not only with C4b and C3b, but also with heparin [120], SAP and protein S (PS) [121], [122]. PS is a vitamin K-dependent anticoagulant and

the interaction with C4bp links the complement and the blood coagulation systems. C4bp circulates in complex with vitamin K-dependent PS, which provides the C4bp with the ability to interact with negatively charged phospholipid membranes.

1.2.2.5. Complement receptor 1-related/gene protein y (Crry)

Crry is a 65 kDa-complement inhibitor broadly expressed in rodents. It contains five SCRs in mice and seven in rats (Fig.1.5B). It inhibits the CP and AP C3 convertases by dissociating the enzymes or by factor I-mediated activity [123]. Crry, together with MCP, exerts a co-factor activity for the factor I-mediated cleavage of C3b and C4b. MCP expression is restricted to male germ cells in mouse and rat, therefore Crry remains the main regulator with cofactor activity in these animals. Similarly to DAF, Crry accelerates the decay of the CP C3 convertase and to a lesser extent the AP C3 convertase [124].

1.2.3. C1-inhibitor

C1 inhibitor is a plasma protein that belongs to the serine protease inhibitor (serpin) family of inhibitors [125]. Upon the interaction with C1-inhibitor, the protease cleaves a peptide bond at the reactive center loop of the C1-inhibitor. This results in a molecular rearrangement that leads to the formation of a covalent bond between the inhibitor and the active site of the serine protease. The C1-inhibitor inactivates complement proteases C1r, C1s and MASP2 and thus regulates the CP and LP [126-129]. In addition to the complement proteases, it also controls the activity factor XII, plasma kallikrein, factor XI, plasmin, and tissue plasminogen activator [130]

1.2.4. CD59

CD59 is a GPI-linked glycoprotein with molecular weight of ~20 kDa. It regulates the terminal pathway and inhibits inappropriate MAC formation on host cells. It binds the α -

chain of C8 within the C5b-C8 complex, preventing binding of more than one copy of C9 to the complex and subsequent insertion of C9 into the membrane [131, 132]. CD59 contains five intrachain disulphide bonds which maintain the disc shape of the molecule [133]. CD59 is broadly expressed being identified on all circulating cells [134]. Two forms of CD59 (CD59a and CD59b) exist in mice, as a result of duplication of the *CD59* gene. CD59a is found in almost all mouse tissues whereas CD59b is identified exclusively in testis [135, 136].

1.3. Complement receptors

C3 is a central player in the complement cascade and its breakdown products have multiple functions in immunity. The C3 derived molecules perform their effector functions through interactions with other molecules. For example, pathogens, immune complexes and dying cells opsonised with C3 fragments can be recognised by complement receptors. Three different C3 receptor families will be described in this section. The RCA gene cluster codes for CR1 and CR2. CR3 and CR4 belong to β_2 integrin family. The recently identified C3 receptor termed Complement receptor of the immunoglobulin superfamily (CRIg) is a type 1 transmembrane Ig molecule.

1.3.1. Receptors encoded by the RCA gene cluster

This group includes two members: CR1 and CR2. Like other members of this family, the extracellular region of CR1 and CR2 is composed of SCRs.

1.3.1.1. Complement receptor type 1 (CR1)

Human CR1 is a ~200 kDa single chain transmembrane glycoprotein that binds C3b and C4b with high activity and iC3b and C3dg with low affinity [39, 67, 137]. It inhibits both CP and AP C3 and C5 convertase due to its decay accelerating activity and co-factor activity for

the factor I-mediated cleavage of C3b to iC3b, C3c and C3dg and of C4b to C4c and C4d. CR1 is expressed on erythrocytes, a subset of T cells, mature B cells, follicular dendritic cells, kidney podocytes, granulocytes and monocytes. A soluble form of CR1, released from the cell membrane by proteolytic cleavage, was found at low concentration in the blood [138-140].

The most common CR1 allotype consists of 30 SCRs. All except the two carboxyl terminal SCRs (SCRs 29 and 30) form large repetitive units called long homologous repeats (LHRs). LHRs A, B and C (but not LHR D proximal to the cell membrane) contain seven SCRs and bear binding sites for C3b and/or C4b, products of complement activation [141]. There are two functional sites interacting with these products or the complement convertases, located in the three amino-terminal SCRs of the LHRs [141-144]. Site 1 (SCRs1-3), located in LHR A binds C4b and very weakly C3b [143]. Site 2 in LHR B (SCRs 8-10) and LHR C (SCRs 15-17), binds C3b and with lower affinity C4b [145].

In addition to its complement inhibitory function, CR1 also plays a major role in immune complex clearance due to its affinity for C3b and C4b. CR1 expressed on erythrocytes is able to capture complement-bound immune complexes and transports them to the liver and spleen where they are eliminated through the action of macrophages [146-148]. CR1 expressed on macrophages and neutrophils binds complement opsonised immune complexes and mediates phagocytosis.

1.3.1.2. Complement receptor type 2 (CR2)

CR2 is a 145kD protein that comprises 15 or 16 SCRs. It binds C3dg and with lower affinity iC3b [149-152]. CR2 is expressed on mature B-cells, thymocytes, a subset of CD4⁺ and CD8⁺ peripheral T-cells and FDCs, basophils, mast cells, keratinocytes and epithelial cells. CR2 together with CD19 and CD81 acts as a B-cell co-receptor complex for antigen receptor mediated signal transduction. Studies using antigens coated with C3d/C3dg to co-ligate CR2 with surface IgM demonstrated that CR2 contributes in B cell activation, generation of immunologic memory and Ig class switching. Uptake of C3dg-coated antigen by B cells results in enhanced signaling via the B cell antigen receptor, lowering the threshold of B cell activation and providing an important survival signal [54].

In addition to C3 fragments, CR2 also binds the Epstein-Barr virus glycoproteins gp350 and gp220. This interaction contributes to the viral infection [153].

1.3.1.3. Murine complement receptor type 1 and complement receptor type 2

Murine type 1 and type 2 complement receptors are products of alternative splicing of single gene *Cr2*. Mouse CR1 comprises 21 SCRs while mouse CR2 contains 15 SCRs (Fig.1.5C). There are two C3b binding sites in the murine CR1-within SCRs 1-2 and SCRs 7-8, and one in CR2 (SCRs 1-2) [154] [155, 156]. One C3d binding site is found in both molecules- SCRs7-8 in CR1 and SCRs1-2 in CR2. Mouse CR1 and CR2 are expressed on B lymphocytes, follicular dendritic cells and activated T cells [156, 157].

1.3.2. β_2 -Integrin family

Two complement receptors belong to the β_2 -integrin family. Complement receptors type 3 and type 4 are transmembrane heterodimers composed of α subunit (CD11b or CD11c respectively) and a common CD18 (β) chain. CR3 and CR4 are expressed mainly on leukocytes. Both of these receptors bind iC3b and facilitate phagocytosis of iC3b-opsonised particles [158, 159]. CR3 and CR4 are also involved in leukocyte adhesive, migratory, phagocytic activities in response to inflammatory stimuli, events that facilitate the host-defence against bacterial pathogens [160].

1.3.3. Type 1 transmembrane Ig superfamily

Complement receptor of the immunoglobulin superfamily (CRIg) also known as V-set and Ig domain-containing 4 (VSIG4) is a recently identified member of the type 1 transmembrane Ig superfamily [161]. Two alternative spliced forms were found in human (long and short) whereas only one form exists in mouse. The longer human form (huCRIg(L)) also known as Z39Ig consists of V and C2-type Ig domain and the short human form and the mouse CRIg contain only a single V-type Ig domain. CRIg is expressed at high

levels in liver macrophages (Kupffer cells), intraperitoneal macrophages, neutrophils and activated dendritic cells. Low level of expression was detected in human adrenal gland macrophages, alveolar macrophages, synovial macrophages in the joints, foam cells in atherosclerotic plaques and lamina propria histiocytes [161-163]. CRIg binds surface attached C3b and iC3b and facilitates the phagocytosis in the liver and plays an important role in removal of intracellular and extracellular pathogens as well as complement-opsonised platelets from the circulation [161, 164, 165]. CRIg binds the β -chain of the C3 fragment but not the α , as other complement receptors do [166]. CRIg expressed on the cell surface does not affect complement activation. However, a study using CRIg-Fc fusion protein demonstrated that binding of CRIg to C3b, a subunit of the AP C3 and C5 convertases, results in complement inhibition [166]. Interestingly, CRIg does not exhibit either decay accelerating or co-factor I mediated activities. Its mode of action is different; it prevents binding of C3b within the convertase to its ligands C3 and C5. The role of CRIg as a complement inhibitor has been confirmed *in vivo* in models of arthritis [167]. In addition to its role as a complement receptor and regulator, CRIg inhibited T-cell proliferation and Il-2 production [163]. Administration of CRIg-Ig fusion protein reduces cytotoxic T-and B-cell response to viral antigen in animals immunized with cytomegalovirus glycoprotein [163].

1.4. Complement and diseases/pathology

The human body is constantly exposed to pathogens and infectious agents and consequently has developed complex, highly efficient immune mechanisms to fight foreign invaders. As a part of the immune system complement plays a key role in enemy elimination. However, when the host's anti-pathogen response is not properly controlled and regulated, the immune system and complement in particular can attack and damage self-tissues. The delicate balance between the self-protective and self-destructive mode of complement is discussed in this section.

1.4.1. Infectious disease and pathogen evasion of complement

The complement system plays a major role in host defense against invading bacteria, fungi, multicellular organisms and viruses. It facilitates phagocytosis of pathogens, stimulates the humoral immune response and chemotactic attraction of immune cells to the sites of infection, stimulates cytokine and histamine synthesis and directly lyses targets. Deficiencies in the terminal pathway components are associated with increased susceptibility to meningococcal infections caused by the Gram-negative bacteria *Neisseria meningitides* [168]. On the other hand, parasites and pathogens, which successfully cause infections and diseases, often protect themselves from host defense by using specific immune escape strategies. Many pathogens have developed mechanisms to break the host's defense barrier and to evade complement attack. Pathogens have learnt how to control and prevent complement recognition and inhibit effector function. There are three main strategies used by pathogens to evade the host complement system.

Some pathogens, such as group B streptococci and gram-negative bacterium *P. aeruginosa* secrete proteases which inactivate products of complement activation: C5a and C3b respectively [169]. Another common complement escape mechanism is binding soluble complement regulators from the host (such as factor H, C4bp) to the pathogen surface [170-172]. The regulators block complement activation and protect the pathogen's surface from complement attack. Some of the proteins secreted by pathogens have the ability to directly inhibit complement activation. For example, *Staphylococcus aureus* produces a staphylococcal complement inhibitor (SCIN) that blocks the three pathways of complement activation by binding to surface-bound convertases [169, 173]. This bacterium secretes another complement inhibitor, extracellular fibrinogen binding protein, which binds the thioester containing C3dg domain of C3b and prevents C3b deposition on to sensitized surfaces. Ticks also produce complement inhibitors. Several anti-complement proteins are found in saliva of blood feeding acari, including *Ixodes* sp. and *Ornithodoros moubata*.

During a blood meal *Ornithodoros moubata* secretes a salivary gland "protein cocktail" able to modulate the host immune and homeostatic system. Some of these proteins belong to a family termed lipocalins. This family is characterised by an eight-stranded anti-parallel β -barrel closed off at one end by an N-terminal helix and stabilised by a C-terminal α -helix that packs against the side of the barrel [174]. The lipocalins are found to modulate the host

inflammatory response by blocking histamine and serotonin, to inhibit platelet and neutrophil aggregation and vasoconstriction, and to block the complement system. The complement inhibitor identified in *Ornithodoros moubata* is termed Ornithodoros moubata Complement Inhibitor (OmCI). OmCI is a 17kDa nonglycosylated protein that belongs to the lipocalin family [175]. It inhibits C5 activity in a broad range of species including rodents and humans without generating immune response [176]. A structural study revealed that the binding of OmCI to C5 does not block the convertase cleavage site but rather leads to conformational changes in C5 molecule which stabilise its global structure [177]. These properties of OmCI could be employed as a therapy in complement mediated disease. This matter will be further discussed in the thesis.

1.4.2. Complement dysregulation and disease

The complement response of the host to infectious agents is a double-edged sword -despite the protective role of complement against microbial invasion, inappropriate activation of the system may have pathological consequences. When complement is not properly controlled it can turn its power towards self-tissues to cause diseases. These include immune complex and autoimmune diseases (such as SLE, autoimmune arthritis and myasthenia gravis), neurodegenerative disorders (such as Alzheimer's disease and multiple sclerosis), cardiovascular diseases (atherosclerosis) and acute conditions such as sepsis and ischaemia reperfusion (IR) injuries. Diseases and animal models involving complement are listed in Table 1.5. Some of these will be discussed in this Chapter.

1.4.2.1. Acute conditions

Although complement activation is often not the primary cause, the tissue damage in certain conditions is complement-mediated. A number of studies provide compelling evidence to implicate complement in IR injury [178-182]. IR injury is a pathological tissue damage caused when blood supply returns to a tissue following a period of ischaemia. IR injury can occur in various clinical situations including myocardial infarction, stroke, haemorrhagic and septic shock [183-185]. Membrane phospholipids and mitochondrial proteins exposed

during the ischaemia serve as neoantigens which activate complement during the reperfusion phase [178, 179]. Restoration of circulation results in complement activation via CP, LP and/or AP [186, 187]. Complement activation triggers release of anaphylatoxins C3a and C5a and MAC formation on the target cells. C3a and C5a can activate endothelial cells and leukocytes. C5a was found to attract inflammatory cells to the site of injury [188]. The incorporation of MAC alters normal function of the target cell by causing direct tissue damage or by modulating the transcription of genes coding for proinflammatory mediators [189, 190]. MAC insertion triggers activation of endothelial nuclear factor κ B and increases the expression of number of adhesion molecules; expression of Il-8 and monocytes chemoattractant protein-1; and activation of platelets, contributing to platelet-leukocyte aggregation. In addition cleavage of C3b results in deposition of iC3b on the target endothelial cells and acts as ligand for CR3. CR3 is usually upregulated in activated leukocytes and contributes to the accumulation of these cells in the extravascular compartment.

In transplantation, the products generated upon the complement activation can modulate the graft rejection by binding to the graft or by modifying the response of macrophages, T and B cells of the recipient. Donor specific antibodies in the blood of the recipient can bind to the vascular endothelium of the transplant and activate complement through the CP. The complement cascade can be also activated through the LP in transplants. MBL binds apoptotic and injured endothelial cells and may be activated by cells undergoing apoptosis [191-194].

1.4.2.2. Autoimmune diseases

Complement has been found to be a key player in the pathology associated with many autoimmune diseases. Autoimmune diseases occur when the immune response is directed against self-antigens and are often characterized by high levels of circulating autoantibodies

Human disease	Models	Evidence for complement implication
Rheumatoid arthritis	Antigen-induced (AIA, antigen-methylated BSA); Collagen type II-induced (CIA); Anti-collagen type II Ab transfer (CAIA); K/BxN serum transfer;	Elevated levels of complement activation products in synovial fluid; Enhanced local production of complement proteins in synovial tissue; Complement deficiency (C3, fB) and complement inhibition (anti-C5 mAb, sCR1) have protective effect;
Multiple sclerosis	EAE, ADEAE, Biozzi (antibody high, ABH);	Elevated levels of complement activation products C3a, C4a and soluble C5b-9 in CSF; Complement deficiency and complement inhibition have protective effect;
Antiphospholipid antibody syndrome	Anti-phospholipid antibody transfer	Complement deficiency (C1q, C4, C3, fB) and complement inhibition (Crry-Ig, anti-fB mAb) have protective effect;
Lupus nephritis	MRL/lpr strain; NZB/W F1	Complement proteins in the glomerulus, predominantly those of the CP; C1, C2 and C4 deficiency predispose to SLE;
Myasthenia gravis	Active immunisation with Acetylcholine receptor (AChR) from Torpedo electric organ of young Lewis rats (acute and chronic phase) and mice (C57bl6); Passive transfer of anti-AChR Abs	Complement deficiency (C5) and complement inhibition (anti-C1q Ab, OmCI, anti-C5) have protective effect;

Table 1.5 Examples for disease associated with complement activation. Animal models and evidence for the role of complement in the disease pathology

Human disease	Models	Evidence for complement implication
Small vessel vasculitis: Cryoglobulinemic vasculitis (immune complex mediated)	-	CP activation; Complement consumption;
Henoch-Schönlein purpura/ IgA nephropathy	-	LP and AP activation; C3, properdin and MAC deposition in the mesangium;
Anti-neutrophil cytoplasmic autoantibody-associated vasculitis (autoimmune disease)	Passive transfer of anti-MPO antibody	C3 and MAC deposition in glomeruli; Complement deficiency and complement inhibition are protective
Asthma	Sensitisation with allergen (OVA, ragweed) in aluminium hydroxide followed by inhalation;	Elevated levels of C3a and C5a in bronchoalveolar lavage fluid; Complement deficiency (C3, C3aR, fB) and complement inhibition (anti-fB mAb, sCR1, futhan) has protective effect and blocked the inflammatory response and airway responsiveness to the allergen;
Atypical haemolytic uremic syndrome	fH deficient mice, with fH SCR1-15 transgenic	Association with “loss-of function” mutation in MCP, fH and fI and “gain of function” mutation in fB; mutation in C3;
Type II membranoproliferative glomerulonephritis (Dense Deposit Disease)	fH deficient mice	Deposition of C3 activation products within the glomerular basement membrane; Reduced circulating C3 levels due to complement consumption; Association with loss-of function mutation in factor H

Table 1.5 (continued) Examples for disease associated with complement activation. Animal models and evidence for the role of complement in the disease pathology

Human disease	Models	Evidence for complement implication
Macular degeneration	Laser-induced Choroidal neovascularization Chronic oxidative damage (model of dry AMD)	C3, C5 and MAC deposition in the retinal lesions; Association with fH polymorphism (Tyr402His); Deficiency in fD and fDprotective from visual loss;
Traumatic brain/spinal cord injury	Mice	Increased complement deposition (C1q, C4, fB, MAC) on neurons and oligodendrocytes; Complement deficiency (C4, C3, fB) and complement inhibition (CR1-Crry) has protective effect to injury;
Guillain-Barre syndrome	Passive immunisation with anti-ganglioside IgM Ab and normal human serum (mice)	Elevated levels of complement activation products in CSF; Complement deficiency (C6) and complement inhibition (sCR1) have protective effect to nerve injury;
Paroxysmal nocturnal haemoglobinuria	-	Complement-mediated intravascular haemolysis due to the lack of GPI anchored protein CD59 and CD55;

Table 1.5 (continued) Examples for disease associated with complement activation. Animal models and evidence for the role of complement in the disease pathology

and the presence of auto-reactive T cells in the affected organs. Complement plays a dual role in the development of autoimmunity. Uncontrolled or excessive complement activation contributes to the pathogenesis of many autoimmune diseases. For example immune complexes accumulate in glomeruli of patients with SLE and activate complement through the CP leading to tissue damage [195]. On the other hand, lack of early complement components facilitates the development of autoimmunity especially SLE [45, 196]. The late complement components have also been associated with the pathogenesis of autoimmune diseases. Increasingly, evidence implicates the terminal pathway as a disease mediator in rheumatoid arthritis and multiple sclerosis. It has been demonstrated that MAC contributes to joint destruction in arthritis and myelin loss in multiple sclerosis. Rheumatoid arthritis and multiple sclerosis will be discussed here.

1.4.2.2.1. Rheumatoid arthritis

Rheumatoid arthritis (RA) is a chronic inflammatory disease that affects mainly peripheral joints. Joint inflammation in RA is a complex process. Strong evidence from both animal and clinical studies demonstrates that complement contributes to the development of the disease [197-199]. RA is characterised by presence of autoantibodies to a variety of antigens such as collagen type II and glucose-6-phosphoisomerase [200]. These are able to form immune complexes within the joints and thus may activate the CP of complement. In addition, AP activation has been also reported in RA [198, 201-203]. It has been found that collagen type II, exposed during the course of disease can activate complement *in vitro* in absence of C4 [201]. Different studies have shown elevated levels of complement activation products in synovial fluids of RA patients [204, 205]. Once activated, complement releases C3a and C5a, causing local inflammation and triggers MAC formation resulting in joint destruction. Increased level of soluble MAC was found in synovial fluid of RA patients [197, 205]. The participation of the terminal pathway in RA was further investigated using animal models. Two models for inflammatory arthritis associated with the terminal complement pathway have been developed. These include collagen-induced arthritis (CIA) and antigen-induced arthritis (AIA). CIA, the most widely used model of arthritis, is induced in a limited number of susceptible inbred strains (DBA/1 and B10.RIII) by immunisation with collagen type II [206]. The disease progression is mediated by cellular and humoral

autoimmune response to the collagen challenge. Both T and B cells play a role in disease pathogenesis. During the early stages of disease, anti-collagen antibodies are generated and bind to the joint cartilage and thus activate complement. The role of complement was confirmed using complement deficient animals. For example C3 deficient mice and mice lacking factor B developed only mild arthritis [207, 208]. The relationship between the terminal pathway and arthritis was also assessed. DBA1 mice lacking C5 were resistant to CIA [209]. Furthermore, blocking C5 with anti-C5 antibody prevented disease onset and ameliorated already established disease [210]. In contrast to CIA, which is poly-articular inflammatory arthritis, in AIA the inflammation is localized in a single joint. When AIA was induced with methylated bovine serum albumin, CD59^{-/-} mice were found to have significantly greater joint swelling, tissue damage and MAC deposition compared to the wild type control mice [211].

Other models used to explore the role of complement in RA are listed in Table 1.5.

1.4.2.2.2. Multiple sclerosis

Multiple sclerosis (MS) is another example of a complex autoimmune disease where the terminal complement pathway contributes to the pathology. MS is a complex, T-cell mediated disease in which myelin and the myelin forming cells are targets. It starts with the formation of acute inflammatory lesions and breakdown of the blood-brain barrier (BBB). The complement system is another important contributor to the pathogenesis of MS, it was implicated in the killing of oligodendrocytes and neurons [212, 213]. Complement activation products such as C1q, C3d and C5b-9 have been detected in white matter lesions in patients with MS [214]. Activation of complement in MS occurs either by antibodies against myelin proteins found in MS patients [215], or directly by myelin and oligodendrocytes themselves [216, 217]. Once complement is activated it triggers MAC formation. MAC is possibly one of the demyelinating effectors in MS. Its assembly on myelin and oligodendrocytes and can induce myelin loss and cell death. Soluble C5b-9 was absent in human cerebrospinal fluid (CSF) from normal donors. However presence of soluble C5b-9 and decreased level of C9 were found in CSF of MS patients, suggestive for C9 consumption due to terminal pathway activation in the central nervous system [218-220]. Wing et al provided other evidence for

involvement of the terminal pathway in MS pathology. Incorporation of human CD59 in rat oligodendrocytes (lacking rat CD59) increased the cell survival when exposed to human complement [221]. The role of the terminal complement pathway in disease pathology was further explored in animal models of MS. Experimental autoimmune encephalomyelitis (EAE) is an acute model of MS used to evaluate the role in complement in MS. The disease is induced either by active immunization with proteins or peptides from the myelin sheath such as myelin oligodendrocyte glycoprotein (MOG), alone or in combination with anti-MOG demyelinating monoclonal antibodies (antibody dependent EAE, ADEAE) [222]. ADEAE induced in rats showed correlation between MAC deposition and spinal cord demyelination [223]. This observation was confirmed by using C6 and CD59 deficient animals [224, 225]. C6 deficient rats failed to develop demyelination and axonal injury after induction of ADEAE, whereas mice lacking the MAC regulator CD59 showed enhanced disease severity. Whereas, these findings demonstrate that the MAC acts as an effector in demyelination and axonal damage, other studies suggest that sublytic C5b-9 may also be beneficial and promote oligodendrocyte survival under certain circumstances [226, 227]. Sublytic dose of C5b-9 inhibited the mitochondrial pathway of apoptosis in oligodendrocytes and contributed to their regeneration [226-228]. The conclusion is therefore that complement plays both proinflammatory and neuroprotective roles in MS.

1.4.2.3. Cardiovascular disease

Complement is involved in the pathogenesis of various cardiovascular diseases including atherosclerosis, arterial aneurism and diabetic angiopathy [229, 230]. When the endothelium lining the luminal side of blood vessels loses its integrity (damage) complement activation occurs and destroys the target cells or promotes cell cycle activation and cell survival [231].

Atherosclerosis is a disease associated with endothelial dysfunction and plaque formation. Atherosclerotic lesions (atheroma) consist of cells, connective-tissue elements, lipids and debris [232, 233]. Plaque rupture and thrombosis take place as disease progresses. In atherosclerosis, complement activation via the AP can be provoked by enzymatic-modified low-density lipoprotein (LDL) [234-236]. In addition, immobilized immunoglobulins, pentraxins (CRP), cholesterol crystals and apoptotic cells can also trigger the complement

cascade in atherosclerotic lesions. Complement activation products and complement receptors have been detected in atherosclerotic lesions [237, 238]. For example C5b-9 was found on smooth muscle cells in early lesions while in advanced lesions it colocalised with apoptotic cells in human atherosclerotic lesions. In advanced lesions the C5b-9 was associated with intact macrophages and macrophage derived debris [239, 240]. As revealed from *in vivo* experiments complement plays a complex role in the disease development however it was clearly shown that terminal pathway plays a crucial role in this pathological process. Schmiedt and colleagues found that C6 deficient rabbits were protected from aortic lesion formation [241]. The role of complement and the terminal pathway in particular was evaluated using mice with targeted deletion of the gene for apolipoprotein E (ApoE^{-/-}). These animals develop severe hypercholesterolemia and atherosclerosis especially when the mice are fed on a high fat diet. The pathology was reversed when ApoE^{-/-} was crossed with C6^{-/-} mice. C6 deficiency significantly reduced plaque area and disease severity while the lack of CD59 had an opposite effect and exacerbated the disease [242]. This finding clearly demonstrates the association of the terminal pathway with the pathology in atherosclerosis. In contrast no difference was observed in disease development in presence or absence of C5 [243]. A different animal model was also developed and used to elucidate the role of complement in atherosclerosis. Mice deficient in LDL receptors were crossed with C1q deficient mice. In contrast to the terminal pathway, the early complement component C1q was found to be protective. C1q deficient mice had larger atherosclerotic plaques with more apoptotic cells compared to the wild type controls. This is likely due to inability of these mice efficiently to clear cell debris and immune complexes in the plaques.

1.4.2.4. Disease with genetically defined mutations of complement inhibitors and/or complement proteins

Complement-related diseases can also be triggered by alterations in the expression and function of complement components and regulators. This group of disorders includes membranoproliferative glomerulonephritis type II (MPGN type II), Atypical haemolytic uremic syndrome (aHUS), Paroxysmal nocturnal haemoglobinuria (PNH) and age-related macular degeneration (AMD). These diseases are examples of complement activity against self-tissues as a result of abnormal complement regulation.

1.4.2.4.1. Membranoproliferative glomerulonephritis type II

Membranoproliferative glomerulonephritis (MPGN) is characterised with proliferation of mesangial and endothelial cells and by thickening of the capillary walls due to immune or intramembranous dense deposits. Three types of MPGN have been described. Type I and III are immune complex mediated disease and type II has no association with immune complexes [244]. MPGN type II, also referred to as dense deposit disease (DDD), is a progressive renal disease often leading to kidney failure. It is characterised with low serum C3 levels, intramembranous dense deposits and C3b and MAC deposition in kidney glomeruli and in vascular walls. Over 80% of the patients are positive for autoantibodies, known as nephritic factors, able to prolong the half-life alternative pathway convertase and thus increase the complement activation. The abnormal complement activation is also accounted for by mutations in the gene encoding fH (the N terminus in particular) that impair the secretion or function of fH and influence the regulation of C3 in circulation [245-248]. The inability of fH to control C3 activation is likely to be a cause of MPGN type II.

1.4.2.4.2. Atypical haemolytic uraemic syndrome

The typical form of Haemolytic uraemic syndrome (HUS) is an epidemic disease that follows a gastrointestinal infection with particular strains of *E. coli*. However, in 5-10% of cases there is no associated *E. coli* infection and this is termed atypical HUS (aHUS). In aHUS the disease occurs in a familial pattern. In contrast to MPGN type II where C3 fragments are accumulated along the glomerular basement membrane, aHUS is characterised by endothelial cell injury and thrombosis leading to haemolytic anemia, thrombocytopenia and renal failure. aHUS is associated with mutation or polymorphisms in genes encoding complement regulators (factor H, factor I and CD46) and complement components (factor B and C3) leading to complement dysregulation [249-252]. The mutations in fH linked to aHUS are clustered at the carboxy-terminus of the protein and thus affect the binding of fH to heparin, C3b and endothelium but not the plasma C3 regulation [253-257]. This prevents overactivation but allows enough complement activity to attack target cells.

1.4.2.4.3. Paroxysmal nocturnal haemoglobinuria

Paroxysmal nocturnal haemoglobinuria (PNH) is an intravascular haemolytic anemia characterised by episodic haemoglobinuria, occurring predominantly at night [258, 259]. PNH is an acquired disease caused by a somatic mutation of the phosphatidylinositol glycan complementation class A (*PIGA*) gene in a hematopoietic stem cell and the expansion of the abnormal haematopoietic clone [260]. This mutation blocks the synthesis of GPI anchors in proteins including CD55 and CD59. Resultant red blood cells, leukocytes and platelets have thus a reduced ability to protect themselves against complement attack. The increased sensitivity to complement results in chronic haemolysis.

To conclude, complement mediates injury and causes diseases either by formation of lytic MAC or by the releasing of the anaphylatoxins C3a and C5a. The MAC may cause inappropriate cell lysis or may activate pro-inflammatory mechanisms to induce cell-activation and thus production of inflammatory chemokines. C3a and C5a induce damage by attracting and activating immune effector cells such as neutrophils, eosinophils and mast cells.

1.5. Anti-complement therapeutics

To prevent complement-mediated destruction of host cells and tissues, complement must be strictly controlled. As described above, despite the presence of a large number of complement regulatory proteins on cells and in fluids, complement may become inappropriately activated in the context of disease. For this reason complement is a promising therapeutic target. A number of anti-complement therapeutics have been developed and tested *in vitro* and *in vivo*.

1.5.1. Cobra Venom Factor

Cobra venom factor (CVF) was the first anti-complement reagent tested in models. It is a structural and functional analogue of C3b found in cobra venom. It binds factor B and forms

a stable AP C3 convertase (CVFBb). Compared to C3bBb the complex has an extended half-life, 7 hours compared to 1.5 minutes, and is resistant to fluid phase regulation [261]. When given to experimental animals, CVFBb continuously activates the AP and consumes all plasma C3. Such complement depletion *in vivo* was useful proof of principle to demonstrate that knocking out the complement system is relevant to many pathologies. However, its use as a long term therapeutic is limited because of its immunogenicity. To address this issue, the C-terminal region of human C3 was replaced with the corresponding region derived from CVF to generate chimeric CVF-like molecule. This “humanised CVF” was less immunogenic with reduced ability to generate neutralizing antibodies [262, 263]. Furthermore, “humanised CVF” with no C5 activating properties has been developed which prevents the release of the pro-inflammatory C5a anaphylatoxin. This reagent was shown to protect from complement-mediated myocardial IR injury in mice [264, 265].

1.5.2. Polyanionic agents

Polyanionic molecules such as low molecular weight heparin, dextran sulphate, polyvinyl sulphate, polylysine and suramin, have been shown to inhibit complement *in vitro* [266]. Heparin inhibits complement at various points including activation of the CP (by binding to C1q), assembly of the C3 convertase and the MAC [267-272]. *In vivo* low molecular weight heparin was used as an anti-coagulant in patients with shock syndromes and to coat extracorporeal circuits in dialysis and cardiopulmonary bypass. Part of its effect in such situations may be due to its properties as a complement inhibitor [273, 274], however its anti-complement capacity *in vivo* has not been fully studied.

1.5.3. Small molecule inhibitors

A number of natural or synthetic small molecules inhibit complement *in vitro* as well as *in vivo*. One such molecule is K-76COOH which blocks complement at the C5 stage and thus inhibiting disease in several complement dependent animal models [275]. Nafamostat mesilate (FUT-175) is an example of a synthetic protease inhibitor. It inhibits complement

by blocking C1r, C1s, fD and the Bb fragment of C3/C5 convertase [276]. Its anti-complement function has been demonstrated in a rat model of adjuvant arthritis [277]. Furthermore, FUT-175 in combination with K-76COOH prolonged graft survival in rats [278]. Other small molecule inhibitors are listed in table 1.6. Together with the advantages (low cost, good tissue penetration, oral administration) they have disadvantages. Usually these molecules are enzyme inhibitors, which have non-specific effects acting on all serine proteases rather than just those of the complement system. Their usage is also limited by their short half-life *in vivo* resulting in their rapid clearance from the body, making them unsuitable for long-term anti-complement therapy in chronic inflammatory conditions.

Molecule	Level of inhibition
K76COOH (K76) An organic acid	C5
FUT-175 (Furan) An organic compound	C1s fD C3/C5 convertases.
BCX-1470 An organic compound	fD C1s
Compstatin A cyclic peptide	C3 (prevents cleavage)
F-OpdChaWR A cyclic peptide	C5aR (antagonist)

Table 1.6 Small molecule anti-complement inhibitors.

1.5.4. Peptide inhibitors

A number of complement inhibitory peptides have been selected from phage display peptide libraries. It has been demonstrated that a peptide interacting with the IgG binding site within C1q inhibits the CP *in vitro* [279]. Another anti-complement peptide derived from a phage display library is compstatin. It was identified from a search for C3 binding peptides by

Sahu et al. [280]. The authors showed that this 13-amino acid cyclic peptide was able to bind C3 and to prevent the cleavage of C3 to C3a and C3b in reversible manner in human serum and in a pure protein system (AP). Other studies independently confirmed the complement inhibitory activity of compstatin on the CP and the AP [281]. Compstatin blocks exclusively human and primate C3 while no binding is observed in mice, rats, guinea pigs and rabbits [280, 282] and thus limiting its characterisation *in vivo*. However, the ability of compstatin to block C3 cleavage was demonstrated *ex vivo* in a model for potential pig to human xenotransplantation. The presence of this peptide significantly increased the survival time of pig kidneys perfused with human complement compared to the controls [283, 284].

Another promising peptide with complement inhibitory potential is C5aR antagonist (Ac-Phe-[Orn-Pro-dCha-Trp-dArg]) [285]. By blocking the binding of C5a to C5aR, this peptide blocked C5a-induced neutrophil chemotaxis and macrophage cytokine production *in vitro* and inhibited neutropenia associated with septic shock induced by lipopolysaccharide in rats [286, 287]. In addition, the C5aR antagonist peptide suppressed the reverse-passive Arthus reaction and endotoxin shock in rats [288, 289]. Its protective role was further proved in a model of intestinal IR injury [290]. The number of *in vivo* studies supporting the therapeutic effect of C5aR antagonist is currently increasing. Jacob et al. have successfully demonstrated that the treatment with the peptide blocks C5a/C5aR signaling while leaving the upstream complement protective events intact and thus decreasing the brain pathology in the MRL/*lpr* lupus mouse model [291].

1.5.5. Recombinant complement receptor 1

Anti-complement reagents based on naturally occurring complement regulators have been developed. Examples for such therapeutics and their application are given in table 1.7 and table 1.8.

Soluble complement receptor 1 (sCR1) was the first recombinant complement regulator developed for therapy. It consists of the extracellular domains of the naturally occurring membrane-associated regulator CR1 (Fig1.6A). sCR1 inhibits complement at C3 and C5 level.

Reagent	Moieties and linker	Expression system (host cells)	Mode of action	Anti-complement effect <i>in vitro</i>	Anti-complement effect <i>in vivo</i>
sCD59	rCD59 (no GPI)	Yeast (<i>Pichia pastoris</i>)	Inhibits MAC formation	Cell (erythrocytes) protection from complement mediated lysis;	NA
CD59-Crry	extracellular domain of rat CD59 (no GPI) linked to rCrry (SCRs1-5)	Yeast (<i>Pichia pastoris</i>)	Multiple hit: Inhibit MAC formation and inhibition of convertases by decay acceleration and cofactor activity	Cell (erythrocytes) protection from complement mediated lysis (greater than the one achieved by CD59)	NA
CR1g-Fc Long-lived	Mouse form: mCR1g (extracellular) linked to mIgG1 Human form: hCR1g mutated from phage display library (extracellular) linked to mIgG1	CHO	Inhibits the AP convertases by blocking substrate binding	Targets C3 fragments and protect cells from complement-mediated lysis;	Protective effect in intestinal IR injury; Protection in arthritis (CIA and CAIA); Modified human form-protective in K/BxN serum transfer mouse model of arthritis;
sCR1 (TP10)	hCR1 (SCRs1-30)	CHO	Decays the convertases (CP and AP) by decay acceleration and cofactor activity	Protects cells from complement-mediated lysis	Protection in models of IR injury: heart, skeletal muscle, intestine, liver; models of acute and chronic inflammatory disease: dermal vascular reaction, trauma, myasthenia gravis, glomerulonephritis, MS, allergic reactions, asthma; Clinical trials: reducing mortality in males on CBP;

Table 1.7 Summary of the recombinant soluble anti-complement reagents. Extracellular-extracellular domain; r-rat, m-mouse; h-human; NA-not assessed;

Reagent	Moieties and linker	Expression system (host cells)	Mode of action	Anti-complement effect <i>in vitro</i>	Anti-complement effect <i>in vivo</i>
OmCI Soft tick protein	Recombinant OmCI	Yeast (<i>Pichia methanolica</i>)	Inhibits C5 activation and MAC	Protects cells from human, mouse and rat complement mediated lysis	Protection in models of myasthenia gravis
CD59-Fc Long-lived	mCD59 linked to Fc of mIgG2a	CHO	Inhibits MAC formation	Protects cells from complement mediated damage;	Protection in mouse model of CNV
DAF-Fc Long-lived	rDAF(SCRs1-4) linked to Fc of hIgG1	CHO	Inhibits complement by decay accelerating activity;	Protects cells from complement mediated damage;	Protection in rat model of AIA;
Crry-Fc Long lived	rCrry(SCRs1-4) linked to Fc of rIgG2a mCrry(SCR1-5) linked to Fc of mIgG1	CHO NS/0	Inhibits the convertases by decay acceleration and cofactor activity	Cofactor activity; Protects cells from complement mediated damage; The mouse form inhibits C3 deposition on zymosan particles;	Protection in rat model of myasthenia gravis; Mouse form has protective effect in nephrotoxic nephritis, mesenteric IR and neurological improvement in traumatic brain injury;

Table 1.7 (continued) Summary of the recombinant soluble anti-complement reagents. Extracellular-extracellular domain; r-rat, m-mouse; h-human; NA-not assessed;

It accelerates the decay of the convertases and has cofactor activity for factor I mediated cleavage of C3b and C4b. sCR1 at nanomolar concentrations is able to inhibit complement *in vitro* and *in vivo*. Its ability to inhibit complement activation has been tested in a variety of animal models such as myocardial, skeletal muscle and intestinal I/R, graft rejection, myasthenia gravis, multiple sclerosis, glomerulonephritis and arthritis [185, 292-304]. Treatment with this reagent reduced the infarct size by 44% in a rat model of myocardial IR injury [185], reduced clinical severity, and also inhibited inflammation and blocked demyelination in a model of multiple sclerosis [300]. sCR1 has been shown to diminish C haemolytic activity in a model of glomerulonephritis and thus significantly reduce the morphological and functional consequences of disease pathology [302]. sCR1 (named TP-10) has been tested in phase I and II clinical trials for respiratory distress syndrome and in patients on cardiopulmonary bypass (CPB) [305, 306]. While 5mg/kg of sCR1 inhibits complement and reduces the mortality in males on bypass, no beneficial effect was found in female patients [307]. In another study, the use of sCR1 in lung transplantation reduced the number of patients requiring intubation and also decrease the time on ventilation and stay in intensive care [308].

sCR1 has been further modified and its half-life increased. Makrides and colleagues extended the half-life of sCR1 by adding an albumin binding site from streptococcal protein G to the C-terminus of the drug. The binding of sCR1 to albumin enabled the reagent to remain longer in the circulation and increased its half-life from 103 to 297 minutes [309]. A targeted CR1 reagent has also been developed. To target sCR1 to cells, Sialyl-lewis X (sLeX) tetrasaccharide groups have been attached to sCR1. These groups are present on neutrophils and bind P-, E- and L-selectins which are upregulated on endothelial surfaces during inflammation. In addition to its complement inhibitory function, the targeted therapeutic was more efficient in reducing neutrophil accumulation than the unmodified sCR1 in a rat model of lung injury [310, 311].

A second strategy has been applied to develop a highly potent membrane-targeted anti-complement therapeutic derived from CR1 known as APT070 (Fig.1.6A). Three N-terminal SCRs of sCR1 have been fused to a peptide containing positively charged amino acids to bind the phospholipid membrane and a terminal myristoyl group to insert into the membrane bilayer. This modification allowed the reagent to target a variety of cells [312].

Reagent	Moieties and linker	Expression system (host cells)	Target	Mode of action	Anti-complement effect <i>in vitro</i>	Anti-complement effect <i>in vivo</i>
Targeting using complement receptor						
CR2-CD59	hCR2 (SCRs1-4) linked to hCD59 (extracellular) via SS(GGGGS) ₃ or (GGGS) ₂ linker	CHO	iC3b and C3dg	Inhibits MAC formation	Inhibition of complement-mediated cell (CHO and erythrocytes) lysis	NA
CR2-DAF	hCR2 (SCRs1-4) linked to hDAF (SCRs1-4) via SS(GGGGS) ₃ or (GGGS) ₂ linker	CHO	iC3b and C3dg	Inactivates the convertases by decay acceleration	Inhibition of complement-mediated cell (CHO and erythrocytes) lysis	Targeting complement activation in SLE mouse models
CR2-Crry	mCR2 (SCRs1-4) linked to mCrry (SCRs 1-5) via (GGGS) ₂ linker	NSO	iC3b and C3dg	Inactivates the convertases by decay acceleration and cofactor activity	Targeting complement activation <i>ex vivo</i> (opsonised cells, FACS); Inhibition of complement-mediated cell (CHO) lysis;	Targeting complement activation in intestinal IR injury; Protection in intestinal IR injury; Improved the disease in CIA;
CR2-fH	mCR2 (SCRs1-4) linked to mfH(SCRs1-5) via (GGGS) ₂ linker	Freestyle 293 cell or CHO	iC3b and C3dg	Inactivates the AP convertases by decay acceleration and cofactor activity	Targeting C3 opsonised zymosan particles;	Disease reduction in CAIA; Protection in laser-induced choroidal neovascularisation and intestinal IR injury;

Table.1.8 Summary of the recombinant targeted anti-complement reagents. Extracellular-extracellular domain; r-rat, m-mouse; h-human; NA-not assessed

Reagent	Moieties and linker	Expression system (host cells)	Target	Mode of action	Anti-complement effect <i>in vitro</i>	Anti-complement effect <i>in vivo</i>
Targeting using antibody specificity						
IgG-DAF	1. Anti-dansyl Ab (m variable and h constant region) linked to hCD59 (extracellular) via SG ₄ SG ₄ SG ₄ S linker	TWS2 cells	Dansyl (Model system)	Inhibits the convertases by decay acceleration	Targeting and complement protection of dansyl-labeled CHO cells;	NA
IgG-CD59	1. Anti-dansyl Ab (m variable and h constant region) linked to hDAF (SCRs2-4) SG ₄ SG ₄ SG ₄ S linker	1. TWS2 cells	1. Dansyl (Model system)		1. Targeting and complement protection of dansyl-labeled CHO cells;	NA
	2. K9/9 scFv linked to rCD59 via GGGGS linker	2. <i>P. pastoris</i> (yeast)	2. Unidentified Ag on rat glomerular and proximal tubular epithelial cells	Inhibits MAC formation	2. Targeting and complement protection of rat proximal tubular epithelial cells;	2. Protection in rat model of puromycin-induced nephrosis;
IgG-Crry	K9/9 scFv linked to rCrry via GGGGS linker	<i>P. pastoris</i> (yeast)	Unidentified Ag on rat glomerular and proximal tubular epithelial cells	Inhibits the convertases by decay acceleration and cofactor activity	Targeting and complement protection of rat proximal tubule epithelial cells (PTEC);	Protection in rat model of puromycin-induced nephrosis;

Table.1.8 (continued) Summary of the recombinant targeted anti-complement reagents. Extracellular-extracellular domain; r-rat, m-mouse; h-human; NA-not assessed

Reagent	Moieties and linker	Expression system	Target	Mode of action	Anti-complement effect <i>in vitro</i>	Anti-complement effect <i>in vivo</i>
Targeting using membrane address tag						
CD59 Targeted	hCD59 with membrane address tag: N-(myristoyl) KSSKSPSKKKKKKPGDC-(S-2-thiopyridyl) C-amide (APT3146) rCD59 with N- (myristoyl)GSSKSPSKKKKKKPGDC-(S-2-thiopyridyl) C-amide (APT542)	<i>E. coli</i>	Cell membrane	Inhibits MAC formation	Protects erythrocyte from complement-mediated lysis; Human form protects PNH-erythrocytes from complement-mediated lysis;	Protection in rat model of AIA;
CR1 Targeted	1. sCR1 glycosylated with SLe ^x (TP20) 2. ATP070 (hCR1 SCR 1-3) with membrane address tag	1. CHO producing enzyme that incorporates sialylated and fucosylated tetrasaccharide sialyl Lewis 2. <i>E.coli</i>	1.E- and P-selectin 2.Membrane targeting	1.Decays the convertases (CP and AP) by decay acceleration and cofactor activity; 2.Decays the convertases (CP and AP) by decay acceleration and cofactor activity;	1. Binds cell expressing E-selectin; Protect cells from complement mediated lysis; Inhibition of neutrophil recruitment and activation; 2. Binds variety of cells;	1. Protection in various preclinical models: mouse stroke, rat lung injury, rat lung allograft, rat myocardial IR; 2. Protection in a model of anti-basement membrane disease; protective effect in kidney transplantation models and AIA;
Crry Targeted	Rat Crry (SCRs1-4) GSGGGSGC-linker Membrane address tag (APT542)	<i>E. coli</i>	Cell membrane	Inhibits the convertases by decay acceleration and cofactor activity	Targeting and complement protection of erythrocytes;	NA

Table.1.8 (continued) Summary of the recombinant targeted anti-complement reagents. Extracellular-extracellular domain; r-rat, m-mouse; h-human; NA-not assessed

APT070 has demonstrated highly protective effect in rat models of vascular shock, kidney I/R and in AIA [313, 314]. It has also shown neuroprotective effect by preventing MAC formation in a model of Miller-Fisher syndrome [315].

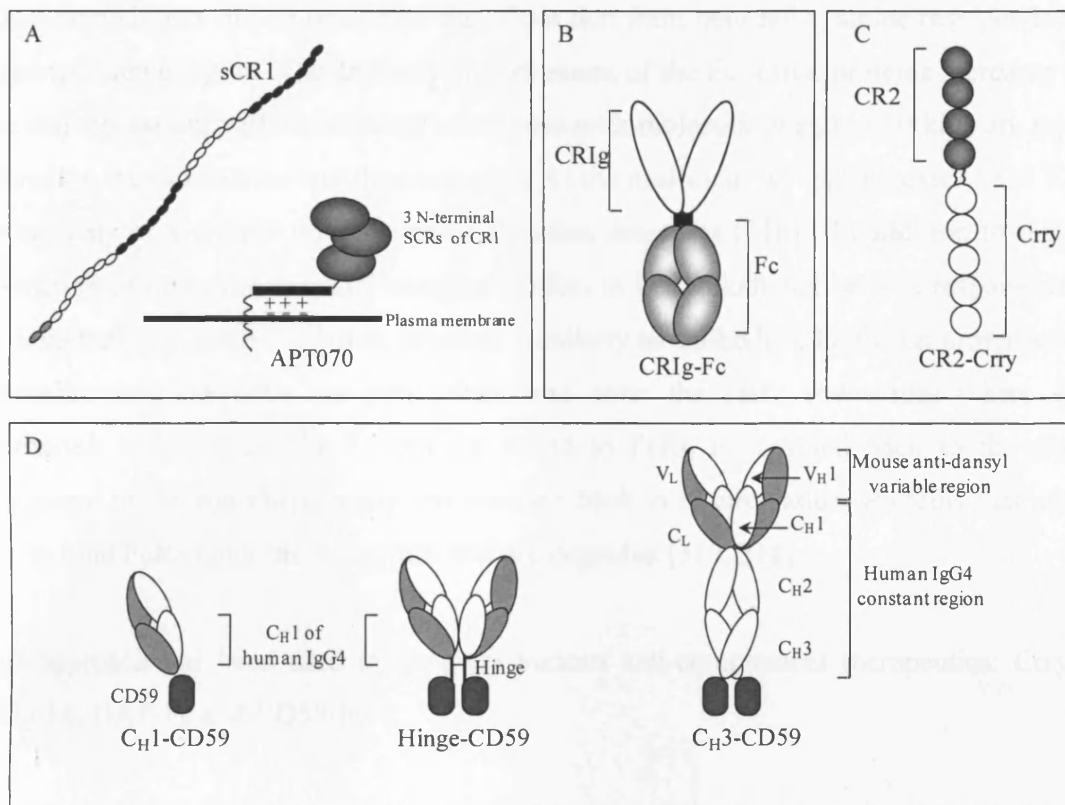


Fig. 1.6. Diagrammatic representation of recombinant anti-complement reagents. A. *sCR1* and *APT070* are reagents based on *CR1*. *sCR1* contains the extracellular domain of *CR1*. *APT070* is composed of three N-terminal SCRs of *CR1* linked to a charged peptide (that binds to the membrane) and a myristoyl tag (which inserts the membrane). B. *CRIg-Fc* is long-lived reagent, composed of the extracellular domain of *CRIg* linked to *Fc* of an antibody. C. The four N-terminal SCRs of *CR2* are linked to the extracellular domain of *Crry* to generate targeted reagent *CR2-Crry*. D. *IgG-CD59* fusion proteins. The extracellular domain of human *CD59* was joined to an antibody at the end of *C_H1*, the hinge or after the entire human *IgG4* constant region. Each construct contains human *IgG* constant region joined to a mouse anti-dansyl variable region.

1.5.6. Complement regulator-Fc fusion proteins

A common strategy employed to increase the half-life of therapeutics is the generation of Fc fusion proteins. The biologically active molecule is attached to Fc domain of antibody. When expressed in mammalian cells the fusion proteins are often secreted as disulfide-linked homodimers due to interchain disulfides that form between cysteine residues located in the IgG hinge region. The antibody-like structure of the Fc fusion proteins increases their size and circulating half-lives. Small molecules with molecular weight <30 kDa are rapidly filtered by the glomerulus and then excreted. As the molecular weight increases (>30 kDa), the capacity of a protein for glomerular filtration decreases [316]. In addition to that, the interaction of Fc to the neonatal receptor (FcRn) in the endothelial cells is responsible for the long half-life of the Fc-fusion proteins. Similarly to antibodies, Fc fusion proteins could internalise into the cells via pinocytosis and enter the early endosomes where FcRn expression is localised. The Fc protein bound to FcRn is recycled back to the plasma membrane of the endothelial cells and released back in to circulation. Proteins that are not able to bind FcRn enter the lysosomes and are degraded [317, 318].

This approach has been used to generate various anti-complement therapeutics: Crry-Fc, CRIg-Fc, DAF-Fc and CD59-Fc.

1.5.6.1. Crry-Fc

A mouse Crry-Fc fusion protein has been generated by linking the major rodent complement regulator Crry to Fc of mouse IgG1 [319]. The therapeutic has been shown to have a half-life of 40 hours. The authors demonstrated that treatment with Crry-Fc inhibited complement in vivo and reduced renal injury in a mouse model of glomerulonephritis [319]. The protective effect of mouse Crry-Fc has been further demonstrated in other animal models such as intestinal IR injury [320], antiphospholipid antibody-induced fetal loss [321], SLE [322], and traumatic brain injury [323]. Recently, our group generated a rat Crry-Ig containing the Fc of rat IgG2a [324]. The therapeutic has been found to abrogate disease in a rat model of myasthenia gravis.

1.5.6.2. CRIg-Fc

The extracellular domain of human complement receptor/regulator, CRIg, has been attached to the Fc portion of mouse IgG1 to generate a CRIg-Fc fusion protein (Fig.1.6B) [161]. CRIg-Fc has been tested in collagen- and antibody-induced models of arthritis. Treatment with this reagent reversed inflammation and bone loss by inhibiting the AP of complement in the joint [167]. Mutant CRIg-Fc with increased C3b binding capacity has recently been created and showed greater therapeutic efficacy compared to the wild type fusion protein when tested in a K/BxN serum transfer model of arthritis [325]. The therapeutic effect of mouse CRIg-Fc has also been studied in a mouse model of intestinal IR injury [326]. It was demonstrated that the treatment with CRIg fusion prior to surgery reduced C3 deposition and cell infiltration and prevented local and remote tissue injury (damage of distant organs).

1.5.6.3. DAF-Fc

A rat DAF-Fc fusion protein has been generated by linking the four SCRs of DAF to human Fc. This reagent has prolonged half-life. It has been found to inhibit the disease in a rat model of AIA [327].

1.5.6.4. CD59-Fc

A mouse CD59-Fc protein has been developed by joining a mouse terminal pathway inhibitor CD59a with the Fc portion of mouse IgG2a. Bora and colleagues have examined the impact of this reagent on disease pathology in a mouse model of choroidal neovascularisation (CNV, laser-induced mouse retinal degeneration model) where the administration of the agent 24 hours before the laser intervention inhibited the development of CNV [328].

1.5.7. Complement regulator-complement receptor fusion proteins

Therapeutic targeting as defined by Smith “implies a relatively selective delivery of a pharmacologically active agent to a disease site, which increases the therapeutic ratio of that agent” [329].

Complement regulators have been targeted to the sites of complement activation by joining them with a complement receptor and thus providing an effective local concentration of the drug with low levels of systemic inhibition. The use of such fusion proteins has been shown to reduce susceptibility to infections due to systemic complement inhibition especially in a long-term treatment of chronic diseases. Various CR2-Complement receptors fusion proteins have been developed (CR2-DAF, CR2-CD59, CR2-Crry and CR2-fH) [330-332]. CR2 is a complement receptor that binds iC3b and C3dg deposited at sites of complement activation.

1.5.7.1. CR2-DAF

Song and co-workers linked the four N-terminal SCRs of human CR2 to the N- or C-terminus of the extracellular domain of human complement inhibitor DAF [330]. *In vitro* studies demonstrated that the fusion protein containing CR2 linked to the N-terminus of DAF bound C3dg with a higher affinity than the fusion protein with CR2 at the C-terminus. This orientation was also found to be more effective in terms of complement inhibition *in vitro*. CR2-DAF at concentration of 18nM was able to provide 50% protection to CHO cells from complement-mediated killing while 74 nM DAF-CR2 was required to achieve the same effect. CR2-DAF was taken further into *in vivo* studies. The authors showed that human CR2-DAF targeted to sites of C activation *in vivo* reduced the clinical score in a mouse model of lupus nephritis [330].

1.5.7.2. CR2-CD59

Human CR2-CD59 fusion proteins have been generated. Similarly to CR2-DAF described above, the four N-terminal SCRs of human CR2 were attached to the N- or C-terminus of

the extracellular domain of human CD59. The targeted CD59 and the N-terminal CD59 in particular was significantly more effective than the nontargeted CD59 in protecting erythrocytes and CHO cells from complement mediated lysis *in vitro* [330].

1.5.7.3. CR2-Crry

To target the major rodent complement inhibitor, Crry, to the sites of complement activation, the extracellular domain of the mouse regulator was linked to the four N-terminal SCRs of mouse CR2 (Fig.1.6C) [331]. CR2-Crry has been successfully targeted to the sites of local and remote complement activation following intestinal IR injury. Significantly lower dose of CR2-Crry was required to achieve equivalent protection compared to non-targeted, long-lived Crry-Ig. In a different *in vivo* study, CR2-Crry improved the neurological recovery and reduced pathology in murine ischaemic stroke and spinal cord injury to a level to that seen in C3 deficient animals [333]. Complement inhibition with CR2-Crry was protective in a model of hepatic IR injury [334]. Conversely, complement inhibition and more precisely blocking production of C3a-des-Arg (acylation-stimulating protein [ASP]) had a negative effect on the liver regeneration in the context of massive liver resection (procedure for removing primary and secondary liver tumors). In a combined model of hepatic IR injury and partial hepatectomy (liver resection), a high dose of CR2-Crry resulted in steatosis, severe hepatic injury and mortality, whereas a low dose of the reagent was found to be protective and improved liver regeneration compared to the control groups [334]. In other words, complement plays a dual role in health and disease. Therefore a balance between complement activation and inhibition has to be considered when developing therapeutic strategies.

1.5.7.4. CR2-fH

Factor H-targeted reagents CR2-fH and CR2-fHfH have been generated by joining mouse CR2 with one or two repeats of the first five N-terminal SCRs of mouse fH [332]. The SCRs 1-4 contain the AP inhibitory activity. It was demonstrated that CR2-fH targeted the site of injury and reduced tissue C3 deposition in the intestine [332]. Both CR2-fH and CR2-fHfH

protected from local intestinal and remote (distant) lung injury in a mouse model of intestinal IR injury. Effective targeting and AP inhibition has been also observed in animal model of CIA [335]. The capacity of CR2-fH to target complement activation has also been demonstrated in a model of CNV [336]. Even delayed treatment after injury provided protection and effectively reduced the choroidal neovascularization in mice [336].

1.5.8. Antibody targeting

Fab arms of antibodies have been used to generate anti-complement therapeutics, which target to different sites. This is a targeting strategy that utilizes the antigenic specificity of monoclonal antibodies to deliver anti-complement protection to specific cells. Such reagents were generated by linking complement inhibitors such as CD59, DAF and Crry to the C-terminus of an antibody recognizing specific cell surface antigens.

1.5.8.1. IgG-CD59

An antibody-targeted CD59 reagent has been generated by linking antibody fragments specific for the hapten 5-dimethylaminonaphthalene-t-sulfonyl (dansyl) to CD59 functional unit (Fig.1.6D) [337]. Using a model system, Zhang and co-workers demonstrated that this reagent successfully targeted dansyl-labeled CHO cells and inhibited complement-mediated lysis. More effective protection was achieved when small antibody fragments comprising just the first antibody constant region (CH1) were used [337] (Fig.1.6D). This indicates that CD59 must be close to the cell surface for effective function.

1.5.8.2. IgG-DAF

The approach used for generating IgG-CD59 has also been applied to target DAF to a surface [338]. SCRs 2-4 of human DAF were used. The IgG-DAF proteins targeted dansylated CHO cells and were able to inhibit complement deposition and cell lysis *in vitro*. This experiment revealed that the construct containing only the CH1 region was the most effective at inhibiting complement deposition, presumably due to spacing from the target

membrane [338]. Spitzer et al have used similar targeting strategy to generate a human DAF (SCRs1-4) reagent that bound specifically to mouse red blood cells and showed its protective effect from complement mediated killing *in vitro* and *in vivo* [339].

1.5.8.3. IgG-Crry

These *in vitro* studies using IgG-CD59 and IgG-DAF have demonstrated the feasibility of the antibody targeted approach to complement inhibition [337, 338]. The same strategy has also been employed for rat Crry [340]. To target the complement inhibitor to the kidney, the extracellular domain of rat Crry was linked to a single chain variable region of antibody specific for an unidentified antigen on rat glomerular and proximal tubular epithelial cell. The reagent, termed tCrry, has been tested in rat model of experimental nephritic syndrome [340]. The administration of tCrry resulted in reduction of tubulointerstitial injury, complement deposition and enhancement in the renal function when compared to the nontargeted Crry.

1.5.9. Blocking antibodies

Many monoclonal antibodies (mAbs) are now in clinical use. The first mAb approved for human use was a murine anti-CD3 mAb, used for the treatment of organ transplant rejection [341]. However, it became evident that murine mAbs have a short half-life, high immunogenicity and suboptimal effector functions when used in humans. To overcome these limitations, mouse mAbs have been engineered to generate chimeric and humanized antibodies [342-344]. The former contains the variable regions of a mouse antibody and the constant regions of a human antibody, while in a humanized mAb, only the complementarity determining regions (CDRs) are of a murine origin. Fully human mAb have been generated by phage display [345]. An alternative approach is the use of human immunoglobulin transgenic mice to generate human antibodies [346]. Monoclonal antibodies against complement have been generated and have emerged as promising therapies.

1.5.9.1. Anti-C5

The terminal pathway and MAC formation have been implicated in pathology of many diseases such as MS, RA and PNH. Neutralizing C5 will inhibit the terminal pathway without interfering with other crucial complement functions such as opsonisation. Inhibition of complement at C5 level in the context of clinical complications can be achieved by using specific anti-C5 antibodies.

Monoclonal antibodies to mouse, rat and human C5 which inhibit C5a generation and membrane attack complex formation have been developed. The efficiency of this has been proved in a number of animal models of diseases where complement is implicated in the pathology. Furthermore, two antibody-based therapeutics have been developed for use in humans and have reached the clinic.

Different research groups have developed anti-C5 mAbs that block complement [347, 348]. The mouse anti-C5 monoclonal antibody (BB5.1) prevents cleavage of C5 *in vitro* and *in vivo* and effectively abrogates disease or tissue damage in a wide range of animal models including nephritis, CIA and myocardial IR injury [210, 348]. Girardi and co-workers studied the effect of C5 inhibition in a murine model of anti-phospholipid syndrome [349]. The researchers found that pre-treatment with anti-C5 antibody is protective against pregnancy loss. BB5.1 administration has improved the function of the lower airways and ameliorated intrapulmonary inflammation in an asthma model [350]. In a murine model of CIA, anti-C5 therapy delays the onset of disease and ameliorates established disease [210].

The C5 blocking capacity of various single chain anti-human C5 antibodies has been demonstrated in preclinical studies. Anti-human C5 scFv clone N19-8 has been shown to prevent C5b-9 deposition in mouse hearts perfused with human plasma [351]. An anti-C5 scFv: TS-A12/22 (reacting with the α -chain of C5 at the C5 convertase cleavage site and inhibits C5 lytic activity and C5a release) and TS-A8 (inhibiting only the C5 lytic activity) have been isolated from a human phage display library [352, 353]. Administration of these two anti-C5 scFv reduced joint swelling, cell count and TNF α levels in synovial lavage fluid in a model of antigen-induced arthritis in rats [352, 353].

Two different human-specific reagents based on mouse anti-C5 antibody (h51.1) have been created [354] and tested in clinical trials. These are humanized monoclonal antibody (Eculizumab, Soliris®, Alexion Pharmaceuticals) and its single chain version (scFv) lacking the constant region (Pexelizumab, Alexion Pharmaceuticals).

The scFv humanized fragment of the murine antibody, Pexelizumab is short-lived reagent and has good tissue penetration. Pexelizumab has been shown to prevent C-mediated myocardial damage during myocardial IR injury and currently two large clinical trials are underway in patients with acute myocardial infarction and undergoing coronary artery bypass surgery [355]. Administration of Pexelizumab reduces total C activity, soluble C5b-9 formation and leukocyte activation in a human phase I trial with patients undergoing coronary artery bypass grafting requiring CPB. It has a beneficial effect on inflammatory markers, myocardial infarction rate and postoperative death rates [356]. The benefit of Pexelizumab on adverse clinical outcomes has been further confirmed in a phase II study in cardiac surgery patients [357]. Moreover, a phase III double-blinded, placebo-controlled study confirmed the impact of Pexelizumab on infarct and mortality reduction in cardiac artery bypass grafting surgery [358-360].

The second humanized anti-C5 reagent, Soliris® is suitable for treatment of chronic diseases and is now approved for treatment of patients with PNH. Its effect has been initially evaluated in a pilot trial for PNH [361]. The effect of the antibody treatment has been measured by a reduction in serum lactate dehydrogenase levels. Blocking C5 using Soliris® has inhibited haemolysis and thus prevented the transfusion requirements of PNH patients. Because of patient improvement, the study has been extended [362]. The efficacy of Soliris® in treatment of PNH has been further confirmed in a double-blind, randomized, placebo-controlled phase III clinical trial [363, 364]. Currently Soliris® is the only treatment for this disease that reduces haemolysis. The use of Soliris® in other diseases is under investigation. Clinical trials are initiated to evaluate the therapeutic effect of Soliris® in aHUS, DDD, kidney transplantation, myasthenia gravis, anti-phospholipid syndrome and other neurological and haematological disorders.

1.5.10. Recombinant CD59

An alternative strategy for blocking the self-destructive capacity of complement whilst leaving the early key complement functions intact, is the use of the terminal pathway regulator CD59. Soluble recombinant CD59, consisting the extracellular domain of the inhibitor, is itself a poor inhibitor of complement in whole serum because of its small size (12kDa) and rapid clearance from the circulation in the kidney. However, generation of forms with long half-life or targeted reagents has meant that this complement regulator has become a potential therapeutic. Membrane targeting of recombinant CD59, using the same lipid targeting peptide as discussed for CR1/APT070, has improved the specific activity to the level of the native protein [365]. Fraser and colleagues demonstrated that membrane targeted CD59 blocked MAC deposition in joints and markedly suppressed disease in a rat model of AIA. This targeting strategy has been applied to human CD59 [366]. The targeted human CD59 bound to PNH erythrocytes *in vitro* and restored CD59 levels to those of normal erythrocytes. Furthermore, these CD59-‘coated’ PNH erythrocytes were protected from complement-mediated lysis when transfused into CD1 mice.

As discussed in section 1.5.8.1, CD59 has been targeted to different cell types by fusion of the protein with a cell-specific antibody or antibody fragment. The rapid clearance of soluble CD59 *in vivo* was overcome by generation of CD59-Fc fusion proteins as explained previously in section 1.5.6.4. Mouse CD59a fused to the Fc of mouse IgG2a generated a reagent that inhibited the development of choroidal angiogenesis in a mouse model of CNV [328]. The deposition of MAC was prevented as well as MAC-mediated release of angiogenic growth factors such as VEGF, β -FGF and TGF- β 2.

1.5.11. Recombinant OmCI

The soft tick lipocalin OmCI, also known as rEV576, was introduced in 1.4.1. Its low immunogenicity and the ability to block MAC formation and C5a release, similarly to the therapeutic anti-C5 antibody described above, suggests that OmCI could be a powerful therapeutic in disease mediated by complement activation. This was proved *in vivo* by us and others. OmCI was able to protect rats from clinical signs of disease in passive and active

models of myasthenia gravis (the models are explained in table 1.5) [176, 367]. A marked reduction in C3 and C9/MAC deposition at the neuromuscular junction and a significant decrease in cellular infiltrate was observed in the animals that received OmCI compared to control rats [176]. Therefore the OmCI-based anti-complement therapy offers a powerful approach for preventing complement-mediated damage in disease. However the usage of OmCI as a therapeutic is limited due to its short half-life of few minutes. Given to experimental C5 sufficient animals, OmCI circulates in complex with C5, however the free OmCI was rapidly cleared in absence of C5 [176]. Thus extending the half-life of OmCI would be rewarding and such long-living inhibitor would be a potent drug, an alternative to anti-C5 antibody treatment, for complement-associated diseases.

1.5.12. Optimal target for complement inhibition

As discussed in this chapter, blocking complement is beneficial in a variety of diseases. However as a part of immune system, complement provides resistance towards infectious agents, eliminates IC and dying cells and helps the development of optimal adaptive immune response, events crucial for maintain the health of a living organism. Each of these important complement functions might be affected with chronic complement inhibition. Evidence for this was provided by findings in humans and experimental animals with complement deficiency. For example, patients and animals lacking early complement components are unable to efficiently process apoptotic cells and immune complexes and prone to develop autoimmune disease [196, 368, 369]. C1q and MBL were shown to bind directly to apoptotic blebs resulting in their opsonisation via the activation of C4 and C3. Deficiencies in C1q, C2 and C4 in humans are associated with SLE. The absence of C1q in mice results in apoptotic bodies and immune deposits accumulation in the glomeruli and the animals develop glomerulonephritis. Furthermore deficiency in C1 and C4, affects the uptake of apoptotic bodies by macrophages [45]. Another key complement component for maintenance of the body homeostasis is C3. C3 bind covalently to IC and thus allowing their solubilisation (transforming big complexes in to small) and transport via the erythrocytes to the liver and spleen for removal by phagocytes. C3b deposited on the pathogens surface facilitates their removal by phagocytosis and clearance.

In contrast to the deficiency in the activation pathways, deficiency or inhibiting complement at later stages does not alter IC clearance or humoral immunity but only results in increase susceptibility to gram-negative bacteria and *Neisseria meningitidis* in particular. However *Neisseria* infection is not a major issue since the bacterium is susceptible to antibiotic treatment. Vaccination against this pathogen is another option to prevent the infection.

1.6. Project Aims

The conclusion therefore is that complement is a host defence system that plays an important role in both innate and adaptive immunity. Besides its beneficial effect in health, complement has a destructive role in various pathological conditions where complement dysregulation can cause tissue damage. In such disorders, complement activation via one of the three activation pathways, occurs leading to the generation of MAC, which can result in tissue damage and cell activation. Therapeutic intervention of complement in the context of disease has aroused enormous interest. Many anti-complement reagents and approaches have been developed and some of them translated into the clinic. Previous research findings revealed the importance to balance the benefit from inhibiting the complement system with potential side effects, such as increased susceptibility to gram-negative bacteria and autoimmune disease caused by poor clearance of IC and cell debris. To avoid complications, only the self-destroying power of the complement should be turned off while leaving untouched crucial function such as opsonisation of pathogens and clearance of immune complexes. This makes the terminal pathway a valuable location for therapeutic intervention.

Therefore, this research effort is to develop anti-complement therapy that does not simply turn the complement off, but modulates its activity. The overall aim of this project is to generate targeted and soluble long-lived reagents which specifically block terminal pathway activity at the level of MAC assembly or C5 activation respectively. The specific aims for this study are:

1.6.1. To generate the optimal targeted CD59-CRIg reagent.

The major side effect of anti-complement therapeutics is the systemic action many of the reagents have on complement and leaving an individual susceptible to infection. This was addressed by developing targeted anti-complement reagents. For example targeted CR2-Crry reagent did not affect the susceptibility of the experimental animals to infections, while the animals that received the non-targeted version, Crry-Fc, lost their pathogen resistance due to inefficient bacterial clearance [331].

A similar approach is applied here to target the terminal pathway inhibitor CD59 to the site of pathology. As noted earlier in this chapter, sCD59 is a poor complement inhibitor in whole serum, probably due to interactions with serum proteins. *In vivo*, sCD59 because of its small size is efficiently cleared by filtration in the kidney, thus targeting CD59 to sites of complement activation and disease is very likely to improve its efficacy. Furthermore the targeting CD59 may reduce the side effect of complement inhibition such as infections with *Neisseria*, particularly in long-term complement suppression. An accurate delivery of CD59 will be achieved by linking the extracellular domain of mouse CD59 to the extracellular region of the mouse complement inhibitor CR1g. CD59-CR1g chimeric molecule is likely to provide good protection to host cells attacked by complement. Targeted human CR2-CD59 reagent has been already developed but its function has been little explored *in vivo*. CR2 binds C3 degradation products iC3b, C3dg and C3d. CR1g binds iC3b and it also interacts with C3b. The advantage of CR1g over CR2 as targeting molecule is that binding of CR1g to the first C3 activation fragment C3b is very likely to provide cell protection earlier in time than CR2 targeted reagents. C3b deposited on cell surface is converted to iC3b (both molecules binds CR1g) by complement regulators. However, in diseases associated with complement dysregulation and absence of complement regulators, the generation of C3 breakdown products iC3b and C3dg will be affected and thus leaving C3b a main target for C3 targeted therapeutics. In such situations CR1g is likely to provide more efficient targeting than CR2.

It has been shown that the orientation of CD59 towards the cell membrane and the other counterpart of the chimeric molecule is of a high importance for the function of the reagent. Such an orientation, in which CD59 is placed close to the membrane has been found beneficial for the activity of CD59 present in chimeric proteins containing DAF or antibody

portion [337, 370]. Another example emphasising the impact of the orientation on the protein function was given by Song et al, where the authors demonstrated that CD59 and DAF linked to the C-terminus of CR2 provided better cell protection [330]. Here CD59-CRIg fusion proteins in a different orientation are generated and their functions are analysed and compared.

To enhance targeting potential, dimeric forms of CD59-CRIg reagents are generated which incorporate an antibody hinge to link the two moieties and promote dimerisation. To the best of my knowledge, the use of antibody hinge to create dimeric forms of reagents targeting complement activation is a novel approach for improving drug efficiency.

1.6.2. To generate a long-lived soluble anti-C5 drug: OmCI-Fc.

C5 is another promising target when blocking the terminal pathway. C5 neutralizing mAbs have been developed and shown their therapeutic effect in preclinical and clinical studies. Moreover anti-C5 mAb is used as a therapy in PNH. Another molecule able to block C5 activation is OmCI. Similarly to anti-C5 mAb, OmCI prevents MAC formation and the release of C5a anaphylatoxin.

As discussed in this Chapter, OmCI is able block the activity of C5 from various species including human, mouse and rat. For this reason the anti-complement effect of OmCI can be validated in preclinical models. The protective role of OmCI was already demonstrated *in vivo*. However, as a small molecule, OmCI is rapidly cleared from the circulation, which necessitates frequent administration and thus limits its clinical utility. To address this issue OmCI is ligated to Fc portion of IgG molecule. The construction of Fc chimeric proteins has been shown to improve pharmacokinetics of therapeutic agents including anti-complement drugs.

1.6.3. To study the capacity of these therapeutics to inhibit complement *in vitro*.

One of the objectives of this study is to assess the ability of CD59-CRIg fusion proteins to target complement activation and protect the target cells from complement-mediated killing. Based on this result, the optimal reagent will be selected and taken for *in vivo* analysis.

Insertion of the Fc fragment could cause conformational change and render the OmCI functionally inactive. To assess this, the complement inhibitory activity of OmCI-Fc is first analysed *in vitro* and compared to OmCI.

1.6.4. To test the therapeutic value of the reagents *ex vivo* and *in vivo* in mice.

Reagents shown to be effective *in vitro*, will be tested for their ability to target complement activation *ex vivo* and *in vivo*.

It is expected that the reagents generated in this project will have the potential to deliver substantial therapeutic benefit and offer a very attractive option for treatment of complement-mediated disease. When humanized, these anti-complement agents may provide a medical solution for patients who have not responded to other treatments. I believe that the results revealed in this study will have implications for improvements in drug design and therapeutic approaches.

Chapter 2. Materials and methods

This chapter will focus on the research methods to be used within the proposed study.

Unless otherwise stated all chemicals were from Sigma Chemical Company or Fisher Scientific UK Ltd.

2.1. Preparation of plasmids encoding the anti-complement therapeutics-molecular biology

The RNA preparation was carried out using diethylpyrocarbonate treated tips and tubes. The DNA manipulations were performed using autoclaved plasticware and solutions.

2.1.1. Solutions

Table 2.1

Solution	Contents
TAE	40mM Tris, 40mM acetic acid, 1mM EDTA pH 7.2
Agarose gel loading buffer	20% glycerol (v/v) in 10x TAE with bromphenol blue
Lauria-Bertani (LB) broth	1% tryptone (w/v), 1%NaCl (w/v), 0.5% (w/v) yeast extract in water
SOC	2% tryptone (w/v), 0.5%yeast extract (w/v), 0.05% NaCl (w/v), 2.5mM KCl, 10mM MgCl ₂ and 20mM glucose

2.1.2. RNA preparation

Mouse liver (BalbC) was harvested and RNA was isolated using GenElute™ Mammalian Total RNA Purification Kit (Sigma) according to the manufacturer's protocol. In brief, the liver was homogenised in guanidine thiocyanate and 2-mercaptoethanol to release RNA and inactivate RNase. The homogenate was spun through a filtration column to remove cellular debris and shear DNA. The filtrate was applied to a silica column to bind RNA, followed

by washing and elution. The concentration of the purified RNA was determined by measuring the absorbance 260nm.

2.1.3. Reverse transcriptase PCR (RT PCR)

cDNA was prepared from the RNA isolated from mouse liver using TaqMan Reverse Transcription reagents (Applied Biosystems, Warrington, UK).

The reaction consisted of:

0.5µg RNA

0.5µl random hexamers

1µl 10xRT buffer

2.2µl 25mM MgCl₂

2µl dNTPs

0.2µl RNase inhibitor

0.25µl Reverse Transcriptase Multiscribe

RNase free water to take the reaction to volume to 10µl

The reaction mix was incubated as follows:

25°C for 10 minutes (to allow the primers to anneal)

42°C for 45 minutes (to extend the DNA)

95°C for 5 minutes (to denature the enzyme)

cDNA was stored at -20°C.

2.1.4. PCR

PCR was used to amplify DNA to be cloned into a vector or to screen bacterial colonies containing plasmids encoding protein of interest. The primers used for amplification,

screening and sequencing were purchased from Invitrogen Life Technologies. The primers were reconstituted using dH₂O to obtain a concentration of 100pmol/μl.

PCR was performed to generate DNA encoding OmCI and the extracellular domains of murine CR1g and CD59 for cloning.

The reaction contained:

100ng template DNA (2μl)

15pmol forward primer (1μl)

15pmol reverse primer (1μl)

1X Platinum ® Blue PCR SuperMix (Invitrogen life technologies) (21μl)

Platinum ® Blue PCR SuperMix contains recombinant *Taq* DNA polymerase, Platinum ® anti- *Taq* DNA polymerase antibody, Mg²⁺, dNTPs, glycerol and blue tracking dye. Platinum® Blue PCR SuperMix is supplied at 1.1x concentration to allow approximately 10% of the final reaction volume to be used for the addition of primer and template solutions.

PCR steps:

1. 94°C-4 minutes (Specific binding of the anti-*Taq* antibody inhibits polymerase activity at room temperature. Activity was restored after this denaturation step)
2. 94°C-30 seconds (Denaturation)
3. 58-65°C-45 seconds (Annealing; temperature dependent upon melting temperature of the primers)
4. 72°C -1.30 minutes (Elongation; times may vary depending on the size of the PCR product, 1 minute per kb)
5. 72°C -15 minutes (Final extension)

Steps from 2 to 4 formed 1 PCR cycle. Each PCR consisted 30 cycles.

2.1.5. Screening PCR (see also Bacterial screening)

For screening PCR, BioMix™ Red (Bioline) was used. BioMix™ Red is a 2x reaction mix containing an ultra-stable *Taq* DNA polymerase, dNTPs, MgCl₂ and inert red dye that permits easy visualisation and direct loading onto a gel. Each reaction contained reagents as followed:

2µl bacterial DNA

25pmol forward primer

25pmol reverse primer

12.5 µl BioMix™ Red

dH₂O to take the final volume to 25µl

The PCR was performed as above.

2.1.6. Agarose Gel electrophoresis

Agarose Gel electrophoresis was used to visualise DNA fragments and PCR products. Agarose (Sigma) was melted in 1xTAE buffer using microwave. The percentage agarose used depends on the size of the DNA fragments. The agarose was allowed to cool to 60-56° and 100ng/ml ethidium bromide was added. An agarose gel was cast using BioRad casting system. The gel was allowed to set and placed into electrophoresis tank (BioRad or Thermo Electron corporation). PCR products containing gel loading buffer or DNA samples with gel loading buffer added were loaded into the gel. DNA size markers were also used. Gels were run at 100V. The DNA bands were visualised using a UV transilluminator (BioRad, ChemiDoc). Images were captured on a digital camera using BioRad Gel Documentation system.

2.1.7. Purification of PCR products

PCR products were purified using a QIAquick PCR purification kit (Qiagen) and a QIAquick Gel Extraction Kit (Qiagen) was used to purify DNA from agarose gels when plasmid DNA was used as a template. The manufacturer's protocol was used for the PCR

purification. In brief, the DNA was bound to a silica membrane in a high-salt buffer, washed and then eluted with low-salt buffer. The concentration was determined by measuring the absorbance at 260nm on a Nanodrop spectrophotometer ND-1000. For accuracy, the reading should be between 0.1 and 1.0. An absorbance of 1 unit at 260nm corresponds to 50µg double stranded DNA per millilitre. To purify PCR products from an agarose gel, DNA was extracted from the gel and purified using manufacturer's protocol in which the agarose gel was dissolved in a gel-dissolving buffer, the DNA bound to a silica matrix, washed and eluted with 10µl of elution buffer. The concentration was determined as above.

2.1.8. Restriction digests

The restriction enzymes used for digestion PCR products or plasmid DNA were purchased from Promega. For digesting 5µg DNA, 3µl (24-30 units) of relevant enzyme was used with 7µl of the recommended buffer and 7µl of 0.1% BSA. The final volume was taken to 70µl with distilled water. All digests were incubated for 2 hours at 37°C. DNA was purified after each digesting step using a QIAquick® PCR purification kit and eluted with 56µl elution buffer provided in the kit.

2.1.9. Ligation

The digested PCR products were ligated into the expression vector pDR2ΔEF1α (gift from Dr. I. Anegon, INSERM U437, Nantes, France) using T4 DNA ligase (Promega). To generate OmCI-Fc, a ligation step in to Signal pIg plus vector (R&D systems) was also performed. For ligation, 90ng plasmid was used and 3-fold molar excess of insert. This was calculated by:

$$3X(90\text{ng vector} \times \text{size of insert in kb})/\text{size of vector in kb}$$

Each ligation reaction contained also 1µl 10x ligase buffer (Promega, 300mM Tris-HCl pH 7.8, 100mM MgCl₂, 100mM DTT and 10mM ATP), 1µl T4 DNA ligase and dH₂O to adjust

the final reaction volume to 10 μ l. This was then incubated at 16°C overnight. The ligated DNA was transformed into bacteria.

2.1.10. Transformation

Chemically competent DH α bacterial cells (Invitrogen Life Technologies) were transformed with ligated DNA by heat shock. 1 μ l of ligated DNA was added to 50 μ l of bacterial cells and mixed gently. The competent cells were incubated on ice for 30 minutes followed by incubation for 60 seconds at 42°C. The cells were immediately transferred back on ice and incubated for 2 minutes. 950 μ l of SOC medium was added and the cells were incubated at 37°C for 1 hour in a shaking incubator. 200 μ l of the bacterial suspension were plated onto LB ampicillin plate (LB containing 1.5% agar and 100 μ g/ml ampicillin plated into a Petri dish) and incubated for 16 hours at 37 °C.

2.1.11. Bacterial colony screening

Bacterial colonies were screened by PCR to detect the efficiency of ligation insert into plasmid. In order to check the orientation of the insert in the vector “internal” and “external” primers were used. “Internal” is one of the primers used to amplify the insert. The “external” primer is specific for the pDR2 Δ EF1 α plasmid. All the primers used for screening are listed in Table 2.2. Single colonies were picked with a sterile pipette tip and resuspended into 20 μ l of dH₂O. 1 μ l of the suspension was spotted onto an LB amp plate. The remaining 19 μ l was boiled for 10 minutes on a heating block to lyse the bacteria. The tubes were cooled down by incubation on ice followed by a centrifugation at 13000 rpm for 8 minutes. 2 μ l of the supernatant containing plasmid DNA was used as a template for the screening PCR. The PCR products were visualised on agarose gel and colonies containing the insert in the correct orientation and size were identified. These were picked from the LB amp plate and seeded in 10ml LB broth and incubated in a shaking incubator for 16 hours (overnight) at 37°C.

Construct	Cloning step	External primer	Internal primer	Annealing temperature (C°)
OmCI-Fc	OmCI into Sig pIg plus	5' pIgpDR2	OmCI 3'	60
	CD33sp-OmCI into pDR2ΔEF1α	pDR 5'	OmCI 3'	60
CRIg-CD59*	CRIg into pDR2ΔEF1α	pDR 5'	CRIg amino 3'	62
	CD59 into CRIg/pDR2ΔEF1α	pDR 5'	CD59carboxy 3'	60
CD59-CRIg*	CD59 into pDR2ΔEF1α	pDR 5'	CD59 amino 3'	62
	CRIg into CD59/pDR2ΔEF1α	pDR 5'	CRIg carboxy 3'	62

Table 2.2 Cloning steps and primers used for DNA screening

*An additional screening step was performed for the reagents containing antibody hinge. The insertion of the hinge was confirmed by PCR using pDR5' (external) and the reverse primer specific for the hinge (internal).

2.1.12. Plasmid isolation

The overnight bacterial culture was spun down at 1300xg for 10 min. The supernatant was discarded. The plasmid DNA was isolated from the bacterial pellet using QIAprep Spin Miniprep kit (Qiagen) according to manufacturer's protocol. In brief, the bacteria were lysed under alkaline conditions. The lysate was subsequently neutralised and adjusted to high-salt binding conditions. The DNA was bound to a silica matrix, following a wash, the DNA was eluted and stored at -20°C.

2.1.13. DNA sequencing

All DNA constructs cloned into plasmids were sequenced using Big Dye™ Terminator Cycle Sequencing Kit (Applied Biosystems). Every sequencing reaction contained 50-100ng of template DNA, 2.5pmol specific forward or reverse primer, 2µl BigDye Premix containing Ampli Taq DNA polymerase, 3µl Better buffer and dH₂O to make the reaction up to 10µl.

The amplification protocol consisted of 25 cycles as follows:

Denaturation: 96°C for 30 seconds

Annealing: 50°C for 15 seconds

Extension: 60°C for 4 minutes

The DNA was precipitated by adding 2µl of 3M Sodium acetate pH5.2, 2µl of 125mM EDTA and 50µl ice cold 100% ethanol. The reaction tubes were incubated for 10 minutes at room temperature and DNA was centrifuged at 13,000 rpm for 30 minutes. The supernatant was discarded and the pellet washed with 200µl 70% (v/v) ethanol. Sequencing was carried out using an ABI model 377DNA sequencer (PerkinElmer; Central Biotechnology Services).

2.1.14. Plasmid dephosphorylation

To prevent self ligation of linearised plasmids during cloning, a dephosphorylation step was carried out. This step was particularly important when the plasmid was cut with a single enzyme (generating sticky ends) or with enzymes forming blunt ends. A shrimp alkaline phosphatase (SAP, Promega) was used in this study. SAP removes phosphate groups from the 5' ends of DNA and RNA and thus prevents re-ligation.

Plasmid DNA digested with restriction enzymes was incubated with SAP at 37°C for 15 minutes in 1xSAP reaction buffer in a final volume of 50µl. The enzyme was inactivated by heating to 65°C for 15 minutes. The plasmid DNA was immediately used for ligation or stored at -20°C.

2.2. Mammalian cell expression

All tissue culture was carried out under sterile conditions in a flow cabinet. All tissue culture reagents were obtained from Invitrogen Life Technologies unless otherwise stated. The cells were grown in a humid atmosphere at 37°C and 5% CO₂.

2.2.1. Media

RPMI-1640 (Roswell Park Memorial Institute 1640) was used for cell culturing. It was supplemented with 50U/ml penicillin/streptomycin, 2 mM L-glutamine and 1mM sodium pyruvate and 10% (v/v) foetal calf serum (FCS). This medium would be called “RPMI-complete” for short. Hygromycin B (O-6-Amino-6-deoxy-L-glycero-D-galactohexopyranosylidene-(1-2-3)-O-β-D-talopyranosyl-(1-5)-2-deoxy-N³-methyl-D-streptamine; A.G. Scientific, Inc.) was used as a selective agent for transfection. Depending upon the stage of cell selection different amounts of hygromycin B were added: 400µg/ml for selection medium, 100µg/ml for transfected cells. Non-transfected CHO cells were grown in hygromycin B free media.

2.2.2. CHO cells

Chinese Hamster Ovary (CHO) cells were used to express the anti-complement therapeutics. A frozen aliquot of the cells was taken from the liquid nitrogen and was rapidly thawed and resuspended in warm RPMI-complete. The cells were centrifuged at 300xg for 5 minutes. The cell pellet was resuspended in 5ml of RPMI and cultured in T25 tissue culture flasks. To subclone or expand adherent cells, the cells were washed with sterile saline and lifted from the flask surface using Trypsin-EDTA. The detached cells were diluted in to RPMI-complete and transferred into new flasks for expansion.

2.2.3. Transfection of CHO cells

The vector pDR2ΔEF1α used for mammalian expression contains the high expression promoter for Elongation Factor 1α and multiple cloning site next to it. In addition to the gene for ampicillin resistance, it carries a hygromycin resistance allowing selection in eukaryotic cells.

CHO cells were transfected using JetPEI™DNA Transfection reagent (Poly plus Transfection). It is a water-soluble polymer, which forms stable aggregates with DNA.

Transfection was carried out in 6 well-plate or T25 tissue culture flasks, according to manufacturer's instructions. Plasmid DNA (3µg or 5µg) was mixed with transfection agent and incubated for 25 minutes at room temperature to allow formation of JetPEY/DNA complexes. The complexes were then applied to the cells. The cells were incubated with the transfection mix in Hygromycin B-free medium for 24-48 hours at 37°C and 5% CO₂. The media was replaced with selective media containing 400µg/ml Hygromycin B. Mock transfected cells were used to monitor the selection. When these non-transfected cells had died, the CHO cells were maintained in media with 100µg/ml Hygromycin B. The efficiency of transfection and protein expression was confirmed by western blot analysis on tissue culture supernatant. Once the protein expression is confirmed, the cells were cloned out.

2.2.4. Cloning by limiting dilution

To select high expressing transfected CHO cells, the cells were cloned out by limiting dilution in 96-well plates. 100µl of medium was placed in the wells. Cells from a tissue culture flask were resuspended to 500 cells/ml medium. 200µl of cell suspension was added to the first three columns. The cells were diluted in 1:2 serial dilution across two 96-well plates to achieve final dilution of 0.26 cell per well. The cloned cells were cultured for 10 days. The supernatant from wells containing a single colony was screened by ELISA or western blot. Cells expressing highest levels of protein were expanded. The same assay was applied for cloning hybridoma cells.

2.2.5. Storage of CHO cells

To freeze down, CHO cells (transfected or non-transfected) harvested from a T80 flask were centrifuged at 300xg for 5 minutes and resuspended into 2ml of freezing medium (10 % DMSO/FCS). The cells were aliquoted into two cryovials (Greiner) and frozen in an isopropanol-containing Freezing container (Nalgene) placed at -70°C. The container provides 1°C/min cooling rate which together with the DMSO prevented the formation of

ice crystals in the cells. After 24 hours at -80°C, the cells were transferred into liquid nitrogen for long-term storage.

2.2.6. High-density expression systems

For efficient protein expression, transfected cells were seeded in a two-compartment bioreactor CELLLine AD1000 or HYPER*Flask* expression systems.

2.2.6.1. Two-compartment bioreactor CELLLine AD1000 for CHO cell culture

CELLLine AD1000 (Integra Biosciences) has two compartments separated by 10kDa semi-permeable cellulose-acetate membrane. This allows the cells, cellular products and protein to remain in the cell compartment and a concurrent continuous removal of any inhibitory waste product. The compartment contains a polyethylene terephthalate matrix that provides a surface for cell attachment. Transfected cells were maintained in transfected cell medium (15-17ml) in the cell compartment.

To inoculate the flasks, the membrane was wetted by placing 50ml media in the medium compartment and 2.5×10^7 cells in 15ml RPMI-complete medium containing 100µg/ml hygromycin B were placed into the cell compartment. A further 950ml RPMI medium was added to the medium compartment. The media in both compartments was changed 10 days after the inoculation and then every 7 days. The medium harvested from the cell compartment was centrifuged at 1000xg for 5 minutes and the supernatant was collected and stored at -20°C. The protein production was assessed by ELISA or Western blot. Prior to any protein purification, the cell culture supernatant was centrifuged at 6000xg for 10 minutes at 4°C and filtered through a 0.22µm filter.

2.2.6.2. HYPERFlask for CHO cell culture

CHO cells expressing anti-complement therapeutics were also maintained in HYPERFlask cell culture vessels (Sigma-Aldrich). These flasks contain ten gas permeable polystyrene growth surfaces that allow air exchange between the layers. CHO cells (1×10^7) expressing fusion proteins were diluted in 100ml RPMI medium containing 100 μ g/ml hygromycin B. The cell suspension was transferred into the HYPERFlask cell culture vessel. The flask was capped and laid on its side to allow the solution to distribute between layers. This ensured that each layer of the flask received the same volume of liquid. The flask was then filled with 450ml of RPMI-complete medium containing 100 μ g/ml Hygromycin B. The tissue culture supernatant was harvested and replaced with fresh medium every six days. The protein production was assessed and the supernatant was stored as described for CELLline AD1000 flask.

2.3. Protein purification

Fusion proteins, complement plasma proteins C3 and C5, and antibodies were purified using chromatography techniques.

2.3.1. Buffers and solutions

The buffers used for protein purification are listed in table 2.3

2.3.2. Clarification of supernatant

Prior to any purification, cell culture supernatant was clarified by centrifugation at 6000xg for 10 minutes. Cell culture supernatant and plasma were filtered using 0.22 μ m filter before applying over chromatography columns.

Name	Contents
Tris buffered saline (TBS)	10mM Tris, 150mM NaCl, 0.01% (w/v) sodium azide, pH7.4
Phosphate buffered saline (PBS)	8.2mM Na ₂ HPO ₄ , 1.5mM KH ₂ PO ₄ , 137mM NaCl, pH 7.4
Coupling buffer	0.2M Na HCO ₃ , 0.5M NaCl, pH8.3
Glycine	0.1M Glycine/HCl pH2.5
Diethylamine	20mM Diethylamine in PBS
IgM binding buffer	20mM Na ₂ HPO ₄ , 0.8M (NH ₄) ₂ SO ₄ , pH7.5
IgM elution buffer	20mM Na ₂ HPO ₄ , pH7.5
IgM regeneration buffer	20mM Na ₂ HPO ₄ , pH7.5, 30% isopropanol
Source Q buffer	10mM K ₂ HPO ₄ , 5mMEDTA, 0.5mM PMSF, 5mM Benzamidine, pH7.8
Source Q elution buffer	10mM K ₂ HPO ₄ , 5mMEDTA, 0.5mM PMSF, 5mM Benzamidine, 1M NaCl, pH7.8
Mono S running buffer	20mM NaPO ₄ , pH6
Mono S elution buffer	20mM NaPO ₄ , 1M NaCl, pH6

Table 2.3

2.3.3. Protein A and G chromatography

To purify antibodies or OmCI-Fc, serum or tissue culture supernatant was passed over prepacked 5ml protein A or G columns (GE Healthcare). Protein A and G are bacterial proteins used for purification of many antibody isotypes from a variety of species. The column was run using an AKTA Prime system (GE Healthcare). Each run consisted of a 2 column volume (10ml) equilibration with TBS, a supernatant load, 6 column volume wash with TBS and a 4 column volume elution with Glycine pH2.5. The elution was collected in

1ml fractions neutralised with 100µl 1M Tris/HCl pH10. The column was washed with HCl pH1.5 and equilibrated in TBS

2.3.4. IgM purification

HiTrap™ IgM Purification HP prepacked column (GE Healthcare) was used to purify IgM. The column was operated with Akta Prime liquid chromatography system. The column was equilibrated with 5 column volumes of IgM binding buffer. Tissue culture supernatant from hybridoma cells producing IgM anti-OmCI mAb containing 0.8M ammonium sulphate was loaded onto the column. The unbound protein was washed out with 15 column volumes of IgM binding buffer. IgM was eluted using 12 column volumes of IgM elution buffer. The column was regenerated with 7 column volumes of IgM regeneration buffer. The elution fractions were assessed by SDS-PAGE.

2.3.5. Gel filtration

Gel filtration chromatography was used to separate proteins based on their size and to estimate the molecular weight of OmCI-Fc and CRlg-CD59 fusion proteins. The chromatographic matrix consists of porous beads and the size of the bead pores defines the size of molecules that may be fractionated. The proteins that are too large to enter the beads pores are eluted from the column first. Smaller molecules are able to enter the pores and are retained by the column. Gel filtration chromatography was performed on Superdex 200 column using an Akta Purifier system. The protein was eluted at a flow rate of 0.5ml/min with a 1.5 column volumes. The elution buffer was chosen to preserve the protein activity. Fractions (0.5ml) were collected and small aliquots were taken for SDS-PAGE analysis. The estimation of the molecular weight is based on the assumption that the protein is globular in shape.

2.3.6. Affinity chromatography

Affinity chromatography was used to purify fusion proteins (OmCI-Fc and CRIG-CD59), complement protein C5 and antibodies (rabbit anti-OmCI polyclonal antibody, anti-OmCI monoclonal antibody of IgM isotype). OmCI-Fc was purified on an anti-OmCI antibody column while anti-CD59 antibody was used to purify CRIG-CD59 fusion proteins. Anti-mouse C5 antibody (BB5.1) was used to generate an affinity column for mouse C5 purification. Prior to the affinity purification, the polyclonal anti-OmCI rabbit serum was passed over a protein A column to isolate the immunoglobulin fraction. This was then subjected to OmCI affinity chromatography and the specific anti-OmCI antibody was purified.

2.3.6.1. Generation of affinity columns

Affinity columns were generated using prepacked NHS-activated Sepharose (5ml or 1ml HiTrap columns) from GE Healthcare. The antibody/protein to be bound were dialysed into coupling buffer two times for 7 hours at 4°C. Before coupling the antibody, the column was washed with 6 column volumes of ice-cold 1mM HCl. The antibody/protein (30mg for 5ml column and 10mg for 1ml column) was injected and column incubated for 30 minutes at 37 °C. The column was then washed with 6 column volumes of 0.5M ethanolamine, 0.5M NaCl, pH8.3 to block the remaining active sites, followed by washing with 6 columns volume of 0,1M acetate, 0.5M NaCl, pH4. These steps were repeated three times. The column was then equilibrated in TBS and stored at 4 °C.

2.3.6.2. Protein purification using affinity columns

To purify proteins, cell culture supernatant or serum (for C5 purification) was passed over an affinity column. The column was run using an AKTA Prime system (GE Healthcare). Each run consisted of a 2 column volume (10ml) equilibration with TBS, a supernatant load, 5 column volume wash with TBS and a 4 column volume elution with glycine pH2.5 (for OmCI-Fc and OmCI) and diethylamine/PBS pH11 (for CRIG-CD59 proteins and mouse C5).

The elution was collected in 1ml fractions neutralised with 100µl 1M Tris pH10 (when eluted with glycine pH2.5) or 1M Tris pH7 (when eluted with diethylamine/PBS pH11). The column was equilibrated in TBS. All buffers and supernatant were filtered through a 0.22µm filter prior to use.

2.3.7. Purification of mouse C3

Two-step PEG4000 cut was used to precipitate mouse plasma proteins prior to C3 purification on anion and cation exchange chromatography. Ion exchange methods separate proteins based upon their differences in charge, anion exchange columns bind negatively charged proteins while cation exchange columns binds positively charged proteins. Proteins were separated using an increased salt gradient. Mouse EDTA-plasma (32 ml) was mixed with 8ml of 20% (w/v) PEG4000 dissolved in Source Q running buffer to achieve a 4% PEG4000 cut. The mixture was stirred at 4°C for 1 hour. The pellet was harvested by centrifugation at 16900xg for 15 minutes. The supernatant was retained and mixed with 20% (w/v) PEG4000 to achieve 15% cut. After 1 hour stirring at 4°C, the precipitate was harvested by centrifugation as before. The pellet was resuspended in 32ml in Source Q running buffer and loaded onto a prepacked anion exchange Source Q column (GE Healthcare). The column was connected to an AKTA Purifier System (GE Healthcare). The proteins were separated using a 0-0.5M NaCl gradient over 15 column volumes. The C3 containing peak was identified by SDS-PAGE (section 2.4.4) and haemolysis assay (section 2.7.2.5). The C3 containing fractions were pooled, dialysed into Mono S running buffer and loaded onto a cation exchange Mono S column. The proteins were separated by a 0-0.5M NaCl gradient over 30 column volumes. C3 was identified by SDS-PAGE and haemolysis assay and dialysed into PBS for storage at -80°C for further studies.

2.3.8. Dialysis of proteins

Fractions containing protein of interests were combined and dialysed in PBS. The dialysing tubing used, had a molecular weight cut off of 12-14 kDa.

2.4. Characterisation of purified proteins

Measuring protein concentration and determination of purity.

2.4.1. Buffers

Buffer	Contents
Sodium Dodecyl Sulphate (SDS) stacking gel buffer	0.5M Tris, 0.4% (w/v) SDS, pH6.8
SDS resolving gel buffer	1.5M Tris, 0.4% (w/v) SDS, pH8.8
Non-reducing loading buffer	0.1M Tris, 10% (v/v) glycerol, 2% (w/v) SDS, 0.01% bromophenol blue, pH6.8
Reducing loading buffer	5% (v/v) β -mercaptoethanol in non-reducing buffer
Running buffer	25mM Tris, 191mM glycine, 1% (w/v) SDS
Coomassie stain	0.2% (w/v) Coomassie blue R250 in 45 % (v/v) Methanol, 10 % (v/v) acetic acid in dH ₂ O
Destaining buffer	20% (v/v) Methanol, 8% (v/v) acetic acid in dH ₂ O
Gel drying buffer	20% (v/v) Methanol, 4 % (v/v) glycerol in dH ₂ O
Transfer buffer	25mM Tris, 191mM glycine, 20 % (v/v) Methanol
Coating buffer for ELISA	0.1M N ₂ CO ₃ , 0.1M NaHCO ₃ , pH9.6
ELISA developing solution	1 OPD tablet, 1 urea hydrogen peroxide tablet dissolved in 20ml dH ₂ O

2.4.2. Protein concentration

The absorbance of proteins at 280nm was measured on NanoDrop ND-1000 Spectrophotometer and the concentration was calculated using the following equation:

Concentration (mg/ml) = Absorbance at 280 nm /Extinction coefficient when the pathlength is 1cm.

The extinction coefficients of fusion proteins were determined using ExPASy (Expert Protein Analysis System) proteomics server (Table 2.4)

Fusion protein	Extinction coefficient
OmCI-Fc	1.3
CRlg-CD59	1.1
CD59-CRlg	1.1
CRlg-hinge IgG3-CD59	1.1
CD59-hinge IgG3- CRlg	1.1
CRlg-hinge IgG2a-CD59	1.1
CD59-hinge IgG2a- CRlg	1.1
CD59-CRlg (cleavable)	1.1
Mouse C3	1.0
Mouse C5	1.0
Antibodies	1.4

Table 2.4 Extinction coefficients of the proteins purified in this thesis

2.4.3. SDS-PAGE analysis

Electrophoretic separation of proteins was carried out using BioRad gel apparatus. The concentration of acrylamide was chosen depending on the proteins to be separated. Higher percentage gel was used for low molecular weight proteins while high molecular weight molecules were run on low percentage gel. Typically gels were poured with a 4 % acrylamide stacking gel and 7.5-15 % acrylamide separating gel (table 2.5 and table 2.6). In general, the protein or protein mixture of interest was mixed with either non-reducing or reducing loading buffer and boiled for 5 minutes. The samples were loaded into the wells of the SDS PAGE gel within a running tank (BioRad) containing buffer. The gel was subjected to electrophoresis at 200V until the dye front had reached the bottom of the gel.

4% stacking gel	amount
Stacking buffer (ml)	1.2ml
40% acrylamide (ml)	506ul
10% Ammonium persulphate (μ l)	50 μ l
dH ₂ O (ml)	3.19ml
TEMED (μ l)	5 μ l

Table 2.5 Content of 4% stacking gel

Percentage resolving gel →	7.5%	10%	11%	12.5%	15%
Resolving gel buffer (ml)	3.75	3.75	3.75	3.75	3.75
40% acrylamide (ml)	2.8	3.75	4.2	4.5	5.62
10% Ammonium persulphate (μ l)	150	150	150	150	150
dH ₂ O (ml)	8.2	7.3	6.8	6.5	5.4
TEMED (μ l)	15	15	15	15	15

Table 2.6 Content of resolving gel

2.4.3.1. Coomassie Blue staining

To visualise 2-5 μ g of protein, SDS PAGE gels were stained with Coomassie Blue R250. Following electrophoresis the gel was incubated with Coomassie Blue R250 stain with

agitation for 30 minutes. Coomassie was removed and the gel was incubated with destaining solution with agitation until the background staining was reduced and the protein bands appeared visible. The gel was then incubated with drying solution for 30 minutes and placed between wet acetate gel drying films (Promega) and stretched within a gel-drying frame overnight to dry by evaporation.

2.4.3.2. Silver staining

To visualise between 100ng-2µg of protein, SDS PAGE gels were silver stained. The gel was treated as followed:

- Rinsed in dH₂O
- Incubate for 20-30 minutes in 50% (v/v) methanol, 10 % (v/v) acetic acid
- Incubate for 20-30 minutes in 5% (v/v) methanol, 7 % (v/v) acetic acid
- Rinsed in dH₂O
- Incubate in 5% (v/v) glutaraldehyde for 20-30 minutes
- Washed in dH₂O, 3x15 minutes
- Soaked in DTT (5µg/ml in dH₂O) for 20-30 minutes
- Rinsed in dH₂O
- Stained with 0.1% (w/v) AgNO₃ in dH₂O for 20-30 minutes
- Rinsed in dH₂O
- Developed in 0.28M Na₂CO₃ containing 0.0185% (v/v) formaldehyde;
Development was stopped by adding 1g citric acid (solid)

All incubation steps were carried out at room temperature with agitation (on a rocker). Following the silver staining procedure, gels were soaked in gel drying buffer and dried as described.

2.4.4. Western blot analysis

Western blot analysis was used to specifically identify proteins separated by SDS-PAGE. Following the electrophoresis, the gel was placed in a tray containing transfer buffer. The 1x

nitrocellulose membrane, 2x blotting paper and 2x fiber pads were soaked in transfer buffer. One fiber pad was placed on one side of an open holder cassette. One blotting paper was then placed on the top of the fiber pad, followed by the gel. The nitrocellulose membrane was placed on the top of the gel followed by the second blotting paper and fiber pad. The cassette was placed into the electrode module with the nitrocellulose membrane closer to the anode and the gel closer to the cathode. The electrode module was placed into a buffer tank Mini Trans Blot Cell (Bio-Rad) which was filled with transfer buffer. The transfer was run at 100V for 1 hour. After the transfer was complete, the membrane was blocked with PBS, 5% (w/v) non-fat dried milk for 30 minutes at room temperature. The blot was washed and incubated with relevant antibody at concentration of 4µg/ml diluted in the blocking buffer overnight at 4C. The blot was washed and probed with an appropriate secondary antibody conjugated with horseradish peroxidase (HRPO) diluted 1/1000 in blocking buffer. The specific primary and secondary antibodies used to detect different proteins are listed in Table 2.7.

Western blot for protein detection	Primary antibody	Secondary antibody
OmCI and OmCI-Fc	Rabbit anti-OmCI pAb	Anti-Rabbit Ig HRPO
OmCI-Fc	-	Anti-mouse Ig HRPO
CRIg-CD59 fusion proteins	Rat anti-mouse CRIg mAb Rat anti-mouse CD59 mAb (mCD59a-7) Rat anti-mouse CD59 mAb (Mel-4)	Anti-rat Ig HRPO
CRIg-CD59 fusion proteins	Mouse anti-mouse CD59 mAb (7A6)	Anti-mouse Ig HRPO

Table 2.7 Antibodies used for protein detection

This incubation was carried out at room temperature for one hour and was followed by a washing step. All washings were performed in 3 steps of 20 minutes each using PBS 0.1% Tween 20/ (v/v). A final wash of 20 minutes in PBS was carried out prior the developing step. Blots were developed using ECLTM Western Blotting Detection Reagents (GE Healthcare). The reagents were mixed 1:1 and the membrane was incubated for 2 minutes.

The membrane was removed and the blot was exposed to Amersham Hyperfilm™ ECL (GE healthcare) and developed in a Compact x2 developer (X-Ograph Ltd).

For densitometry analysis of the Western blot images, ImageJ 1.43u (Wayne Rasband National institute of health, USA, Windows version) was used.

2.4.5. Dot blot

Proteins (1-2µl) were applied directly on a nitrocellulose membrane as a dot. The membrane was allowed to dry and then was blocked at room temperature for one hour in 5% milk/PBS. The blots were probed and developed as with Western blots.

2.4.6. ELISA

ELISAs were used to identify and quantify recombinant fusion proteins (OmCI-Fc and CRIG-CD59) and to screen hybridoma cells and serum for presence of antibodies. ELISA plates (96-well plates, Nunc) were coated with 100µl per well of a protein or antibody at 3-5µg/ml in coating buffer. The wells were blocked with 200µl of 1% BSA/PBS (w/v) and incubated with the sample of interest or standard in an appropriate dilution (100µl per well). The wells were incubated with 100µl of detection antibody at 4µg/ml followed by 100µl of a HRPO conjugated secondary antibody at 1/1000. The ELISA was developed using ELISA developing solution prepared with o-phenylenediamine dihydrochloride (OPD; SIGMAFAST OPD; Sigma Life Science). The reaction was stopped with 50µl of 10% H₂SO₄. Absorbance was read at 490nm.

ELISA	Capture	Test sample or protein	Detection antibody or test antibody	Secondary antibody
Quantification of pOmCI and OmCI-Fc; Half-life;	MBI-Om3	Cell culture supernatant, purified protein or serum of mice injected with OmCI proteins	Rabbit anti-OmCI	Anti-rabbit Ig HRPO
Quantification of CRIG-CD59 proteins in tissue culture supernatant or mouse plasma	Mouse anti-mCD59 mAb (7a6)	Cell culture supernatant or pure protein	Rat anti-mCRIG mAb or rat anti-mCD59 mAb (mCD59a-7)	Anti-rat Ig HRPO
Screening for production and detection of mouse anti-OmCI Ab	-	OmCI	Mouse serum or cell culture supernatant	Anti-mouse Ig HRPO
	Rabbit anti-OmCI	OmCI		
	Rabbit anti-OmCI	(negative screening)		
Screening for rat anti-mCRIG and anti-mCD59 Ab	-	CRIG-CD59	Rat serum or cell culture supernatant	Anti-rat Ig HRPO
	-	CD59-Fc		

Table 2.7 ELISAs for detection and quantification of recombinant proteins and antibodies.

2.4.7. Estimation of protein molecular weight

The molecular weight of fusion proteins was determined using their mobility in SAS PAGE or in the matrix of gel filtration column.

2.4.7.1. Mobility in SDS PAGE

To calculate apparent molecular mass of fusion proteins by their relative mobility a 7.5% SDS PAGE was used. To generate a standard curve, protein standards with known molecular weight were used (Protein Ladder, New England Biolabs). Relative mobility for

each standard was determined by measuring the distance from the top of the separating (resolving) gel to the middle of the dye front in millimetres, measuring the distance from the top of the gel to the middle of the band, and dividing the second measurement by the first. This is Rf. It is between 0 and 1. Rf was plotted versus log molecular mass and standard curve was generated. Rf for each fusion protein was calculated and the molecular mass was determined using the standard curve.

2.4.7.2. Mobility in Superdex 200

To determine the molecular weight of fusion proteins, the Superdex 200 column was calibrated with standards of known apparent molecular weight (Gel filtration high molecular weight calibration kit, GE Healthcare) using the manufacturer's protocol. Briefly, Blue Dextran 2000 at concentration of 1mg/ml (100 μ l) was loaded onto the column to determine the void volume (V_0). A mixture of the standard proteins (100 μ l) was then applied onto the column and the elution volumes (V_e) of the proteins were determined. An elution volume parameter K_{av} was calculated ($K_{av}=(V_e-V_0)/(V_c-V_0)$; V_c is the geometric volume of the column). K_{av} was plotted versus molecular mass and standard curve was prepared. K_{av} for each fusion protein was calculated and the molecular weight was determined from the standard curve.

2.5. Generation of monoclonal antibodies (mAbs)

Mice or rats were used to generate mAbs.

2.5.1. Medium

RPMI 1640 supplemented with 50U/ml penicillin/streptomycin, 2mM L-glutamine and 1mM sodium pyruvate was used as hybridoma culture medium. Depending upon the stage of hybridoma developing HAT (Hypoxanthine, Aminopterin, Thymidine) or HT

(Hypoxanthine, Thymidine) was added. The percentage of FCS varied depending on the cell culture system used.

Medium for hybridoma cell culture	Additives	Use
HAT medium	1xHAT; 15% FCS	Selection of hybridoma cells
HT medium	1XHT; 15% FCS	Cloning and expansion of hybridoma cells post-culture with Aminopterin
Hybridoma medium	15% FCS	Culture of hybridoma cells
CL1000 complete	10% Low Ig FCS	Culture of hybridoma cells in a High density CL1000 system-cell compartment
CL1000 incomplete	-	Culture of hybridoma cells in a High density CL1000 system-media compartment

2.5.2. Immunisation protocol

Female BALB/C mice or Lewis rats were immunized with 50µg of antigen. The antigens used in this project were pOmCI (for generation of anti-OmCI mAbs) and CRIG-CD59 (generation of anti-CRIG and anti-CD59 mAbs). The antigen for immunization was diluted in saline (100 µl final volume) and mixed with 100µl of Freund's complete adjuvant (Sigma Life Science), using two glass Hamilton syringes connected with a luer fitting. Emulsion was prepared by repeated passage of the oil-water mixture through the narrow-bore syringe connector. A droplet test was performed to monitor the quality of the emulsion. The antigen was administrated subcutaneously. Two booster immunizations were carried out with the same dose of antigen emulsified in Freund's incomplete adjuvant (Sigma Life Science) at three-week intervals. Ten days after the final injection, the mice were tail-bled and sera were tested for antibody titer by ELISA, further boost were carried out if the titre was low. A final intraperitoneal (*ip*) injection of 50µg of antigen in 200µl saline (without adjuvant) was performed four days before the fusion experiment.

2.5.3. Droplet test

The quality (thickness) of antigen emulsion was assessed using droplet test [371]. A drop of the mixture (adjuvant and antigen) was placed in a Petri dish with cold water and the integrity of the drop was observed. The emulsion was ready to administer when the drop retained its shape.

2.5.4. Preparation of splenocytes

The mouse or rat which had been challenged with antigen was sacrificed by cervical dislocation. The spleen was harvested, placed in a vessel containing ice cold RPMI 1640 and kept on ice. The spleen was transferred in a Petri dish containing 2ml RPMI 1640 and the excess fat and fibrous tissue was removed. Single cell suspension was prepared by pressing the spleen using the plunger of a 10ml-syringe and passing it through a cell strainer (40 μ m, Falcon™BD). The cell suspension was collected in a 50 ml-falcon tube. The splenocytes were washed three times in cold RPMI 1640. All handling of cells was performed in a laminar flow hood.

2.5.5. Preparation of myeloma cells

SP2/0-Ag14 (SP2/0) myeloma cells were cultured before the fusion. SP2/0 cells in an exponential growth phase were harvested by centrifugation at 145xg for 5 minutes. The cells were washed in cold serum-free RPMI 1640.

2.5.6. Preparation of macrophage

Macrophages were used as a feeder layer to produce soluble factors that increase hybrid growth. To obtain peritoneal macrophages, a BALB/C mouse was sacrificed 24 hours prior to the cell fusion. 10 ml of cold serum-free RPMI was injected into the peritoneal cavity using

21-gauge needle. The medium was then withdrawn. The medium containing peritoneal macrophages was centrifuged at 145xg for 5 minutes and washed with RPMI. The cells were resuspended in HAT or HT containing medium and plated in 24-well plates (for fusion) or in 96-well plates (for cloning). The cells were checked for contamination at the fusion at time of cloning.

2.5.7. Cell fusion

Hybridomas were produced by fusing spleen cells from the immunised BALB/C mouse or Lewis rat with myeloma SP2/0 cells (2.5×10^7) using polyethylene glycol 1500 (PEG, Roche). Washed myeloma and spleen cells were mixed, pelleted and drained of all medium. PEG (1.5ml) was added slowly to the dry cell pellet over a 1-minute period with gently agitation and then kept without agitation for a further 1 minute. The fusion suspension was then diluted with 50 ml of warm RPMI 1640 medium; the first 20ml was added drop-wise over several minutes. The cells were spun down and the pellet resuspended in HAT-containing medium. The cells were plated in 24-well plates containing peritoneal macrophages as feeder cells. At day 10 the wells were screened for the desired antibody by ELISA.

Cells from wells that came up positive on ELISA were cloned by limiting dilution method (Method 2.2.4) and transferred to 96-well plates with feeder cells. The HAT medium was replaced by HT (Hypoxanthine Thymidine) containing RPMI 1640.

2.5.8. CELLine CL1000

CELLine CL1000 high density system was used to scale up the antibody production. CELLine CL1000 is similar to CELLine AD100 (section 2.2.6.1) but it does not have polyethylene terephthalate matrix (required for culturing adherent cell). The procedures for cell seeding and culturing are identical to these explained in section 2.2.6.1.

2.5.9. Isotyping of mAbs

2.5.9.1. Isotyping of mouse mAbs

Roche Applied Science's IsoStrip Mouse Monoclonal Antibody Isotyping Kit was used to determine the isotype of the anti-OmCI monoclonal antibodies. Culture supernatant (150µl) containing test antibody was added to a development tube containing coloured latex. An isotyping strip was placed into the tube and incubated until a blue band appear in either kappa or lambda section and in the class or subclass sections of the strip.

2.5.9.2. Isotyping of rat mAbs

An antibody-based rat immunoglobulin isotyping ELISA kit (Southern biotechnology associate) was used to determine the isotype of rat anti-mouse CRiG and anti-mouse CD59a antibodies. 96-well plates were coated with 3µg/ml CRiG-CD59 or CD59-Fc fusion proteins diluted in coating buffer (100µl per well) and incubated for one hour at 37°C. The plates were washed with ELISA washing buffer. The wells were blocked with 1% BSA/PBS for one hour at 37°C followed by incubation with hybridoma supernatant. The binding of the antibody to the antigen was detected with HRPO-conjugated anti-rat immunoglobulin secondary antibody. The ELISA was developed by adding substrate solution (OPD). The reaction was stopped with 50µl of H₂SO₄ and the absorbance was measured at 490nm.

2.6. Protein manipulations

2.6.1. Labelling with horseradish peroxidase (HRPO)

Monoclonal antibodies were conjugated with HRPO using EZ-Link® Plus Activated peroxidase kit (Pierce) following the manufacturer's instructions. Monoclonal antibody (1mg) was dialysed into carbonate buffer (0.1M N₂CO₃, 0.1M NaHCO₃), pH9.4 and was added to the lyophilized activated peroxidase. Sodium cyanoborohydride (10µl) was added

to the mixture. Following 1 hour incubation at room temperature, a quenching buffer was added and allowed to react for additional 15 minutes.

2.6.2. Chemical cross-linking of CRlg-3-CD59 and CD59-3-CRlg

A chemical cross-linker 1,8-bis (maleimido) diethylene glycol (BM(PEG)₂; Pierce Biotechnology) was used to improve dimerisation of CRlg-3-CD59 and CD59-3-CRlg and to link the sulfhydryl groups (-SH) in the hinges from different molecules. BM(PEG)₂ is a bismaleimide crosslinker for conjugation between sulfhydryl groups (-SH). It has a spacer arm with polyethylene glycol groups. Reaction of a sulfhydryl to the maleimide group results in formation of a stable thioether linkage resistant to reducing agents and physiological buffer conditions. Prior to cross-linking, fusion protein (170µl) at concentration of 6mg/ml (in PBS/5mMEDTA) was mixed with 17µl of the mild reducing agent 2-Mercaptoethylamine.HCl (2-MEA; Thermo Scientific) at concentration of 6mg/100µl. The reaction was incubated for 90 minutes at 37°C. 2-MEA selectively reduces hinge-region disulphide bonds. The reaction was cooled down to room temperature and 2-MEA was separated from the fusion protein using HiTrapTM Desalting column (GE Healthcare) and AKTA Prime system. The run consisted of column equilibration with PBS/5mM EDTA, loading of fusion protein containing 2-MEA and elution with PBS/5mM EDTA buffer. The buffer and the sample were filtered through a 0.22µm filter prior to use. The peak fractions were pooled and concentrated to 2mg/ml using Vivspin500 MWCO 10,000 (GE Healthcare)

BM(PEG)₂ was dissolved in dimethylsulfoxide (DMSO) to achieve 5mM final concentration. The cross-linker was added to the fusion proteins at two-fold molar excess (0.1mM of BM(PEG)₂ to 0.05mM of protein). Following incubation of 1 hour at room temperature the reaction was passed over a desalting column using PBS as a running buffer. The efficiency of dimerisation was assessed by SDS PAGE on 7.5% gel.

2.6.3. Papain digest

For cleavage of CD59-2a-CRIg and CD59-3-CRIg, immobilised papain (Pierce, Rockford, IL, USA) was used according to manufacturer's protocol. The immobilised papain (200µl) was washed in digestion buffer containing 20mM Na₂HPO₄, 10mM EDTA and 20mM cysteine, pH7.0. Digestion buffer (100µl) was added to 100µl of the reagents (1mg/ml) and this was mixed with the immobilised papain. The reaction was incubated at 37°C and test samples were withdrawn at 30 minutes, 1 hour, 2 hours and 19 hours for analysis. The cleavage efficiency was assessed by SDS-PAGE on 15% gel.

2.6.4. 3C rhinovirus protease digest

For cleavage of CD59-CRIg cleavable reagent, recombinant human rhinovirus protease 3C (HRV 3C; Novagen, Darmstadt, Germany) was used. CD59-CRIg cleavable reagent (50µg) was incubated with 1µl (2 units) of the enzyme for 16 hours at 4C in presence of protease cleavage buffer supplied with the enzyme. The 10x protease cleavage buffer contained 1.5M NaCl, 0.5M Tris-HCl with pH7.5. The protease (2000U/ml) was supplemented with 150mM NaCl, 50mM Tris-HCl, 1mM EDTA, 0.5mM reducing agent THP and 50% glycerol, pH8.0. The cleavage efficiency was assessed by SDS-PAGE on 15% gel.

2.6.5. Labelling of CD59-2a-CRIg

CD59-2a-CRIg was labelled with the amine-reactive fluorescent labelling dye HiLyte™ 488 SE using AnaTag™ HiLyte Fluor™ 488 Protein Labeling Kit (AnaSpec). The labelling was performed according to the manufacturer's protocol. CD59-2a-CRIg diluted PBS was mixed with 1M bicarbonate buffer (buffer B) at 1/10 (v/v) ratio to obtain pH9. The HiLyte™ 488 SE was dissolved in 30µl DMSO and was added to CD59-2a-CRIg. The reaction was mixed thoroughly. The reaction mixture was wrapped in foil to protect from direct light and incubated on a rotator for 1 hour at room temperature. The protein conjugate was purified on a pre-packed desalting column equilibrated with 25ml of elution buffer. The buffer was allowed to drain to the top frit and the reaction mixture was loaded on the column. When the

entire sample entered the column, 10ml of the elution buffer was added. The coloured material separated into two bands. The faster-running band contained the labeled CD59-2a-CRIg (CD59-2a-CRIg/488) and the slower-running band contained the free dye. The labeled protein was collected and the degree of substitution (DOS) of the conjugate was calculated using the following equation:

DOS= Molar concentration of Dye / Molar concentration of the protein

Molar concentration of dye= $(A_{499} \times \text{dilution factor}) / \epsilon_{\text{HiLyte Fluor}^{\text{TM}} 488}$

Molar concentration of the protein= $((A_{280} - 0.19 \times A_{499}) \times \text{dilution factor} /) / \epsilon_{\text{CD59-2a-CRIg}}$

Where: A_{499} is the maximum absorbance of the dye measured at 499nm

A_{280} is the absorption of the labelled protein at 280nm

$\epsilon_{\text{HiLyte Fluor}^{\text{TM}} 488} = 68,000 \text{ cm}^{-1} \text{ M}^{-1}$ is the extinction coefficient of the dye

$\epsilon_{\text{CD59-2a-CRIg}} = 36,000 \text{ cm}^{-1} \text{ M}^{-1}$ is the extinction coefficient of the CD59-2a-CRIg

2.7. Functional analysis

The functional analysis of OmCI-Fc and CRIg-CD59 fusion proteins and the ability of purified mouse C3 and C5 to restore complement activity.

2.7.1. Buffers and reagents

Buffer	Contents
Complement Fixation Diluent (CFD; Oxoid)	2.8mM Barbituric acid, 145.5mM NaCl, 0.8mM MgCl ₂ , 0.8mM CaCl ₂ , 0.9mM Sodium Barbital, pH7.2
Alternative pathway (AP) buffer	5mM Sodium barbitone, 150mM NaCl, 7mM MgCl ₂ , 10mM EGTA
Terminal pathway (TP) buffer	10mM EDTA, PBS
Biacore running buffer	10mM HEPES, 150mM NaCl, 0.005% (v/v) Surfactant P20, pH7.4
FACS buffer	1% (w/v) Bovine Serum Albumin (BSA), PBS

2.7.2. Classical pathway haemolysis assay

2.7.2.1 Preparation of erythrocytes

Sheep erythrocytes were used for human and rat classical pathway haemolysis assays and rabbit erythrocytes were used for mouse assays. The cells were washed into CFD and diluted to 4% (v/v). To sensitise rabbit erythrocytes, mouse anti-rabbit erythrocyte polyclonal serum was diluted 1/500 in CFD and incubated 1:1 with cells for 30 minutes at room temperature. Sheep erythrocytes were sensitised by 30-minute incubation at 37°C with equal volume of amboceptor (rabbit anti-sheep erythrocytes, Behring Diagnostics) diluted 1/250 in CFD.

2.7.2.2. Titration of serum for inhibition assays

To establish the amount of mouse, rat and human serum required to cause 70% lysis a haemolysis assay was carried out using a serum titration. The serum was diluted and 1:2 dilution series were set up beginning at 1/5 for mouse serum and 1/10 for human and rat serum. Each concentration (50µl) was incubated with 50µl antibody coated erythrocytes and 50µl CFD in a round-bottom 96-well plate. Control wells were incubated for 100% lysis in which the serum was substituted for 0.01% (v/v) Triton and 0% lysis in which the serum was substituted for 50µl CFD. Each concentration was analysed in duplicate. The plate was incubated for 30 minutes at 37°C. The remaining erythrocytes were pelleted by centrifugation at 900xg for 5 minutes. The supernatant (100µl) from each well was transferred into a flat-bottom 96-well plate. The absorbance at 415nm was measured and percentage lysis (haemoglobin released) was calculated as follows:

$$\% \text{ lysis} = 100 \times (\text{Test}_{A415} - 0\%_{A415}) / (100\%_{A415} - 0\%_{A415})$$

The concentration of serum giving 70%-80% lysis was used in subsequent assays.

2.7.2.3. Function of OmCI and OmCI-Fc

To compare the function of pOmCI and OmCI-Fc, the proteins were diluted and 1:2 serial dilutions were prepared starting from 84nM of OmCI-Fc and 102nM of pOmCI. Antibody-coated erythrocytes (50µl) were incubated with 50µl of the OmCI proteins from the dilution series and 50µl of serum (human, mouse or rat) diluted to give 70%-80% lysis in the absence of inhibition. Controls for 100% and 0% lysis were included. Each incubation was carried out in duplicate. The assays were incubated at 37°C for 30 minutes. Following the incubation the remaining cells were pelleted and the absorbance at 415 was measured. The percentage lysis was calculated and plotted against the log of concentration (x-axis). The concentration of inhibitor causing 50% lysis (EC50) was determined using GraphPad Prism5 software.

2.7.2.4. Functional analysis of mouse C5

Antibody sensitised rabbit erythrocytes (50µl) were incubated with 1 in 2 serial dilutions (50µl) of C5 deficient serum (DBA2, mouse strain with naturally occurring C5 deficiency) or C5 deficient serum reconstituted with the purified C5 at physiological concentration (50µg/ml). Serial dilution of serum from wild type mouse (BalbC) was also used as a positive control for complement-mediated lysis. The assay was carried out in CFD. Complement-mediated killing of the rabbit erythrocytes was determined after 30 minutes incubation at 37°C by measuring the haemoglobin release of the cells at 415nm. 100% and 0% lysis controls were also included. Maximum lysis was obtained by adding 0.01% Triton to the target cells. For 0% lysis-CFD was added to the erythrocytes. The percentage of lysis was calculated as described.

2.7.2.5. Assay for identification of C3-containing fractions

Elution fractions obtained from anion- and cation-exchange chromatography (section 2.3.7) were screened for presence of mouse C3 using classical pathway haemolytic assay.

Antibody sensitised rabbit erythrocytes (50µl) were incubated with 22% C3 deficient mouse serum (45µl) and 5µl of each elution fraction for 30 minutes at 37°C. Controls for 0% and 100% lysis were included. Percentage of lysis was determined.

2.7.3. Alternative pathway haemolysis

The capacity of the CR1g-CD59 fusion proteins to inhibit complement was assessed using alternative pathway assay.

2.7.3.1. Titration of rat serum

Guinea pig erythrocytes (GPE) were washed into AP buffer and diluted to 2% (v/v). To establish the amount of serum needed to cause 90% lysis, rat serum diluted in 10-fold 1:2 serial dilution beginning at 1 in 2. The serum (50µl) from dilution series was incubated with 50µl GPE and 100µl AP buffer. Control wells containing either 50µl of 0.01% (v/v) Triton or AP buffer instead of serum were included to obtain 100% and 0% lysis respectively. The assay was carried out in duplicate. The plate was incubated at 37°C for one hour. The absorbance at 415 was measured and percentage of lysis was calculated as described for the classical pathway haemolysis assay.

2.7.3.2. Function of CR1g-CD59 fusion proteins

To compare the function of CR1g-CD59 fusion proteins, they were diluted in a 1:2 serial dilution. The dilution series began with 150µg/ml of CD59-CR1g, CD59-3-CR1g, CR1g-3-CD59 and with 80µg/ml of CR1g-CD59. GPE (50µl) were incubated with 50µl of the inhibitor proteins from the concentration titre and 50µl of anti-CR1g (generated in this project) or anti-CD59 (7a6) antibodies (300µg/ml). Rat serum (50µl) at concentration that caused 90% lysis in absence of inhibition was added to the wells. Controls for 100% and 0%

lysis were included. The plate was incubated at 37°C for one hour and absorbance at 415 was measured. The percentage of lysis was determined.

2.7.4. Terminal pathway assay

2.7.4.1. Generation of C5b-7 sites on GPE using C8 depleted human serum

GPE were washed and resuspended in CFD at 4% (v/v). C8 depleted human serum, generated by passing normal human serum over monoclonal anti-C8 affinity column (generated previously in house), was diluted in CFD to prepare two 1:2 serial dilutions beginning at 1 in 2 and 1 in 3. GPE (50µl) were incubated with 50µl of the serum from dilutions. The plate was incubated for 30 minutes at 37°C. The serum concentration causing 15% lysis was used to generate GPE-C5b-7. GPE were incubated for 30 min at 37°C with an equal volume of C8 depleted human serum at a dose that gives 15% of lysis. The resulting cells (GPE-C5b-7) were washed and resuspended at 2% in TP buffer.

2.7.4.2. Generation of C5b-7 sites on GPE using purified C5b-6 and C7 human proteins

GPE were washed and resuspended in CFD at 2% (v/v). GPE (2ml) were incubated with 15µg C5b-6 for 5 minutes at 37°C, followed by 10µg C7 for 15 min at 37°C. The GPE-C5b-7 were washed and resuspended in 2ml TP buffer.

2.7.4.3. Titration of mouse serum

To develop the terminal pathway assay, C3 deficient mouse serum was used. The mouse serum was diluted in TP buffer and two 1:2 dilution series beginning at 1 in 2 and 1 in 3 were prepared. The amount of mouse serum that gave 50% lysis was determined by incubating 50µl of GPE-C5b-7 for 30 min at 37°C with 50µl dilutions of mouse serum and 50µl TP buffer. Percentage of lysis was determined as described for the classical pathway.

2.7.4.4. Function of CR1g-CD59 fusion proteins

The function of CR1g-CD59 was assessed in three different terminal pathway assays listed in table 2.8.

Terminal pathway haemolysis assay	Source of C5b-6 and C7	Source of C8 and C9	Presence of CR1g-CD59 proteins
Assay 1: In absence of C3	Purified human proteins	C3 deficient mouse serum	Throughout the assay
Assay 2: Non-wash assay in presence of C3	C8 depleted human serum	C3 deficient mouse serum	Throughout the assay
Assay 3: Wash assay in presence of C3	C8 depleted human serum	C3 deficient mouse serum	Washed before the addition of C8 and C9

Table 2.8 Terminal pathway haemolysis assays

To assess the function of the terminal pathway CR1g-CD59 inhibitors, these reagents were diluted in TP buffer and 1 in 2 or 1 in 3 dilution series were prepared. As a control, a 1:3 serial dilution of CR1g-fH fusion protein was used.

Assay 1 and 2: GPE-C5b-7 (50µl) were incubated with 50µl of dilutions of CR1g-CD59 fusion proteins for 10 minutes at room temperature. The predetermined concentration of mouse C3 deficient serum (usually 1/3000; 50µl) was then added to the wells and incubated for 30 minutes at 37°C.

Assay 3: GPE-C5b-7 (50µl) were incubated with 50µl of dilutions of CR1g-CD59 fusion proteins for 30 minutes at 37°C. The cells were pelleted and washed with TP buffer. The predetermined concentration of mouse C3 deficient serum (usually 1/3000; 50µl) and 50µl of TP buffer were added to the wells and incubated for 30 minutes at 37°C.

Controls, 0% (buffer only) and 100% (0.1% triton) were included in all three assays. Following pelleting of cells by centrifugation, lysis was quantified by measuring absorbance at 415nm. Percentage of lysis was calculated as described.

2.7.5. Binding OmCI-Fc and pOmCI to C5

The ability of pOmCI and OmCI-Fc to bind human and mouse C5 was assessed by surface plasmon resonance (SPR) using Biacore® T100 instrument (GE Healthcare). The binding of a molecule in the soluble phase (the analyte) to a ligand molecule immobilised on a sensor surface was directly measured. In Biacore® the samples are delivered to the sensor surface using a micro-fluidic system. The sensor surface is a glass slide coated with thin gold film mounted in a plastic carrier. Binding events cause changes in the refractive index at the surface layer. The value is plotted as response units (RU). For carboxymethylated dextran-coated chip (CM5) used in this study, 1000RU correspond to 1ng protein/mm² sensor surface [372].

2.7.5.1. Preparation of pOmCI and OmCI-Fc surface

Fifty RU of pOmCI was amine coupled to the chip surface of flow cell 2 (CM5 chip, Biacore) using 1-ethyl-3(3-dimethyl aminopropyl) carbodiimide/N-hydroxy-succinimide as instructed by the manufacturers (NHS/EDC coupling kit; Biacore). The immobilization was performed at 100µg/ml in acetate buffer, pH 4.0. Flow cell 1 was activated with NHS/EDC but left uncoated as negative control. Both Flow cells were deactivated with 0.1M ethanolamine pH8.5.

OmCI-Fc was amine coupled to the chip surface of flow cell 4 NHS/EDC coupling kit. The immobilization was performed at 3.5µg/ml in acetate buffer, pH 4.5 using the immobilization wizard control template, with target immobilization set at 150 RU. Flow cell 3 was activated with NHS/EDC but left uncoated as negative control. Both Flow cells were deactivated with ethanolamine.

2.7.5.2. Binding of OmCI-Fc and pOmCI to human and mouse C5. Affinity analysis

To assess the affinity of pOmCI and OmCI-Fc with C5, human and mouse C5 were diluted in a 5-fold 1:2 serial dilution in a biacore running buffer. Each concentration was injected

across the OmCI-Fc and pOmCI surface with 180 second contact time followed by a 300 second dissociation buffer, flow rate 10 μ l/min. The C5 concentration began at 54nM. A regeneration cycle was run after each concentration. One cycle contained consecutive 30 second pulses of 20mM diethylamine in PBS, pH11 followed 10mM Glycine-HCl, pH2.5 (BIAcore). Each cleaning cycle began and finished with the high pH buffer. Each protein concentration was injected in duplicate or triplicate. Data were evaluated using Biacore evaluation software. The affinity interaction was analysed by 1:1 Langmuir binding.

2.7.6. MBI-Om1-OmCI binding interaction

To investigate the interaction of MBI-Om1 (anti-OmCI mAb) with OmCI, Bicare 3000 instrument was used. The experiments performed are listed in table 2.9. The ligands were diluted in 10mM citrate buffer pH4.5 immobilised on CM5 chip using amine coupling (section 2.7.5.1). Bicare running buffer was used to dilute analyte 1 and analyte 2. The regeneration cycle, consisting of two injections of glycine pH2.5, was run after each MBI-Om1-OmCI binding interaction. The biacore analysis was performed at flow rate of 10 μ l/min.

Ligand/RU immobilised	Analyte 1	Analyte 2
MBI-Om1 1000RU	OmCI (20 μ g/ml and 200 μ g/ml)	-
Protein A 500RU	MBI-Om1 (500 μ g/ml)	OmCI (200 μ g/ml)
Human C5 4000RU	OmCI (200 μ g/ml)	MBI-Om1 (100 μ g/ml)

Table 2.9 Experiments carried out to characterise MBI-Om1-OmCI interaction

2.7.7. Binding CRIG-CD59 proteins to mouse C3b and iC3b

The ability of CRIG-CD59 fusion proteins to bind mouse C3b and iC3b was assessed by SPR using Biacore ® T100 instrument.

2.7.7.1. Preparation of C3b surface

Human C3b was amine coupled on flow cell 2 of CM5 sensor chip using NHS/EDC coupling kit. The immobilization was performed at 3.3µg/ml in acetate buffer, pH 4.5 using the built-in immobilization wizard control template, with target immobilization set at 100 RU. Flow cell 1 was activated with NHS/EDC but left uncoated as negative control. Both Flow cells were deactivated as above.

Mouse C3b was generated by cleavage of mouse C3 by alternative pathway convertase assembled on the chip surfaces. An alternative pathway convertase was formed from the covalently immobilised human C3b together with a mixture of factor B and factor D (CompTech, Inc) injected across the chip surfaces at concentration of 200 µg/ml and 5 µg/ml respectively for 120 seconds at flow rate of 10 µl/min. Mouse C3 at a concentration of 400µg/ml was immediately injected for 120 seconds at flow rate of 5µl/min. C3bBb complex (alternative pathway convertase) cleaved mouse C3 to C3b deposited on the chip surface. Injections of a mixture of factor B and factor D and mouse C3 were repeated until approximately 800RU of mouse C3b was deposited on the chip surface. Convertases was decayed by injection of DAF (16µg/ml) for 30 seconds. The surface was stabilised by a 30 second injection of 0.1M acetate buffer containing 1M NaCl, pH4.0 to remove any loosely bound mouse C3b. Biacore running buffer supplemented with 1mM MgCl₂ was used as running or dilution buffer.

2.7.7.2. Preparation of iC3b surface

Mouse iC3b surface was prepared by cleavage of C3b (coated on the chip surface) with factor I and factor H as a co-factor. Human factor I (CompTech, Inc) at concentration of 5µg/ml and human factor H (68µg/ml) diluted in biacore running buffer were injected across the C3b surface for 300s at 5µl/min. The surface was regenerated by a 30 second injection of 0.1M acetate buffer containing 1M NaCl, pH4.0.

2.7.7.3. Binding of CR1g-CD59 proteins to C3b and iC3b. Affinity analysis

To measure binding affinity of fusion proteins for mouse C3b, two-fold dilution series of CR1g-CD59 fusion proteins were prepared in a biacore running buffer and injected sequentially over the C3b or iC3b chip surface for 120s. Data was collected at 25 °C at a flow rate of 20µl/min. The proteins were allowed to dissociate for 180s. The surface was regenerated between binding cycles by a 30s injection of 0.1M acetate buffer containing 1M NaCl, pH4.0. Each concentration was injected in duplicate. Data from a reference cell was subtracted to control for bulk refractive index changes. The equilibrium dissociation constant for fusion proteins was determined by using steady-state analysis.

2.7.8. Binding of CR1g-2a-CD59 to C3b-opsonised red blood cells-flow cytometry

CD59 deficient mouse erythrocytes were washed into CFD containing 0.1% (w/v) gelatin and diluted to 4% (v/v). polyclonal Rabbit anti-mouse erythrocytes (generated in house) was diluted 1 in 12.5 and incubated 1:1 with the mouse erythrocytes for 30 minutes on ice. The antibody-sensitised cells were washed into CFD/gelatin and diluted to 2% (v/v). To coat in C3b/iC3b, the antibody sensitised mouse erythrocytes were exposed to 20% C6^{-/-} mouse serum diluted in CFD at 37°C for 30 minutes. C3^{-/-} mouse serum was used as a negative control for C3 deposition. The cells were washed and resuspended in CFD/gelatin.

C3b/iC3b deposition was confirmed by flow cytometry. Cells (5µl) incubated with C6 or C3 deficient mouse serum were transferred into 96-well plate (round bottom) and washed. The cells were incubated with 100µl of anti-mouse C3 antibody (Clone 3/26, HyCult) at concentration of 10µg/ml for 30 minutes at room temperature. The plate was washed and 100µl of Phycoerythrin (PE) conjugated anti-rat IgG antibody (Jackson ImmunoResearch Laboratories) diluted 1:100 was added. After 20-minute incubation at room temperature the cells were washed and resuspended. FACS buffer was used to wash and resuspend the cells and to dilute the antibodies. The cell suspension was transferred to FACS tubes (BioRad) and fluorescence intensity was measured on FACSCalibur flow cytometer (Becton Dickenson, Oxford, UK), using CELLquest software.

CD59 deficient erythrocytes (20 μ l) coated in C3b/iC3b along with cells that had been exposed to C3-/- serum were transferred into 96-well plate (round bottom) and washed in CFD. The cells were incubated with 100 μ l of CD59-2a-CRIg monomer or dimer (separation is explained in section 2.3.5) at concentrations of 50 μ g/ μ l, 20 μ g/ μ l and 0 μ g/ μ l (diluted in CFD/gelatin) for 30 minutes at 37°C. The wells were washed and resuspended in FACS buffer. Cell suspension (5 μ l) was transferred into a new plate and CD59-2a-CRIg binding was detected by incubating the cells with 100 μ l of rat anti-CD59 mAb at concentration 10 μ g/ml diluted in FACS buffer. The plate was incubated for 30 minutes at room temperature and washed. PE conjugated anti-rat IgG antibody was then added and allowed to react with the cells for 20 minutes at room temperature. The cells were washed and fluorescence intensity was measured.

2.7.9. Binding of anti-CD59 mAb (mCD59a-7) to mouse -flow cytometry

CD59 sufficient and deficient mouse erythrocytes (0.05%) were washed in FACS buffer and incubated with mCD59a-7 mAb (10 μ g/ml in FACS buffer) for 30 minutes at room temperature. Following washing step, the cells were incubated with 100 μ l of PE conjugated anti-rat IgG antibody diluted 1:100. After 20-minute incubation at room temperature the cells were washed and resuspended. The fluorescence intensity was measured as described in section 2.7.8.

2.8. *In vivo* and *ex vivo* analysis

2.8.1. Animals

DBA2 (DBA/2OlaHsd) and C57Bl/6 mice were obtained from Harlan LaboratoriesTM. CD59-/- mice have been previously generated [373]. The animals were maintained according to Home Office guidelines within the Biomedical Services Unit at School of Medicine, Cardiff University.

2.8.2. *In vivo* clearance of OmCI-Fc and pOmCI in DBA2 mice

pOmCI was mixed with OmCI-Fc and diluted in PBS. Male DBA2 mice (n=3) were injected *iv* with 200µl of the mixture containing 75µg of OmCI-Fc and 150µg of pOmCI. The animals were tail bled at the following time points 5, 10 and 30 minutes, 1, h, 12, 25, 48, 72 and 96 hours post injection. The blood (20µl) was collected in tubes coated in lithium heparin (Microvette ® CB300 blood collection system). Presence of pOmCI and OmCI-Fc in plasma was assessed by Western blot. Test mouse plasma (0.25µl) along with plasma from a naïve mouse was subjected to electrophoresis on 11% polyacrylamide gel and transferred to a nitrocellulose membrane. Mixture (0.25µl) of purified pOmCI and OmCI-Fc at concentration of 150µg/2ml and 75µg/2ml (assuming 2ml blood in mouse) respectively was used as a positive control. The blot was developed using affinity-purified rabbit polyclonal anti-OmCI Ab (4µg/ml) followed by anti-rabbit Ig-HRPO (1:1000) as described in section 2.4.5. Protein levels were determined by densitometry analysis using ImageJ 1.43u (Wayne Rasband National institute of health, USA, Windows version) and presented as percentage of purified pOmCI or OmCI-Fc mixture used as a positive control.

2.8.3. *In vivo* half-life of OmCI-Fc and pOmCI in C57Bl/6 mice

Two groups of 5 C57Bl/6 mice were injected *iv* with 500µg of pOmCI or 200µg of OmCI-Fc. The animals were tail bled at the following time points 5, 10 and 30 minutes, 1, h, 12, 25, 48, 72 and 96 hours post injection. The blood (20µl) was collected in tubes coated in lithium heparin (Microvette ® CB300 blood collection system). Pharmacokinetic analysis of the proteins was performed by determining the plasma concentration of injected proteins by ELISA (section 2.4.6 table 2.7) using pOmCI or OmCI-Fc standard curves respectively. For each time point the protein concentration was calculated and expressed percent of the injected dose against time. The log of the percentage protein (y-axis) was plotted against the time in hours (x-axis). The data was analysed using two-compartment model. The half-life was calculated from the slope (determined using GraphPad Prism 5) of the linear region of the curve.

β half-life = $0.693 / \text{slope}$

2.8.4. *In vivo* complement inhibitory activity of OmCI-Fc and pOmCI

The *in vivo* complement inhibitory activity (CH50) of OmCI-Fc and pOmCI was assessed in C57Bl/6 mice. The animals were injected with either OmCI-Fc or pOmCI. A third group of mice received pOmCI followed by injection OmCI-Fc to study the combine effect of these reagents. Blood was collected at various time points. Serum samples were obtained by tail vein section and collected in capillary tubes (Microvette ® CB300 blood collection system). Blood was allowed to coagulate at room temperature for 10 minutes and serum was collected after centrifugation at full speed for 10minutes in a benchtop centrifuge. C5 activity or complement activity was measured. Doses of OmCI-Fc and pOmCI used in these experiments are listed in table 2.10.

pOmCI injection at time 0 hour	OmCI-Fc injection at time 1 hour	Route of administration	Mice per group	Activity measured
200µg	-	<i>iv</i>	5	Complement
-	300µg	<i>iv</i>	5	Complement
200µg	50µg	<i>iv</i>	1	C5
200µg	150µg	<i>iv</i>	1	C5
200µg	300µg	<i>iv</i>	5	Complement
200µg	-	<i>sc</i>	2	Complement
-	300µg	<i>sc</i>	2	Complement

Table 2.10 Experiments carried out to determine haemolytic inhibitory capacity of OmCI-Fc and pOmCI. Route and dose of OmCI reagents injected in mice and activity measured

2.8.4.1. Complement activity

For each animal, serum was diluted in CFD and 1 in 2 dilution series beginning at 22% (v/v) serum was prepared. Serum (50µl) from each concentration was incubated with 50µl antibody coated rabbit erythrocytes (described in section 2.7.2.1) in a round-bottom 96-well plate for 20 minutes at 37°C. To establish 0% and 100% lysis, 50µl rabbit erythrocytes were

incubated with 50µl CFD and 50µl 0.01% Triton. The assay was carried out in duplicate. Following the incubation the cells were pelleted by centrifugation at 900xg for 5 minutes. Supernatant (80µl) from each well was transferred to a flat-bottom 96-well plate and the absorbance at 415nm was measured. Percentage lysis was calculated as described in section 2.7.2.2 and was plotted against log of serum concentration (%) used. Haemolytic activity was quantified by the amount of the test serum necessary to kill 50% of antibody-sensitised rabbit erythrocytes (CH50). CH50 was determined as described in Complement Methods and Protocols [374, 375] and expressed as percent of the activity prior to pOmCI or OmCI-Fc administration (at time -1 hour).

$\% \text{ haemolytic activity} = 100 \times (\% \text{ serum collected at time -1 hour causing 50\% lysis} / \% \text{ serum collected at various time points causing 50\% lysis})$

2.8.4.2. C5 activity

Experimental serum collected at various time points from animals injected with OmCI-Fc and pOmCI was diluted and one in two dilution series beginning at 10% (v/v) was prepared. Serum (25µl) from each concentration was incubated with 50µl antibody coated rabbit erythrocytes and 25µl of 25% C5 deficient mouse serum (obtained from C5 deficient DBA2 mice) in a round-bottom 96-well plate for 20 minutes at 37°C. All the dilutions were performed in CFD. Percentage haemolysis and CH50 were determined as described in section 2.8.5.1.

2.8.5. Induction of antibody-dependent experimental autoimmune encephalomyelitis (ADEAE)

Mice were immunised *sc* at a single site close to the base of the tail with 200µl of an emulsion containing 50µg recombinant mouse myelin oligodendrocyte glycoprotein consisting of amino acids 1-117 of the extracellular Ig domain (rMOG; provided by Dr. H Reid, Monash University, Clayton, Victoria, Australia) in complete Freund's adjuvant

supplemented with 2.5mg/ml Mycobacterium tuberculosis H37 Ra (Difco Labs, Detroit, MI, USA) on day 0. Mice also received 200ng pertussis toxin (endotoxin of *Bordetella pertussis*; Sigma) *ip* in PBS on days 0 and 2. On day 8 mice were injected with 500µg mouse anti-mouse MOG mAb clone Z12 [223]. Mice were weighed and monitored daily for signs of clinical disease, scored as followed: 0, no clinical signs; 1, tail atony; 2, hind-limb weakness; 3, hind-limb paralysis; 4, moribund; 5, dead. Animals that achieved a clinical score of 2 (day 11) at monitoring were divided in two groups (n=2) and injected with 200µl of 100µg of CD59-2a-CRIg or PBS *iv*. Mice were sacrificed via anaesthesia with *ip* injection of sodium pentobarbitone 15 minutes or 3 hours after injection and perfused via the aorta with PBS with outflow through the transected renal vein. The Spinal cord was promptly removed, embedded in optimum cutting temperature (OCT) compound (Raymond A Lamb Limited, Eastbourne, UK), snap-frozen on dry ice and stored at -80°C until required. Transverse spinal cord sections (10µm) were cut using a cryostat and mounted onto glass slides. The sections were allowed to dry for one hour at room temperature and stored at -80°C.

2.8.6. Induction of atherosclerosis

Male ApoE^{-/-}/CD59^{-/-} double knock out mice were fed on a high-fat diet containing 21% (w/w) pork lard supplemented with 0.15% (w/w) cholesterol (Special Diet Services, Whitham, UK) for 8 weeks starting at 8 weeks of age. Animals were housed in a specific pathogen-free environment. Mice were injected with 200µl of 200µg CD59-2a-CRIg or PBS *iv*. Body weights were measured and animals were sacrificed 30 minutes or 1 hour post administration. At sacrifice, blood samples were collected via cardiac puncture. The mice were anaesthetised with sodium pentobarbitone via *ip* injection. After arterial perfusion with PBS via the abdominal aorta with outflow through the incised jugular veins, brachiocephalic arteries were removed with a piece of the aortic arch and the stump of the right subcavian artery still attached to aid orientation during histological processing. These were immediately embedded in OCT compound and snap-frozen in liquid nitrogen. This experiment was carried out in collaboration with Dr. Tim Hughes who harvested the brachiocephalic arteries. Serial transverse sections, of 7µm thickness, were cut along the brachiocephalic artery, starting from the proximal end.

2.8.7. Immunohistochemical analysis

Frozen sections from the spinal cord or brachiocephalic artery from mice with ADEAE and atherosclerosis respectively (for C3 deposition and CD59-2a-CRIg targeting) and liver (for anti-CRIg mAb analysis) were left to air dry for 20 minutes before fixation in ice-cold acetone for 10 minutes on ice. Spinal cord from a naïve mouse was used as a negative control in the ADEAE experiment and for anti-CRIg mAb characterisation. Sections were washed in PBS before marking with a pap pen and blocking in 10% Normal goat serum diluted in 30 min at room temperature. The sections were stained for C3b deposition or analysed for *ex vivo* or *in vivo* CD59-2a-CRIg targeting. Sections were then incubated with the relevant Abs, isotype control or CD59-2a-CRIg diluted in 1%BSA/PBS for 1 h at room temperature (Table 2.11). In between antibody incubations, the slides were washed three times in PBS for five minutes each. Following incubation with the secondary fluorescently labelled antibody for 30 minutes at room temperature, the slides were counterstained with DAPI (diamidino-2-phenylindole; Sigma-Aldrich) diluted 1:400 in 1%BSA/PBS for 20 minutes. Incubations with antibodies, CD59-2a-CRIg reagent and DAPI were performed at room temperature in a humid chamber. Following washing in PBS and H₂O the sections were air dry and mounted in Vectashield (Vector Laboratories) to prevent fading of the fluorescent signal. Fluorescence microscopy and digital image collection were carried out using Nikon ECLIPSE 80i fluorescence microscope and a Nikon Digital Camera DXm1200F.

Purpose	Targeted reagent	Detecting antibody	Fluorescently labelled antibody (Secondary antibody)
C3 deposition	-	5µg/ml Rat anti-mouse C3 clones 2/11 and 11H9 (HyCult Biotechnology) or rat IgG1 (Caltag Laboratories) isotype control	Alexa Fluor ® 594 donkey anti-rat IgG (H+L) (1:100; Invitrogen)
CD59-2a-CRIG <i>ex vivo</i> targeting	100µg/ml CD59-2a-CRIG/488 (section 2.6.5)	-	-
CD59-2a-CRIG <i>in vivo</i> targeting	-	5µg/ml rat anti-mouse CD59 mAb (mCD59a-7) or rat IgG1 (Caltag Laboratories) isotype control	Alexa Fluor ® 488 goat anti-rat IgG (H+L) (1:100; Invitrogen)
Anti-CRIG mAb characterisation	-	5µg/ml rat anti-mouse CRIG mAb or rat IgG1 (Caltag Laboratories) isotype control	Alexa Fluor ® 488 goat anti-rat IgG (H+L) (1:100; Invitrogen)

Table 2.11 Reagents, antibodies and their working dilutions used for immunohistochemical analysis.

Chapter 3. Cloning and expression of anti-terminal pathway therapeutics

The aim of the work described in this chapter was to clone and express a set of therapeutic agents with potential to inhibit the terminal pathway, these were based either on OmCI or CD59. Two types of anti-complement therapeutics were designed in this research study. OmCI-Fc is a long-lived reagent and CD59-CRIg proteins were engineered to target the site of pathology.

The C5 inhibitor OmCI, is a small protein which is cleared from the body within 30 minutes when injected into experimental animals. This has restricted its therapeutic application only to acute disease and conditions. In order to develop a long-lived reagent suitable for therapy of chronic complement-mediated disease, DNA technology was used in this project to join together the nucleotide sequences encoding for the tick protein, OmCI, and the mouse Fc of IgG2a so that it was expressed as an antibody-like OmCI-Fc fusion protein. The generation of Fc fusion proteins is a strategy employed to increase the serum half-life of protein drugs. Linking of immunoglobulin Fc fragment to complement regulators has been shown previously to increase the half-life of complement regulators and generate effective agents for anti-complement therapy [319, 320, 327].

The second type of anti-complement reagents makes use of the terminal pathway inhibitor, CD59. The MAC regulator has previously been generated in soluble form, however it is a poor inhibitor of complement in a whole serum, a consequence of its small size and its predisposition to bind plasma lipoproteins [376]. To overcome this limitation, CD59 was modified in such a way as to specifically deliver its complement inhibitory activity to the sites of complement activation where it is most needed. This was achieved in this project using the complement receptor, CRIg. CRIg binds complement activation products C3b and iC3b. To develop this efficient and targeted inhibitor, the DNA encoding the functional domain of mouse CD59 was linked to the extracellular domain of mouse CRIg in a chimeric molecule, thus combining the properties of both CD59 and CRIg. It has been shown previously in other CD59-containing constructs that the orientation of the protein moieties within the chimeric molecule and the distance between CD59 and the target surface affected its therapeutic capacity [330, 370, 377]. CD59 was functionally active when fused to the N-terminus of CD59-Crry molecule, however it worked better when linked to the C-terminus of CR2 (CR2-CD59). To address this, DNA constructs encoding CD59 fusion proteins in

different orientations were designed and generated in the current study. The CRlg-CD59 reagents were further modified to increase the targeting efficiency. To achieve this, the ability of antibodies to associate into dimers was utilised and the hinge of mouse IgG3 and IgG2a was incorporated within the CRlg-CD59 chimeric molecule to promote dimerisation. Two antibody hinge domains were tested. IgG3 has the longest upper hinge among the mouse antibody, therefore potentially providing flexibility to the chimeric molecule which may be beneficial for the function [378]; IgG2a core hinge has three cysteines able to form three disulfide inter-chain bonds [379] which may result in more stable CRlg-CD59 dimer.

The detailed design of these agents will be introduced and the strategies that were used to clone these agents into the expression system of choice will be explained step-by-step. Furthermore, generation of stable lines secreting these proteins and approaches used to optimise the yield in static culture systems will be discussed. The purification and functional characterisation of these agents will be described in Chapter 5.

DNA technology has transformed modern science. Advances in DNA technology including polymerase chain reaction (PCR), recombinant DNA techniques, gene therapy, and DNA microarray have already begun to shape medicine and biotechnology. DNA technology allows for the production of biological products including drugs at bulk quantities. By putting human, animal or plant genes into the genetic material of bacteria, mammalian or yeast cells, these cell systems can be used as protein factories to produce recombinant proteins for medical and therapeutic use. The design and production of recombinant proteins (including therapeutic proteins) are processes involving methods and techniques from different fields of basic science- molecular biology, biochemistry, microbiology, and cell biology. Recombinant proteins are proteins encoded by DNA that has been artificially generated. Moreover DNA from two or more sources can be incorporated into a single recombinant molecule to create one recombinant fusion protein. The approach offers an opportunity to create highly efficient therapeutics which combine the functional properties derived from each of the original proteins. This attractive strategy was used in this project to generate targeted drugs based on the complement inhibitor CD59.

Once the DNA encoding the protein of interest is generated it is amplified using PCR to provide material for further manipulations. The amplification products can be “cut” with restriction endonucleases and “glued” into “carrier molecule” using DNA ligase. This is

used as a “transport vehicle”. In order to transfect cells for expression of recombinant protein or drug, the DNA encoding the molecule has to be replicated and purified. This usually can be done in bacterial cells such as *E. coli*. This organism has been studied for many years by molecular biologists and it is now known that its genome contains 4.2 million base pairs. The bacterium also possesses extrachromosomal DNA molecules known as plasmids that can replicate independently of the nuclear DNA. These plasmids are closed single pieces of supercoiled DNA which can be stably inherited by daughter cells. They have the ability to replicate to high copies within each bacterial cell. Therefore the plasmids can be used as a “transport vehicle” known as a “vector”. The introduction of recombinant plasmid into bacterial cells is referred to as transformation. Replicating the vector will amplify the DNA of interest inserted into the plasmid. This will generate enough material for further manipulations. Plasmid vectors are also used to transfer DNA from the prokaryotes to eukaryotic cells to generate the recombinant proteins. In order to achieve correct glycosylation and to avoid contamination with bacterial toxins, a mammalian cell line was chosen to express the recombinant therapeutic proteins. For this project Chinese Hamster Ovary (CHO) cells were used. These cells are one of the most popular hosts for production of therapeutics. They are able to perform appropriate and efficient post-translational modifications of complex proteins and the glycosylation pattern of recombinant proteins produced in CHO cells is very similar to that of native proteins [380]. Glycosylation is particularly essential for Fc fusion proteins (OmCI-Fc in this project). It is crucial for the structure and many effector functions of the antibody Fc domain [381-384].

3.1. Design of anti-complement therapeutics

The experiments described in this chapter are:

1. Generation of a soluble, long-lived anti-complement therapeutic: OmCI-Fc (Fig.3.1).
 - Cloning cDNA encoding the soft tick salivary protein, OmCI, into the pDR2 expression vector which also contains DNA encoding the mouse IgG2a Fc domain.
 - Transfection of CHO cells with the engineered plasmid constructs and analysis of protein expression.

- Bulk production of OmCI-Fc

2. Generation of targeted anti-complement therapeutics: CRIg-CD59, CD59-CRIg, CRIg-3-CD59*, CD59-3-CRIg*, CRIg-2a-CD59*, CD59-2a-CRIg*, and finally the cleavable control protein CD59-CRIg. These agents are illustrated schematically in Fig 3.2. (* 3 stands for hinge of mouse IgG3 and 2a stands for hinge of mouse IgG2a).

- Cloning cDNA encoding extracellular domain of mouse CRIg into the pDR2 Δ EF1 α vector to generate CRIg-pDR2 vector.
- Cloning cDNA encoding extracellular domain of mouse CD59a into CRIg-pDR2 vector.
- Cloning cDNA encoding the hinge region of mouse IgG2a or IgG3 into CRIg-CD59-pDR2 vector between CRIg and CD59.
- Transfection of CHO cells with the engineered plasmid constructs and analysis of protein expression.
- Bulk production of CD59-CRIg fusion proteins.

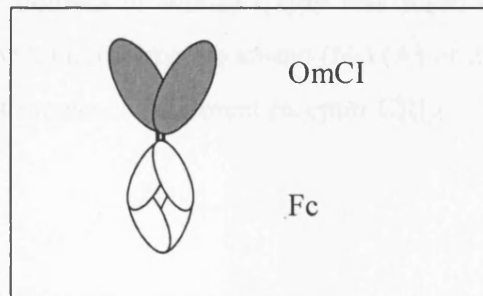


Fig. 3.1 Schematic diagram of OmCI-Fc. To generate the chimeric antibody-like molecule, the Fab fragments of mouse IgG2a were replaced with OmCI. Two molecules of OmCI were linked to Fc portion of mouse IgG2a antibody. Fc comprises hinge, CH2 and CH3 domains of the antibody molecule.

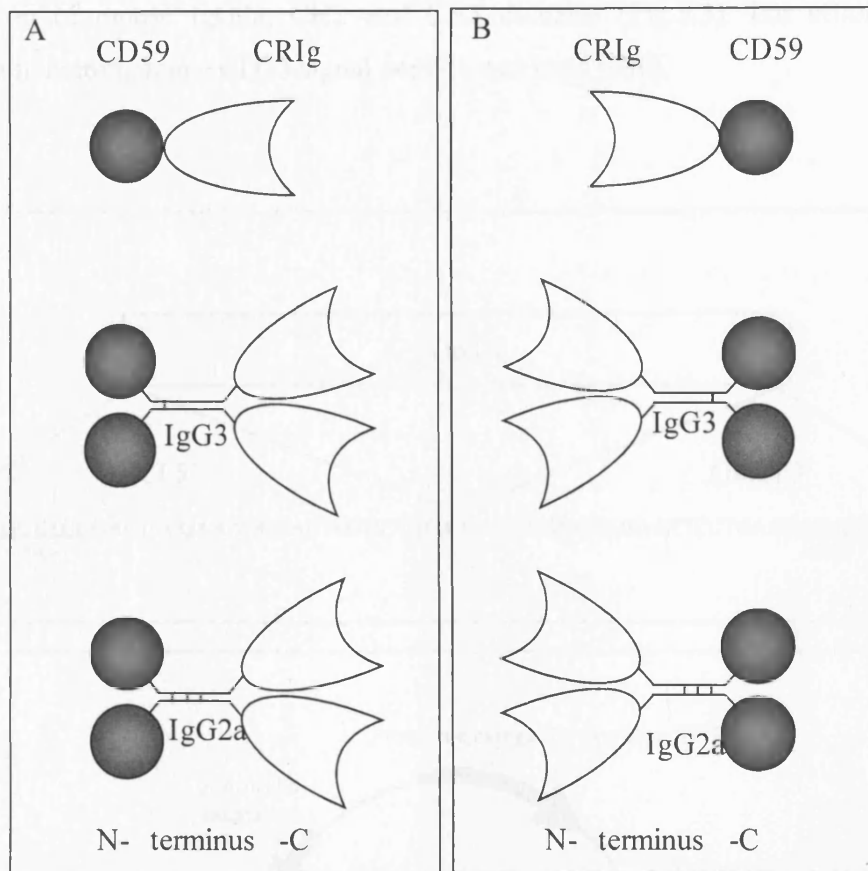


Fig.3.2 Diagram of CD59 containing fusion proteins. To generate CD59 targeted reagents, the extracellular domain of mouse CD59 was fused directly or through a hinge (taken from mouse IgG3 or IgG2a) either to amino (N-) (A) or carboxy (C-) terminus (B) of the extracellular domain of mouse complement receptor CRIg.

3.2. Generation of OmCI-Fc

Fc fusion proteins are promising dimers designed to be effective as a long-term agents *in vivo* [385]. The aim of this project is to increase the molecular weight and prolong the half-life of the C5 inhibiting protein, OmCI, to generate a powerful long lasting anti-complement drug (Fig.3.1). This will be achieved by linking OmCI to Fc antibody domain to increase the molecular weight of the protein and also bind to the FcRn, to protect the Fc coupled molecule from degradation via a recycling mechanism. Thus OmCI-Fc is an antibody-like molecule with the C5 binding protein replacing the Fab arms (Fig.3.1). The expression vector was engineered to contain DNA encoding OmCI upstream of DNA encoding the

hinge region of mouse IgG2a, CH2 and CH3 domains (Fig.3.3). For efficient protein production in mammalian a CD33 signal peptide was used [386].

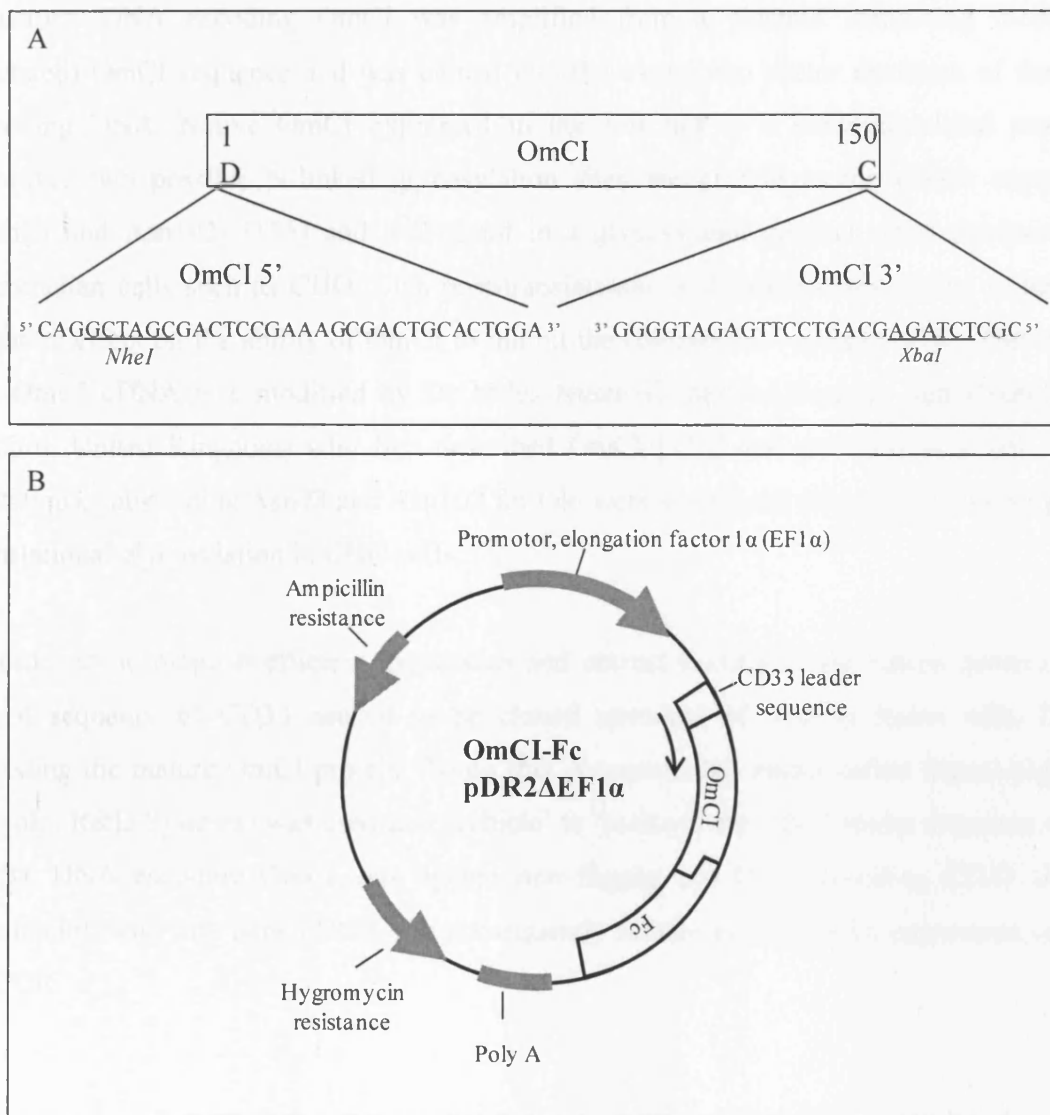


Fig. 3.3 Schematic representation of the expression plasmid pDR2ΔEF1α encoding OmCI-Fc fusion protein. A. OmCI cDNA was amplified. The sequences and positions of primers used for amplification of OmCI are shown. The incorporated restriction sites are underlined. B. The OmCI cDNA digested with restriction enzymes was ligated into plasmid in a frame with sequence encoding Fc portion of mouse IgG2a. CD33 leader sequence was used for efficient expression of OmCI-Fc.

3.2.1. Cloning strategy

The strategy used to generate plasmid encoding OmCI-Fc protein was shown in Fig.3.4. The Fc domain of mouse IgG2a was cloned in pDR2ΔEF1α (Fig.3.4A) to create the Fc-pDR2 construct. DNA encoding OmCI was amplified from a plasmid containing modified (mutated) OmCI sequence and was cloned into the expression vector upstream of the Fc-encoding DNA. Native OmCI expressed in the soft tick is a nonglycosylated protein. However two possible N-linked glycosylation sites are present in the cDNA sequence (Asn78 and Asn102) [175] and will result in a glycosylated product when produced in mammalian cells such as CHO. This post-translational modification was shown to have a negative effect on the ability of OmCI to inhibit the complement cascade [175]. Therefore, the OmCI cDNA was modified by Dr Miles Nunn (Centre for Ecology and Hydrology, Oxford, United Kingdom) who first described OmCI [175] and provided as a gift. Two mutations, substituting Asn78 and Asn102 for Gln were introduced (Fig.3.5) to abolish post-translational glycosylation in CHO cells.

In order to accomplish efficient expression and correct folding of the fusion protein, the signal sequence of CD33 needed to be cloned upstream of, and in frame with, DNA encoding the mature OmCI protein. To do this, a commercial vector called Signal pIgPlus (SigpIg, R&D Systems) was used as a 'vehicle' to 'pick up' the CD33 leader sequence (Fig. 3.6B). DNA encoding OmCI was ligated into SigpIg and DNA encoding CD33 signal peptide in frame with OmCI DNA was subsequently subcloned into the Fc-expression vector by PCR.

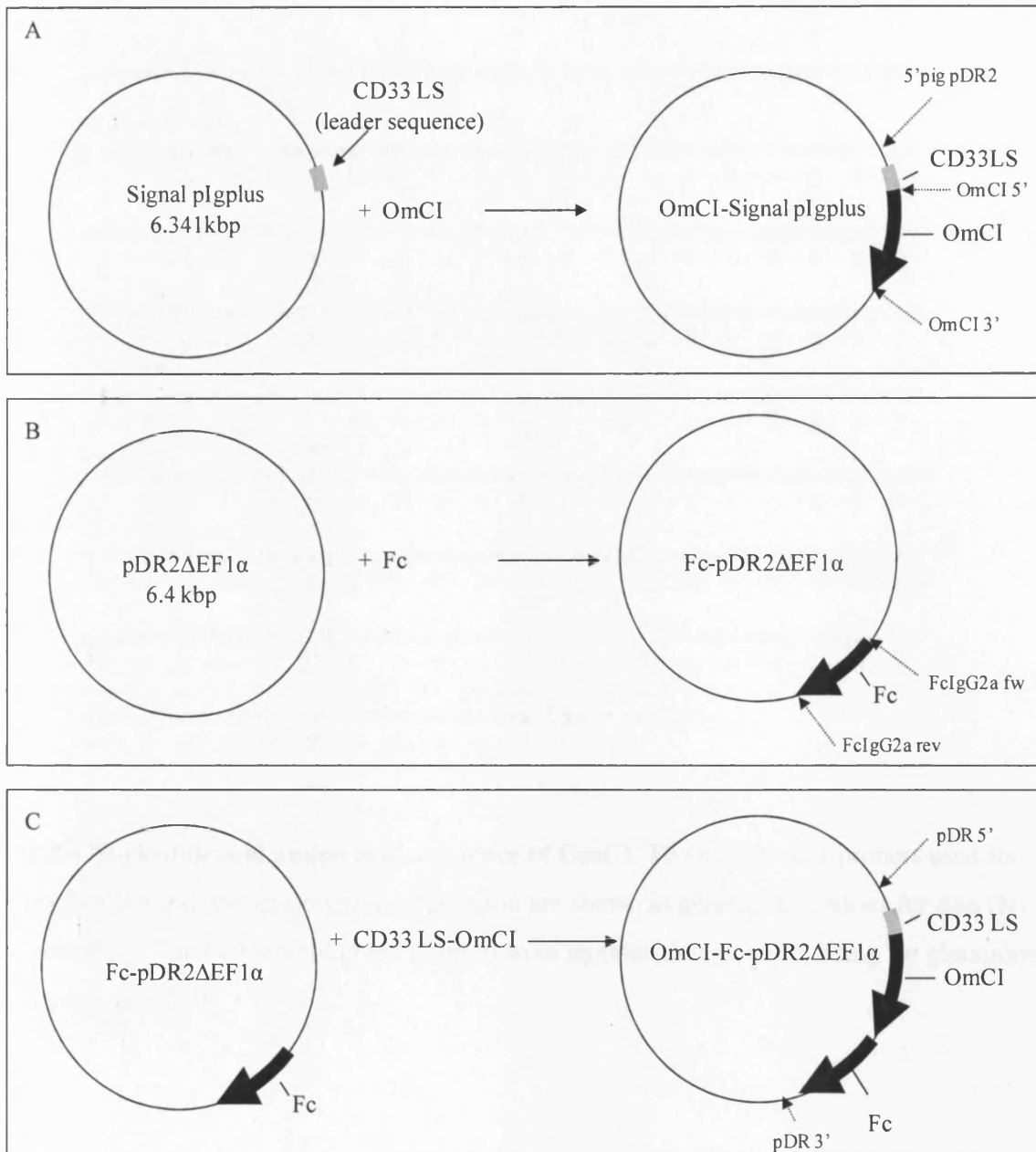


Fig.3.4 Generation of OmCI-Fc encoding construct. Cloning strategy. A. DNA encoding the sequence of OmCI was cloned into Signal pIgplus vector in frame with and downstream of the CD33 leader sequence. B. DNA encoding the Fc of mouse IgG2a was ligated into pDR2ΔEF1α to generate Fc-pDR2 vector. C. Signal pIgplus vector encoding OmCI was used as a template to amplify sequence encoding CD33 leader sequence-OmCI. The PCR product was cloned into Fc-pDR2 vector in frame with and upstream of the DNA encoding IgG2a Fc. Positions of primers used for cloning and sequencing are shown with dotted arrows.

taagagctcaaaatgctgggttttggtgaccctgattttctccttttctgcaacatcgca

OmCI 5' primer

tatgctgacagcgaaagcgactgcactggaagcgaacctgttgacgccttccaagctttc

·D·S·E·S·D·C·T·G·S·E·P·V·D·A·F·Q·A·F·

agtgagggcaaagaggcatatgtcctgggtgaggtccacggatcccaaagcgagggactgc

·S·E·G·K·E·A·Y·V·L·V·R·S·T·D·P·K·A·R·D·C·

ttgaaaggagaaccagccggagaaaagcaggacaacacgttgccggtgatgatgacgttt

·L·K·G·E·P·A·G·E·K·Q·D·N·T·L·P·V·M·M·T·F·

caa

aaagaatggcacagactgggcttcaaccgattggacgtttactttggacggcgcaaaggta

·K·N·G·T·D·W·A·S·T·D·W·T·F·T·L·D·G·A·K·V·

Q

caa

acggcaacccttggtaacctaaccctcaaaataggggaagtgggtctacgactcgcaaagtc

·T·A·T·L·G·N·L·T·Q·N·R·E·V·V·Y·D·S·Q·S·H·

Q

cactgccacgttgacaaggtcgagaaggaagttccagattatgagatgtggatgctcgat

·H·C·H·V·D·K·V·E·K·E·V·P·D·Y·E·M·W·M·L·D·

gcgaggagggttgaagtggaagtcgagtgctgcccgtcaaaagcttgaagagttggcgtct

·A·G·G·L·E·V·E·V·E·C·C·R·Q·K·L·E·E·L·A·S·

OmCI 3' primer

ggcaggaaccaaagtgtatccccatctcaaggactgctaggcggcc

·G·R·N·Q·M·Y·P·H·L·K·D·C·*·

Fig.3.5 Nucleotide and amino acid sequence of OmCI. The positions of primers used for amplification and restriction site incorporation are shown in **green**. The codons for Asn (N) at positions 78 and 102 (highlighted in blue) were mutated to codons encoding for glutamine (Q) (shown in red).

3.2.1.1. Cloning of DNA encoding mouse IgG2a Fc

Fc, consisting hinge region, C_H2 and C_H3 of mouse IgG2a (Fig.3.7) was previously cloned into pDR2ΔEF1α vector in our lab. Briefly, DNA encoding the Fc of IgG2a was amplified from a hybridoma cell line secreting monoclonal mouse IgG2a antibody. The Fc was amplified using sense primer FcIgG2a fw and anti-sense-FcIgG2a rev (primers listed in Table 3.1). FcIgG2a fw contained a BamHI restriction site at the 5' end and overlapped the DNA encoding the hinge of IgG2a. Primer FcIgG2a rev introduced a SmaI restriction site at the 3' end.

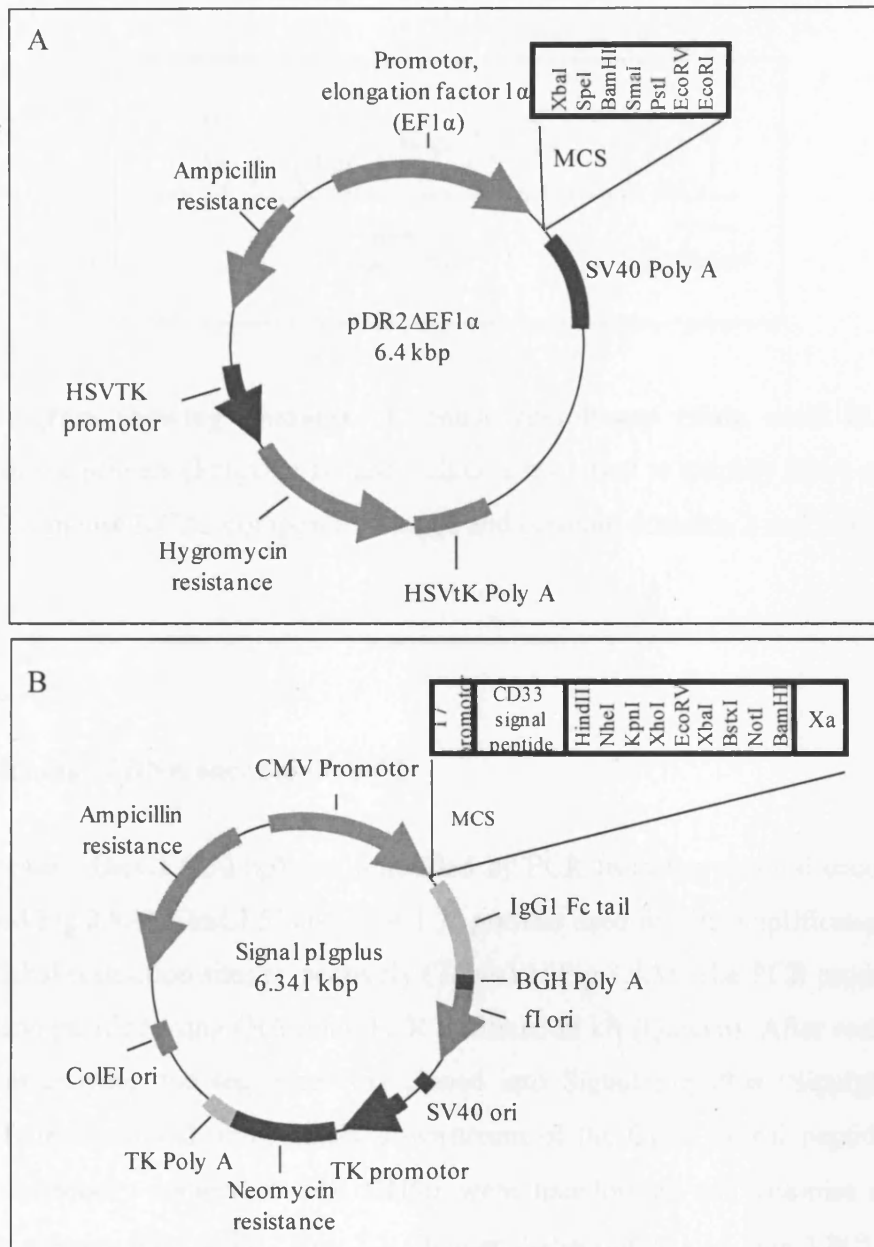


Fig.3.6 Vectors used for cloning. A. pDR2ΔEF1α expression vector. B. Signal pIgplus expression vector encoding CD33 leader sequence.

The amplification product was purified, digested with relevant enzymes and ligated in to pDR2ΔEF1α to generate Fc-pDR2 construct (Fig.3.4 B). Chemically competent cells DH5α were transformed with the construct by heat shock and bacterial colonies were screened for presence of the insert (Chapter 2, sections 2.1.10 and 2.1.11). A positive colony was selected and expanded and the plasmid was purified by QIAquick® spin miniprep purification kit. The fidelity of the Fc sequence was confirmed by sequencing Chapter 2, sections 2.1.13).

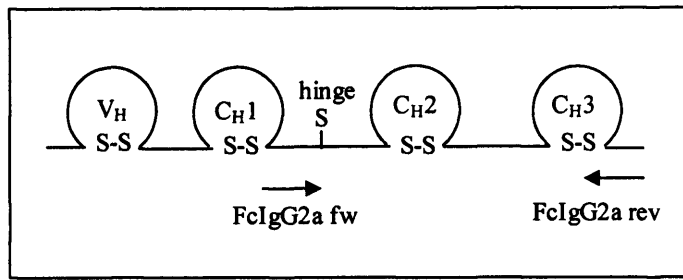


Fig.3.7 Diagram showing domains of mouse IgG heavy chain used in OmCI-Fc. Positions of the primers (FcIgG2a fw and FcIgG2a rev) used to amplify DNA encoding the Fc portion of mouse IgG2a, composed of hinge and constant domains 2 and 3 (C_H2 and C_H3) are shown.

3.2.1.2. Cloning of DNA encoding OmCI

cDNA encoding OmCI (450 bp) was amplified by PCR from the plasmid encoding OmCI (Fig.3.5 and Fig.3.8A). OmCI 5' and OmCI 3' primers used for the amplification contained NheI and XbaI restriction sites respectively (Table3.1; Fig.3.3A). The PCR product was gel-extracted and purified using QIAquick PCR purification kit (Qiagen). After restriction with the relevant enzyme, the sequence was cloned into Signal pIg Plus (SigpIg) (Fig.3.8B) vector in frame with and immediately downstream of the CD33 signal peptide sequence. Bacterial chemically competent cells DH5 α were transformed and colonies screened by PCR using primers located in Table 2.2 Chapter 2 (Section 2.1.11, Fig.3.8C). A positive colony was grown up and plasmid encoding CD33 signal peptide-OmCI was purified using QIAprep[®] spin Miniprep kit (Qiagen). OmCI-SigpIg vector was then used as a template to amplify a sequence encoding CD33 signal peptide-OmCI. Both, sense primer 5'pig pDR2 and anti-sense primer OmCI 3' used for this PCR reaction incorporated XbaI restriction sites at 5' and 3' ends of the amplification product. The position of the primers is shown in Fig3.4. CD33 signal peptide-OmCI DNA sequence was then purified from the plasmid template using QIAquick PCR purification kit (Qiagen), digested with XbaI (Fig.3.8D) and ligated into Fc-pDR2 previously restricted with XbaI and SpeI, OmCI-encoding DNA was in frame with and upstream of the Fc DNA. The usage of SpeI restriction enzyme to digest Fc-pDR2 was possible since it generates 'sticky ends' compatible with XbaI (used in CD33

signal peptide-OmCI digest). Chemically competent cells DH5 α were transformed using heat shock. Bacterial colonies were screened by PCR for expression of the insert (Fig.3.8E). A positive colony was selected, grown up and plasmid DNA was purified. Sequencing confirmed that no errors had been introduced by PCR.

Construct	Primer name and sequence	Incorporated restriction sites
OmCI 5'	CAGGCTAGCGACTCCGAAAGCGACTGCACTGGA	NheI
OmCI 3'	CGCTCTAGAGCAGTCCTTGAGATGGGG	XbaI
5'pig pDR2	CGATCTAGATAACTAGAGAACCCACTG	XbaI
FcIgG2a fw	CGCGGATCCGGTGGTGGTGGCAGTGGTGGT	BamHI
FcIgG2a rev	GCGCCCGGGTCATTTACCTGGAGTCCTGGAGAAGC	SmaI
pDR5'	CAAGCCTCAGACAGTGGTTC	-
pDR3'	ATGTCTGGATCGGTGCGGGGC	-

Table 3.1 Primers used for generating OmCI-Fc fusion protein. The primer name and primer sequence are listed. The introduced restriction sites are shown in boldface.

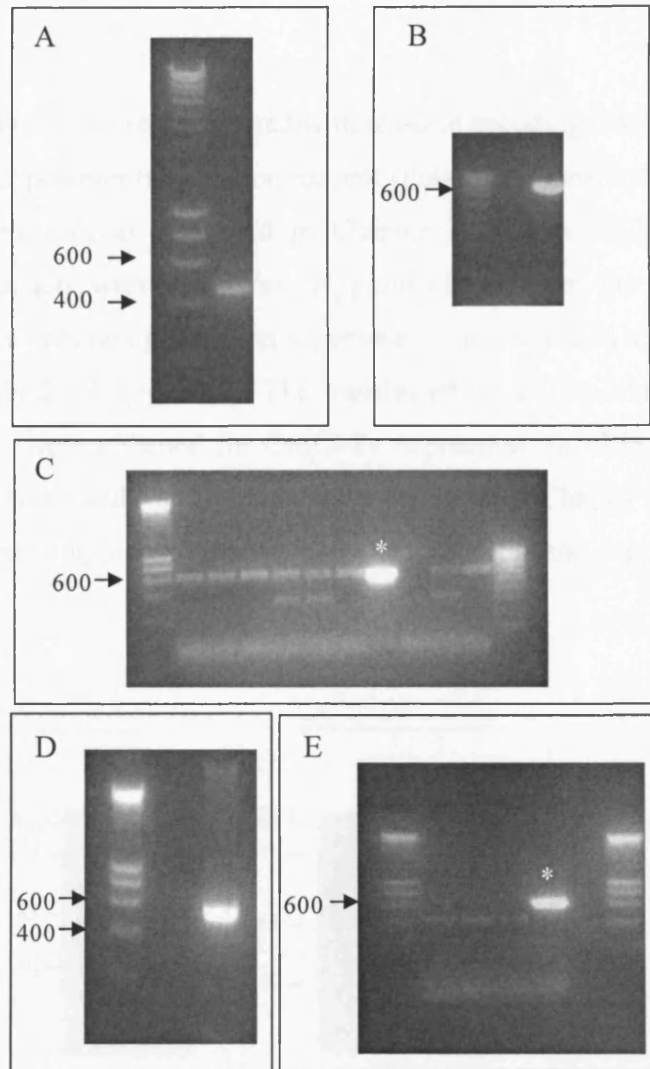


Fig.3.8 Generation of OmCI-Fc. PCR amplification and bacterial screening. A. DNA encoding OmCI (450bp) amplified and visualised by gel electrophoresis. B. Signal pIgplus (Sig pIg) vector was digested with NheI and XbaI restriction enzyme and 3 μ l of the reaction was loaded on agarose gel. C. PCR screen of colonies containing Sig pIg vector encoding OmCI. Primers 5'pig pDR2 and OmCI 3' were used for the amplification. A band with an identical size (~600bp) appeared in 9 out of 10 tested colonies. However only the band with the highest intensity (indicated by asterisk) came up positive for insert after sequence analysis. D. DNA encoding CD33 signal peptide-OmCI, obtained by PCR from Sig pIg vector encoding OmCI was digested with XbaI and visualised by gel electrophoresis. E. DNA encoding CD33 signal peptide-OmCI was subcloned into Fc-pDR2 vector in a frame with Fc. Competent bacterial cells were transformed and bacterial colonies tested by PCR for insert. Primers pDR2 5'and OmCI 3' were used for the amplification. Positive colony is indicated by asterisk.

3.2.2. Transfection

For expression, CHO cells were transfected with plasmid encoding OmCI-Fc fusion proteins using JetPEI cationic polymer transfection reagent (Poly Plus Transfection) according to the manufacturer's instructions as described in Chapter 2, section 2.2.3. Stable lines were established by selection with 400 $\mu\text{g/ml}$ Hygromycin B over the course of 4 days. Expression of the recombinant proteins in supernatant was confirmed at day five by western blot analysis (section 2.4.4, Fig.3.9A). The transfected cells were cloned out by limiting dilution. The clones were screened for OmCI-Fc expression by ELISA and Western blot (Fig.3.9B). The methods used for screening were explained in Chapter 2, sections 2.4.4 and 2.4.6. The cells expressing high levels of protein were selected and expanded.

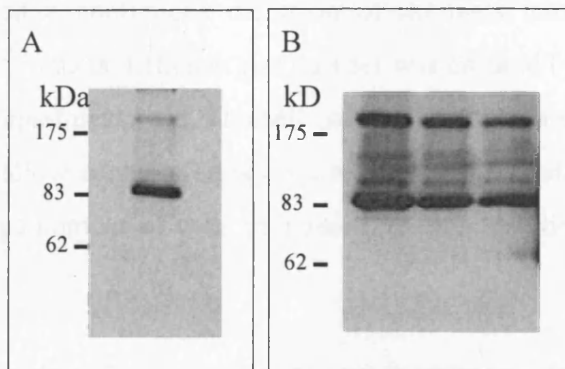


Fig.3.9 Western blot analysis for OmCI-Fc expression and clone selection

A. OmCI-Fc expression. Tissue culture supernatant from CHO cells expressing OmCI-Fc was harvested and subjected to SDS-PAGE on 7.5% gel under nonreducing conditions and a western blot was carried out using affinity purified rabbit anti-OmCI polyclonal antibody. Molecular weight markers are shown on left. OmCI-Fc appeared as a band with molecular weight of 83 kDa. The additional, higher molecular weight band is likely to represent protein aggregates. B. Clone screening. CHO cells expressing OmCI-Fc were cloned out by limiting dilution in 96-well plate. Tissue culture supernatant from wells containing a single colony was subjected to western blot. The three tested clones expressed similar levels of OmCI-Fc.

3.2.3. Large-scale protein expression

To scale up OmCI-Fc production two high-density cell culture systems were tested. The selected clones expressing OmCI-Fc were expanded and transferred into either a two-compartment bioreactor CELLLine AD1000 (Integra Bioscience) or High Yielding Performance Flask (Corning @HYPERFlask Cell culture vessel).

3.2.3.1. Integra CELLLine AD1000flasks

CELLLine AD 1000 consists of two compartments separated by a 10kDa semi-permeable cellulose acetate membrane (Fig.3.10). The cells were cultured in the small compartment and the medium compartment was filled with medium as described in section 2.2.6.1. The membrane allowed a continuous diffusion of nutrients into the cell compartment and removal of waste products. Efficient gas transfer was ensured by a silicone membrane which forms the cell compartment base. The cell compartment contains a polyethylene terephthalate matrix design to allow adherent cells such as CHO cells to attach. This technology allows the culture of large number of cells in a small volume resulting in a high concentration of secreted protein.

CHO cells secreting OmCI-Fc were harvested from T80 flasks in log phase of growth. They were pelleted and resuspended in 15ml of RPMI medium supplemented with 10% low Ig FCS. The cells were then inoculated into CL AD1000flask. Ten days later tissue culture supernatant from the cell compartment was harvested and tested for OmCI-Fc. The presence of OmCI-Fc was confirmed by western blot analysis (Fig.3.11) and the yield quantified by ELISA using a standard curve. For western blot analysis, the proteins were separated on 7.5% gel and transferred to a nitrocellulose membrane. The membrane was probed with affinity purified rabbit anti-OmCI polyclonal antibody (generated in house). As expected, two bands were detected. The band with approximate molecular weight of 90kDa was OmCI-Fc (Fig.3.11). The higher molecular weight band was probably an aggregation product.

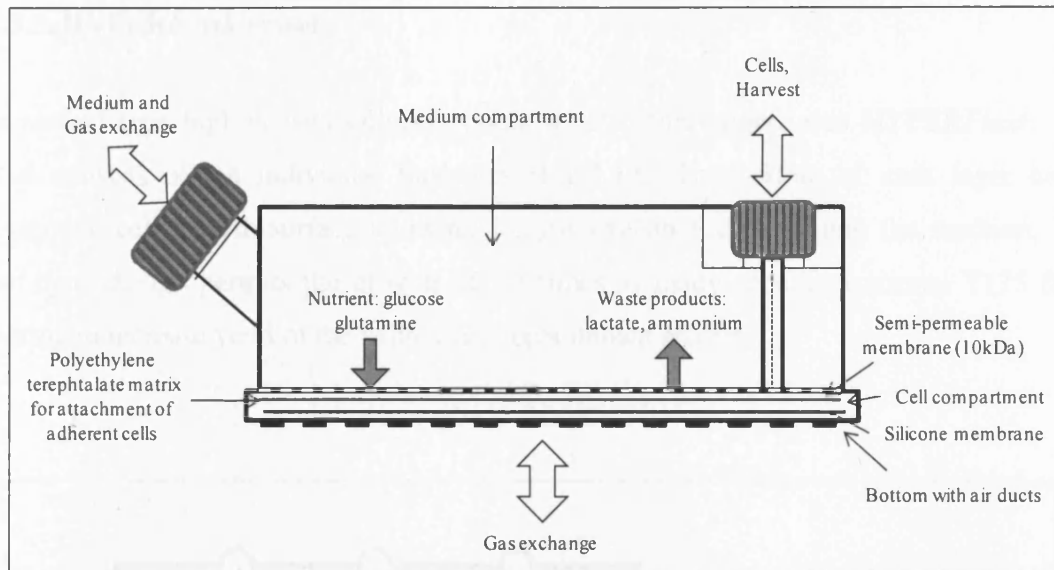


Fig.3.10 Schematic representation of CELLine AD1000. CELLine AD1000 is a high density tissue culture system consisting of cell and medium compartments. The cells are cultured in high density in the cell compartment and fed by nutrients from the medium compartment passing over a semi-permeable membrane. The protein of interest is secreted in the cell compartment. Efficient gas transfer of the cell compartment is ensured by a silicone membrane. The medium is gassed via the lid.

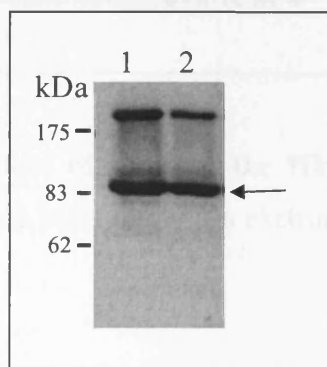


Fig. 3.11 Western blot analysis of cells expressing OmCI-Fc fusion protein. Supernatant was harvested from CHO cells expressing OmCI-Fc cultured in CELLine AD 1000 (lane1) flask and HYPERFlask vessel (lane 2), proteins were separated on a 7.5% gel and transferred to nitrocellulose membrane. The western blot was probed with rabbit anti-OmCI polyclonal antibody. OmCI-Fc was detected in the supernatant from both types of high-density culture systems. OmCI-Fc appeared as a major band with approximate molecular weight of 90kD in both supernatants (indicated with arrow). High molecular weight aggregates were seen on both lanes.

3.2.3.2. HYPERFlask vessel

The second type high-density culture system used in this project was HYPERFlask. The vessel consists of ten individual flaskettes (Fig.3.12). The bottom of each layer has a polystyrene cell growth surface allowing for gas exchange directly into the medium. The multi-layer design permits the growth of ten times as many cells as a normal T175 flask resulting in increase yield of the expressing recombinant protein.

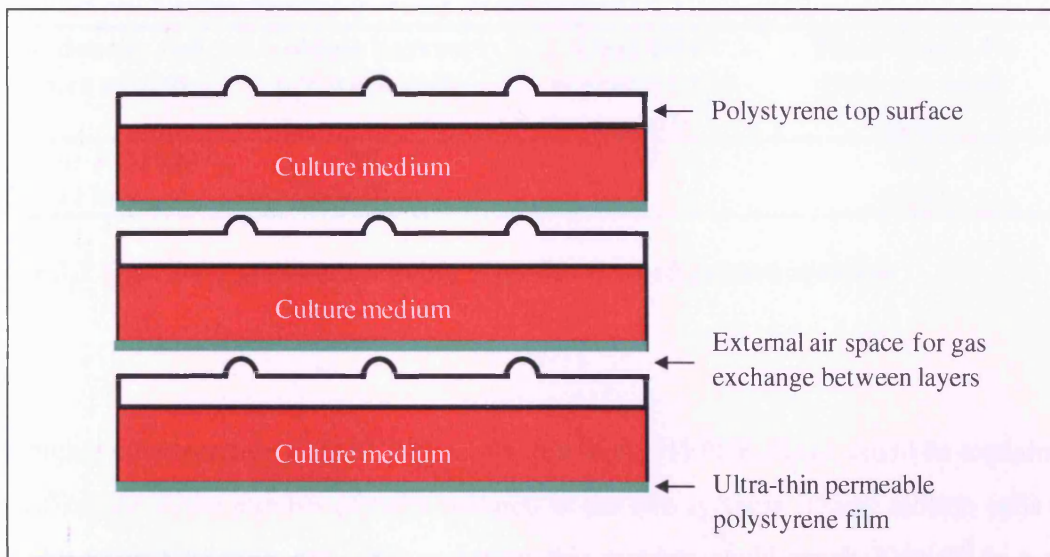


Fig.3.12 Schematic representation of three of the HYPERFlask vessel's ten culture layers. The air gaps between each layer allow gas exchange through the ultra-thin bottom growth surfaces.

CHO cells secreting OmCI-Fc were into HYPERFlask vessel. The tissue culture supernatant was harvested every six days and replaced with fresh medium as described in section 2.2.6.2. Protein production was confirmed by western blot analysis (Fig.3.11). Similarly to OmCI-Fc obtained from the CELLline AD 1000 flask, two bands were observed after probing with Rb anti-OmCI. OmCI-Fc appeared as a band with apparent molecular weight of 90kDa. This result suggested that OmCI-Fc fusion protein expressed in CELLline AD 1000 flask and HYPERFlask had an identical molecular mass and a similar level of aggregate formation.

To determine the level of OmCI-Fc expression, a quantitative ELISA was performed on tissue culture supernatant arising from both culture systems. The assay was described in method section 2.4.7. OmCI-Fc was calculated using a standard curve (Fig.3.13). The analysis revealed that the cells cultured in the HYPER *Flask* produced OmCI-Fc at concentrations 4µg/ml. However 450ml tissue culture supernatant was obtained every six days giving 1800µg of the recombinant protein per harvest contrasting with the weekly yield of 10.5µg in the CELLline AD1000 (Table3.2).

High density cell culture system	Volume harvest per week (ml)	OmCI-Fc concentration (µg/ml)	Total OmCI-Fc yield per week (µg)
CELLline AD1000	15	0.7	10.5
HYPER <i>Flask</i>	450	4	1800

Table 3.2 OmCI-Fc production using high-density cell culture systems

The higher concentration of OmCI-Fc expressed in the HYPER *Flask*, could be explained by the difference in the number of cells cultured in the two systems. Thirty million cells could be cultured in CELLline AD 1000, whereas this number could reach 200×10^6 in a single HYPER*Flask*. HYPER *Flask* was more efficient in terms of protein production and therefore was used to bulk-up OmCI-Fc fusion protein.

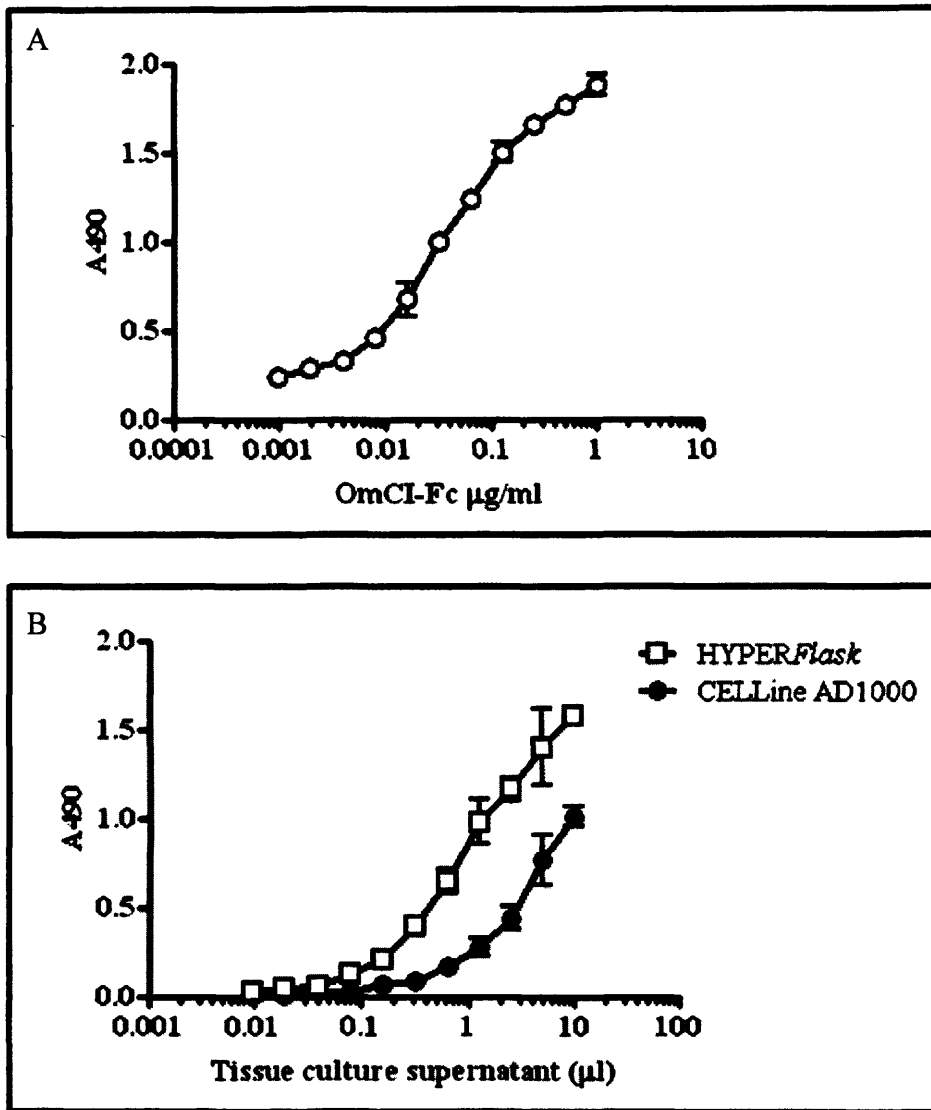


Fig.3.13 ELISA analysis of OmCI-Fc expression level of CHO cells cultured in CELLLine AD1000 flask and HYPERFlask vessel. Tissue culture supernatant, 15ml and 450ml was harvested from CELLLine AD1000 flask and HYPERFlask vessel respectively. Serial dilutions from the tissue culture supernatant and pure OmCI-Fc were prepared and added to ELISA plate coated with mouse anti-OmCI mAb. OmCI-Fc was detected with affinity purified rabbit anti-OmCI polyclonal antibody. A standard curve was generated from the pure OmCI-Fc (A). The amount of tissue culture supernatant added to the wells was plotted (X-axes) versus the absorbance at 490nm (Y-axes) (B). Higher level of OmCI-Fc was detected in tissue culture supernatant from HYPERFlask vessel (open square) comparing to CELLLine AD1000 flask (black circle). To determine the concentration of OmCI-Fc, a cubic-spline curve was fitted to the standards and the unknown values were interpolated from the standard curve. The analysis was performed using GraphPad Prism 5.0 software.

3.3 Generation of fusion proteins consisting of CRIG and CD59

To generate fusion proteins, the extracellular domain of mouse CRIG was linked to either the N terminus or the C terminus of mouse CD59a. DNA encoding the membrane-anchoring domains was excluded from these constructs as illustrated in Fig.3.14.

3.3.1 Construction of expression plasmids

3.3.1.1 CRIG-CD59, CRIG-3-CD59 and CRIG-2a-CD59

To generate CRIG-CD59, CRIG-3-CD59 and CRIG-2a-CD59 fusion proteins (Fig.3.2A), DNA encoding extracellular domain of murine CRIG was required. Total RNA was isolated from mouse liver and RT-PCR was performed. The cDNA generated by RT-reaction was used as template to amplify the extracellular domain (including the signal sequence) of mouse CRIG (Fig.3.14). The PCR was carried out using primers containing restriction sites. The forward primer CRIG amino5' introduces XbaI and the reverse primer CRIG amino3' introduced a BamHI restriction site (Fig.3.15A). Following purification of the PCR product (Fig.3.15C), it was digested with XbaI and BamHI and ligated into pDR2 Δ EF1 α vector. Chemically competent cells DH5 α were transformed using heat shock. Bacterial colonies were screened by PCR for inclusion of the insert. A positive colony was selected, grown up and plasmid DNA was purified. The DNA sequence of the insert was checked by sequencing analysis.

DNA encoding the 72 N-terminal amino acids of mouse CD59a was amplified from a vector that had previously been engineered in house to contain mouse CD59a encoding sequence (Fig.3.15B and C). PCR primers containing BamHI and EcoRV restriction sites were used. The reverse primer was designed to introduce a stop codon prior to Asp-74, to which the GPI anchor attaches (Fig.3.15B) and thus deleting the GPI-addition signal sequence from the CD59 DNA construct. The DNA obtained from this PCR did not contain the CD59 leader sequence. The PCR product was extracted from the agarose gel and digested with BamHI and EcoRV. The plasmid containing CRIG sequence (CRIG-pDR2) was also subjected to the same digestion procedure followed by a dephosphorylation step (Method 2.1.14). The

CD59a insert was ligated into CRIG-pDR2 in frame and downstream of CRIG to create a construct encoding CRIG-CD59 fusion protein.

```

CRIG amino 5'
gagctaccagcacttccaggttcttcagcagcaagaggatggaaggatgaatagaagtag

Signal sequence →
cttcaaataaggatggagatctcatcaggcttgctgttctctgggccacctaatagtgctca
·M·E·I·S·S·G·L·L·F·L·G·H·L·I·V·L·
IgV → CRIG carboxy 5'
cctatggccacccacccctaaaaacacctgagagtgtagacagggacctggaaaggagatg
T·Y·G·H·P·T·L·K·T·P·E·S·V·T·G·T·W·K·G·D·
tgaagattcagtgcatctatgatccctgagaggetacaggcaagttttggtgaaatggc
V·K·I·Q·C·I·Y·D·P·L·R·G·Y·R·Q·V·L·V·K·W·

tgtaagacacggctctgactccgtcaccatcttcctacgtgactccactggagaccata
L·V·R·H·G·S·D·S·V·T·I·F·L·R·D·S·T·G·D·H·

tccagcaggcaaagtacagaggccgctgaaagtgagccacaaagttccaggagatgtgt
I·Q·Q·A·K·Y·R·G·R·L·K·V·S·H·K·V·P·G·D·V·

ccctccaaataataaccctgcagatggatgacaggaatcactatacatgtgaggtcacct
S·L·Q·I·N·T·L·Q·M·D·D·R·N·H·Y·T·C·E·V·T·
ggcagactcctgatggaaaccaagtaataagagataagatcattgagctccgtgttcgga
W·Q·T·P·D·G·N·Q·V·I·R·D·K·I·I·E·L·R·V·R·
aatataatccacctagaatcaataactgaagcacctacaaccctgcactcctctttggaag
K·Y·N·P·P·R·I·N·T·E·A·P·T·T·L·H·S·S·L·E·
caacaactataatgagttcaacctctgacttgaccactaatgggactggaaaacttgagg
A·T·T·I·M·S·S·T·S·D·L·T·T·N·G·T·G·K·L·E·
amino/carboxy 3' Trans membrane domain →
agaccattgctggttcagggaggaacctgccaatctttgccataatcttcatcatctccc
E·T·I·A·G

intracellular
tttgctgcatagtagctgtcaccataccttatatcttggctccgctgaggacattccaac

domain →
aagagtatgtctatggagtgagcaggggtttgccaggaagacaagcaactctgaagaaa

```

Fig.3.14 Nucleotide and amino acid sequence of mouse CRIG. Variable region (IgV) of CRIG is shown in boldface. The signal sequence is highlighted in green. The positions of primers used for amplification and restriction site incorporation are shown in red. To generate vector construct encoding fusion protein with CRIG fused to the N-terminus of CD59 (CRIG-CD59 or CRIG-hinge-CD59) CRIG encoding DNA was amplified using primers CRIG amino 5' and CRIG amino 3'. The PCR product contained sequence encoding the signal peptide (in green) and IgV. To generate reagents in reverse orientation (CD59-CRIG or CD59-hinge-CRIG), primers CRIG carboxy 5' and CRIG carboxy 3' were used. This gave rise to DNA encoding IgV of CRIG but not the signal peptide. For these reagents CD59 signal peptide was used. Primer CRIG carboxy 3' adds stop codon to the 3' end of the PCR product.

The common BamHI restriction site in both CRIG and CD59 cDNA formed a link between the DNA fragments (Fig.3.15D). DH5 α chemically competent bacteria were transformed and colonies screened by PCR for insert expression. A positive colony was selected, grown up and plasmid DNA was isolated. The sequence was checked for fidelity.

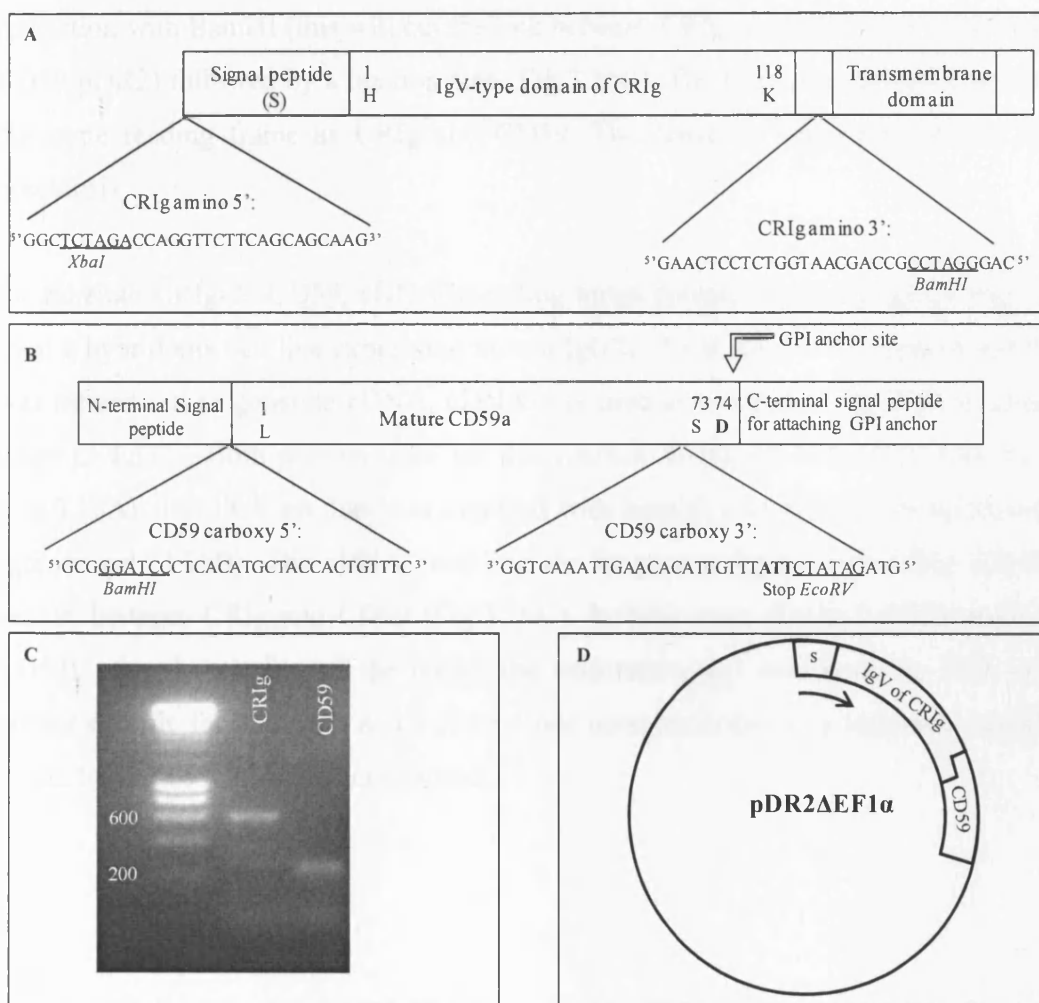


Fig.3.15 CRIG-CD59: construction of expression plasmid. Schematic diagrams of mouse CRIG (A) and mouse CD59 (B). The sequences and positions of primers used for amplification of extracellular domains of CRIG and CD59a are shown. The incorporated restriction sites are underlined. The stop codon is shown in boldface. The amplification products were visualised by gel electrophoresis (C), digested with appropriate enzymes and ligated into expression vector pDR2 Δ EF1 α to create CRIG-CD59 encoding construct (D).

In order to generate CRlg-3-CD59, cDNA, encoding hinge of mouse IgG3 was amplified by PCR. Total RNA was isolated from mouse spleen and reverse transcribed. The generated cDNA was used as a template to PCR-amplify the hinge of IgG3 (Fig.3.16A). The primers used for this PCR amplification step were designed to add BamHI restriction sites to 5' and 3' end of the hinge. The size of the amplification product was confirmed on agarose gel (Fig.3.16B). The PCR product and the plasmid encoding CRlg-CD59 were subjected to restriction with BamHI (this will cut the link between CRlg and CD59 in the plasmid, CRlg-CD59-pDR2) followed by a ligation step (Fig.3.16C). The hinge was cloned between and in the same reading frame as CRlg and CD59. The construct was processed as described previously.

To generate CRlg-2a-CD59, cDNA encoding hinge domain of mouse IgG2a was obtained from a hybridoma cell line expressing mouse IgG2a. Total RNA was prepared and RT-PCR was carried out to generate cDNA. cDNA was used as a template for PCR to amplify the hinge of IgG2a. Both primers used for this reaction contained restriction sites for BamHI (Fig.3.16A). The PCR product was digested with BamHI enzyme after being visualised on agarose gel (3.16B). The cDNA encoding the hinge was ligated into CRlg -CD59-pDR2 vector, between CRlg and CD59 (Fig.3.16C). In both cases (CRlg-3-CD59 and CRlg-2a-CD59), after the cloning of the hinge, the orientation was confirmed by PCR using one primer specific for the insert and a second one complementary to a sequence outside of the insert. Sequence fidelity was confirmed.

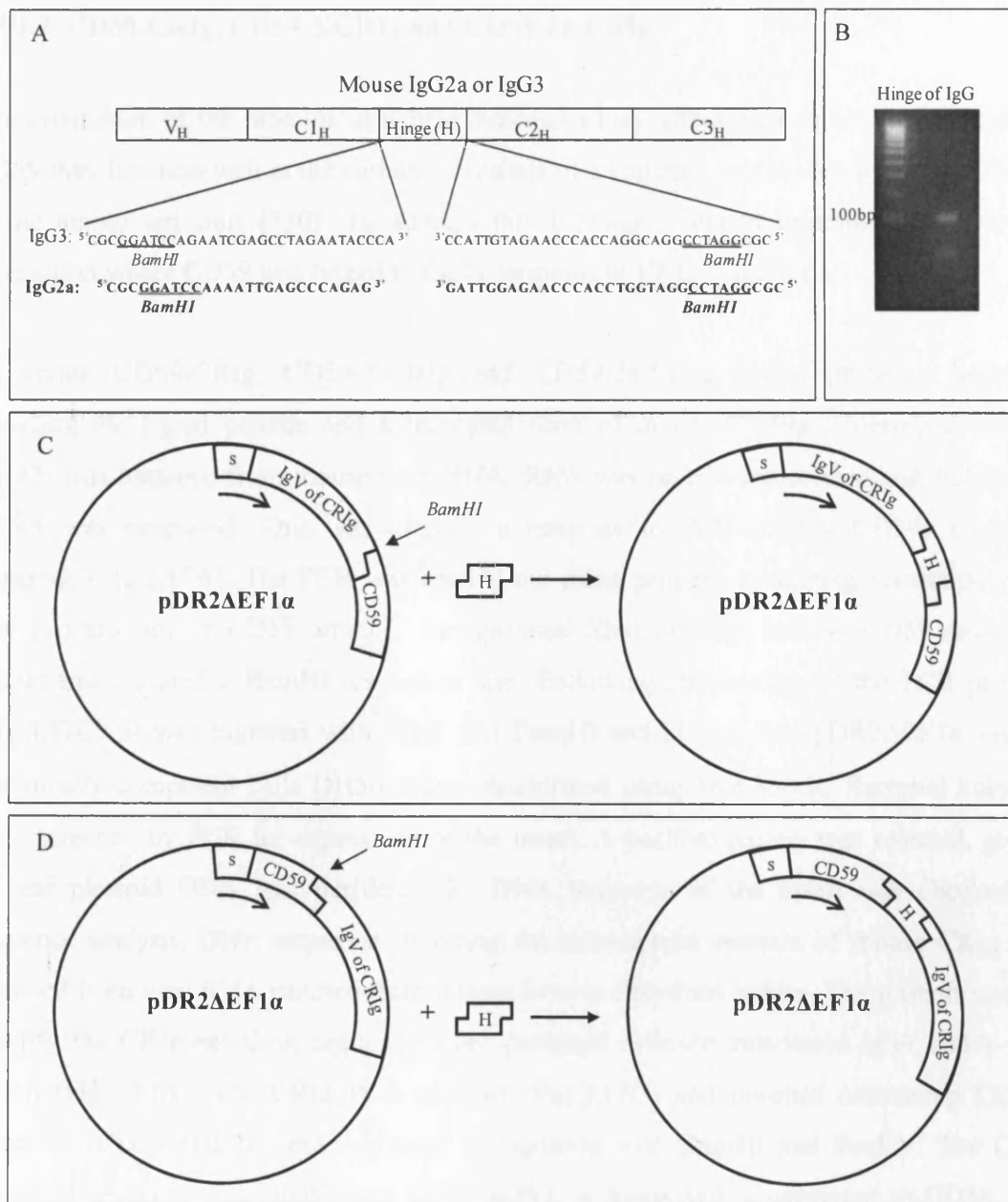


Fig.3.16 CR Ig-3-CD59, CR Ig-2a-CD59, CD59-2a-CR Ig and CD59-2a-CR Ig: construction of expression plasmid. Schematic diagrams of mouse IgG cloning strategy. The sequences and positions of primers used for amplification the hinges are shown. The primers for IgG2a are boldfaced. All primers incorporated BamHI restriction sites (underlined). The amplification products were visualised by gel electrophoresis (B), digested with appropriate enzyme and ligated into linearised expression vector pDR2ΔEF1α encoding CR Ig-CD59 (C) and CD59-CR Ig (D).

3.3.1.2. CD59-CRIg, CD59-3-CRIg and CD59-2a-CRIg

The orientation of the proteins in hybrid molecules may affect their function, for example CD59 may function well at the carboxy terminus of a chimeric protein but it is less efficient at the amino terminus [330]. To address this I designed fusion proteins in the reverse orientation where CD59 was linked to the N-terminus of CRIg (Fig.3.2B).

To create CD59-CRIg, CD59-3-CRIg and CD59-2a-CRIg fusion proteins, sequence encoding the signal peptide and a truncated form of mouse CD59a (C-terminal residue Lys72) was obtained from mouse liver RNA. RNA was reverse transcribed and full-length cDNA was generated. This was used as a template to PCR-amplify CD59a encoding sequence (Fig.3.17A). The PCR was carried out using primers containing restriction sites. The forward primer CD59 amino5' incorporated XbaI and the reverse CD59 amino 3' primer incorporated a BamHI restriction site. Following purification of the PCR product (Fig.3.17C), it was digested with XbaI and BamHI and cloned into pDR2 Δ EF1 α vector. Chemically competent cells DH5 α were transformed using heat shock. Bacterial colonies were screened by PCR for expression of the insert. A positive colony was selected, grown up and plasmid DNA was purified. The DNA sequence of the insert was checked by sequence analysis. DNA sequence encoding the extracellular domain of mouse CRIg was obtained from total RNA isolated from mouse liver as described before. The primers used to amplify the CRIg-encoding sequence were designed to insert restriction sites and a stop codon (Fig.3.17B). The CRIg PCR product (Fig.3.17C) and plasmid containing CD59a sequence (CD59-pDR2) were subjected to digestion with BamHI and EcoRV. The CRIg encoding sequence was cloned into CD59-pDR2 in frame and downstream to CD59. The common BamHI restriction site in both CRIg and CD59 cDNA formed a link between the DNA fragments (Fig.3.17D). DH5 α chemically competent bacteria were transformed and colonies screened by PCR for insert expression. A positive colony was selected, grown up and plasmid DNA was isolated. The sequence was checked for fidelity.

CD59-3-CRIg and CD59-2a-CRIg were generated using an identical approach to that described above (Section 3.3.1.1; Fig.3.16 A and D).

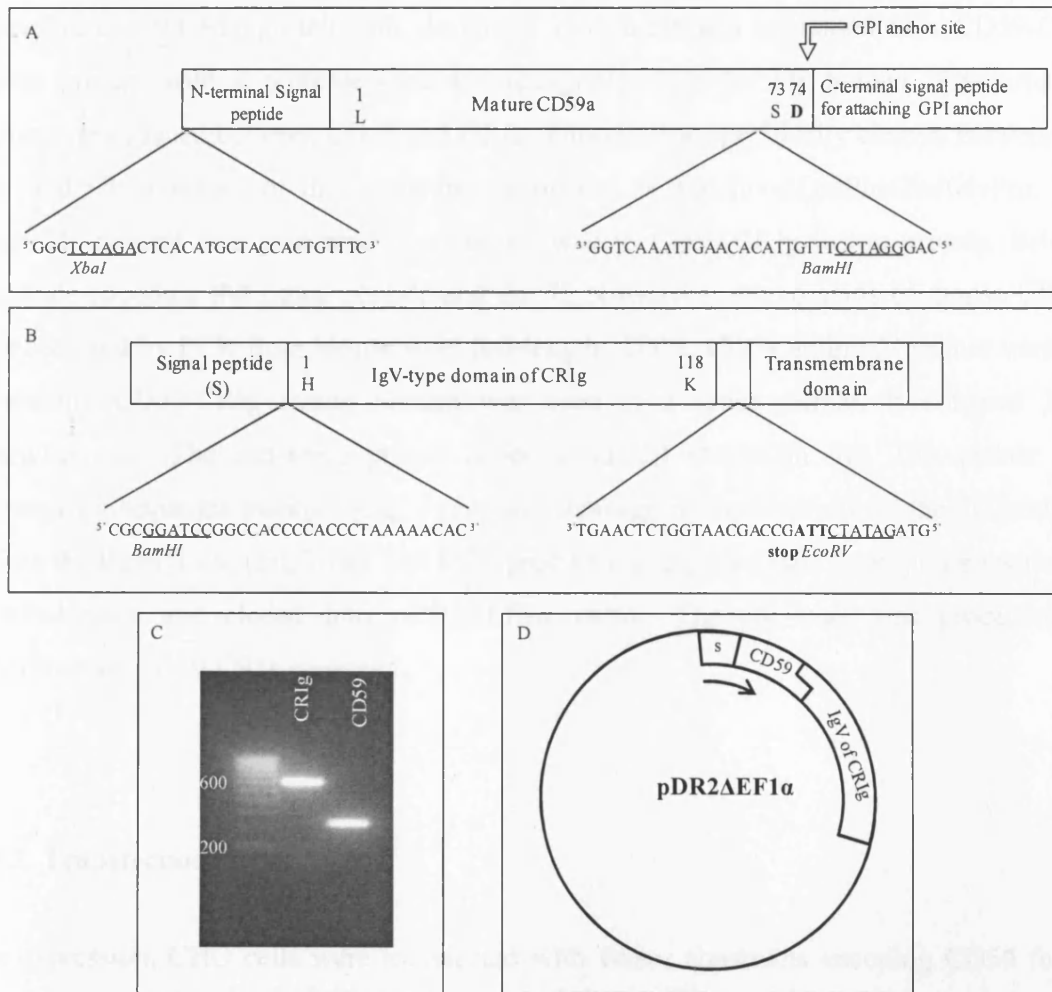


Fig.3.17 CD59-CR1g: construction of expression plasmid. Schematic diagrams of mouse CD59 (A) and mouse CR1g (B) cloning strategies. The sequences and positions of primers used for amplification of extracellular domains of CR1g and CD59a are shown. The incorporated restriction sites are underlined. The stop codon is shown in boldface. The amplification products were visualised by gel electrophoresis (C), digested with appropriate enzymes and ligated into expression vector pDR2ΔEF1α to create CD59-CR1g encoding construct (D).

3.3.1.3. Generation of cleavable CD59-CR1g

Soluble CD59 and soluble CR1g were required as controls for various assays used to assess function of the chimeric reagents. To create control soluble CD59 and CR1g which were identical to those in the constructs described above, but NOT fused to other domains, a

cleavable CD59-CRIg protein was designed. This agent was expressed as a CD59-CRIg fusion protein with a protease cleavage recognition site for the human rhinovirus 3C protease introduced between CD59 and CRIg. This enzyme specifically cleaves between the Gln and Gly residues of the recognition sequence of IleGluValLeuPheGln/GlyPro. The cleavable reagent was generated in a similar way to CD59-CRIg fusion protein. Briefly, sequence encoding the signal peptide and the 72 N-terminal amino acids of mouse CD59a was obtained by PCR from mouse liver full-length cDNA. CD59 amino 5' primer used for generating CD59-CRIg fusion protein was used as a sense primer. It contains XbaI restriction site. The anti-sense primer contains BamHI restriction site. This primer also contained a sequence incorporating a protease cleavage recognition site of the 3C protease before the BamHI site (Fig.3.18). The PCR product was digested with appropriate restriction endonucleases and cloned into pDR2ΔEF1α vector. The construct was processed as described for CD59-CRIg construct.

3.3.2. Transfection

For expression, CHO cells were transfected with vector constructs encoding CD59 fusion proteins using JetPEI cationic polymer transfection reagent (Poly Plus Transfection) according to the manufacturer's instructions and as described in method 2.2.3. Stable lines were established by selection with 400 µg/ml Hygromycin B. Expression of the recombinant proteins in supernatant was confirmed by western blot probed with anti-CD59 or anti-CRIg mAb (Fig.3.19). This assay revealed that the transfection was successful. CD59-CRIg and CRIg-CD59 proteins appeared as a single band, while two bands were seen for the fusions containing antibody hinge. The bands are likely to represent different oligomeric forms of the proteins: monomers and dimers. The transfected cells were cloned out by limiting dilution and cells expressing high levels of protein were detected using western blot analysis (Fig.3.19C). The selected clones were expanded and transferred into the two-compartment bioreactor CELLline AD1000. Cell culture supernatant was harvested weekly.

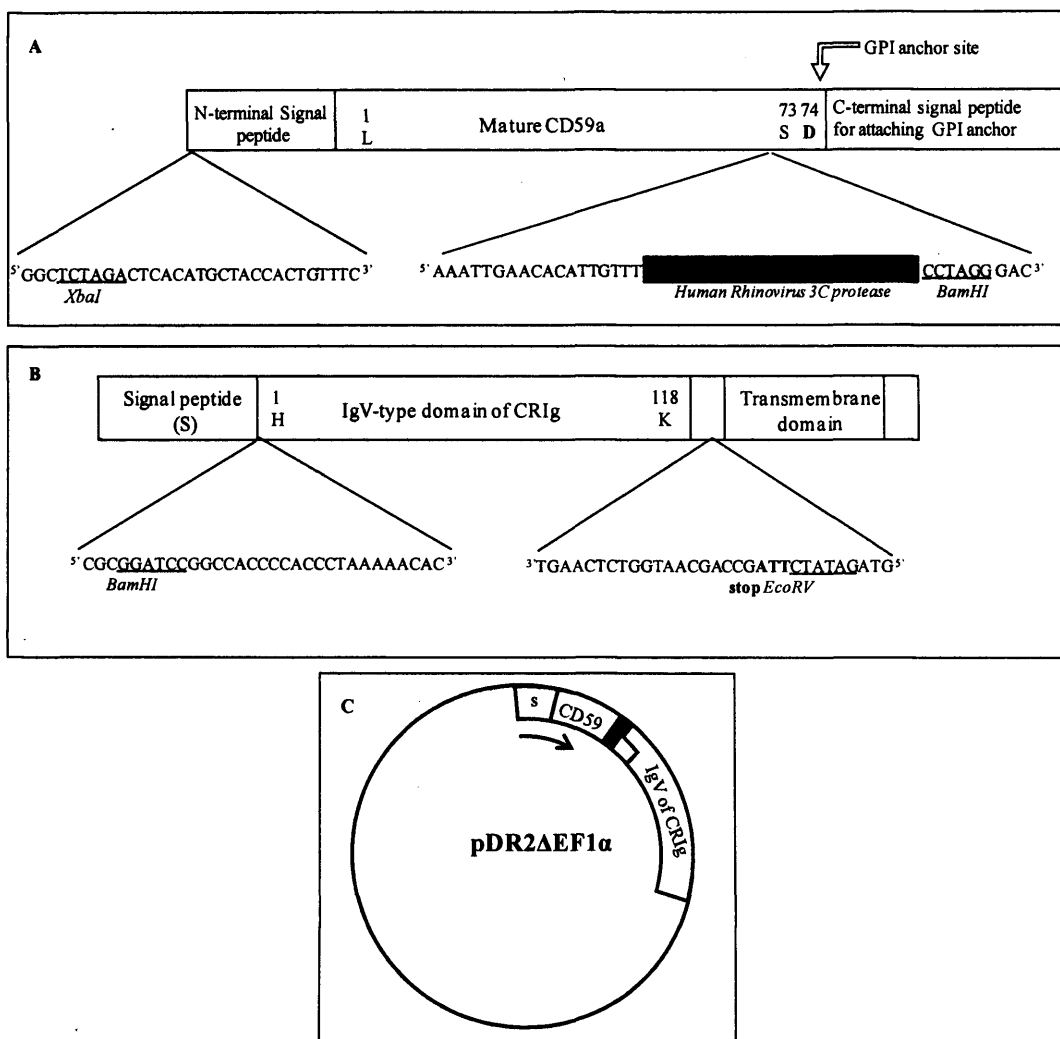


Fig. 3.18 Cleavable CD59-CR1g: construction of expression plasmid. Schematic diagrams of cloning strategy to introduce a human rhinovirus 3C protease site. The sequences and positions of primers used for amplification of extracellular domains of mouse CD59a (A) and CR1g (B) are shown. The incorporated restriction sites are underlined. The PreScission recognition site is encoded by the antisense primer for CD59 (shown in grey box). The stop codon is shown in boldface. The amplification products were digested with appropriate enzymes and ligated into expression vector pDR2 Δ EF1 α to create a cleavable CD59-CR1g-encoding construct (C). The protease recognition site is shown in grey.

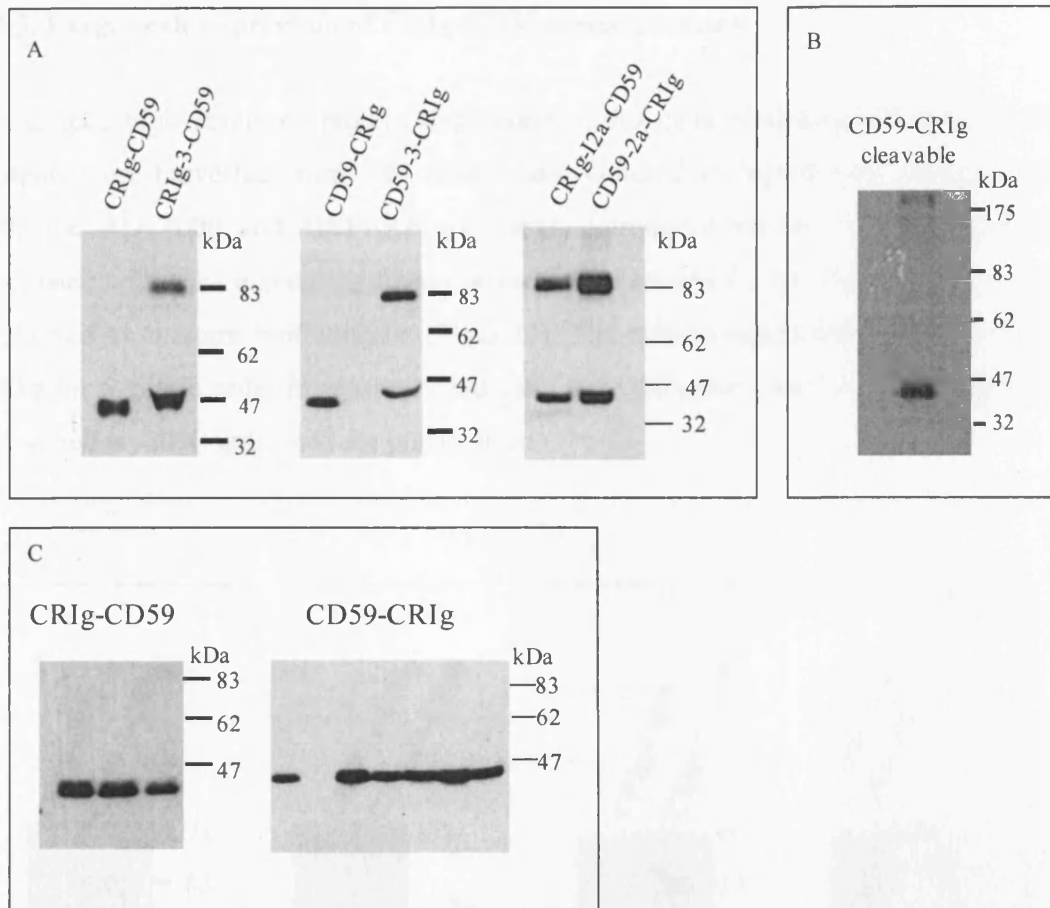


Fig. 3.19 Western blot analysis for protein expression and clone selection. Tissue culture supernatant from CHO cells expressing CRIg-CD59, CRIg-CD59, CRIg-IgG3 hinge-CD59, CD59-3-CRIg, CRIg-2a-CD59 and CD59-2a-CRIg, (A) and cleavable CD59-CRIg (B) was subjected to SDS-PAGE and the proteins were transferred onto a nitrocellulose membrane. The blot was probed with anti-CD59 mAb (A) or anti-CRIg mAb (B). Molecular mass markers are shown to the right of each panel. One band of 40kDa was observed for CRIg-CD59 (A), CD59-CRIg (A) and CD59-CRIg cleavable reagent (B). CRIg-hinge-CD59 and CD59-hinge-CRIg gave two forms with molecular weights corresponding to monomeric and dimeric forms. Example of screening of cells expressing CRIg-CD59 and CD59-CRIg fusion proteins (C). Transfected cells were expanded and cloned out by limiting dilution in 96-well plate format. Tissue culture supernatant from wells containing single colonies was subjected to western blot analysis. The three tested CRIg-CD59 producing cell clones gave positive result. One out of ten tested wells containing CD59-CRIg did not express this protein.

3.3.3. Large-scale expression of CRIG-CD59 fusion proteins

To achieve high levels of protein expression, CHO cells producing CRIG-CD59 fusion proteins were harvested from T80 flasks and cultured in high-density culture systems. CELLline AD 1000 and HYPERFlask flasks, introduced earlier in this chapter, were inoculated with cells expressing fusion proteins (see section 2.2.6). Protein expression was confirmed by western blot analysis (Fig.3.20). The culture supernatant was centrifuged at 700xg for 5 min in order to separate dead cells from the culture medium. The tissue culture was stored at -20°C until used for purification

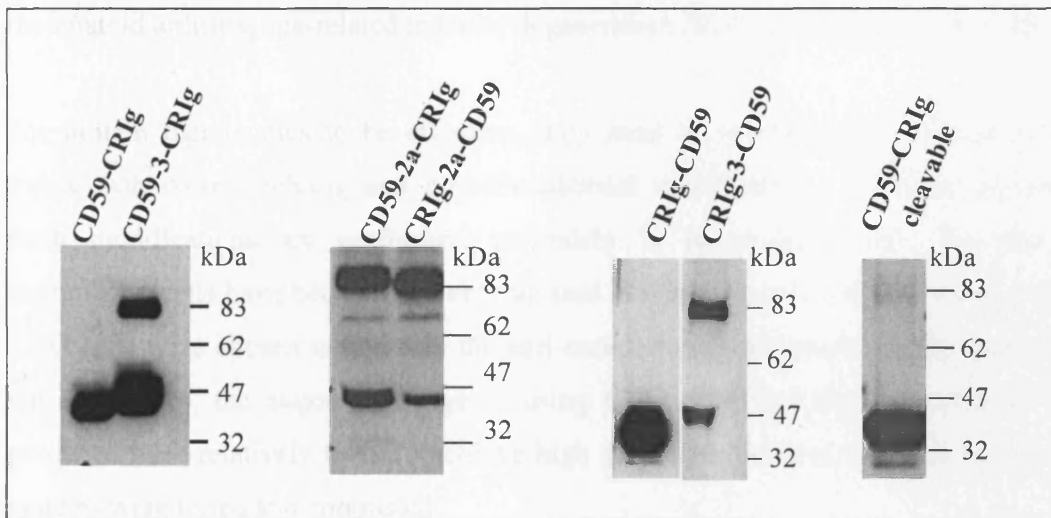


Fig. 3.20 Western blot analysis of tissue culture supernatant from cells cultured in high-cell density cell systems. Tissue culture supernatant from CHO cells cultured in high-density cell culture systems expressing CRIG-CD59 constructs with or without the IgG3 or IgG2a hinge was subjected to SDS-PAGE and the proteins were transferred to a nitrocellulose membrane. The blot was probed with anti-CD59 mAb. Molecular mass markers are shown to the right of each panel. One band of 40kDa was observed for CRIG-CD59, CD59-CRIG and CD59-CRIG cleavable. CRIG-2a-CD59 and CD59-2a-CRIG gave two forms with molecular weights corresponding to monomeric and dimeric forms.

3.4. Discussion

Complement has been implicated in a number of diseases. It either causes or exacerbates pathology. Reagents which inhibit complement have shown benefit in many models of diseases. Many of these therapeutics block complement systemically, and thus suppress vital complement functions such as opsonisation. Complications including infection and immune complex disease may arise after long-term treatment. I have designed drugs which may retain the physiologically important complement functions (such as opsonisation) and suppress only pathological ones. Here I describe agents which neutralise late events of complement activation and MAC formation. MAC is intimately involved in host tissue destruction and pathology of diseases such as multiple sclerosis, myasthenia gravis, rheumatoid arthritis, age-related macular degeneration [211, 224, 328, 365, 387-389].

For protein therapeutics to be effective, they must be synthesised in biologically active forms with correct folding and post-translational modifications, including glycosylation. Such modifications are performed accurately in mammalian cells. For this reason mammalian cells have been extensively utilised as a host for protein production [390, 391]. CHO cells were chosen to generate the anti-complement therapeutics in this study. Despite the advantages, the major challenge in using CHO cells was that the yields of proteins produced were relatively low. To achieve high protein expression, two high-density culture systems were tested and contrasted.

To generate soluble long-lived complement blocking agent, the Fc portion of mouse IgG2a antibody was fused to C5 inhibitor, OmCI. Plasmid encoding OmCI-Fc was generated and CHO cells were successfully transfected. Protein expression was confirmed with western blot analysis. The protein production was scaled-up using high-density cell culture systems. Out of the two culture systems tested, the *HYPERFlask* flask demonstrated better yields and was therefore used for production of OmCI-Fc. However, overall level of OmCI-Fc expression remained low. In future studies this could be improved by engineering the vector and host cell or by changing the format of transfection- from stable to transient. Large-scale transient gene expression has been proved to be more efficient in the production of many therapeutic proteins especially at the early development phase [392-394]. The choice of the vector and particularly the promoter driving the expression could be crucial in terms of protein production rate [395]. The fusion proteins including OmCI-Fc were expressed under

promoter for human EF1 α . To increase the levels of protein expression a promoter from Chinese hamster EF1 α could be used. The level of protein expression driven by sequences from the Chinese hamster EF1 α gene was found higher than expression controlled by a human EF1 α promoter [396].

The targeted anti-complement therapeutics were generated by joining DNA sequences encoding the extracellular domains of mouse CRIg and CD59a. It has previously been shown that orientation of the protein domains within chimeric fusion proteins may cause loss of function [330]. In order to generate an optimally-targeted reagent, constructs encoding fusion proteins in different orientations were engineered (Table 3.3). CRIg was linked either to the amino (N-) or carboxy (C-) terminus of CD59.

N-terminus	Spacer	C- terminus	Fusion protein
CRIg	-	CD59a	CRIg-CD59
CD59a	-	CRIg	CD59-CRIg
CRIg	Hinge IgG3	CD59a	CRIg-3-CD59
CD59a	Hinge IgG3	CRIg	CD59-3-CRIg
CRIg	Hinge IgG2a	CD59a	CRIg-2a-CD59
CD59a	Hinge IgG2a	CRIg	CD59-2a-CRIg
CD59a	Human Rhinovirus 3C protease recognition site	CRIg	CD59-CRIg cleavable

Table 3.3 CD59 containing targeted reagents

In addition to restriction of function caused by blockade of one or other protein terminus, function may be sterically restricted due to the close proximity of the two molecules. To avoid steric hindrance, the hinge region of mouse IgG3 or IgG2a was introduced to distance CRIg from CD59. The Ig hinge consists of three parts: an upper hinge permitting Fab rotation and movement; a core hinge containing possible interchain disulfide bonds; and a lower hinge allowing Fc movement. In addition to distancing the two moieties, it was expected that the hinge would promote dimerisation and introduce avidity effects and thus better surface localisation and targeting as is the case with native antibody. Mouse IgG3 hinge was initially chosen as it possessed a long upper hinge (14 amino acids), which theoretically would provide high flexibility. However, experiments described in Chapter 5 illustrated that this hinge, which contains a single cysteine residue capable of forming one

disulfide bridge, did not promote efficient dimerisation. Despite its long upper hinge (14aa) it has been found that mouse IgG3 hinge has a rigid structure, possibly due to a Pro-Pro-Gly sequence near the inter-chain disulfide bond [378]. This sequence can cause a turn of a polyproline helix that restricts the motion of the Fab arms. To increase flexibility and improve dimerisation, additional constructs comprising the hinge of mouse IgG2a were generated [397]. The “core” hinge of IgG2a contains three cysteines that could form three separate disulfide bridges [379]. I hypothesised that this would increase the chance of formation of stable dimers.

To compare function of the reagents, a control fusion protein was also engineered. Cleavable CD59-CRIg fusion protein was generated by incorporating the human rhinovirus 3C protease recognition site immediately after the CD59 sequence. This will allowed generation of soluble CD59 and soluble CRIg, which will be used as control proteins when testing function of CD59 and CRIg units within the fusion proteins (described in later chapters).

Plasmids encoding all CD59 fusion proteins (listed in Table 3.3) were purified and used to transfect CHO cells. Stable cell lines were generated by selection and protein expression was confirmed by Western blot. The blot was developed with either anti-CD59 or anti-CRIg monoclonal antibodies (generation of the anti-CRIg antibody is described in Chapter 4). CRIg-CD59, CD59-CRIg and cleavable CD59-CRIg gave rise to single bands with apparent molecular weight of 40kDa. The modified reagents containing antibody hinge migrated as two bands. The lower band with apparent molecular mass of 45kD represented a monomeric form. Incorporation of the hinge increased the molecular mass of CRIg-hinge-CD59 and CD59-hinge-CRIg monomers compared to the CRIg-CD59 and CD59-CRIg reagents. The higher band (83kDa) is likely to represent a dimeric form of the reagent, the result of disulfide bond formation between hinges from two molecules.

In summary, this chapter describes the cloning strategy, successful generation and large-scale expression of anti-terminal pathway therapeutics. Their purification and functional characterisation is detailed in the following chapter.

Chapter 4. Production of monoclonal antibodies against OmCI, mouse CR1g and mouse CD59

4.1 Introduction

The aim of this project was to generate and characterise anti-complement therapeutics. This Chapter describes the production of monoclonal antibodies (mAbs) specific to the anti-complement reagents generated in the study. These antibodies would provide essential tools for purification and characterisation of the therapeutics. In section 4.2 the production, characterisation and the purification of anti-OmCI monoclonal antibodies is discussed, whereas section 4.3 is focused on anti-CR1g and anti-CD59 mAbs.

Activation and clonal expansion of antigen-specific B cells is one of the body's protective mechanisms against foreign antigen. Each B cell clone secretes its unique (monoclonal) antibody that recognizes a specific binding site (epitope) on the antigen surface. Their high specificity and high sensitivity makes monoclonal antibodies indispensable tools for research, diagnostics and therapy. The generation of monoclonal antibodies involves *in vitro* and *in vivo* procedures (Fig.4.1). The technology for monoclonal antibody production from hybridoma cells (hybridomas) was first described in 1975 [398]. The hybridomas are hybrid cells generated by the fusion of cancer cells, such as myeloma, with B-lymphocytes (splenocytes) from the spleen of animals challenged with the target antigen. The hybrid cells possess the key features of both parental cell types, immortality and specific antibody secretion respectively. Cloning of hybridoma cells by limiting dilution ensures isolation of clones producing antibodies identical in their epitope-binding region.

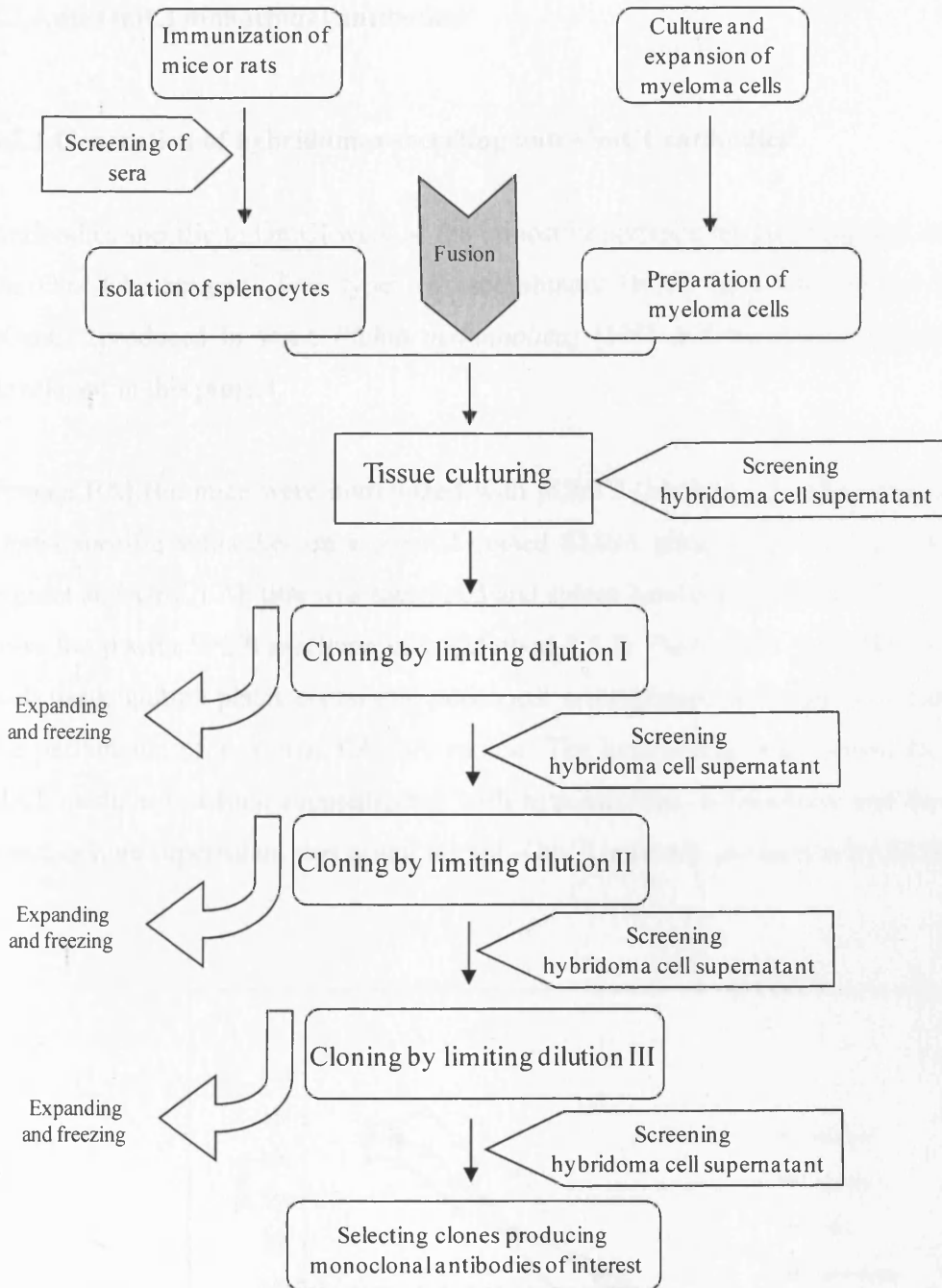


Fig. 4.1 Diagram showing the typical steps for monoclonal antibody production. These include antigen challenge of animals, splenocyte preparation and fusion with immortal myeloma cells to generate antibody producing hybridoma cells. Three round of clonal selection are usually necessary to generate clones producing specific monoclonal antibodies.

4.2 Anti-OmCI monoclonal antibodies

4.2.1 Generation of hybridomas secreting anti-OmCI antibodies

Antibodies specific to OmCI were of the utmost importance for purifying and characterising the OmCI-Fc reagent. Two types of recombinant OmCI were used in the experiments: pOmCI (produced in yeast *Pichia methanolica*) [175] and the fusion protein, OmCI-Fc, developed in this project.

Female BALB/c mice were immunized with pOmCI (Method 2.5). Sera were analysed for OmCI specific antibodies on a pOmCI coated ELISA plate (Fig.4.2). The mouse with the highest anti-OmCI Ab titre was sacrificed and spleen harvested (Method 2.5.4). Splenocytes were fused with SP2/0 myeloma cells (Method 2.5.7). Fused cells were distributed into 24-well tissue culture plates containing peritoneal macrophages as feeder cells harvested from the peritoneum of a normal BALB/c mouse. The hybridomas were grown for ten days in HAT medium (medium supplemented with hypoxanthine, aminopterin and thymidine) and tissue culture supernatant was tested for anti-OmCI antibody production by ELISAs.

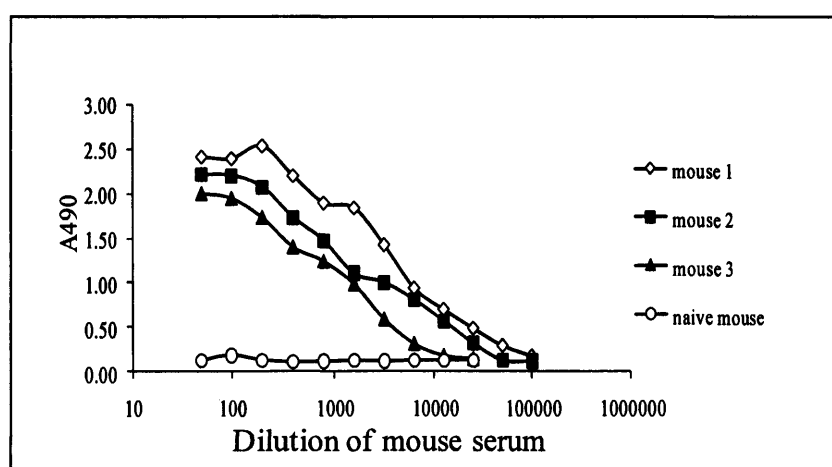


Fig.4.2 Pre-fusion ELISA screen of sera from mice immunised with pOmCI. Serum from three test mice or from a naïve mouse was tested by ELISA for immunoreactivity with OmCI. The spleen from the mouse with highest antibody titer against OmCI (open diamond) was used for fusion.

4.2.2. ELISA for screening hybridoma cells secreting anti-OmCI mAbs

Supernatants from the hybridoma cells were screened for specific antibody production by ELISA. Three different ELISAs were developed (Fig.4.3).

A direct ELISA was initially used for screening (Fig.4.3A). Hybridoma supernatant was incubated on a plate coated with pOmCI. Bound antibody was detected with HRP-conjugated anti-mouse Ig. Two OmCI-specific clones were selected and two monoclonal antibodies were developed. The antibody subclass was determined using *IsoStrip* test (Roche) using the method recommended by the manufacturer. The analysis revealed that the mAbs were of IgG1 (MBI-Om1) and IgM (MBI-Om2) isotype. The characterisation of the antibody, discussed in section 4.2.4, showed that the mAb obtained from this screening selectively bound denatured antigen (directly coated on the plate or transferred to membranes by western blot) but not in conditions which preserved the native conformation of OmCI (captured on ELISA plate or flowed across biacore chip). This antibody selectivity can be attributed to the set up of the screening assay.

To generate mAb which recognised the native conformation of OmCI, the hybridoma cells were screened on a capture ELISA (“positive” screening) (Fig.4.3BI). To maintain the native conformation of OmCI, the antigen was captured on the plate coated with affinity-purified rabbit anti-OmCI polyclonal antibody. Tissue culture supernatant from hybridoma cells was added to the wells. The bound antibody was detected with HRPO-conjugated anti-mouse Ig, similarly to the previous ELISA. To confirm the specificity of the antibodies a “negative” screening was also performed (Fig.4.3BII). This was identical to the positive screening but instead of antigen (pOmCI) the wells were incubated with buffer only. The clones with positive response to pOmCI and negative to the buffer were selected. Four hybridoma clones passed both levels of selection and four anti-OmCI monoclonal antibodies were obtained. The isotype of the antibodies were determined as described before. One of the specific monoclonal antibodies was identified as IgG2b and the remaining three belonged to IgG1 isotype. To assess whether IgG2b (MBI-Om3) was suitable for purifying OmCI-Fc reagent, this antibody was further characterised.

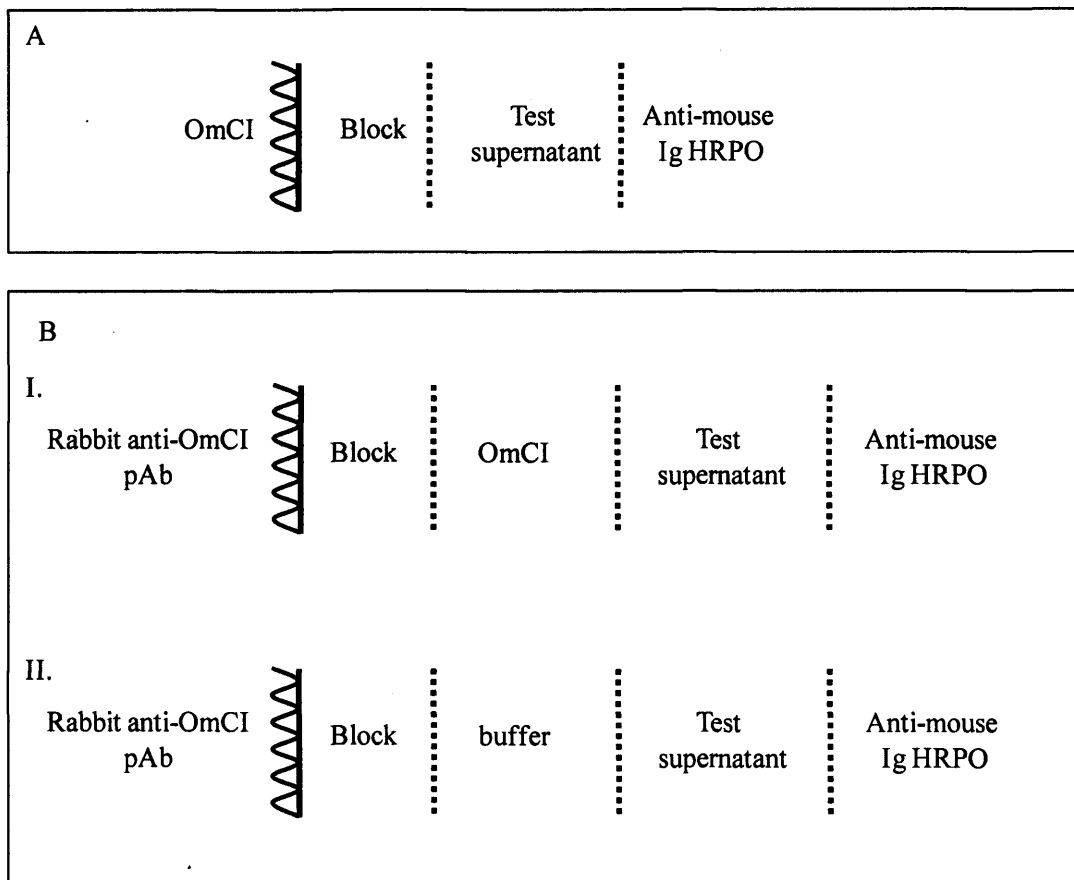


Fig. 4.3 ELISA based strategies for screening hybridoma supernatant for OmCI reactivity. OmCI (3 μ g/ml) was coated directly (A) or captured with rabbit anti-OmCI polyclonal antibody (pAb) (B) on an ELISA plate. Antibody-containing tissue culture supernatant (100 μ l) was added to the wells and antibody binding was detected with HRPO conjugated anti-mouse Ig. Washing steps are indicated with a dotted line. The antigen was denatured when coated directly on the plate and one monoclonal antibodies against denatured OmCI was developed (A). To ensure identification of hybridomas secreting antibodies recognizing native antigen, OmCI was captured with specific pAb (BI). The specificity of the screening approach was increased by introducing second “negative” screening steps (BII).

All six hybridoma clones which gave a positive signal on ELISA were cloned three times by limiting dilution (Detailed method in Chapter 2, section 2.2.4) on peritoneal macrophages from a normal BALB/c mouse as feeder cells after which they were clonal.

4.2.3. Large-scale production of Anti-OmCI antibodies

As a result of cell fusion and cloning, six clones secreting monoclonal antibodies recognising OmCI were obtained. Three clones secreting anti-OmCI mAbs: MBI-Om1 (IgG1), MBI-Om2 (IgM), MBI-Om3 (IgG2b) were expanded and high expression level of the antibody was achieved using Two-compartment bioreactor CELLLine technology (Integra Biosciences CL1000 flasks). This cell culture system is similar to CELLLine AD1000 (section 2.5.8) but does not contain a polyethylene terephthalate matrix. To avoid bovine Ig contamination from the FCS in the medium when purifying the antibody, ultra low bovine immunoglobulin FCS was used. The CELLLine CL1000 high expression system requires only small amount of serum containing media therefore the usage of ultra low bovine immunoglobulin FCS was economical. Cell culture supernatant was collected weekly and the monoclonal antibodies were purified.

4.2.4. Purification of Anti-OmCI antibodies

4.2.4.1. Purification of anti-OmCI mAbs of IgG isotype (MBI-Om1 and MBI-Om3)

Protein A and protein G affinity chromatography are the most commonly used approaches for IgG purification. Protein A and protein G are both bacterial proteins (from *Staphylococcus aureus* and Group G *Streptococcus*, respectively), which bind to the Fc portion of IgG. A Protein G column was used to purify the antibodies of IgG isotype as the Fc of mouse IgG1 and IgG2b have higher affinity for protein G than to protein A. The method was described in Chapter 2, section 2.3.3. The supernatant containing anti-OmCI IgG was passed over the column, the column was washed and bound protein was eluted using elution buffer. The absorbance at 280nm was used to identify fractions that contained protein. These fractions were combined and the antibody was dialysed against PBS. The purity of the protein was assessed by SDS-PAGE. The proteins were visualised using Coomassie blue staining. A typical antibody pattern was observed (Fig.4.4). MBI-Om1 and MBI-Om3 migrated as one prominent band under non-reducing conditions. As can be seen from Fig.4.4, two distinct bands corresponding to the heavy and light chains were observed under reducing conditions. As may be noted from the figure, the heavy chain of

MBI-Om3 appeared as a double band under reducing conditions. This may suggest that MBI-Om3 was not clonal.

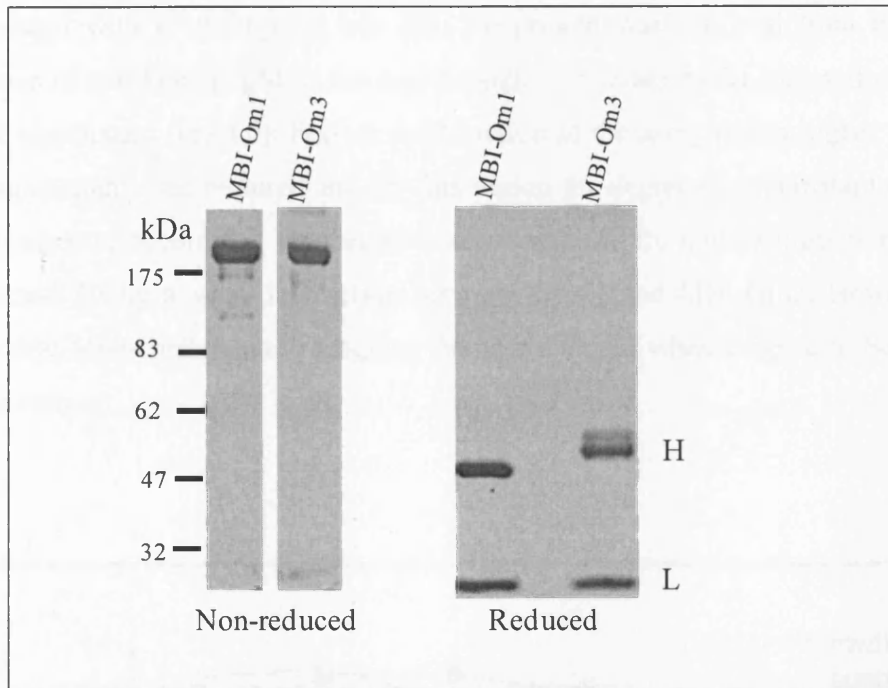


Fig.4.4 SDS PAGE analysis of purified monoclonal antibodies against OmCI. mAbs of IgG class were purified by chromatography on protein G column and subjected to SDS-PAGE analysis under non-reducing and reducing conditions and proteins were stained with Coomassie Blue. MBI-Om1 and MBI-Om3 appeared as one prominent band under non-reducing condition. The antibodies migrated as two bands under reducing condition, corresponding to the light (L) and heavy (H) chains of antibody. The difference in molecular weight between the antibodies may be due to the isotype difference or difference in glycosylation.

4.2.4.2. Purification of MBI-Om2 (IgM)

Two chromatography-based methods were tested in order to purify anti-OmCI monoclonal antibody of IgM isotype.

The first approach used to purify MBI-Om2 was affinity chromatography. Supernatant containing the monoclonal antibody was passed over the OmCI column, generated previously (Method 2.3.6). The column was washed with Tris buffer and bound antibody was eluted with a buffer with low pH. No protein was obtained from the elution. The presence of anti-OmCI IgM in the run through was tested by ELISA and compared to the initial supernatant (Fig.4.5). Further optimisation of the assay (using higher dilutions of the test supernatant) was required and for this reason the degree of supernatant depletion could not be assessed accurately. The negative result obtained from the affinity purification can be accounted for by a weak interaction between OmCI and MBI-Om2. However it is more likely that MBI-Om2 cannot recognise the native OmCI when coupled to Sepharose matrix on the column.

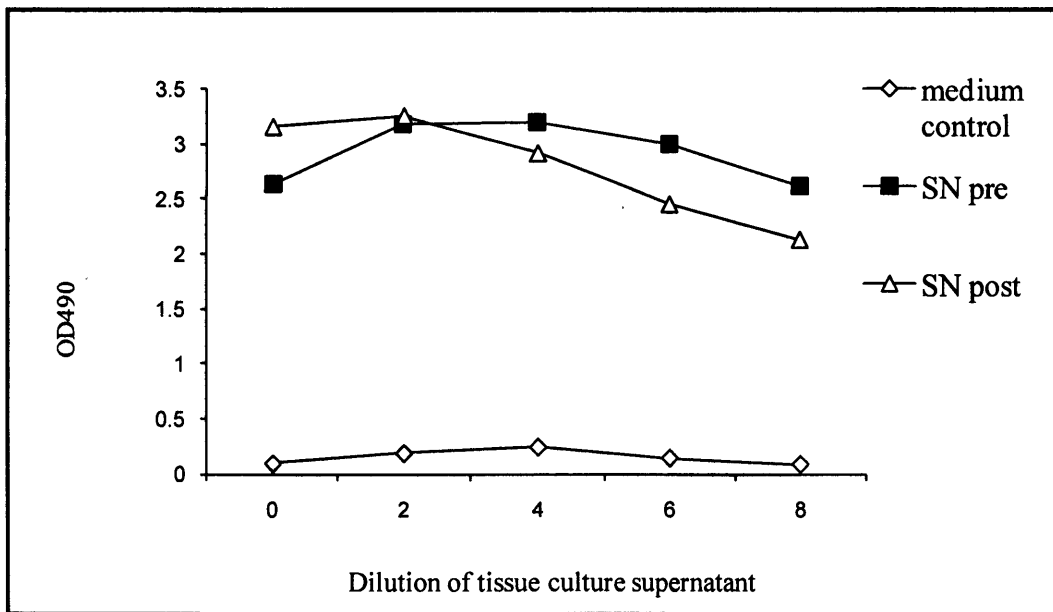


Fig.4.5 ELISA of the purification of anti-OmCI IgM mAb by OmCI column. To assess the degree of supernatant depletion brought about by the OmCI column and hence the expected yield, an ELISA was carried out as follows. The plate was coated with OmCI, blocked and incubated with a sample of supernatant from before and after the column (1:2 serial dilutions). The plate was probed with anti-mouse IgM HRPO. Anti-OmCI IgM antibody was detected in both the pre column supernatant and the run through. It A higher dilution of the tissue culture supernatant was required for more accurate analysis.

The second strategy performed to purify MBI-Om2 was based on thiophilic chromatography on a prepacked thiophilic adsorption medium, 2-mercaptopyridine coupled to Sepharose™ High Performance (HiTrap™ IgM Purification HP; GE Healthcare). This approach relies upon the affinity of a sulphur-containing ligand, immobilized on a matrix, for immunoglobulins in the presence of high concentrations of lyotropic salts. Elution of IgM is mediated by removal of these salts [399]. The tissue culture supernatant was adjusted to a high salt (0.8M ammonium sulphate) concentration before applying on the column. The supernatant was passed over the column which had been preequilibrated with binding buffer pH 7.5. Unbound protein was washed away with binding buffer and bound IgM was eluted by decreasing the ionic strength of the buffer. Fractions containing protein were identified by their absorbance at 280nm, combined and dialysed against PBS. SDS-PAGE analysis revealed that the eluted protein contained IgM antibody (Fig.4.6). Multiple bands found on the gel indicated low purity of the preparation (Fig.4.6). Additional purification steps such as gel filtration were required to achieve pure IgM preparation and for this reason the antibody was not characterised further.

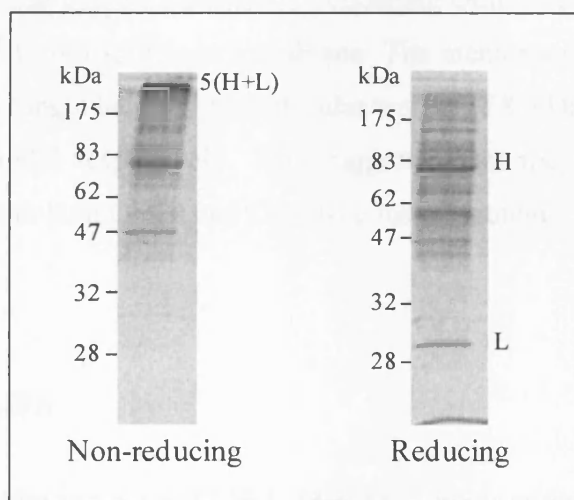


Fig. 4.6 SDS PAGE analysis of the purification of anti-OmCI IgM mAb. The product from HiTrap IgM Purification HP was resolved on a 7.5% gel under non-reducing and reducing conditions and Coomassie stained. The major, high molecular band indicated as 5(H+L) is likely to represent IgM pentamer. Two main bands with apparent molecular weight of 20 kDa and 80kDa were seen under non-reducing conditions. These corresponds to IgM heavy (H) and light (L) chains. Multiple bands were also found indicating that the product was not pure.

4.2.5. Characterisation of anti-OmCI mAbs

In order to develop a tool to purify and characterise the OmCI-Fc protein, the selected anti-OmCI monoclonal antibodies were analysed. An important feature for good antibodies is their ability to recognise the antigen in native conformation. The specificity of MBI-Om1 and MBI-Om3 was evaluated by Western blot analysis and ELISA. In addition to that a SPR analysis was performed to characterise MBI-Om1. To be able to test the specificity of the antibodies, they were conjugated with Horseradish peroxidase (HRPO) using EZ-link Plus Activated Peroxidase (Pierce) as described in method section 2.6.1.

4.2.5.1. Characterisation of MBI-Om1 (IgG1)

4.2.5.1.1. Western blot analysis

pOmCI protein and tissue culture supernatant containing OmCI-Fc were subjected to SDS-PAGE and transferred to nitrocellulose membrane. The membrane was probed with MBI-Om1-HRPO (Fig.4.7). Single bands with molecular weight of 83kDa and 17kDa were found for OmCI-Fc and pOmCI respectively. This suggested that the antibody raised against pOmCI was reactive with both OmCI and OmCI-Fc fusion protein.

4.2.5.1.2. Capture ELISA

As shown by Western blot and direct ELISA, MBI-Om1 binds antigen that has been directly immobilised on the surface (plastic plate or on nitrocellulose membrane following SDS PAGE). To check whether MBI-Om1 was able to bind the antigen in its native conformation, a capture ELISA was performed. Rather than the antigen being directly attached to the plate, it was captured by polyclonal anti-OmCI antibody or by its ligand C5. C5 and the polyclonal antibody were able to bind the antigen and thus maintain its native shape on the plate. However, MBI-Om1 failed to bind OmCI captured on the plate in this way. This result suggested that the monoclonal antibody was specific to denatured but not to native OmCI. However, as this was the first antibody generated, there was no positive

control that could be used to confirm that OmCI was indeed captured on the plate. This encouraged further analysis of the binding.

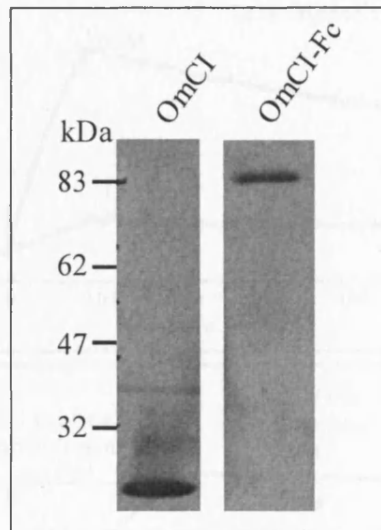


Fig.4.7 Western blot analysis of MBI-Om1-HRPO binding to OmCI and OmCI-Fc. pOmCI (pure protein) or OmCI-Fc (supernatant) was resolved by SDS-PAGE and transferred to a nitrocellulose membrane. The membrane was probed with MBI-Om1-HRPO.

4.2.5.1.3. Surface Plasmon Resonance (SPR)

To confirm that the result obtained from the capture ELISA was real and the antibody recognised only the denatured antigen, the MBI-Om1/OmCI interaction was further analysed using SPR. MBI-Om1 (1000RU) was covalently immobilized through free amines to a carboxy-methylated sensor chip. pOmCI (1 μ M and 10 μ M) diluted in a biacore running buffered saline was injected across the mAb surface. Having the antigen in solution minimized the risk of masked or altered epitopes due to immobilization of the antigen to a surface. Fig.4.8A showed that pOmCI bound MBI-Om1 in a dose dependent manner. Nevertheless crude fitting of the curves to a 1:1 interaction model indicated 100-1000-fold weaker than normal antibody binding. This might be due to a non-specific binding to the chip matrix or that antibody was denatured during purification. To orientate the mAb and to analyse the interaction from the 'opposite direction', 500RU of protein A was immobilised

on a chip and MBI-Om1 was captured. Either pOmCI or running buffer was injected (Fig.4.8 B).

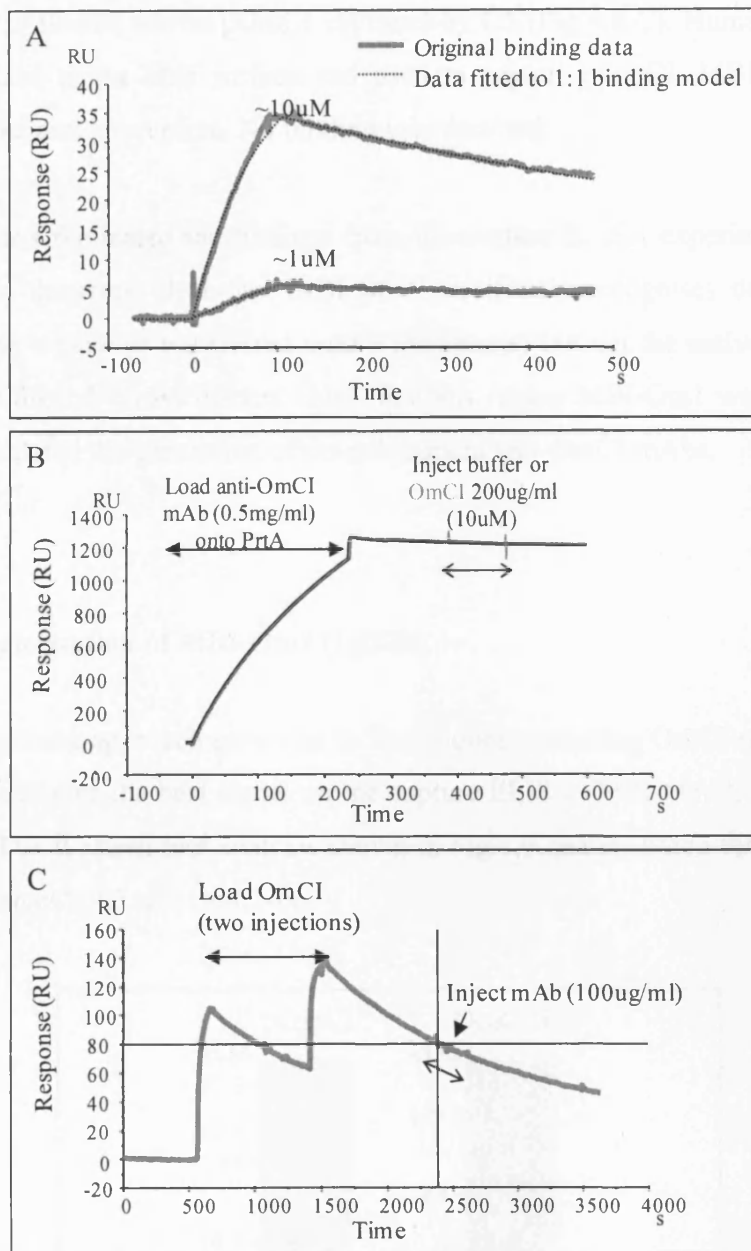


Fig.4.8 Biacore analysis of MBI-Om1 binding to pOmCI. pOmCI was flowed over a chip immobilized with the mAb. The binding response was fitted to 1:1 Langmuir binding model to obtain the dissociation constant ($K_D=0.9\mu\text{M}$) (A). To orientate anti-OmCI mAb, it was captured with protein A onto the chip surface. OmCI (grey) or buffer control (black) was flowed across the surface. No difference between the test sample and the negative control was observed in terms of binding (B). OmCI was captured on a chip with C5 and the mAb loaded over the chip. No binding was detected (C). The result from this experiment demonstrate that anti-OmCI mAb did not recognise native OmCI.

No detectable antigen-antibody binding was observed since the binding profile for the antigen and the buffer control were exactly the same. An identical result was achieved when the antibody was flowed across pOmCI captured by C5 (Fig.4.8 C). Human C5 (4000RU) were immobilized to the chip surface and used to capture pOmCI. MBI-Om1 was then flowed across the antigen surface. No binding was detected.

These SPR assays replicated the findings from the capture ELISA experiments. In light of the above, it is therefore clear that MBI-Om1 specifically recognises denatured antigen (when coated on a plate or transferred onto a membrane) but not the native form (captured on the plate or flowed across biacore chip). For this reason MBI-Om1 was of limited use. This result stimulated the generation of the subsequent anti-OmCI mAbs.

4.2.5.2. Characterisation of MBI-Om3 (IgG2b)

The double screening approach gave rise to four clones producing OmCI-reactive antibody. The antibody that gave the best signal on the capture ELISA (MBI-Om3), was purified and characterised. The Western blot analysis shown in Fig.4.9 demonstrated that MBI-Om3 was able to react with pOmCI and OmCI-Fc.

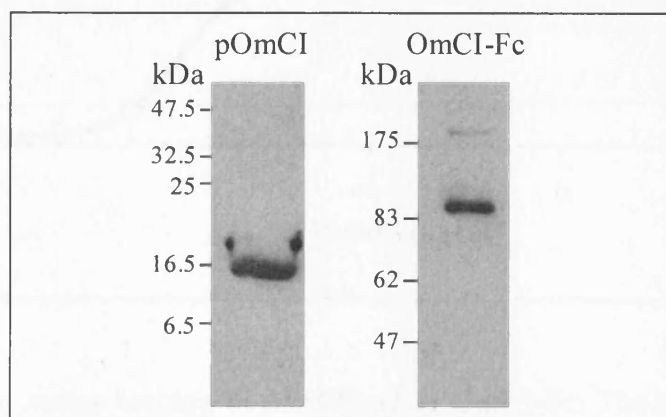


Fig.4.9 Western blot analysis of MBI-Om3-HRPO binding to OmCI and OmCI-Fc. pOmCI (pure protein) or OmCI-Fc (supernatant) was resolved by SDS-PAGE on 15% gel (pOmCI) or 7.5% gel (OmCI-Fc) and transferred to a nitrocellulose membrane. The membrane was probed with MBI-Om3-HRPO.

One of the reasons to develop anti-OmCI mAb was to enable purification of the OmCI-Fc fusion protein. To do so the antibody needed to be coupled to the matrix of a chromatography column. The capacity of MBI-Om3 immobilised on a solid phase to bind OmCI-Fc was verified in ELISA format. MBI-Om3 was used to capture OmCI-Fc (present in tissue culture supernatant) on to the plate. Using an antibody to bind OmCI-Fc on a plate will retain the antigen in its native form. The binding was then detected with rabbit anti-OmCI polyclonal antibody. The analysis revealed that MBI-Om3 antibody was able to recognise OmCI-Fc fusion protein in a dose dependent manner (Fig.4.10). Most importantly, the results indicated that this monoclonal antibody, coupled to chromatography column had potential to bind OmCI-Fc protein and to purify it from tissue culture supernatant. This antibody was used to generate an affinity column that was able to purify OmCI-Fc as described in Chapter 5. For this reason the last three anti-OmCI mAbs generated during the double screening were not characterised at this time.

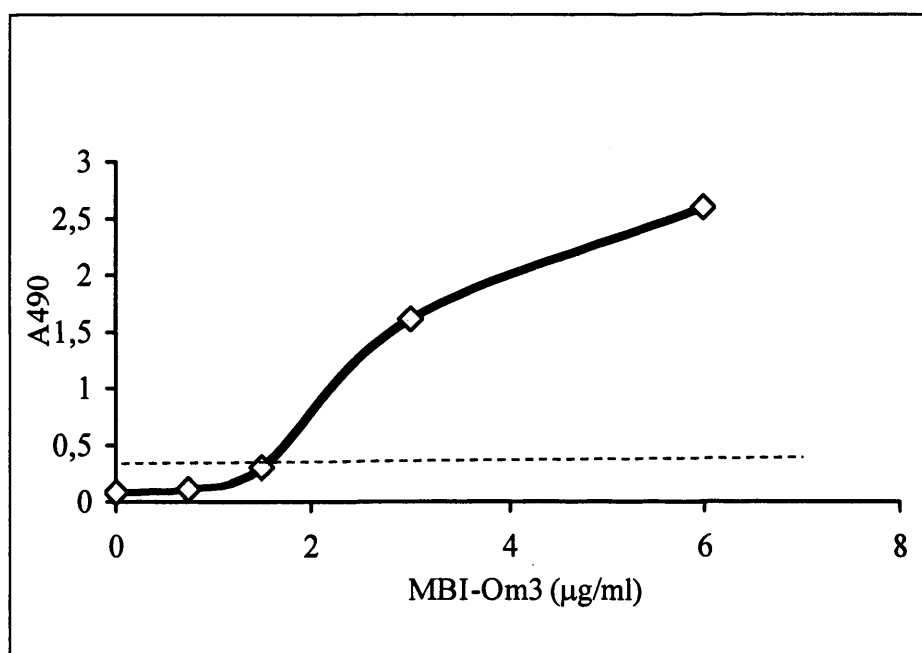


Fig.4.10 ELISA to assess binding of MBI-Om3 to OmCI-Fc. The plate was pre-coated with various concentrations of MBI-Om3 and 100µl of tissue culture supernatant containing OmCI-Fc fusion protein were added. The plate was then incubated with rabbit anti-OmCI polyclonal Ab following by incubation with anti-rabbit Ig-HRPO. The test antibody coated on the plate bound OmCI-Fc in a dose dependent manner. The medium background control is presented with a dotted line.

4.3. Rat anti-mouse CRIG and rat anti-mouse CD59a monoclonal antibodies

To purify and characterise the CRIG-CD59 reagents, availability of good mAbs was an indispensable requirement. Anti-CRIG and -CD59 mAbs were generated by immunising rats with recombinant CRIG-CD59 fusion protein (generation of CRIG-CD59 was described in Chapter 3). Supernatants from the hybridoma cells were screened on a plate coated with the antigen used for immunisation. A second ELISA, with CD59-Fc coated on the plate, was also performed in order to discriminate the cells producing anti-CRIG Ab from those secreting antibody specific for CD59. The ability of the antibodies to bind native CRIG and CD59 (expressed on cells) was validated.

4.3.1. Generation of rat anti-mouse CRIG and rat anti-mouse CD59a monoclonal antibodies

Female Lewis rats (10-12 weeks old) received 50 μ g CRIG-CD59 fusion protein initially emulsified in Freund's complete adjuvant, followed 2 weeks later by similar booster injection emulsified in Freund's incomplete adjuvant. Two more booster injections were administered at 2-week intervals. After the third immunisation, the rats were test bled and the serum tested for reactivity with CRIG-CD59. The animal showing the strongest reactivity with the antigen was selected for fusion (Fig.4.11). This animal was given a final immunisation by the *ip* route with 50 μ g of CRIG-CD59 fusion protein diluted in PBS and 2 days later the spleen was harvested. The splenocytes were isolated and fused with mouse myeloma SP2/O cells using polyethylene glycol as fusogen as described in Chapter 2. The cell mixture was plated in 24-well plates containing a feeder layer of mouse peritoneal macrophages. Hybridomas were selected by growing in HAT medium. 10-12 days following the fusion, the cell supernatant was screened. Cells were harvested from the selected wells and plated out at limiting dilution into wells containing feeder cells. Screening and cloning were repeated to obtain monoclonal populations.

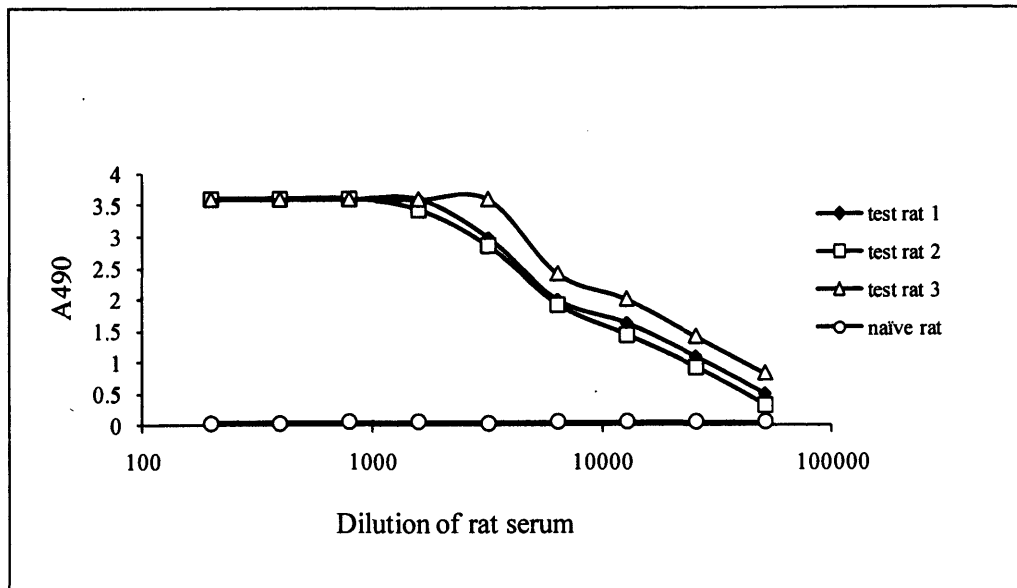


Fig. 4.11 ELISA to test specific antibody titre of rats immunised with CRlg-CD59 fusion protein. Rats immunised with CRlg-CD59 or non-immunised (open diamond) were bled and serum samples were incubated in wells coated with CRlg-CD59 antigen. The binding was detected with anti-rat IgG-HRPO. The rat with the highest antibody titer (open triangle) was boosted and the spleen harvested.

4.3.2. Screening ELISA

The hybridomas were screened for anti-CRlg and anti-CD59 antibodies by ELISA. Because the rat was immunised with CRlg-CD59 fusion protein, it was possible that the antibodies produced by the hybridomas could be reactive to either CRlg or CD59. To identify the specificity of the antibodies, double screening was performed. ELISA plates were coated with purified CRlg-CD59 or CD59-Fc fusion protein (generated previously in-house). Supernatant from growing hybridoma cells was added and the binding of the antibody to the coated antigen was detected by HRPO labelled anti-rat Ig. The specificity of the antibodies was determined by comparing the binding signal of each well to CRlg-CD59 and CD59-Fc. The antibodies that reacted with both, CRlg-CD59 and CD59-Fc, proteins were initially assumed to be CD59-specific and these that bound CRlg-CD59 only as CRlg-specific. Hybridomas producing anti-CD59 and anti-CRlg antibodies were selected and cloned at least three times by limiting dilution. Stable clones were expanded. Three monoclonal

antibodies were generated: one against CRlg and the remaining two against CD59 (named mCD59a-7 and mCD59a-8). ELISA-based isotype analysis (Method 2.5.9.2) was performed using HRPO-labelled secondary antibodies specific for rat immunoglobulins: IgM, IgG1, IgG2a, IgG2b and IgG2c. The analysis revealed that the three mAbs were of IgG1 isotype.

The cells producing mCD59a-7 and the anti-CRlg antibodies were expanded for large-scale antibody production (as described for anti-OmCI mAbs). The two mAbs were purified and further characterised.

4.3.3. Purification of rat anti-mouse CRlg and rat anti-mouse CD59a monoclonal antibodies

The anti-CRlg mAb and mCD59a-7 were of rat IgG1 subclass and were therefore purified using protein G affinity chromatography (as described for anti-OmCI mAb of mouse IgG isotype). The purified mAbs were subjected to SDS-PAGE analysis. As shown in Fig.4.12, the antibodies migrated as a single band under non-reducing conditions. Two bands, representing the heavy and the light chains, were found on the reducing. The result of the purity analysis demonstrated that purification using HiTrap protein G column yielded very pure preparations.

4.3.4. Characterisation of rat anti-mouse CRlg and rat anti-mouse CD59a monoclonal antibodies

The reason for generating anti-CRlg and anti-CD59 mAbs was to develop tools to characterise the CD59-CRlg reagents. Therefore an extensive analysis of the anti-CRlg and mCD59a-7 antibodies was needed. The ability of mAbs to bind recombinant and native antigens was verified.

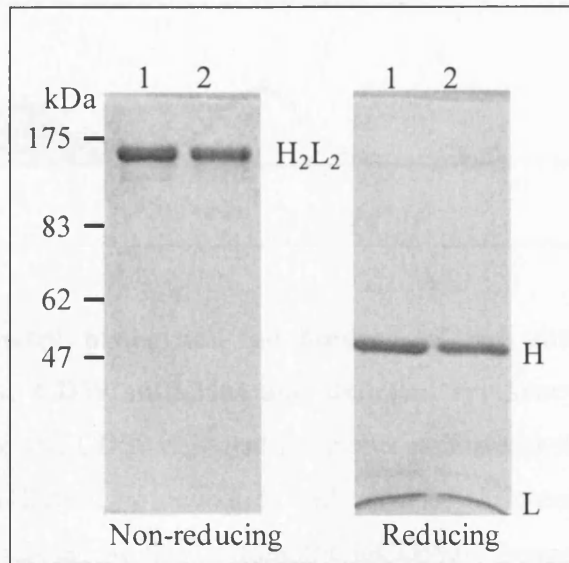


Fig.4.12 SDS-PAGE analysis of purified rat monoclonal antibodies specific to mouse CRIg or CD59a. Purified anti-CRIg (lane 1) and anti-CD59 (lane 2) Abs were electrophoresed under non-reducing and reducing conditions. The proteins were stained with Coomassie Blue. One band as observed under non-reducing condition. This consisted of two heavy and two light chains (H₂L₂). Two bands corresponding to the heavy (H) and light (L) chains of the antibodies were found under reducing conditions.

4.3.4.1. Characterisation of anti-CD59 mAb

The specificity of rat anti-mouse CD59 (mCD59a-7) mAb was confirmed by FACS analysis. CD59a deficient and sufficient mouse erythrocytes were isolated from CD59^{-/-} or WT mice. The cells were washed and resuspended in FACS buffer (1% BSA, PBS). After incubation with serial dilutions of mCD59a-7, the cells were pelleted. The unbound antibody was washed out and mCD59a-7 bound to the cells was detected with phycoerythrin-conjugated donkey anti-rat Ig, cells were analysed by flow cytometry. The result clearly demonstrated that mCD59a-7 was able to bind the cells expressing CD59 but not the erythrocytes derived from CD59 deficient mouse (Fig.4.13).

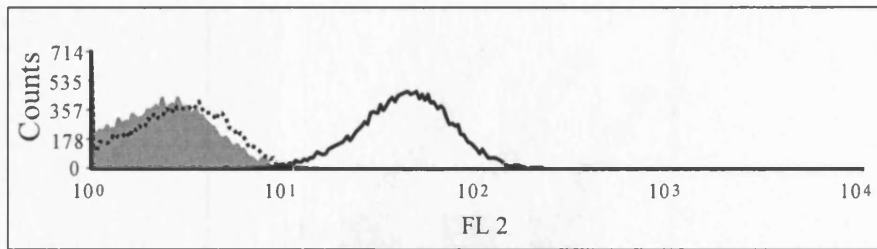


Fig.4.13 Flow cytometry histogram for binding of rat anti-mouse CD59a mAb (mCD59a-7) to mouse CD59 sufficient and deficient erythrocytes. Erythrocytes were isolated from wild type and CD59 deficient mice and incubated with 6 μ g/ml of mCD59a-7 monoclonal antibody, followed by incubation with phycoerythrin-conjugated donkey anti-rat Ig. The binding was analysed by flow cytometry. mCD59a-7 bound CD59 expressing cells (solid line) and no detectable reactivity was observed with CD59^{-/-} erythrocytes (filled area). Antibody isotype control is the dotted line.

4.3.4.2. Characterisation of anti-CRIg mAb

The specificity of the anti-CRIg mAb was analysed by western blot and immunohistochemistry. To check whether the antibody recognised CRIg but not a neo-epitope formed after the fusion with CD59, CRIg containing fusion proteins (different to the one used for the antigen challenge, CRIg-CD59) were subjected to SDS-PAGE and transferred to nitrocellulose membrane (Fig.4.14). The membrane was probed with the purified anti-mouse CRIg mAb. The fusion proteins migrated as two forms -monomers and dimers. The antibody was able to detect CRIg in both forms of all fusion proteins. Furthermore it recognised a fusion protein CRIg-2a-factor H, which did not contain CD59. These data suggested that the antibody-binding site is exclusively within the CRIg moiety of the hybrid molecules but not in CD59 or in the join between them.

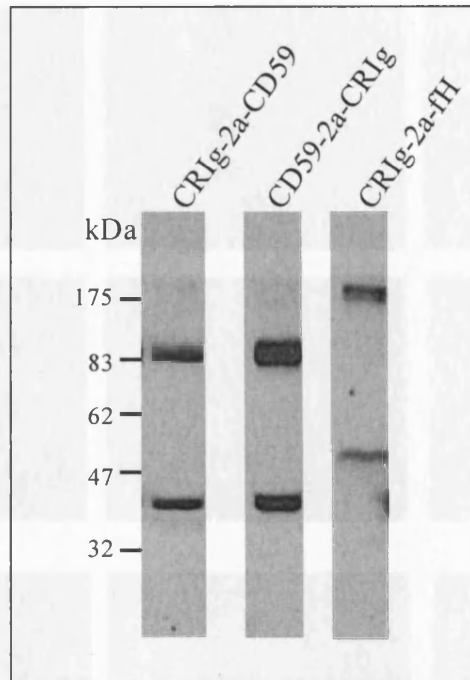


Fig.4.14 Western blot analysis of monoclonal antibody against mouse CRiG. CRiG-2a-CD59, CD59-2a-CRiG and CRiG-2a-fH were subjected to SDS PAGE under non-reducing conditions and transferred to a membrane by Western blot. The blot was incubated with the test anti-CRiG mAb. Molecular weight markers are shown on the left. The test antibody recognised the monomeric and dimeric forms of all three fusion proteins. It reacted with N-terminal and C-terminal CRiG (within CRiG-2a-CD59 and CD59-2a-CRiG respectively). The monoclonal antibody also bound in CRiG-2a-fH, a negative control fusion protein, which did not contain CD59.

To investigate whether the anti-CRiG mAb recognised a native antigen, immunohistochemical analysis was performed. CRiG is a complement receptor expressed on resident macrophages and Kupffer cells in the liver [161]. Therefore a liver from a BalbC mouse was harvested and frozen sections were prepared. The tissue was stained for CRiG using the anti-CRiG mAb. An isotype control was also included. The microglia in brain tissue do not express CRiG therefore frozen section from mouse spinal cord was used as a negative control. The anti-CRiG antibody specifically bound liver but not spinal cord tissue (Fig.4.15). The analysis demonstrated that anti-CRiG mAb specifically binds denatured (shown by western blot) as well as native CRiG (shown by immunohistochemistry).

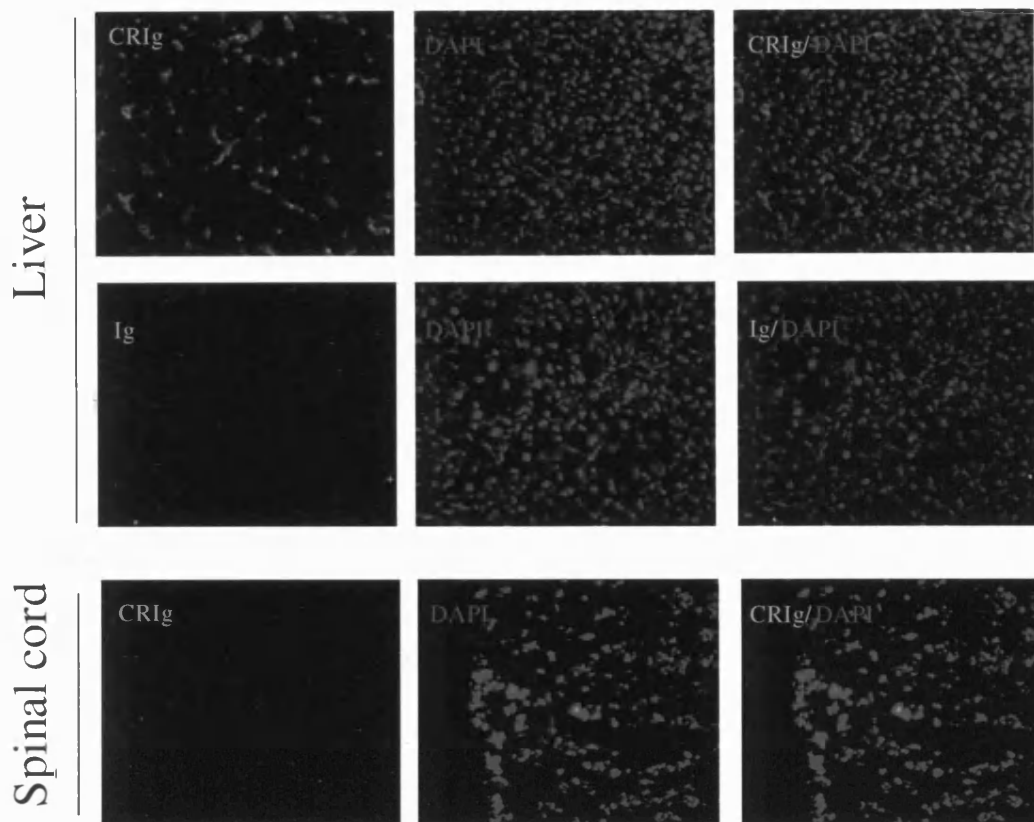


Fig.4.15 CRIg staining. Immunostaining was performed on sections obtained from mouse liver (positive control tissue) and spinal cord (negative control tissue) using monoclonal anti-CRIg antibody (green channel) at a concentration of 3.5 μ g/ml. DAPI staining (blue channel) was used to detect the nuclei. The anti-CRIg antibody specifically recognised CRIg expressed in liver. No staining was found in the control tissue or when isotype control antibody was used.

4.4. Discussion

Specific antibodies are key tools for the purification and characterisation of newly generated recombinant proteins. The main focus of the work in this chapter was the development of antibodies specific for complement regulators; this involved generation of hybridomas secreting antibody specific for pOmCI, OmCI-Fc, CRIg and CD59, followed by their purification and characterisation. These antibodies were important not only for efficient purification of the recombinant complement inhibitors but also for *in vitro*, *ex vivo* and *in vivo* characterisation of these therapeutic agents.

Conventional hybridoma technology was used to generate the monoclonal antibodies. The first steps were antigen preparation and antigen challenge of animals. Mice and rats were used for generation of hybridomas secreting specific antibody. The choice of species depended on the origin of the antigen used for immunisation. The immune system usually does not respond to self-antigens. Rats are not used for the production of antibodies to rat proteins and mice for antibodies to mouse proteins. For this reason mice were used for production of antibodies to soft tick glycoprotein OmCI and rats for the generation of antibodies to mouse CRIg and mouse CD59.

Six hybridoma clones producing mouse anti-OmCI mAbs were selected and the isotype of the antibodies was determined. The specificity of the antibodies was found to be dependent on the design of the screening approach. Three ELISAs were developed for detection and selection of OmCI reactive antibodies. Two antibodies, of IgG1 and IgM isotypes, which recognised denatured OmCI, were generated when the hybridoma clones were screened on a pOmCI-coated plate. Many studies have demonstrated a tendency of immobilised proteins to undergo conformational changes and denaturation as a consequence of their binding to the plastic surface [400-402]. The pOmCI coated directly on the plate was presumably partially or completely denatured and therefore the selected antibodies from this screening turned out to be specific for the denatured protein. The denaturation problem was overcome by capturing pOmCI using specific rabbit polyclonal antibody on the plate and thus maintaining its native conformation. A double screening approach was introduced to select clones producing antibodies that are highly specific to OmCI. The specificity of the clones was verified on a “negative” control ELISA incubated with buffer instead of pOmCI (Fig4.3). The double screening approach proved to be particularly effective for identifying positive

hybridoma clones which were reactive against native OmCI. Hybridomas from the four original fusion wells were taken successfully through the cloning process and four highly specific anti-OmCI mAbs were developed and one of IgG2b isotype was purified and characterised.

The isotype of the antibodies was important for the choice of purification strategy. The antibodies of the subclasses IgG1 (MBI-Om1) and IgG2b (MBI-Om3) were readily purified by protein G affinity chromatography and the purification of IgM (MBI-Om2) required thiophilic chromatography followed by further polishing steps. Because an additional purification step such as gel filtration was required to obtain pure MBI-Om2, only the two other mAbs of IgG isotype were further characterised. Methods such as ELISA, western blot and biacore analysis were used to characterise the antibodies. The result from the detailed analysis revealed that MBI-Om1 recognised denatured OmCI, but not native protein. MBI-Om3 was specific to native OmCI. Furthermore, it was able to capture OmCI-Fc on the ELISA plate indicating that it might also work well for affinity chromatography. MBI-Om3 proved to be the key tool in the purification of OmCI-Fc fusion protein and its *in vivo* characterisation.

A similar approach was used to generate anti-mouse CRlg and anti-mouse CD59a mAbs. When rats were immunised with CRlg-CD59 recombinant fusion protein, two kinds of antibodies were produced in the animals. One set of antibodies was elicited by CRlg in the fusion protein, and the other was elicited by CD59. Both antibody types would be useful tools in this project. In order to identify and discriminate such antibodies, two different fusion proteins, CRlg-CD59 and CD59-Fc, were used as coating antigens in the screening ELISA. Two clones producing antibodies reactive with both CRlg-CD59 and CD59-Fc were obtained. These were considered as CD59 specific antibodies (mCD59a-7 and mCD59a-8). mCD59a-7 was purified and its specificity for native protein was confirmed by flow cytometry using CD59-deficient and sufficient mouse erythrocytes.

Among the hybridomas screened on the two fusion proteins, one clone reacted with CRlg-CD59, but not with CD59-Fc antigen. The antibody secreted from the cells was considered as CRlg specific. It was purified and its capacity to interact with recombinant antigen was analysed by Western blot. The mAb was able to detect CRlg in a number of fusion proteins, including protein that did not contain CD59 moiety (CRlg-factor H). This suggested that the

epitope for this mAb was located within CRIG but not in CD59. Furthermore the anti-CRIG mAb recognised native CRIG as shown from the immunohistochemical analysis of mouse liver.

In conclusion, two monoclonal antibodies specific for mouse CD59a and one against mouse CRIG were generated and characterised. These antibodies would be used to characterise the anti-complement therapeutics generated in this project.

Chapter 5. Purification and biochemical characterisation of anti-complement therapeutics

The generation and expression of the anti-complement reagents was described in Chapter 3. The focus is now moved to the purification and biochemical characterisation of OmCI-Fc and CRIG-CD59 fusion proteins and their ligands (complement proteins C3 and C5). To assess CRIG-CD59 targeted inhibitory activity, soluble CRIG and soluble CD59 are required. This Chapter explains the generation of control proteins containing CRIG and CD59 but not fused to each other.

5.1. OmCI-Fc

5.1.1. Purification of OmCI-Fc

Different chromatographic methods could be employed for purifying Fc fusion proteins and the choice of the approach depends on the type of the protein. As a potential therapeutic it is necessary that OmCI-Fc is of high purity, that it has functional activity and is in sufficient amount for *in vitro* and *in vivo* analysis. A thorough study was carried out to determine the optimal purification approach and two chromatography strategies were investigated and compared.

5.1.1.1. Purifying via the Fc portion

Protein A and protein G chromatography (described in Chapter 4) is based on the affinity interaction of the Fc domain with these bacterial proteins and can be employed for purification of Fc fusion proteins. Fc of mouse IgG2a (used in OmCI-Fc) has good affinity for protein G and A. However the bovine antibodies present in the FCS used to supplement cell culture media also have a good affinity for protein G and will compete with OmCI-Fc for binding to the column. To avoid contamination with bovine immunoglobulins, CHO cells expressing OmCI-Fc were cultured in medium supplemented with low Ig FCS. The

tissue culture supernatant was passed over the protein 5ml G or protein A column, the column was washed and bound protein was eluted at low pH (pH2.5). No protein was found in any of the fractions when absorbance at 280nm was measured. Elution with high pH buffer (PBS containing diethylamine, pH 11) was then tested and again no protein was detected in any of the eluted fractions.

To confirm that OmCI-Fc did not bind to protein G and protein A and to determine whether it bound but could not be dissociated during the elution step, an ELISA was performed. The analysis showed a very little depletion of the supernatant after it had passed through protein A column (Fig.5.1A). A similar result was obtained with protein G (data not shown). As this method gave no purified OmCI-Fc protein, another chromatography approach was investigated. Anti-OmCI antibody columns were generated and used for OmCI-Fc purification.

5.1.1.2. Purifying via the OmCI domain

Specific polyclonal and monoclonal anti-OmCI antibodies were tested for their suitability to purify OmCI-Fc.

5.1.1.2.1. Polyclonal anti-OmCI affinity chromatography

Immunoglobulins from rabbit anti-OmCI polyclonal serum were purified on a protein G column (Method 2.3.3) and 30 mg was used to prepare an anti-OmCI affinity column (5ml HiTrap). Supernatant containing OmCI-Fc was passed over the column, the column was washed with TBS and bound protein was eluted with glycine pH 2.5. When no protein was found in the eluate, a buffer with a high pH (PBS containing 20mM diethylamine, pH11) was run over the column. No protein was detected in any of the eluted fractions. ELISA-based analysis was carried out to assess the degree of OmCI-Fc depletion. Similarly to the result obtained with protein A and G chromatography, a very little depletion of the run through was seen when compared to the tissue culture supernatant prior the purification (Fig.5.1B).

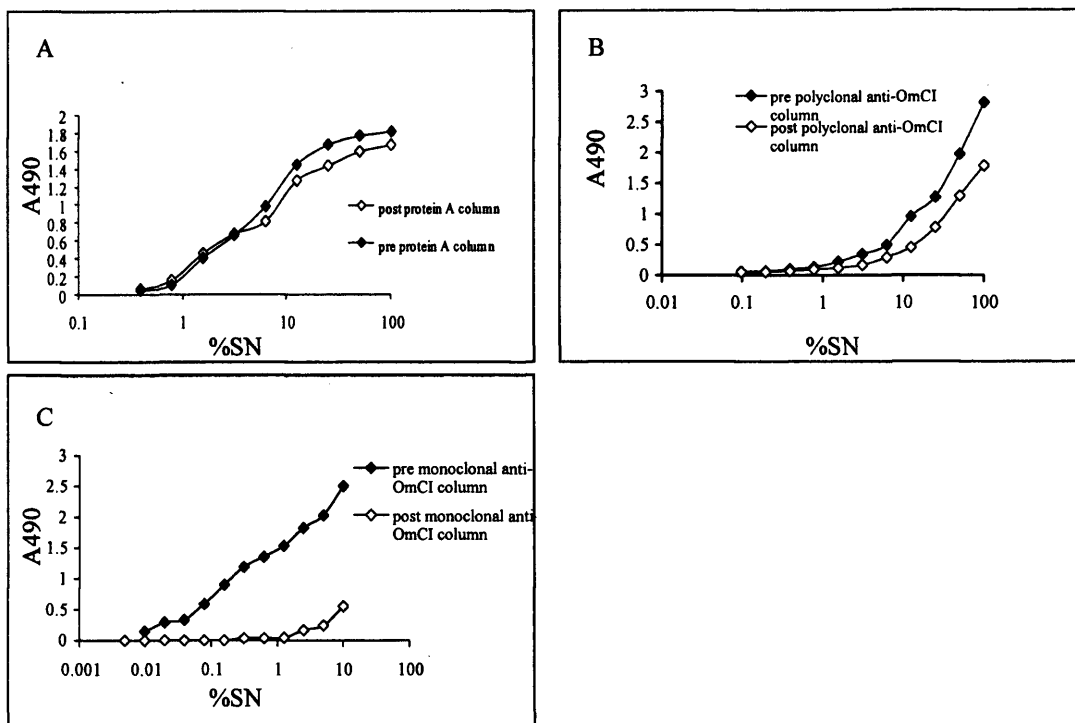


Fig.5.1 ELISA to determine efficiency of purification of OmCI-Fc. To assess the degree of supernatant depletion achieved by protein A (A), polyclonal anti-OmCI (B) and monoclonal anti-OmCI (C) affinity chromatography, an ELISA was carried out as follows. The plate was coated with rabbit anti-OmCI polyclonal antibody, blocked and incubated with a sample of supernatant from before and after the column (1:2 serial dilutions). The plate was probed with anti-mouse IgG HRPO. OmCI-Fc was detected in both the pre column supernatant and the run through. Very little difference was seen between the two supernatants suggesting that OmCI-Fc failed to bind the protein A or the polyclonal anti-OmCI column (A and B). Only a small amount of protein was detected in supernatant after passing over the monoclonal affinity column. The monoclonal affinity column was adopted as the method for purification of OmCI-Fc from supernatant.

5.1.1.2.2. Monoclonal anti-OmCI affinity chromatography

The antibody (MBI-Om3, IgG2b) that recognised native OmCI and passed the double screening test analysis (explained in Chapter 4, section 4.2.4) was used to generate an affinity column. MBI-Om3 (27mg) was coupled to prepacked Sepharose. Tissue culture supernatant from cells expressing OmCI-Fc cultured in *HYPERFlask* was loaded onto the

column. The unbound protein was washed out and the protein associated with the anti-OmCI Ab was eluted with a glycine buffer (pH 2.5). The fractions containing eluted protein were identified, neutralised, pooled and dialyzed against PBS. An ELISA analysis was conducted to determine the efficiency of purification. Almost no OmCI-Fc was detected in the run through (Fig.5.1C).

5.1.2. Biochemical characterisation of OmCI-Fc

The purity of OmCI-Fc isolated from tissue culture supernatant using anti-OmCI monoclonal antibody (MBI-Om3) column was verified by SDS-PAGE. The molecular weight of the recombinant protein was determined using its relative mobility in the gel and by gel filtration chromatography.

5.1.2.1. SDS-PAGE characterisation of OmCI-Fc

The overall purity and the molecular weight of the recombinant protein purified on an anti-OmCI column was determined by SDS-PAGE. OmCI-Fc eluted from the affinity column and dialysed in PBS was subjected to SDS-PAGE on a 7.5% gel. The protein was visualised by staining with Coomassie blue (Fig.5.2). Two bands were seen under non-reducing condition. This was consistent with the result obtained from the western blot analysis of the tissue culture supernatant (Chapter 3, Fig.3.11).

The apparent molecular mass of the protein was estimated using its relative mobility. The calculation for protein molecular mass is explained in section 2.4.7.1 of Chapter 2. The major band was with apparent molecular weight of 90 kDa, agreeing with the mass predicted for OmCI-Fc. A higher molecular weight band was also observed. Initially this band was defined as a product of aggregation since there was reactivity with antibody specific for OmCI on Western blot analysis (Fig.3.11)). However, three bands were seen under reducing conditions (Coomassie staining, Fig.5.2), when only one was expected for pure OmCI-Fc. The band with the highest intensity (51 kDa) represented the polypeptide backbone of OmCI-Fc. The molecular weight of the two additional bands corresponded very well with a

C5 profile under reducing conditions: α -chain (127 \pm 5 kDa) and β -chain (74 \pm 2kDa) [403]. It is likely that the OmCI-Fc expressed from the CHO cells bound bovine C5 from the FCS in tissue culture medium. It appeared that the first band seen on the Western blot represents the OmCI-Fc while the higher molecular weight band was mostly bovine C5 and a bit of OmCI-Fc aggregating material. This suggests that the anti-OmCI mAb (MBI-Om3) used in this analysis but also used to purify OmCI-Fc binds the free Fc fusion protein and also the C5 complex. There is good possibility that bovine C5 has been co-purified with OmCI-Fc.

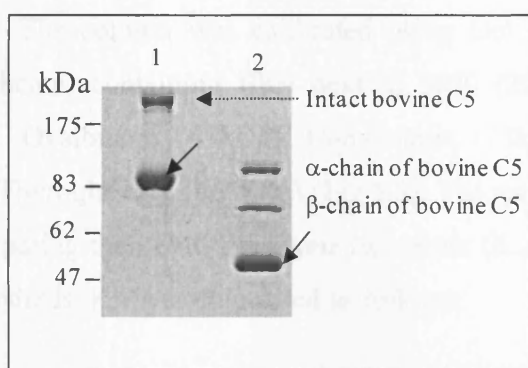


Fig.5.2 SDS-PAGE of purified OmCI-Fc fusion protein. Purified OmCI-Fc was subjected to SDS-PAGE on a 7.5% under non-reducing (lane1) and reducing conditions (lane2) and stained with Coomassie Blue. The protein migrated as two bands under non reducing conditions (lane 1). The band, indicated with arrows, with apparent molecular weight of 90kDa corresponded to OmCI-Fc. The additional higher molecular band (indicated with dotted arrow) was likely to represent bovine C5 from the cell growing medium, co-purified with OmCI-Fc. Three bands were visible under reducing conditions. The polypeptide chain of OmCI-Fc is indicated with arrows. The higher molecular weight bands represent the α - and β -chain of bovine C5. Molecular weight markers are shown on the left.

5.1.2.2. Gel filtration of OmCI-Fc

Gel filtration was used to remove C5 contamination from OmCI-Fc protein and as an alternative way to determine the apparent molecular weight of the fusion protein.

This method separates the proteins and peptides based on their size. Separation was achieved using a porous matrix of dextran chains covalently linked to highly cross-linked agarose particles (Superdex) to which the molecules have different degrees of access. Smaller molecules have greater access and larger molecules are excluded from the matrix. Therefore proteins are eluted from the column in decreasing order of size, with the largest molecules (bovine C5 in this case) eluting from the column first.

Gel filtration also allows an estimation of the molecular weight of protein or multiprotein complexes. The molecular weight estimation is based on the assumption that the proteins have a globular shape. The column was calibrated using Gel filtration High Molecular Weight Kit (GE Healthcare) containing Blue dextran 2000 (2000kDa, for column void volume determination), Ovalbumin (43kDa), Conalbumin (75kDa), Aldolase (158kDa), Ferritin (440kDa), and Thyroglobulin (669kDa) (Fig.5.3). The molecular weight of proteins was determined by comparing their elution volume parameter (K_{av}) with the values obtained from the calibration standards. K_{av} was calculated as follows:

$$K_{av}=(V_e-V_o)/(V_c-V_o)$$

V_o is elution volume of molecules larger than the largest pores in the matrix and therefore remains in the buffer and pass straight through the packed bed.

V_c is the geometric volume of the column.

V_e is elution volume.

To measure the molecular weight and to remove bovine C5, OmCI-Fc purified from tissue culture supernatant on an anti-OmCI column was applied to a Superdex 200 10/300GL column (GE Healthcare) equilibrated with PBS. Eluted proteins were detected by monitoring their UV absorbance at 280nm. Three peaks were detected (Fig.5.4A). Peak fractions were pooled and the purity of the protein was analysed by SDS-PAGE on a 7.5% gel (Fig.5.4B). The protein was visualised by silver staining. Aggregates and C5 were eluted in the first two peaks, traces of OmCI-Fc were also visible. The majority of OmCI-Fc protein was eluted in the third peak with characteristic elution volume of 12.30ml (between 440kDa-ferritin and 158-aldolase), corresponding to apparent molecular weight of 174kDa. The molecular mass obtained from the gel filtration was greater than the molecular mass measured by SDS-PAGE analysis (Table 5.1). The variation could be explained by a non-spherical shape of the fusion proteins. No aggregates or C5 were detected in the OmCI-Fc peak. Using gel

filtration chromatography as a polishing purification step C5 and aggregates free OmCI-Fc protein preparation was obtained.

Reagent	Mass based on amino acid sequence (kDa)	Experimental mass SDS-PAGE (kDa)	Experimental mass Gel filtration (kDa)
OmCI-Fc	83	83	174
CRIG-CD59	30	33	93.68
CD59-CRIG	30	33	87.11
CRIG-3-CD59 m/d	32/64	39/94	110/295
CD59-3-CRIG m/d	32/64	39/94	123/276
CD59-2a-CRIG m/d	32/64	40/96	118/280
CRIG-2a-CD59 m/d	32/64	40/96	n/a
Cleavable CD59-CRIG	30	33	96

Table 5.1 Experimental molecular mass of anti-complement reagents determined by SDS-PAGE and Gel filtration analysis or based on the amino acid sequence. m, monomer; d, dimer; n/a, not available;

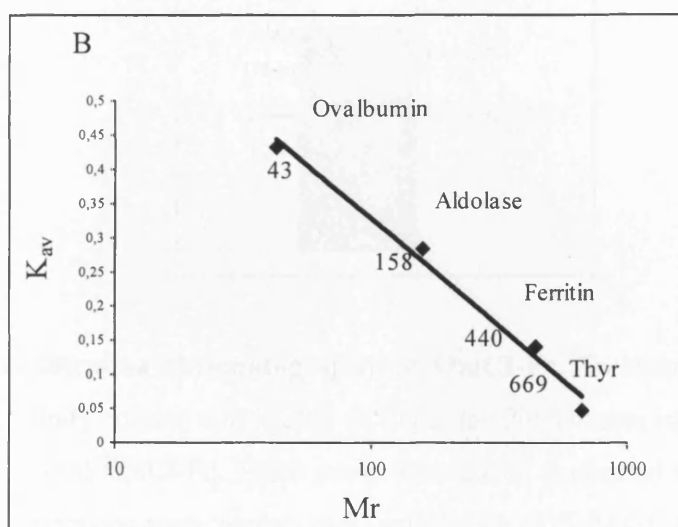
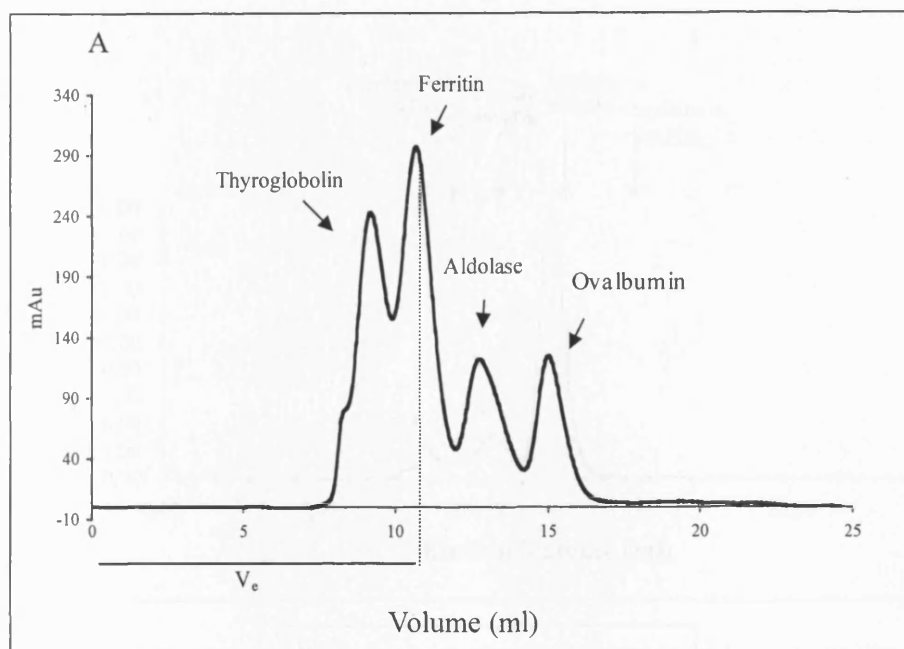


Fig.5.3 Calibration of SD200 gel filtration column. A. Gel filtration chromatography of a series of protein molecular mass standards on a pre-packed Superdex 200 column. Standards were: thyroglobulin (669kDa), ferritin (440kDa), aldolase (158 kDa), ovalbumin). The elution volume V_e of ferritin is shown on the histogram. B. Standard curve. The standard curve for a particular gel filtration media is a plot of K_{av} of the standards versus log of their molecular weight, and the data shown here has been derived from panel A. The curve was used estimate the molecular mass of anti-complement reagents.

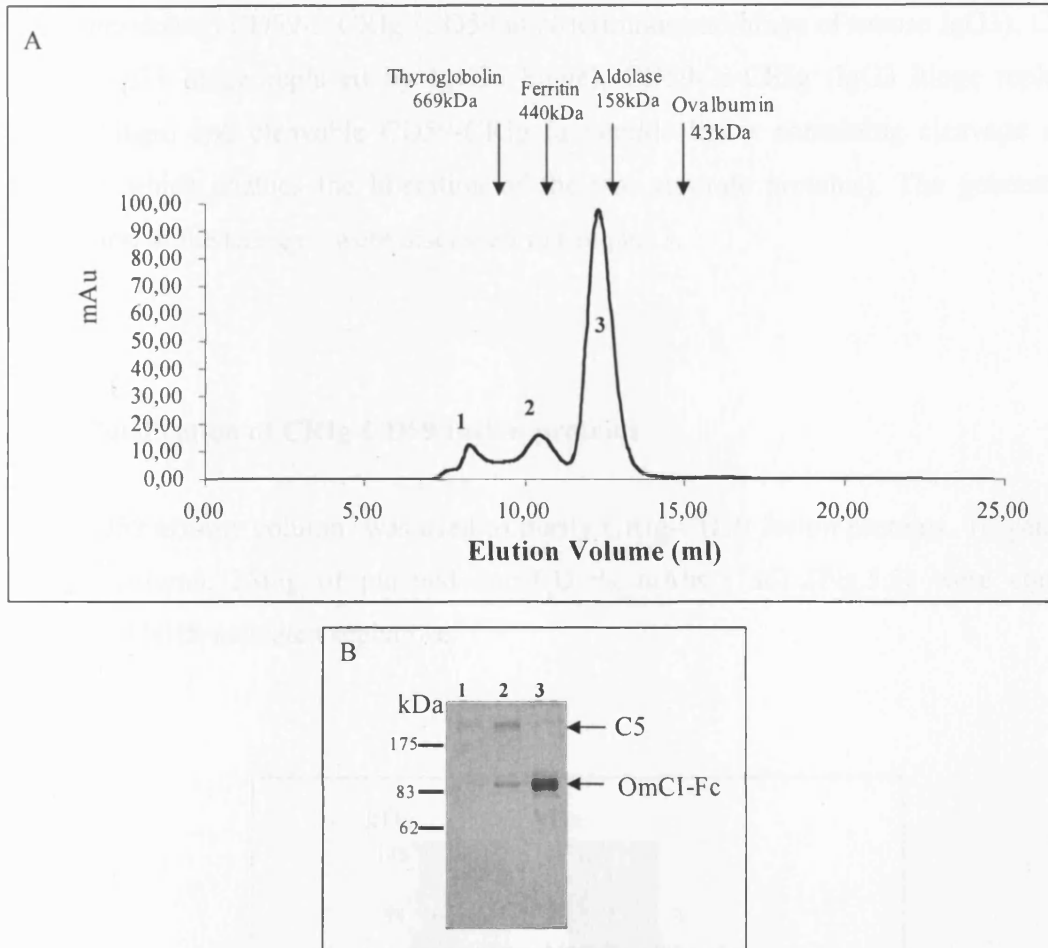


Fig. 5.4 Gel filtration chromatography of OmCI-Fc. To remove aggregates OmCI-Fc purified on affinity column was loaded on Superdex 200 column equilibrated in PBS. A. Gel filtration profile of OmCI-Fc. Three peaks were eluted (indicated with a numbers from 1 to 3). The peak fractions were pooled and analysed by SDS-PAGE on 7.5% gel. The protein was visualised by silver staining (B). Each peak is indicated with its corresponding number. OmCI-Fc was eluted as peak 3 at 12.30ml between Ferritine and Aldolase and corresponds to 174kDa apparent molecular weight. No contamination of C5 was detected. C5 was eluted early, in peaks 1 and 2. Trace of OmCI-Fc was also found in these peaks.

5.2. CR1g-CD59 fusion proteins

Seven CR1g-CD59 fusion proteins have been generated: CR1g-CD59 (CD59 at C-terminus), CD59-CR1g (CD59 at N-terminus), CR1g-3-CD59 (CD59 at C-terminus and hinge of mouse

IgG3 introduced) CD59-3-CRIg (CD59 at N-terminus and hinge of mouse IgG3), CRIg-2a-CD59 (IgG3 hinge replaced by IgG2a hinge), CD59-2a-CRIg (IgG3 hinge replaced by IgG2a hinge) and cleavable CD59-CRIg (a peptide linker containing cleavage sites for protease which enables the liberation of the two separate proteins). The generation and expression of the reagents were discussed in Chapter 3.

5.2.1. Purification of CRIg-CD59 fusion proteins

Anti-CD59 affinity column was used to purify CRIg-CD59 fusion proteins. To generate an affinity column, 28mg of purified anti-CD59a mAbs (7a6) (Fig.5.5) were coupled to prepacked NHS-activated sepharose.

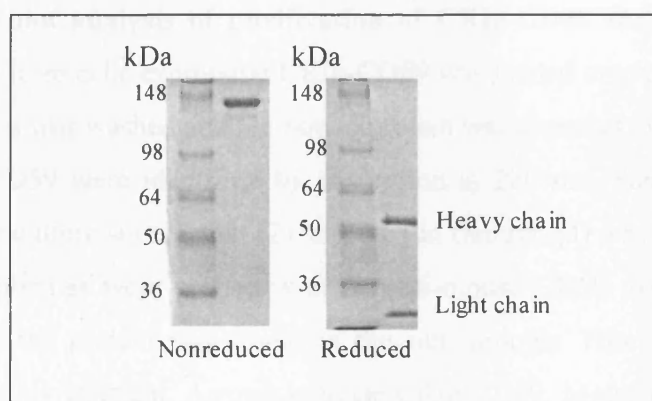


Fig. 5.5 SDS-PAGE analysis of anti-mouse CD59 mAb. Anti-mouse CD59 mAb was purified on protein G column and visualised on SDS-PAGE (under reduced and non-reduced conditions) by Coomassie staining.

Supernatant containing CD59 fusion protein was passed over the column. The column was washed with TBS and the fusion protein was eluted at high pH. Protein-containing fractions were identified, combined and dialysed against PBS and analysed by Western blot. The blot was developed with a rat anti-mouse CD59 mAb. The efficiency of purification is shown in Fig.5.6, where CRIg-CD59 is illustrated as an example. As may be noted in the figure CRIg-

CD59 was not detected in the run through, suggesting that the supernatant was completely depleted (Fig.5.6).

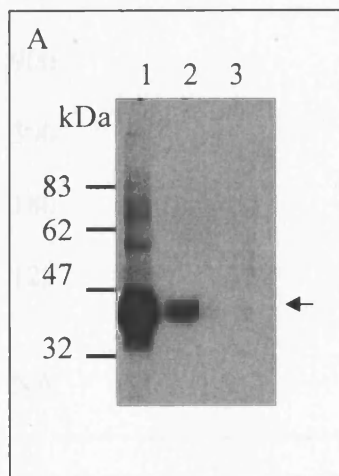


Fig. 5.6 Western blot analysis of purification of CRlg-CD59 fusion proteins. Tissue culture supernatant from cells expressing CRlg-CD59 was loaded onto an anti-CD59 affinity column. The column was washed and the bound protein was eluted at high pH. The fractions containing CRlg-CD59 were identified by absorption at 280 nm. Samples from the peak fractions (1), tissue culture supernatant (2) and the run through (3) was subjected to western blot analysis. Membranes were probed with rat anti-mouse CD59 mAb (mCD59a-7). No detectable level of the protein was found in the run through. This result suggested that purification was highly efficient. Arrows indicate CRlg-CD59. Molecular weight marker is shown on left.

The concentration of the reagents was calculated by measuring absorbance at 280nm and the rate of protein expression was determined. Table 5.2 shows the amount of purified protein produced per week in CELLline AD 1000 and HYPER*Flask*. The data revealed that the rate of protein production was greater in HYPER*Flask*, which was consistent with the result obtained from OmCI-Fc expression discussed in Chapter 3 (section 3.2.3.2, table 3.2). The purified proteins were concentrated and analysed by SDS-PAGE (Fig.5.7).

Reagent	Yield ($\mu\text{g}/\text{weekly harvest}$)	
	CELLine AD 1000 (20ml harvest)	HYPERFlask (500ml harvest)
CR Ig-CD59	93	700
CD59-CR Ig	900	NA
CR Ig-3-CD59	300	900
CD59-3-CR Ig	180	875
CR Ig-2a-CD59	125	NA
CD59-2a-CR Ig	NA	NA

Table.5.2 High-density tissue culture system and production of recombinant proteins expressed as μg per harvest. NA-not assessed

5.2.2. Biochemical characterisation of CR Ig-CD59 fusion proteins

5.2.2.1. SDS-PAGE analysis of CR Ig-CD59 fusion proteins

CD59 containing fusion proteins were analysed by SDS PAGE on 7.5% gel. The apparent molecular mass of the proteins was estimated using their relative mobility (Rf) as described in Chapter 2. The result is summarised in Table 5.1.

As can be noted in Fig. 5.7, the CR Ig-CD59 fusion protein, the construct in reverse orientation CD59-CR Ig and the cleavable CD59-CR Ig migrated as a single band with apparent molecular weight of 34kDa under nonreducing conditions. This confirmed the western blot analysis of crude supernatant, where one band of apparent molecular weight of 33kDa was detected with anti-CD59 mAb in the supernatant.

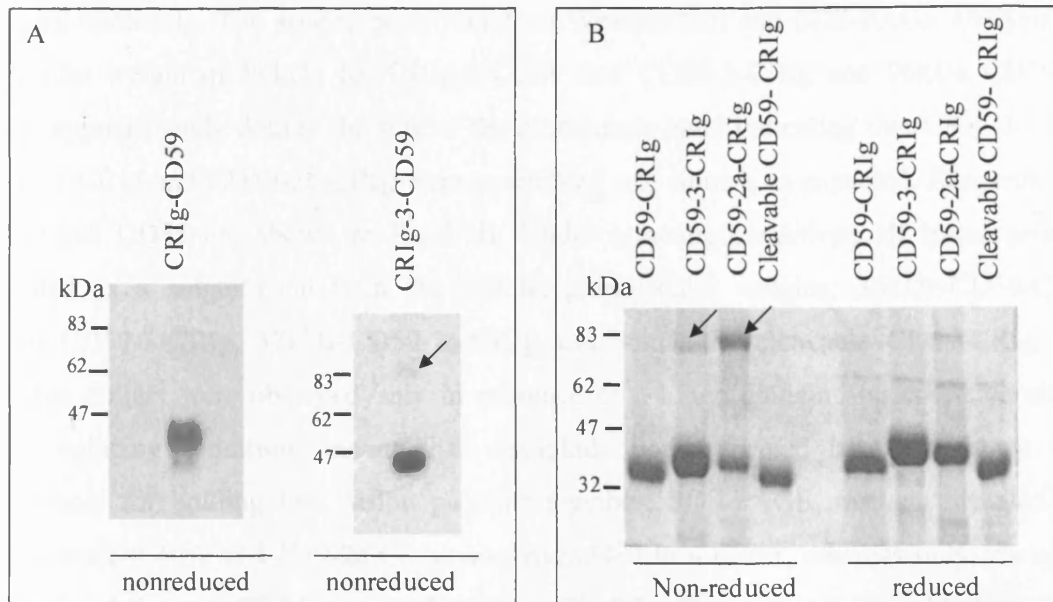


Fig.5.7 Purification of CR Ig-CD59 fusion proteins. Proteins were purified by anti-CD59 affinity chromatography, subjected to SDS-PAGE on a 7.5% gel and stained with Coomassie Blue. A. SDS-PAGE analysis of fusion proteins CR Ig-CD59 and CR Ig-3-CD59 under non-reducing conditions. CR Ig-CD59 migrated as a single band. Two bands were seen for CR Ig-3-CD59. The major band had approximate molecular weight of 33kDa. The faint band (indicated with arrows) is likely to represent a dimeric form of the protein. B. SDS-PAGE analysis of fusion proteins CD59-CR Ig, CD59-3-CR Ig, CD59-2a-CR Ig and cleavable CD59-CR Ig under non-reducing (left) and reducing conditions (right). Two bands were seen for CD59-3-CR Ig and CD59-2a-CR Ig under non-reducing condition. The arrows indicate the dimeric forms. All proteins migrate as a one band under reducing conditions. Loading is indicated above lanes.

The reagents containing antibody hinge: CR Ig-3-CD59, CD59-3-CR Ig and CD59-2a-CR Ig and CR Ig-2a-CD59 were resolved into two bands with molecular mass identical to this observed by western blot analysis of cell culture supernatant (Chapter 3). This result suggested that the proteins existed as two forms. The smaller band had apparent molecular weight of 39kDa (CR Ig-3-CD59 and CD59-3-CR Ig) and 40kDa (CD59-2a-CR Ig), slightly higher than CR Ig-CD59 or CD59-CR Ig proteins. This band is likely to represent monomeric configuration of the proteins. The increase in molecular mass of CR Ig-3-CD59, CD59-3-CR Ig, CD59-2a-CR Ig and CR Ig-2a-CD59 was due to the IgG hinge incorporated in the

chimeric molecule. The second band found on Western blot and SDS-PAGE analysis had molecular weight of 94kDa for CR Ig-3-CD59 and CD59-3-CR Ig and 96kDa CD59-2a-CR Ig, approximately double the size of the monomeric band indicating that CR Ig-3-CD59, CD59-3-CR Ig and CD59-2a-CR Ig were assembled into dimers as expected. Reagents with N-terminal CD59 are shown in Fig.5.7B. Under reducing conditions all tested proteins migrated as a single band with the following molecular weights: 36kDa-CD59-CR Ig, 38kDa-CD59-3-CR Ig, 37kDa-CD59-2a-CR Ig and 36kDa-the cleavable CD59-CR Ig. The fact that dimers were observed only in presence of a hinge domain and could be altered under reducing conditions means that disulphide bonds formed between hinges were responsible for holding two fusion proteins together. SDS-PAGE analysis revealed that approximately 40% of CD59-2a-CR Ig was assembled in a dimer, whereas only 5% of the protein, containing IgG3 hinge was dimerised (Fig.5.7). The molecular weight obtained by SDS-PAGE analysis was slightly higher than the molecular weight from the amino acid sequence (Expert Protein Analysis System) (Table 5.1). This difference could be explained by post-translational modifications such as glycosylation. CR Ig-CD59 fusion proteins possess two potential N-linked glycosylation sites, one in the CR Ig moiety and one in CD59.

5.2.2.2. Gel filtration analysis of CR Ig-CD59 fusion proteins

Analytical gel filtration was used to confirm the ratio of monomer and covalent dimer and to precisely calculate their molecular weights.

Samples were loaded on Superdex 200 column equilibrated in PBS. CR Ig-CD59 and CD59-CR Ig were eluted as a single peak. The reagents containing hinge of antibody gave a distinct profile shown in Fig.5.8. Two peaks were observed for CR Ig-3-CD59, CD59-3-CR Ig and CD59-2a-CR Ig suggesting that these proteins indeed existed in two forms- monomer and covalently associated dimer (Fig.5.8 A and B). To prove that two peaks represent different oligomeric organization of the same protein, western blot analysis was performed (Fig.5.8C). Both elution peaks were recognized by anti-CD59 mAb and gave bands corresponding to the molecular weight of a monomer and dimer of the analysed fusion protein.

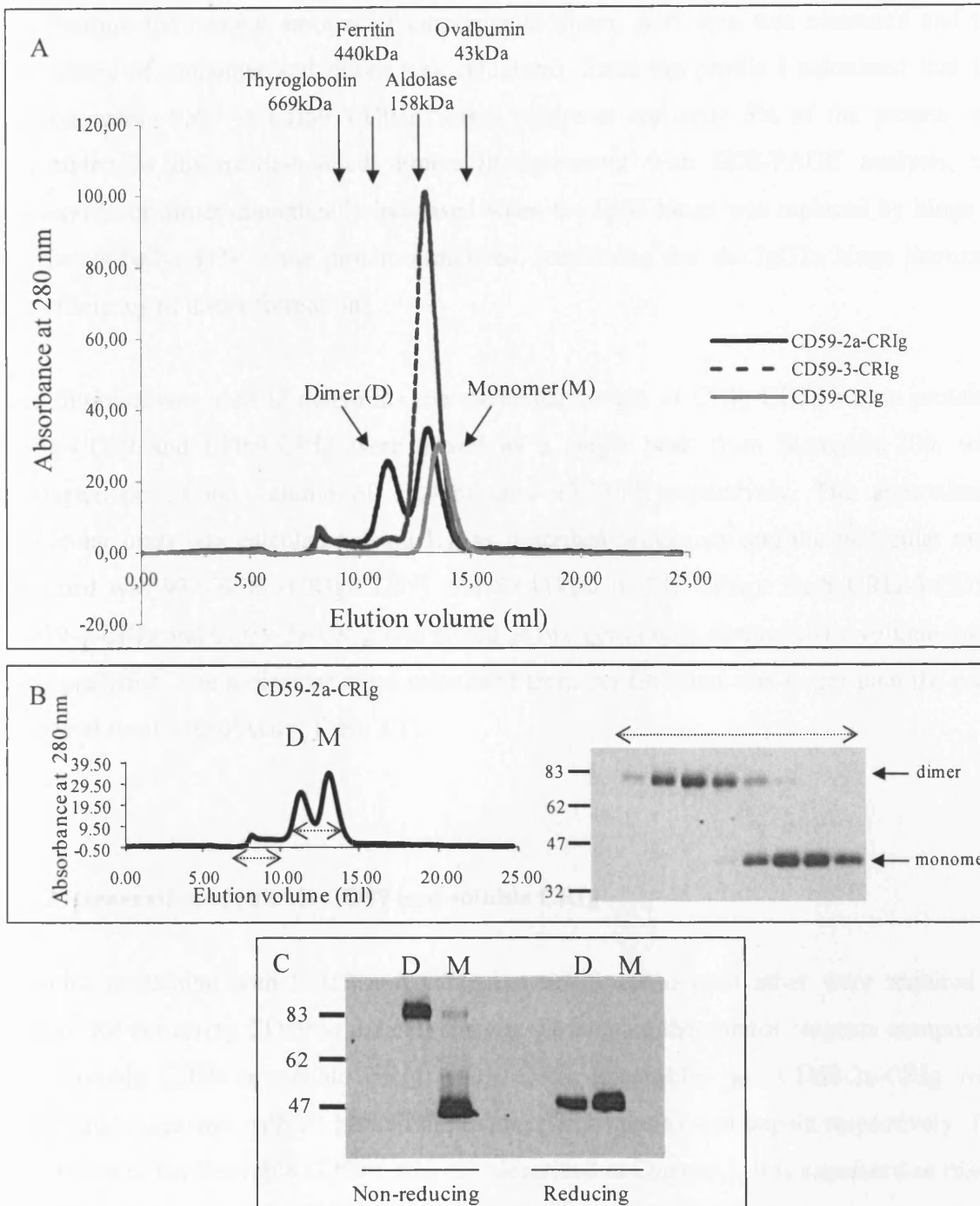


Fig.5.8 Gel filtration chromatography of CD59-CRIg (N-terminal CD59) fusion proteins. A. Gel filtration profile. CD59-CRIg was eluted as a single peak. Two peaks were observed for CD59-3-CRIg and CD59-2a-CRIg. The earlier eluted peak represents a dimer and the late represents a monomer. Elution position of protein standards and their molecular weights are indicated. B. Gel filtration elution profile of CD59-2a-CRIg and SDS-PAGE analysis. Elution fractions across (indicated with dotted double arrow) the dimer and monomer peaks were analysed by SDS-PAGE. The first peak contained dimer and the second-monomeric CD59-2a-CRIg. C. Western blot analysis of pooled fractions.

To measure the relative amount of monomer to dimer, peak area was measured and the percentage of monomer and dimer was calculated. From the profile I calculated that the approximately 95% of CD59-3-CRIg was a monomer and only 5% of the protein was assembled in disulphide-bonded dimer. In agreement with SDS-PAGE analysis, the percentage of dimer dramatically increased when the IgG3 hinge was replaced by hinge of IgG2a antibody, 45% of the protein dimerised, confirming that the IgG2a hinge increased the efficiency of dimer formation.

Gel filtration was used to determine the molecular weight of CRIg-CD59 fusion proteins. CRIg-CD59 and CD59-CRIg were eluted as a single peak from Superdex 200, with characteristic elution volume of 13.58ml and 13.73ml respectively. The approximate molecular mass was calculated using K_{av} as described previously and the molecular mass obtained was 93.69kDa (CRIg-CD59) and 87.11kDa (CD59-CRIg). Each CRIg-3-CD59, CD59-3-CRIg and CD59-2a-CRIg was eluted as two peaks with characteristic volume lower than predicted. The molecular mass calculated from gel filtration was larger than the mass achieved from SDS-PAGE (Table 5.1).

5.2.3. Generation of soluble CD59 and soluble CRIg

Proteins containing both CD59 and CRIg but not fused to each other were required to control for delivering CD59 to the cell surface. To prepare the control reagents comprising only soluble CD59 or soluble CRIg, CD59-CRIg (cleavable) and CD59-2a-CRIg were subjected to cleavage with 3C human rhinovirus (HRV) protease or papain respectively. The generation of the cleavable CD59-CRIg was described in Chapter 3. It is expressed as fusion protein with a protease cleavage recognition site of the 3C HRV protease introduced between CD59 and CRIg. The cleavage was performed in presence of 0.01mM reducing agent Tris (hydroxypropyl) phosphine (THP), using recombinant 3C HRV protease (Novagen) following the manufacturer's protocol. After 16 hours incubation with the 3C HRV protease at 4°C, the cleavable CD59-CRIg was subjected to SDS-PAGE analysis to assess the cleavage efficiency. As seen in Fig 5.9A, the majority of the fusion protein was split to its components CD59 and CRIg. Only small amount of the dimeric protein remained intact.

To investigate the effect of the reducing agent, THP, on CD59, a Western blot analysis was performed (Fig.5.9B). The three-dimensional structure of the CD59 molecule is maintained by five disulfide bonds [404]. Presence of THP might reduce the disulfide bonds holding the molecule and thus impair the protein structure. The functional activity of CD59 depends on the binding interaction with C8 and C9 in regions exposed during assembly of MAC. For this reason conformational alterations in CD59 caused by breaking the disulfide bridges are likely to affect its function.

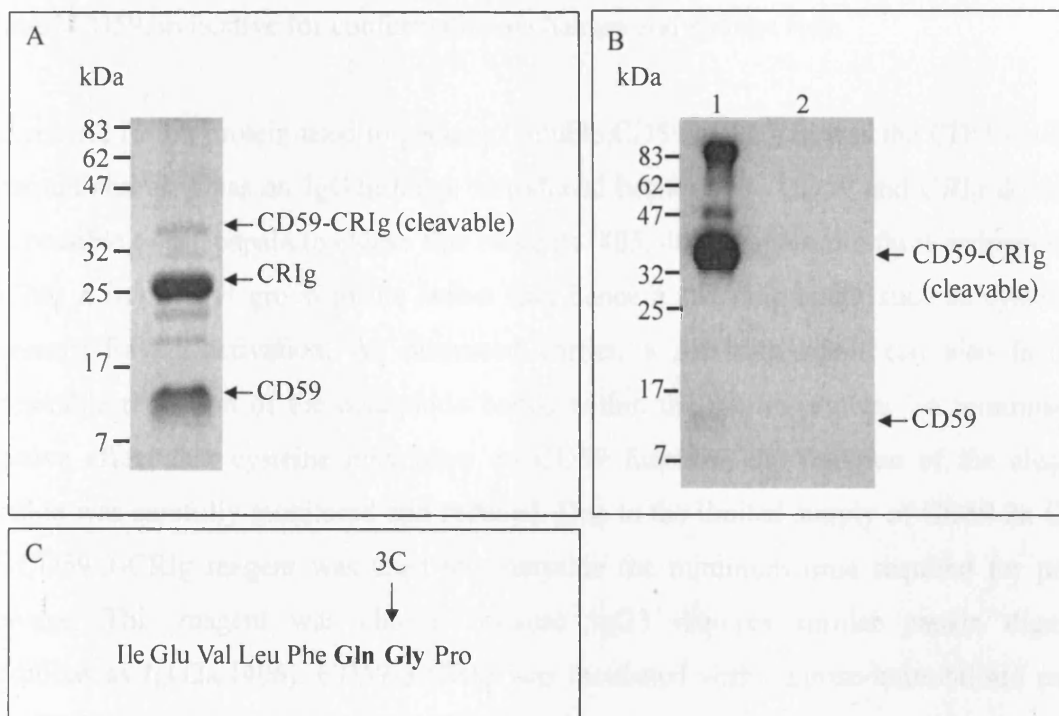


Fig. 5.9 CD59-CRIg cleavage with 3C rhinovirus protease (3C HRV). A. SDS-PAGE analysis illustrating fusion protein cleavage. CD59-CRIg (cleavable) was digested with 3C HRV protease. After separation on 15% gel, the proteins were visualised with Coomassie Blue. B. Western blot analysis of CD59-CRIg (cleavable) reagent following digest. CD59-CRIg cleaved with 3C HRV protease was subjected to Western blot analysis under non-reducing (lane 1) and reducing conditions (lane 2). Rat anti-mouse CD59 mAb was used to detect the proteins. The higher molecular weight bands are likely to represent aggregates. The arrows indicate the positions of the non-cleaved fusion protein and digestion products CRIg and CD59. C. Amino acid sequence of the 3C rhinovirus protease cleavage site. The cleavage site (3C) is indicated with arrow and the amino acids are shown in bold.

To analyse whether CD59 lost conformational epitopes after being exposed to THP, the cleaved CD59-CRIg fusion protein was resolved on a 15% gel and transferred to a nitrocellulose membrane. A rat anti-mouse CD59 mAb was used for detection. As seen in Fig. 5.9B, the mAb was not able to recognise CD59 under reducing conditions confirming that it specifically binds a conformational epitope within the antigen. Under non-reducing conditions, a major band was seen on the western blot corresponding to the intact CD59-CRIg. This suggests that the fusion protein was not completely reduced and a small portion remained noncleaved (also seen in Fig 5.9A). Only a very faint band was obtained for the cleaved CD59, indicative for conformational changes and epitope loss.

The second fusion protein used to generate soluble CD59 and CRIg was the CD59-2a-CRIg construct and as it has an IgG2a hinge introduced between the CD59 and CRIg domain it was possible to use papain to cleave this reagents [405, 406]. Papain is a thiol-endopeptidase that has a sulphhydryl group in the active site, hence a reducing agent such as cysteine is necessary for its activation. As discussed earlier, a reducing agent can also facilitate undesirable reduction of the disulphide bonds within the fusion protein. To minimise the negative effect that cysteine may have on CD59 function, the duration of the cleavage reaction was carefully monitored and reduced. Due to the limited supply of CD59-2a-CRIg, the CD59-3-CRIg reagent was used to determine the minimum time required for papain cleavage. This reagent was chosen because IgG3 requires similar papain digestion conditions as IgG2a [406]. CD59-3-CRIg was incubated with agarose-immobilised papain (Pierce) at 37 °C in a shaking water bath. The reaction was performed in the presence of 20mM cysteine.HCl. Aliquots were taken at various time and analysed by SDS-PAGE and Western blot (Fig.5.10). SDS-PAGE analysis demonstrated that CD59-3-CRIg was almost entirely cleaved to soluble CRIg and CD59 within an hour of incubation time (Fig.5.10A). To investigate whether cysteine affected the CD59 structure the proteins were subjected to western blot analysis. Probing with rat anti-mouse CD59 mAb confirmed that the majority of CD59-3-CRIg was cleaved and soluble CD59 was generated one hour after incubation (Fig.5.10B). The analysis revealed that the antibody epitope on CD59 remained intact suggesting cysteine did not have a dramatic effect on the CD59 conformation.

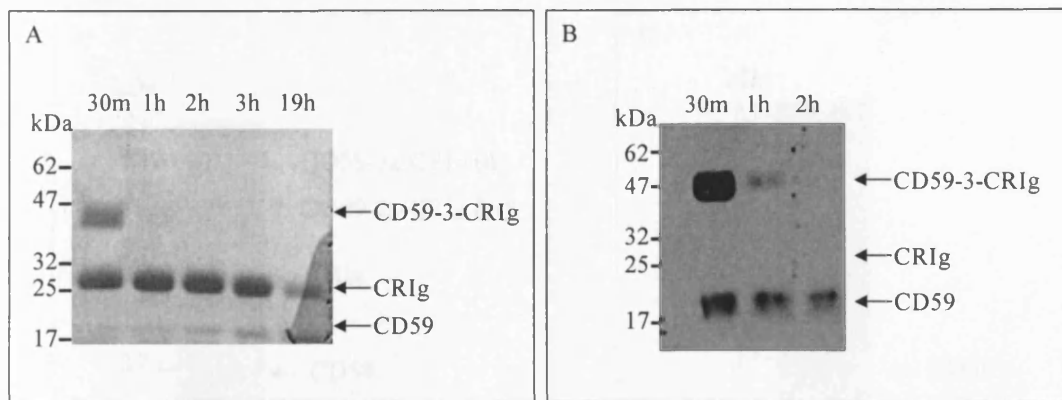


Fig.5.10 Papain digest of CD59-3-CRIg. CD59-3-CRIg was used to determine the minimum time required for generation of soluble CRIg and CD59. The fusion protein was incubated with immobilised papain. Aliquots were removed from the reaction after 30 minutes, 1, 2, 3 and 19 hours and subjected to SDS-PAGE on 15% gel under nonreducing conditions (A) and a Western blot was carried out using rat anti-mouse CD59 mAb (B). Molecular weights in kDa are indicated on the right. The arrows indicate the anticipated size of the intact fusion proteins and its cleavage products.

Following the same protocol, CD59-2a-CRIg was subjected to a papain digest for one hour at 37°C. Papain digest of the IgG2a and IgG3 antibodies results in formation of Fab and Fc fragments, but no (Fab)₂ [406]. For this reason no CD59 dimers were expected. The cleavage efficiency was analysed by SDS-PAGE and Western blot analysis (Fig. 5.11 A and B). Consistent with the CD59-3-CRIg digest, one-hour incubation with papain was sufficient to dissociate most of the fusion protein and generate soluble CRIg and CD59. The cleaved reagent, containing soluble CD59, soluble CRIg and very small percentage of intact monomer and dimer, was dialysed in PBS.

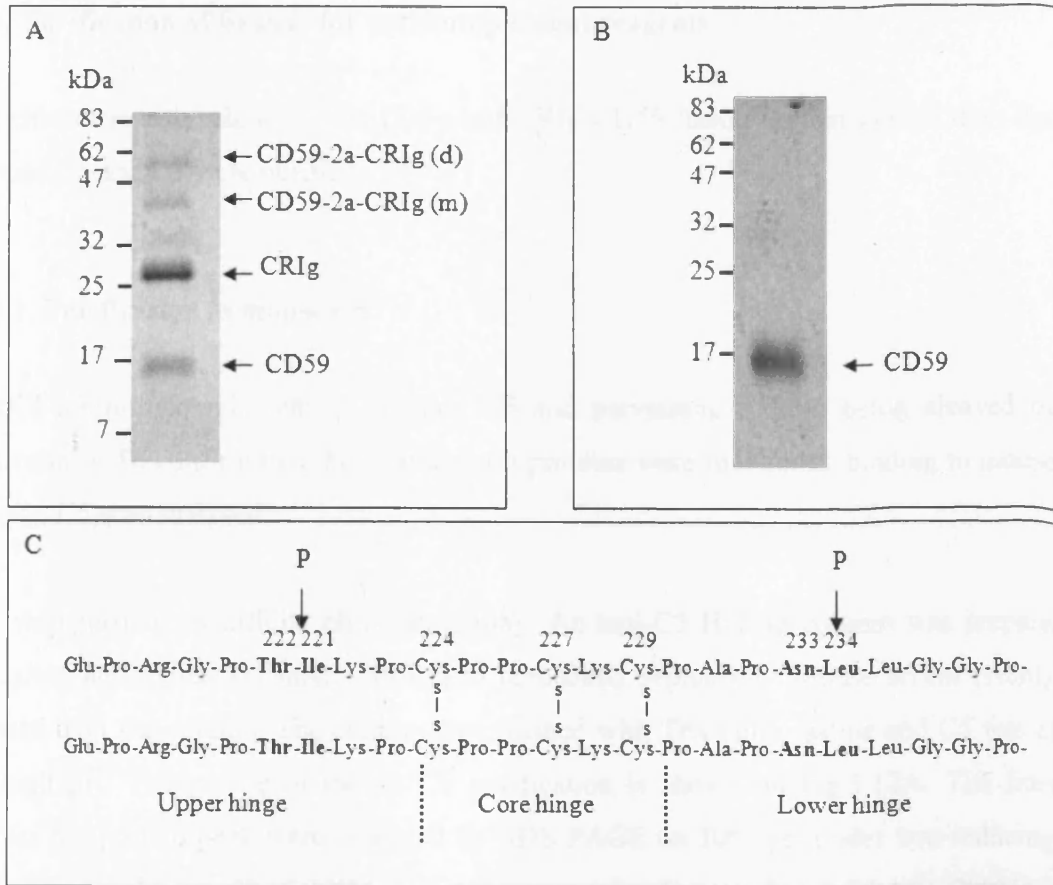


Fig.5.11 Generation of soluble CRIG and CD59. A. SDS-PAGE analysis illustrating papain cleavage of CD59-2a-CRIG. CD59-2a-CRIG was subjected to a papain cleavage for 1 hour at 37°C. After separation on 15% gel, the proteins were visualised with Coomassie Blue. Arrows indicate the positions of non-cleaved CD59-2a-CRIG monomer and dimer and released CRIG and CD59. B. Western blot analysis of CD59-2a-CRIG following digest. CD59-CRIG cleaved with papain for 1 hour was subjected to Western blot analysis under non-reducing condition. Rat anti-mouse CD59 mAb was used to detect the proteins. Arrows indicated the positions of the non-cleaved CD59-2a-CRIG dimer and digestion product CD59. C. Amino acid sequence of the hinge region of mouse IgG2a. The hinge region is composed by core hinge flanked by upper and lower hinge. The positions of disulfide bonds (S-S) responsible for protein dimerisation are indicated. The papain (P) cleavage sites are indicated in bold.

5.3. Purification of ligands for anti-complement reagents

To characterise the ability of OmCI-Fc and CR1g-CD59 fusion protein to bind their ligands, mouse C5 and C3 were purified.

5.3.1. Purification of mouse C5

OmCI inhibits complement by binding C5 and preventing it from being cleaved by the convertase. To confirm that the recombinant proteins were functional, binding to mouse and human C5 was analysed.

C5 was purified by affinity chromatography. An anti-C5 HiTrap column was prepared by coupling anti-mouse C5 mAb (BB5.1) to prepacked Sepharose. Mouse serum (10ml) was passed over the column. The column was washed with Tris buffer saline and C5 was eluted at high pH. The profile of mouse C5 purification is shown on Fig.5.12A. The fractions across the protein peak were analysed by SDS PAGE on 10% gel under non-reducing and reducing conditions (Fig.5.12B). The apparent molecular weight of C5 was 200kD (non-reducing condition) and the α - and β - chain showed molecular mass of 115kD and 83kD (reducing condition). A minor contamination was detected across the peak fractions. The fractions containing C5 were pooled and immediately dialysed against PBS. The protein concentration was determined by measuring absorbance at 280nm.

The functional activity of the affinity purified C5 was assessed by haemolysis assay described in detail in Chapter 2, section 2.7.2.4. Antibody-sensitised rabbit erythrocytes were attacked by C5-deficient mouse serum and the ability of the purified mouse C5 to restore complement killing was analysed. C5 was able to restore the complement activation of the C5^{-/-} serum and lysed the target cells via the classical pathway (Fig.5.12C). This suggested that C5 obtained from mouse serum in affinity purification was functionally active and that affinity purification of C5 from mouse serum did not destroy its haemolytic function. The difference in level of lysis caused by the wild type serum and the C5^{-/-} serum with C5 added back was probably due to difference in level of complement activation in the different mouse strains used in this experiment.

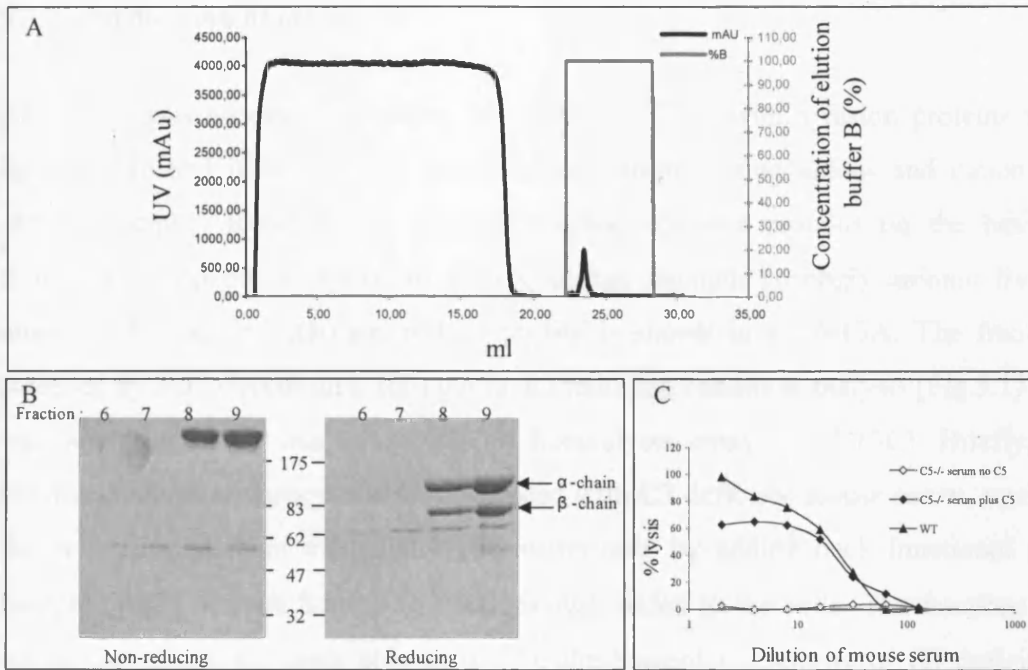


Fig.5.12 Purification of C5 from mouse plasma. A. Profile of affinity purification of C5. Mouse plasma was passed over an anti-mouse C5 affinity column. C5 was eluted in a single peak. Peak fractions were analysed by SDS-PAGE (B). Coomassie staining revealed a band of intact C5 with apparent molecular mass of 210-220kDa under non-reducing condition and bands at 115kDa and 83kDa, corresponding to the intact C5 and α - and β - chains (indicated with arrows), respectively under reducing condition. A minor contamination (probably albumin) was seen in fractions across the peak. The ability of C5 to restore the complement cascade in C5 deficient mouse serum was assessed by the ability of the serum to lyse antibody-sensitised rabbit erythrocytes (C). The cells were incubated with serial dilutions of C5 deficient mouse serum (open circle), C5 deficient serum reconstituted with the purified mouse C5 at concentration of 50 μ g/ml (black diamond) added back or dilutions of wild type serum (black triangle). The purified C5 was able to restore complement-mediated lysis of the C5 deficient serum.

5.3.2. Purification of mouse C3

Mouse C3 was necessary to assess the ability of CRiG within fusion proteins to bind its ligands C3b and iC3b. C3 was purified from plasma using anion- and cation exchange chromatography. Ion-exchange chromatography separates proteins on the basis of their charge type and on the basis of relative charge strength (strongly anionic from weakly anionic). The anion exchange elution profile is shown in Fig.5.13A. The fractions were screened by SDS-PAGE on a 10% gel under reducing condition analysis (Fig.5.13B) and C3 was identified. This was confirmed by haemolysis assay (Fig.5.13C). Briefly, antibody sensitised rabbit erythrocytes were incubated with C3 deficient mouse serum, unable to lyse the cells. Complement mediated lysis occurs only by adding back functional active C3. Sample (10 μ l) of each Source Q fractions was added to the cells. The fractions (C6-C11) containing mouse C3 were able to restore the haemolytic activity of C3 deficient mouse serum. The C3-containing peak was dialysed against 20mMNaPO₄ pH6.0 and subject to cation exchange chromatography on Mono S column with a gradient of 0 to 500mM NaCl over 20 column volumes (Fig.5.14A). The peak containing C3 was identified by SDS-PAGE (Fig.5.14B) analysis and presence of C3 was confirmed by haemolysis assay (Fig.5.14C).

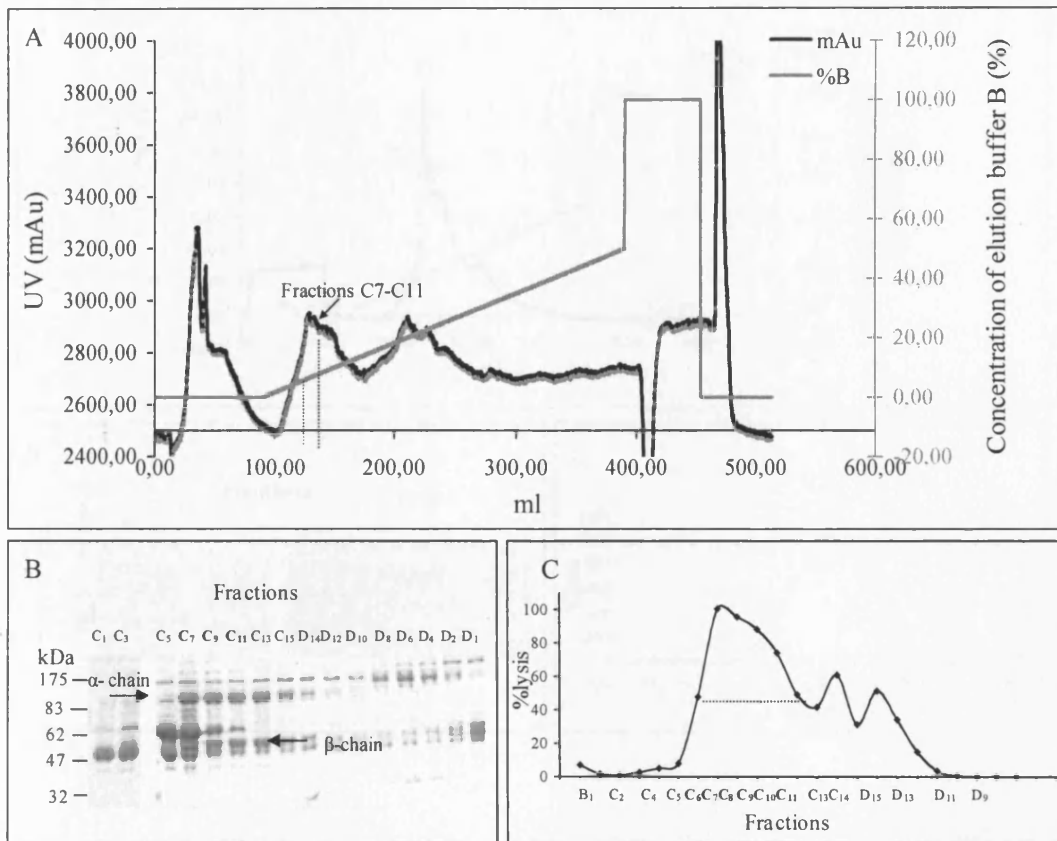


Fig.5.13 Purification of mouse C3 by anion exchange chromatography.

A. Chromatogram of the anion exchange of mouse C3. The product from the 15% cut of mouse plasma was loaded onto Source Q column. The proteins were separated using an increasing salt gradient, presented as a change in conductivity (%B; gray). B. SDS-PAGE analysis of the Source Q fractions. The elution fractions were loaded on 10% gel under reducing conditions. The protein was visualized by staining with Coomassie Blue. The fraction number is shown above each lane. Fractions C7 to C11 showed typical C3 profile. α - and β -chains are indicated with arrows. C. Haemolytic activity of Source Q fractions. Fractions positive for C3 on SDS-PAGE and adjacent fractions were analysed on haemolysis assay. Antibody-sensitised rabbit erythrocytes were incubated with C3 deficient mouse serum and fraction samples was added. Fractions from C6 to C11 (bold) were able to restore complement activity to the C3-deficient serum and were processed further.

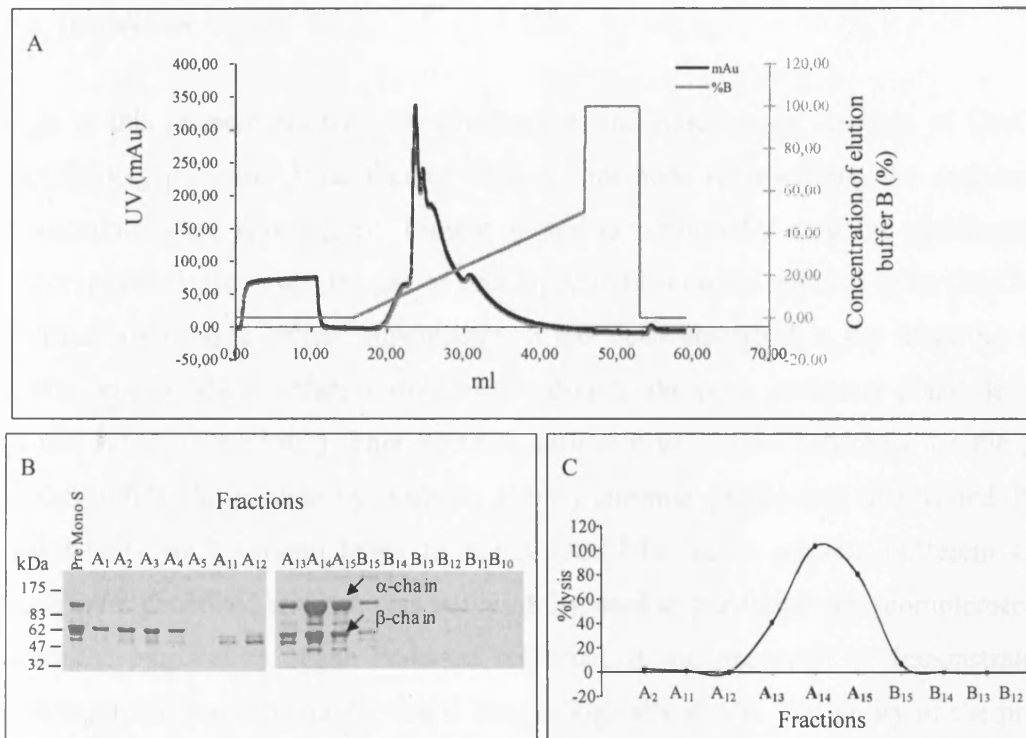


Fig. 5.14 Purification of mouse C3 by cation exchange chromatography.

A. Chromatogram of the cation exchange of mouse C3. Source Q fractions C6-C11 were pooled, dialysed against 20mMNaPO₄ pH6.0 buffer and loaded onto Mono S column. The proteins were separated using an increasing salt gradient, presented as a change in conductivity (%B, gray). B. SDS-PAGE analysis of the Mono S fractions. The elution fractions were loaded along with a protein sample before being loaded on the column (Pre MonoS) on 10% gel under reducing conditions. The protein was visualized by staining with Coomassie Blue. The fraction number is shown above each lane. Fractions A13 to A15 showed typical C3 profile. α - and β -chains are indicated with arrows. C. Haemolytic activity of MonoS fractions. Fractions positive for C3 on SDS-PAGE and adjacent fractions were analysed on haemolysis assay. Antibody sensitised-rabbit erythrocytes were incubated with C3 deficient mouse serum and fraction samples were added. Fractions from A13 to A15 (bold) were able to restore complement activity of the C3 deficient serum and were dialysed against PBS and stored at -80°C until needed.

5.4. Discussion

Data in this chapter illustrate the purification and biochemical analysis of OmCI-Fc and CD59-CRIg proteins. A number of different methods for purifying the anti-complement therapeutics were investigated. Protein A and G are usually used for purification of Fc-fusion proteins. However, the use of protein A and G column resulted in no OmCI-Fc being purified from tissue culture supernatant. It has been described in the literature that some fusion proteins show different ability of binding to the same stationary phase despite being of the same isotype [407]. This effect is attributed to a steric hindrance on the protein A surface [407]. Purification by antibody affinity chromatography was then tested. Polyclonal rabbit anti-OmCI column failed to purify OmCI-Fc fusion protein. Different anti-OmCI mAb were generated and one was successfully used to purify this anti-complement reagent. After the purification of the Fc-based construct, it was necessary to demonstrate that the fusion protein was structurally sound and biologically active. The purity of the protein was analysed by SDS-PAGE. OmCI-Fc migrated as a band with molecular weight of 90kDa under non-reducing condition and 51kDa (polypeptide backbone) under reducing. The analysis revealed a contamination with bovine C5 from the FCS in the cell-growing medium. This was removed by a gel filtration step.

The second part of the chapter deals with the purification and the biochemical analysis of targeted CD59-CRIg fusion proteins. CD59-CRIg, CRIg-CD59, CD59-3-CRIg, CRIg-3-CD59, CD59-2a-CRIg, CRIg-2a-CD59 and cleavable CD59-CRIg were purified from culture supernatant by affinity chromatography. The molecular mass of fusion proteins was determined by SDS-PAGE analysis and gel filtration and compared to the mass calculated based on amino acid sequence. SDS-PAGE analysis was also used to control the quality of purified proteins. Gel filtration chromatography clearly revealed that CRIg-CD59, CD59-CRIg and cleavable CD59-CRIg were monomeric, whereas CRIg-3-CD59 and CD59-3-CRIg and CD59-2a-CRIg were eluted as two peaks meaning that they exist in two forms- monomer and dimer. Calibration of the gel filtration column allowed the generation of a standard curve used to determine the molecular weight of the recombinant proteins. The molecular mass obtained from gel filtration has found to be higher than the mass calculated from the SDS-PAGE analysis and the molecular weight from the electrophoresis was larger than the mass estimated from the amino acid sequence (Table 5.1). This could be explained with enhanced level of post-translational modification. CRIg-CD59 fusion proteins

contained two potential N-linked glycosylation sites-one within CRIg and one in the CD59 moiety. In addition, the high content of proline, serine and threonine predispose to O-linked glycosylation [408]. This could result in highly glycosylated proteins with increased molecular mass. The Fc domain of IgG (used in OmCI-Fc) is also highly glycosylated.

The discrepancy in the molecular weight obtained from SDS-PAGE and gel filtration analysis could be explained with a high hydration of the particle in solution, characteristic for extended molecules with large specific surface accessible to the solvent. Extended molecules have larger Stokes radius (Stokes-Einstein radius, hydrodynamic radius, radius of the hydrated molecules in solution) and therefore larger resistance to motion compare to spherical molecules (Stoke radius identical to the effective radius) with the same molecular weight. It might be that the CD59-CRIg proteins have hydrodynamic radius larger than the effective radius and therefore are eluted earlier than expected for globular proteins with their molecular mass. The monomeric CRIg-CD59 were eluted substantially earlier than ovalbumin, a 43kDa globular protein and OmCI-Fc was eluted before the aldolase (158kDa) (Fig.5.4 and Fig.5.8).

As revealed by the analysis, the ratio of monomer to dimer within the CD59-2a-CRIg and CD59-3-CRIg preparations was different. This means that IgG3 and IgG2a hinge could offer different levels of protein dimerisation. The difference could be explained by the different number of cysteins found in the two hinges. IgG2a hinge has three cystiens and a potential to form three hinge disulphide bonds, whereas IgG3 has only one. It is highly likely that the two additional cysteines in the IgG2a hinge increased the efficiency of assembling disulfide-bonded dimers and/or their stability. The formation of disulfide-bonded dimers would increase the avidity of the reagent to the target (C3b/iC3b coated) surface which might be extremely beneficial for therapy.

Chapter 6. *In vitro* functional analysis of OmCI-Fc and CD59-CRIg fusion proteins

The aim of the work in this chapter was to characterise the function of the anti-complement therapeutics *in vitro*. OmCI-Fc and CD59-CRIg are chimeric proteins. Linking two molecules in one fusion protein may alter the way in which OmCI-Fc and CD59-CRIg bind their ligands. For this reason it is vital to assess the ability of the reagents to bind C5 (for OmCI-Fc) and C3b/iC3b (for CD59-CRIg). Furthermore, measuring the affinity of CD59-CRIg fusion proteins for C3b will address the important question whether dimerisation improves the binding capacity of these reagents. To confirm that the targeting strategy works, the ability of CD59-CRIg agents to bind C3b-coated will be evaluated by flow cytometry. Haemolysis analysis will be undertaken to assess the ability of OmCI-Fc and CD59-CRIg reagents to prevent complement activation. As a result of these *in vitro* analyses, the best anti-complement fusion proteins will be expanded and selected for *in vivo* testing.

6.1. *In vitro* characterisation of OmCI-Fc

6.1.1. Binding of OmCI-Fc and pOmCI to C5; affinity analysis.

Surface plasmon resonance (SPR) was used to measure the affinity of OmCI-Fc for mouse and human C5 and to investigate whether the fusion to antibody Fc domain affected the C5 binding capacity of OmCI. The experiments were carried out on a Biacore T100. The method is described in detail in Chapter 2, section 2.7.5. Briefly pOmCI or OmCI-Fc was amine coupled on CM5 biacore chip. For efficient amine coupling the ligand must be positively charged and therefore diluted in immobilization buffer 0.1-1 units in pH below its pI. The optimal pH for OmCI-Fc and pOmCI coupling was determined in a pre-concentration injection. Fifty resonance units (RU) of pOmCI (100 μ g/ml) were immobilised on the chip surface using a manual protocol in 10mM acetate pH4.0 as a dilution buffer. One hundred and fifty RU of OmCI-Fc (3.5 μ g/ml in 10mM acetate pH4.5) were coupled on the chip surface using the immobilisation wizard. The remaining free covalent-binding sites of the carboxymethylated dextran surface were blocked (Fig.6.1).

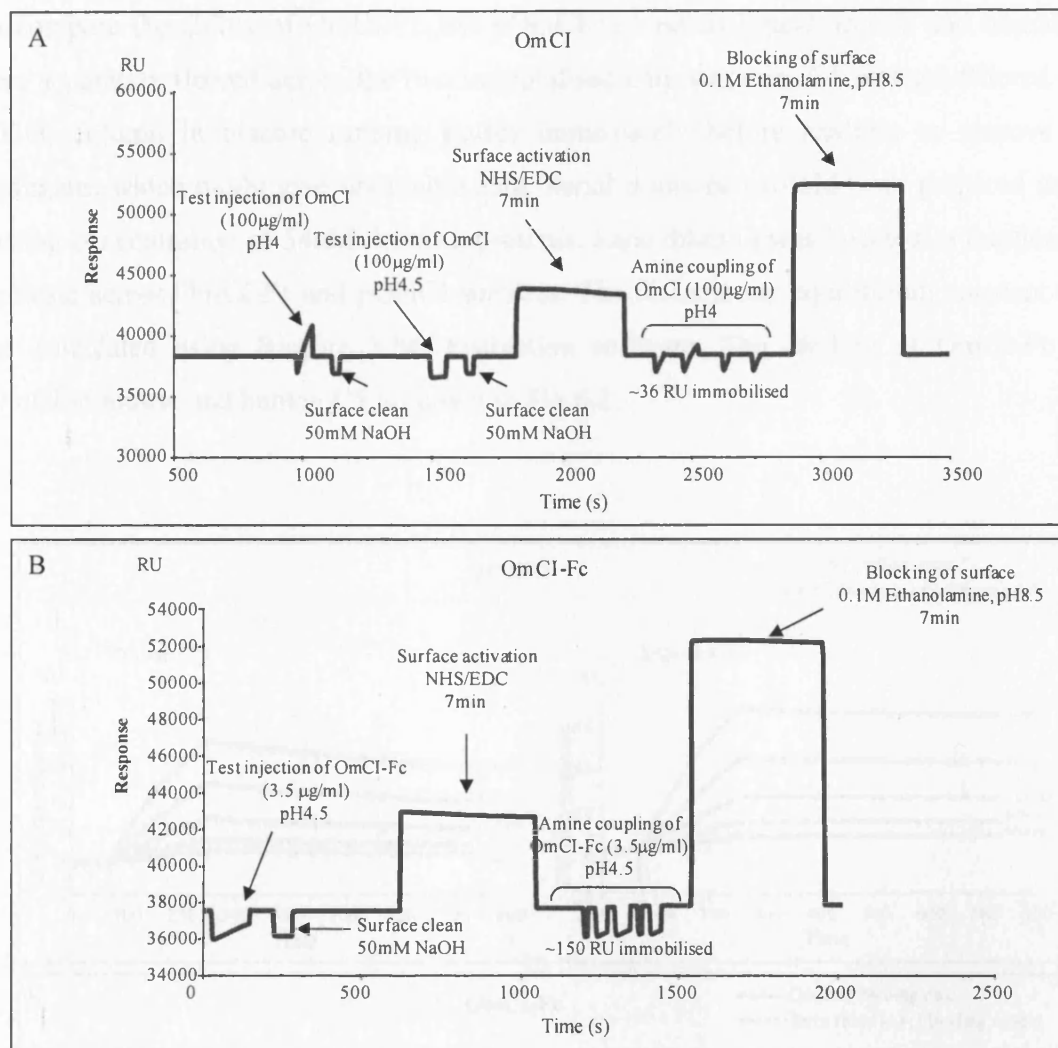


Fig.6.1 Sensograms illustrating preparation of the chip surface. All steps were performed at a flow rate of 5µl/min at 25°C. **A. Immobilisation of OmCI.** The chip surface was prepared using manual immobilisation. The surface was cleaned by injecting 50mM NaOH and activated with N-hydroxysuccinimide (NHS) and 1-ethyl-3(3-dimethylaminopropyl)-carbodiimide hydrochloride (EDC), mixed 1:1. OmCI, diluted in acetate buffer pH4.0, was injected until 36RU were immobilised. The surface was blocked with ethanolamine. **B. Immobilisation of OmCI-Fc.** OmCI-Fc diluted in acetate buffer pH4.5 electrostatically adhered to the chip. The surface was cleaned with 50mM NaOH and activated as above. OmCI-Fc, diluted in acetate buffer pH4.5, was injected until 150RU were immobilised. The surface was blocked.

To compare the ability of OmCI-Fc and pOmCI to bind its ligand, mouse and human C5 were separately flowed across the two immobilised chip surfaces. C5 was gel-filtered on a SD200 column in biacore running buffer immediately before analysis to remove any aggregates which might give unreliable data. Serial dilutions twofold were prepared with a starting concentration of 54nM for both proteins. Each dilution was injected in duplicate or triplicate across OmCI-Fc and pOmCI surfaces. The dissociation equilibrium constant (K_D) was calculated using Biacore 3000 evaluation software. The binding of OmCI-Fc and pOmCI to mouse and human C5 is shown in Fig.6.2.

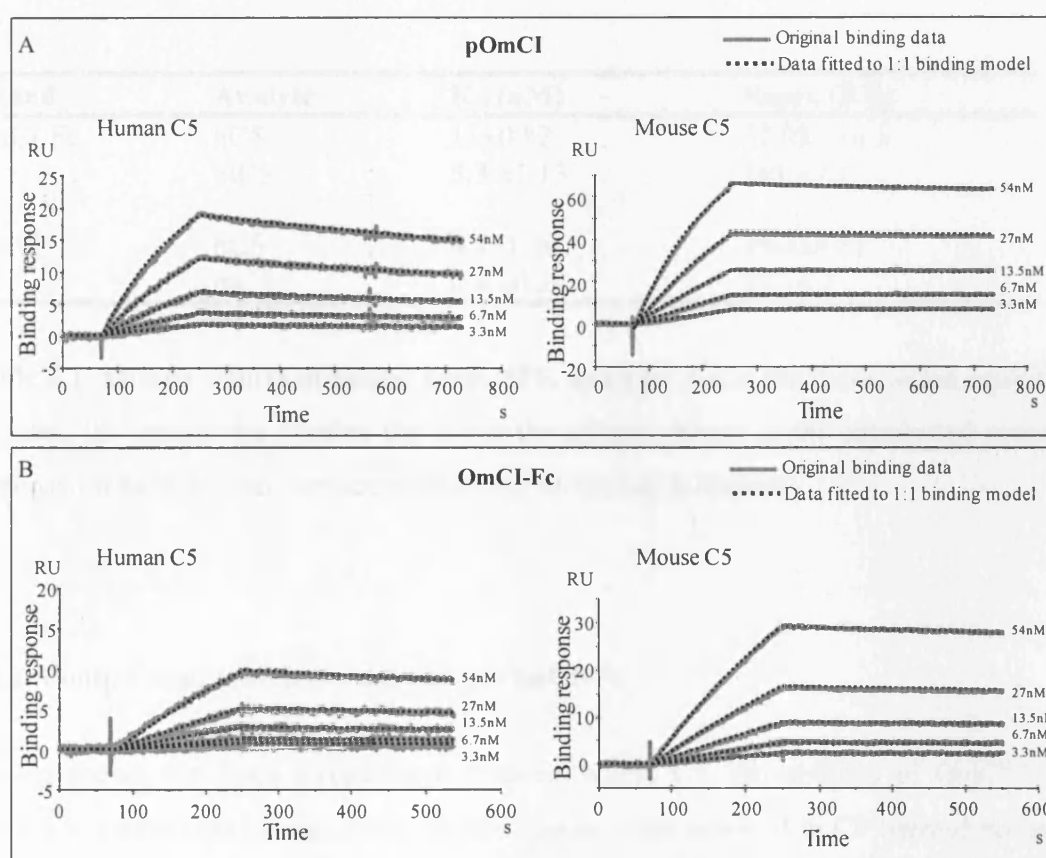


Fig.6.2 SPR sensograms illustrating the OmCI-C5 interaction. pOmCI (A) and OmCI-Fc (B) were immobilised on a sensor surface and a dilution series of five different concentrations of human and mouse C5 was injected over the surface. Binding experiments were performed two times. The protein binding interaction is shown in resonance units with a grey line. The binding response was fitted to 1:1 Langmuir binding model (shown with black dotted line) to derive kinetic rate and affinity constants.

OmCI-Fc and pOmCI bound human and mouse C5 with high, nanomolar affinity. While no difference in the binding profile was observed, the evaluation of the affinity data showed changes in binding properties occurring as a result of engineering OmCI. Table 6.1 presents a summary of the affinity data obtained from the interactions. The affinity of OmCI-Fc for C5 was lower than pOmCI. The K_D values of OmCI-Fc and pOmCI with human C5 were greater than those obtained with the mouse protein. pOmCI had an affinity with mouse C5 of 0.4 ± 0.24 nM, while the K_D with human C5 was 4.7 ± 1.26 nM. A similar observation was made for the Fc protein. OmCI-Fc had enhanced binding affinity with mouse C5 ($K_D = 5.3 \pm 1.13$ nM) when compared to the human protein ($K_D = 10.10$ nM).

Ligand	Analyte	K_D (nM)	Rmax (RU)
OmCI-Fc	hC5	11 ± 0.82	32.02 ± 16.5
	mC5	5.3 ± 1.13	101 ± 7.1
pOmCI	hC5	4.7 ± 1.26	29.4 ± 4.17
	mC5	0.4 ± 0.24	72 ± 4.3

Table 6.1 Affinity values obtained from SPR analysis. K_D is the dissociation equilibrium constant, the greater the number the lower the affinity. Rmax is the anticipated maximum response for each protein (surface saturation); m-mouse; h-human;

6.1.2. Complement inhibitory activity of OmCI-Fc

Having shown that both recombinant proteins bound C5, the abilities of OmCI-Fc and pOmCI to inhibit complement from various species were assessed in CP haemolysis assays. Antibody-sensitised sheep erythrocytes (EAsh) were used for the rat and human complement assay and sensitised rabbit erythrocytes (EArb) were the target for mouse complement. The assays are described in detail in method 2.7.2. Briefly, EAsh or EArb were exposed to human, rat or mouse serum at concentrations that caused 70% lysis and a dilution of OmCI-Fc or OmCI (1:2 serial dilution). Haemoglobin release from the cells was measured and complement-mediated lysis was determined. Approximately one third the mass of OmCI-Fc is contributed by the Fc domain, for this reason the results are presented in molar

concentration of OmCI moiety. Percentage lysis was plotted against inhibitor concentration in nM and the amount of inhibitor causing 50% lysis was calculated (IH₅₀).

pOmCI and OmCI-Fc effectively inhibited lysis by all three species of sera tested (mouse, rat and human) in a dose dependent manner (Fig.6.3). OmCI-Fc and pOmCI showed a different profile of complement inhibition, consistent among the assays. Both inhibitors followed a sigmoidal dose-response curve, however the OmCI-Fc curve was shallower than the curve obtained for the pOmCI. Nevertheless, both proteins were highly potent at preventing cell lysis with IH₅₀ in the range of 1.7-7.1nM. OmCI-Fc provided 50% inhibition of mouse complement at 6.1nM and pOmCI had IH₅₀=7.1nM. The amount of pOmCI required to achieve 50% cell lysis by human and rat serum, was 1.9nM and 2.7nM respectively. OmCI-Fc at 1.7nM provided 50% cell protection in the human assay and 2.0nM OmCI-Fc was sufficient to achieve the same effect in the rat assay. A direct comparison with the mouse assay was not appropriate because of the different target cells used in this assay. Table 6.2 compares the inhibitory activities of OmCI-Fc and pOmCI.

Source of complement	OmCI-Fc		pOmCI	
	nM	SD	nM	SD
Human	1.67	0.008	1.94	0.1
Rat	2.01	0.46	2.67	0.1
Mouse	6.13	0.4	7.06	0.008

Table 6.2 Concentrations of OmCI-Fc and pOmCI resulting in 50% inhibition of cell lysis (IH₅₀). SD, standard deviation of two (human and mouse assay) or four measurements (rat assay).

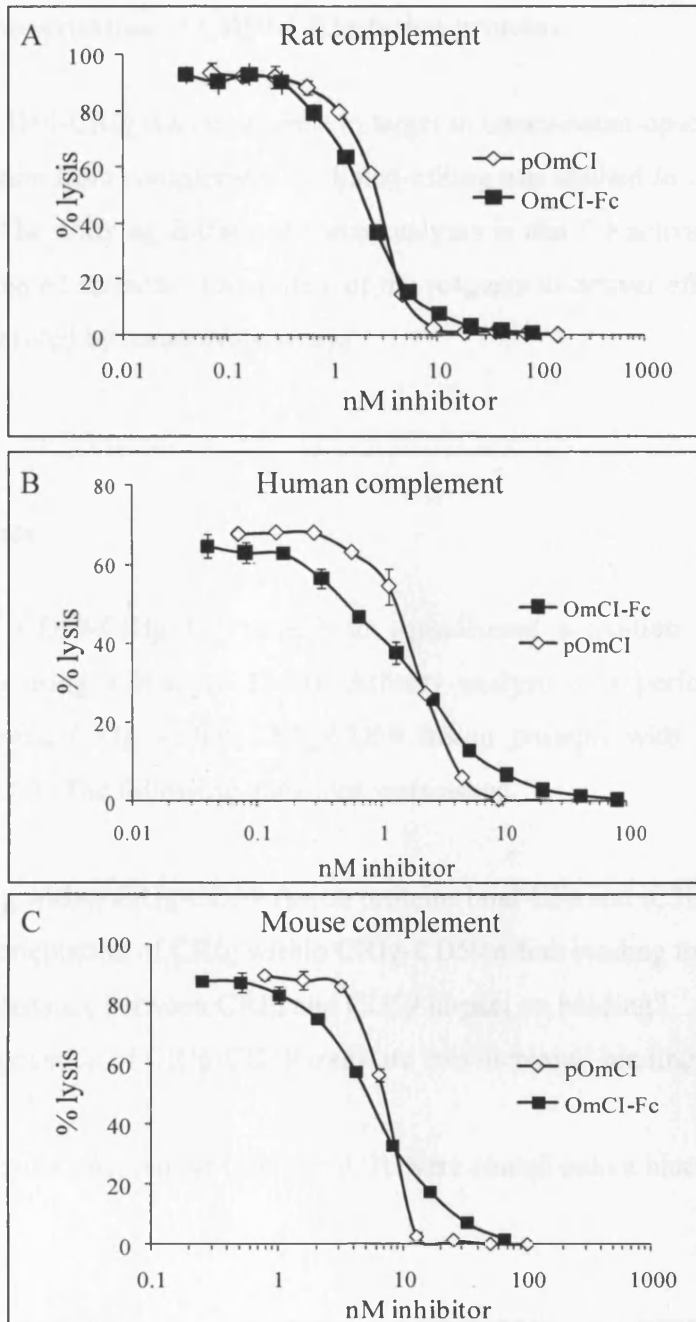


Fig.6.3 Complement inhibitory activity of OmCI-Fc and pOmCI. Antibody sensitised sheep erythrocytes were incubated with a dilution of OmCI-Fc and pOmCI and attacked by rat (A) or human (B) complement. Antibody sensitised rabbit erythrocytes were used to test the effect of pOmCI and OmCI-Fc on mouse complement (C). Both, OmCI-Fc and pOmCI inhibited lysis in a dose dependent manner. Each data point represents the mean value \pm SD of a single experiment performed in triplicate.

6.2. *In vitro* characterisation of CD59-CRIg fusion proteins

The capacity of CD59-CRIg fusion proteins to target to complement-opsonised cells in order to provide protection from complement mediated-killing was studied *in vitro* using SPR and flow cytometry. The unifying feature of these analyses is that C3 activation was promoted generating C3b-coated surfaces. The ability of the reagents to deliver effective complement inhibition was analysed by haemolysis assays.

6.2.1. SPR analysis

The capacity of CD59-CRIg to “target” to complement activation products was first analysed *in vitro* using a Biacore T100). Affinity analysis was performed to study the interaction of mouse CRIg within CRIg-CD59 fusion proteins with its natural ligands, mouse C3b and iC3b. The following questions were asked.

1. Does CRIg within CRIg-CD59 fusion proteins bind C3b and iC3b?
2. Does the orientation of CRIg within CRIg-CD59 affect binding to C3b?
3. Does the distance between CRIg and CD59 impact on binding?
4. Does dimerisation of CRIg-CD59 translate into increased binding avidity?

To address these questions, mouse C3b and iC3b were coated onto a biacore chip.

6.2.1.1. Preparation of the C3b surface

To investigate the potential of CD59-CRIg fusion proteins to target cells tagged with C3 fragments, a C3b “opsonised” chip surface was prepared to resemble a C3b-coated cell.

A small nidus of human C3b was first immobilised on the chip surface (~50RU). An initial alternative pathway C3 convertase was assembled on the sensor chip by injecting mixture of fB and fD across the nidus of human C3b in the presence of Mg²⁺ (1mM) (Fig.6.4). This C3 convertase (containing human C3b) was able to cleave mouse C3 resulting in deposition of

mouse C3b on the surface. This procedure was repeated. Each cycle, comprising injection of fB and fD to form convertase on both mouse and human C3b, followed by mouse C3, gradually increased the amount of C3b deposited on the chip, (~700RU). Once C3b was deposited, DAF was flowed across the surface to dissociate any active convertase and non-covalently bound C3b was removed using regeneration buffer.

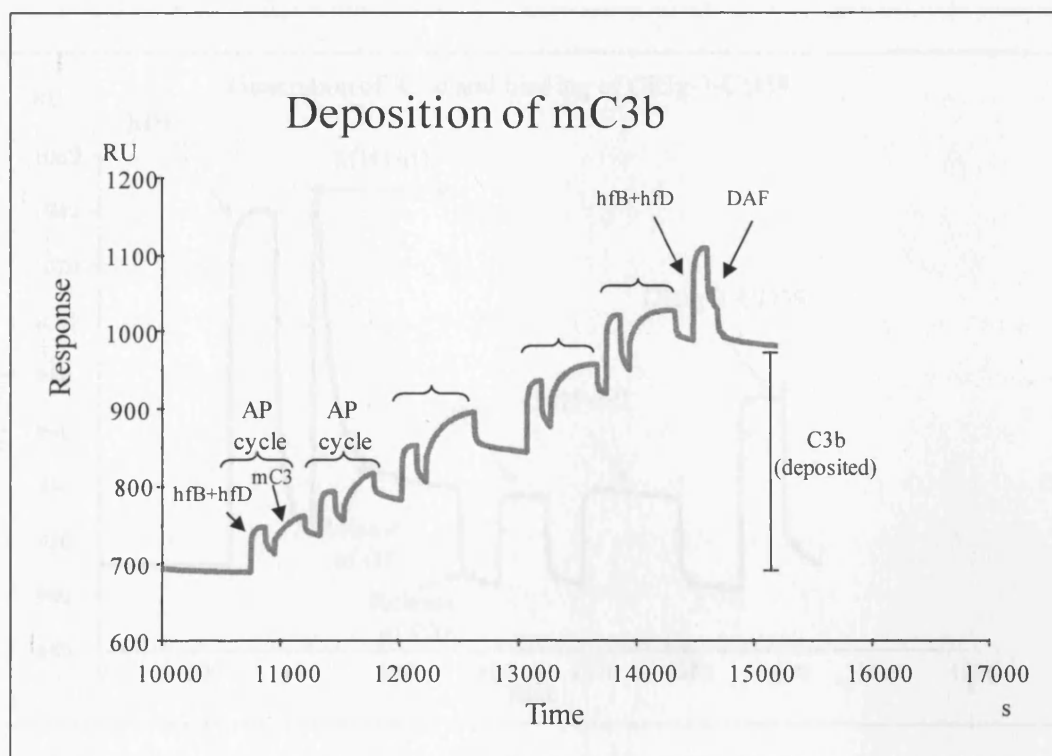


Fig.6.4 Preparation of a mouse C3b surface. A mouse C3b “opsonised” chip surface was generated via the AP using the C3 convertase. A small nidus of human C3b was immobilized onto a CM5 biacore chip and used as initial target to build a C3b_{hu}Bb convertase by injecting human factor B and factor D. Mouse C3 was flowed across the convertase surface and C3b was generated which bound covalently to the chip. The AP was amplified by repeated cycling of fB and fD followed by mouse C3. Convertases and non-covalently bound C3b were decayed by injection of DAF and regeneration buffer.

6.2.1.2. Preparation of iC3b surface

iC3b is a C3b degradation product generated by cofactor mediated factor I cleavage of C3b. Factor I in the presence of factor H (cofactor) was used to cleave mouse C3b deposited on the sensor chip. The deposition of iC3b was explained in section 2.7.7.2. Briefly human factor H and factor I were injected across the C3b surface resulting in release of C3f and generation of iC3b bound to the chip surface (Fig.6.5).

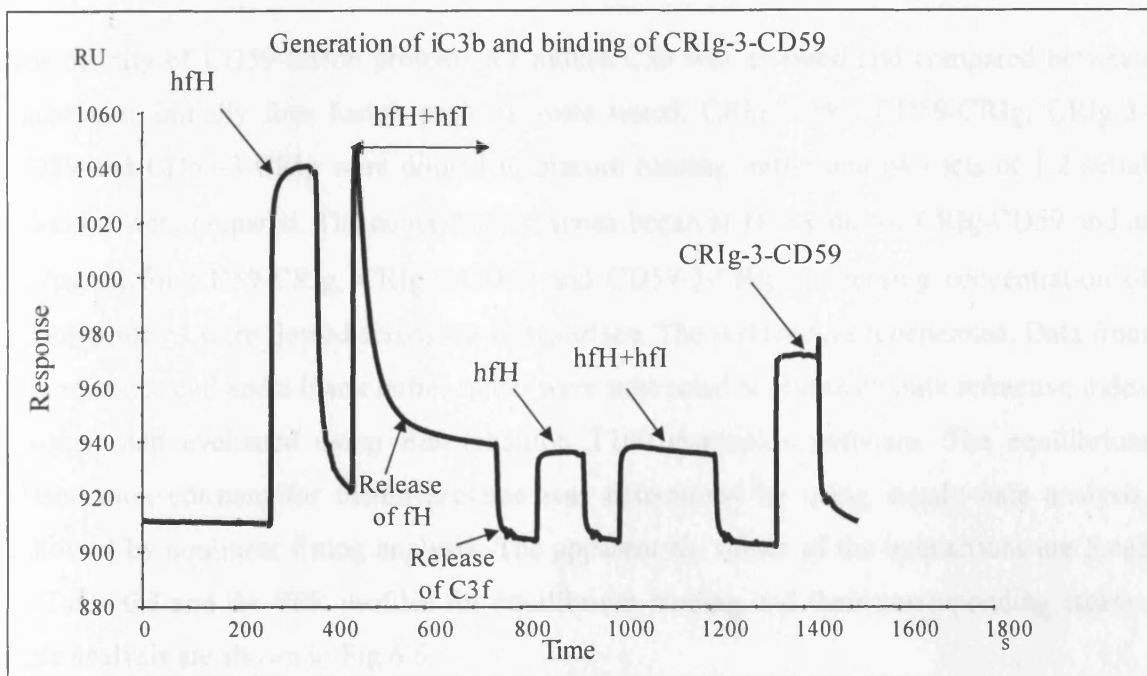


Fig. 6.5 Preparation of a mouse iC3b surface and binding of CR1g-3-CD59. A mouse iC3b surface was generated by cleaving C3b, previously deposited on the chip. Human factor I and factor H were injected over the C3b surface. This resulted in generation of iC3b bound to the chip and C3f released in the fluid phase. fH alone was then injected to confirm that no C3b was left on the surface. A second injection of fH and fI verified that C3b was entirely converted to iC3b. CR1g-3-CD59 was flowed over the surface and binding was detected.

To confirm that C3b was entirely converted to iC3b, factor H alone was flowed over the surface prior to and after the combined fH/fI injection. Because fH can bind only C3b and not iC3b, the absence of binding to the chip indicated when there was no C3b left. This was further verified when a second injection of fH/fI was applied and no binding or release of C3

fragments was observed. Once the iC3b surface was created, CR1g-3-CD59 was flowed across the chip. The positive interaction indicated that CR1g retained its ability to react with iC3b after being fused to CD59.

6.2.1.3. Interaction of CR1g-CD59, CD59-CR1g, CR1g-3-CD59 and CD59-3-CR1g with C3b

The affinity of CD59-fusion proteins for mouse C3b was assessed and compared between constructs; initially four fusion proteins were tested. CR1g-CD59, CD59-CR1g, CR1g-3-CD59 and CD59-3-CR1g were diluted in biacore running buffer and two sets of 1:2 serial dilutions were prepared. The concentration series began at 181 µg/ml for CR1g-CD59 and at 727 µg/ml for CD59-CR1g, CR1g-3-CD59 and CD59-3-CR1g. Increasing concentration of fusion proteins were flowed across the C3b surface. The surface was regenerated. Data from the reference cell and a blank buffer inject were subtracted to eliminate bulk refractive index changes and evaluated using Biaevaluation T100 evaluation software. The equilibrium dissociation constant for fusion proteins was determined by using steady-state analysis, followed by nonlinear fitting analysis. The apparent K_D values of the interactions are listed in Table 6.3 and the SPR profiles for equilibrium binding and their corresponding steady-state analysis are shown in Fig 6.6.

Reagent	K_D (µM)
CR1g-CD59	2.3
CD59-CR1g	6
CR1g-3-CD59	NA
CD59-3-CR1g	5.2
CD59-2a-CR1g monomer	5
CD59-2a-CR1g dimer	0.7

Table 6.3 K_D for interaction of CD59-CR1g fusion proteins with C3b. K_D is the dissociation equilibrium constant, the greater the number the lower the affinity. NA, not assessed;

CRlg-CD59 had a K_D of $2.3\mu\text{M}$ (Fig.6.6 A). The same reagent with CRlg at the C-terminus (CD59-CRlg) had a three-fold weaker affinity with the surface ($K_D=6\mu\text{M}$) (Fig.6.6 B).

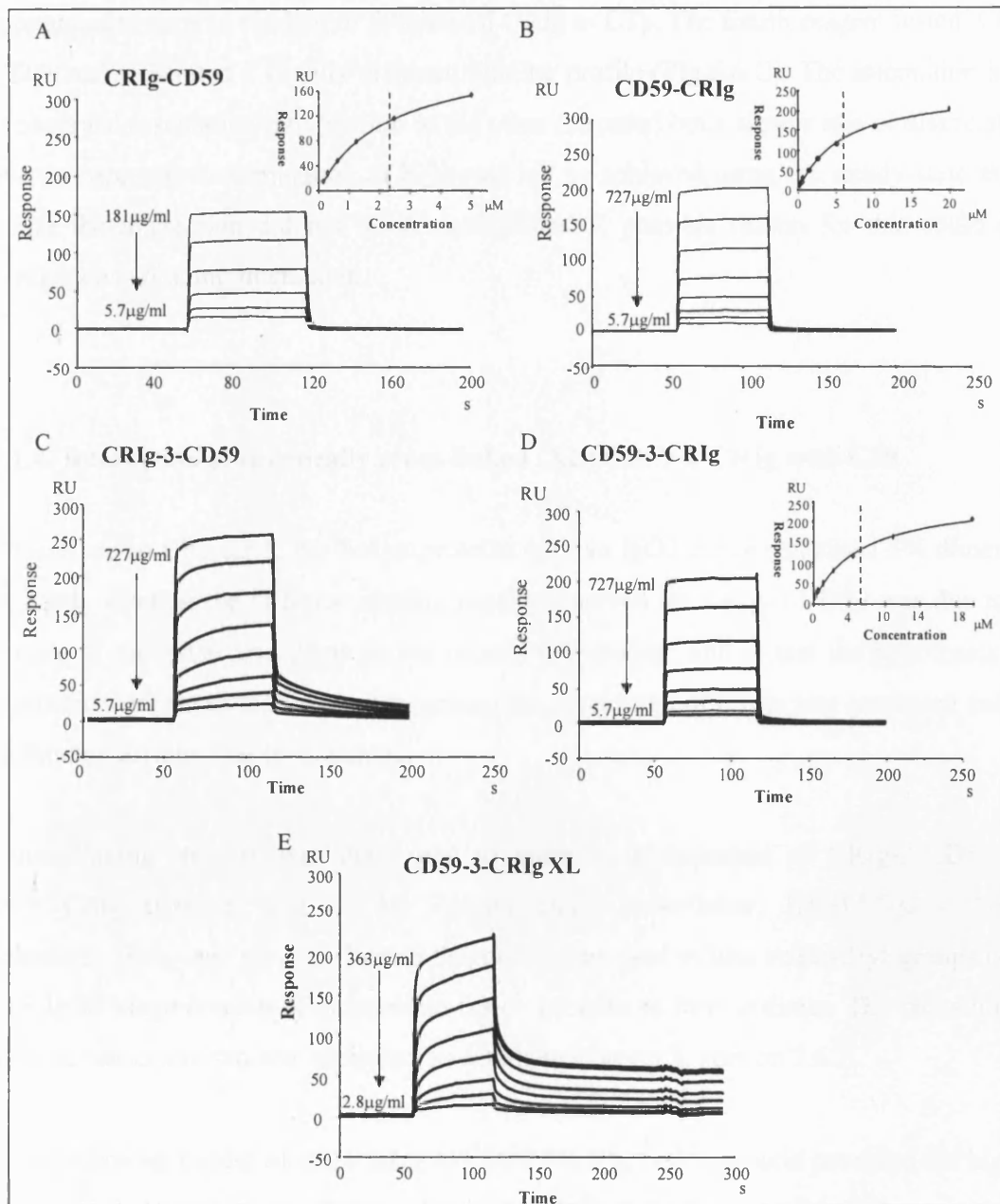


Fig.6.6 Equilibrium binding of CD59-CRlg fusion proteins to C3b. Representative SPR sensorgrams of the interaction between C3b and either CD59-CRlg (A), CRlg-CD59 (B), CD59-3-CRlg (C), CRlg-3-CD59 (D) and CD59-3-CRlg crosslinked (XL). Each protein was injected across the surface at a range of concentrations as indicated on each sensorgram. When possible, inset plots show the corresponding steady-state affinity analysis.

This suggests that orientation of CRIg has an effect on binding to C3b. N-terminal CRIg binds tighter to its ligand. The affinity of CD59-CRIg was comparable to CD59-3-CRIg ($K_D = 5.2 \mu\text{M}$) (Fig.6.6 D), implying that the space between CD59 and CRIg was not of high importance in terms of binding of C-terminal CRIg to C3b. The fourth reagent tested, CRIg-3-CD59, demonstrated a slightly different binding profile (Fig.6.6 C). The interaction had a fast observed association rate (similar to the other reagents) but a slower rate of dissociation. However, accurate determination of K_D could not be achieved using the steady-state model because the interaction did not reach equilibrium. A possible reason for this could be a heterogeneous binding interaction.

6.2.1.4. Interaction of chemically cross-linked (XL) CD59-3-CRIg with C3b

As described in Chapter 5, the fusion proteins with an IgG3 hinge contained 5% dimer. To investigate whether the different binding profile observed for CRIg-3-CD59 was due to the presence of monomer and dimer in the protein preparation, and to test the hypothesis that dimerisation improved binding and targeting, the percentage of dimer was increased and the C3b binding affinity was re-evaluated.

A cross-linking strategy was developed to enhance dimerisation of CRIg-3-CD59 and CD59-3-CRIg proteins (Fig. 6.7A). Bisamaleimide cross-linker, BM(PEG)2 (1,8-*bis* (maleimido) diethylene glycol; Thermo Scientific) was used to link sulphhydryl groups (-SH) of the IgG3 hinge domain of monomeric fusion proteins to form a dimer. The cross-linking condition was optimised and explained in details in Chapter 2, section 2.6.2.

A two-fold molar excess of crosslinker to CD59-3-CRIg fusion protein provided the highest percentage of dimerisation and was selected as the final reaction condition. As assessed by SDS-PAGE analysis, the dimerisation was increased by 30% and approximately 35% of the protein was assembled in a dimer (Fig.6.7 B). The affinity of CD59-3-CRIg XL with C3b was studied. As with the other CD59-CRIg fusion proteins, a serial dilution of CD59-3-CRIg XL was prepared, starting at 363 $\mu\text{g/ml}$, and was flowed across the C3b coated chip surface. The binding sensorgram is shown on Fig 6.6 E. Similarly to CRIg-3-CD59 interaction (Fig.6.6 C), the injection time of CD59-3-CRIg XL was not sufficient for the

binding reaction to reach equilibrium. The K_D was estimated at 1.4 μM using steady state analysis although this was likely a significant under-estimate due to the unusual and heterogenous kinetics which made it difficult to reach equilibrium. It was clear that crosslinking increased binding significantly (at least 3.7-fold as estimated by K_D) when compared to CD59-3-CRIg; a portion of the bound ligand bound very stably with a slow off-rate.

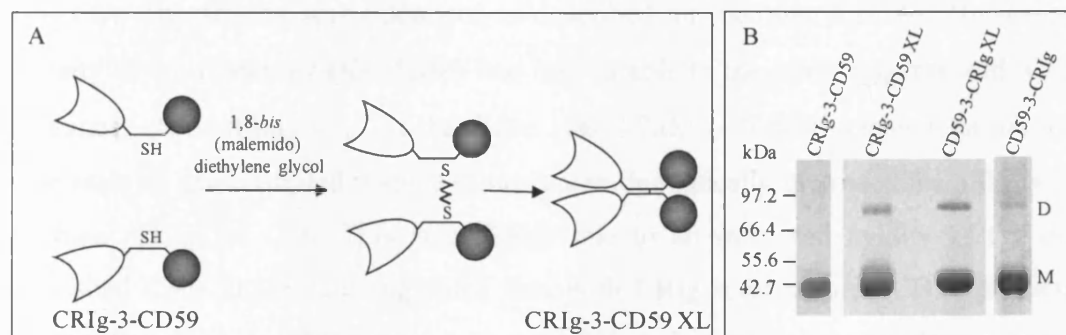


Fig.6.7 Chemical crosslinking of CD59-3-CRIg fusion proteins. A. Schematic diagram representing CR Ig-3-CD59 crosslinking. Crosslinking reaction of CR Ig-3-CD59 or CD59-3-CRIg with BM(PEG)2 (1,8-*bis* (maleimido) diethylene glycol) was performed in PBS (pH7.5) containing 5mM EDTA. The reaction mixture was incubated for one hour at room temperature and the excess of nonreacted reagent was removed by a desalting column. B. SDS-PAGE analysis of dimerisation. The efficiency of crosslinking was assessed by SDS-PAGE analysis under non-reducing conditions. Proteins before and after the crosslinking are visualised using Coomassie Blue. Monomer and dimer are indicated.

6.2.1.5. Interaction of monomeric and dimeric forms of CD59-2a-CRIg with C3b

The effect of dimerisation on binding to C3b was further analysed. SPR was used to establish the affinity of CD59-2a-CRIg monomer and dimer for mouse C3b.

The generation of CD59-2a-CRIg proteins was explained in Chapter 3. We hypothesised that the three sulfhydryl groups present in IgG2a hinge (compared to only one cysteine in IgG3 hinge) would lead to a higher percentage of stable dimers being formed. SDS-PAGE

analysis and gel filtration explained in Chapter 3 confirmed this and revealed that 45% of the protein was assembled in dimer.

Using gel filtration chromatography, CD59-2a-CRIg monomer and dimer were separated on Superdex 200 column (Fig.5.8B) and their affinity to C3b was analysed. Similarly to the other reagents, the monomer and dimers were diluted in a 1:2 serial dilution in biacore running buffer. Each concentration was flowed over the C3b coated chip in duplicate (Fig.6.8). The affinity was calculated as described for the other CD59-CRIg reagents. The affinity of the monomer ($K_D=5\mu\text{M}$) was comparable to the other reagents with CRIg at C-terminus. The affinity (K_D) of the dimer was $0.7\mu\text{M}$ or 7-fold greater than the monomer. The analysis demonstrated that the dimerisation dramatically increased the affinity of the C-terminal CRIg for C3b. This is probably due to an increased avidity of the dimer for deposited C3b. These data suggested that both CRIg molecules in CD59-2a-CRIg dimer were able to bind simultaneously to separate C3b molecules and contribute to avidity.

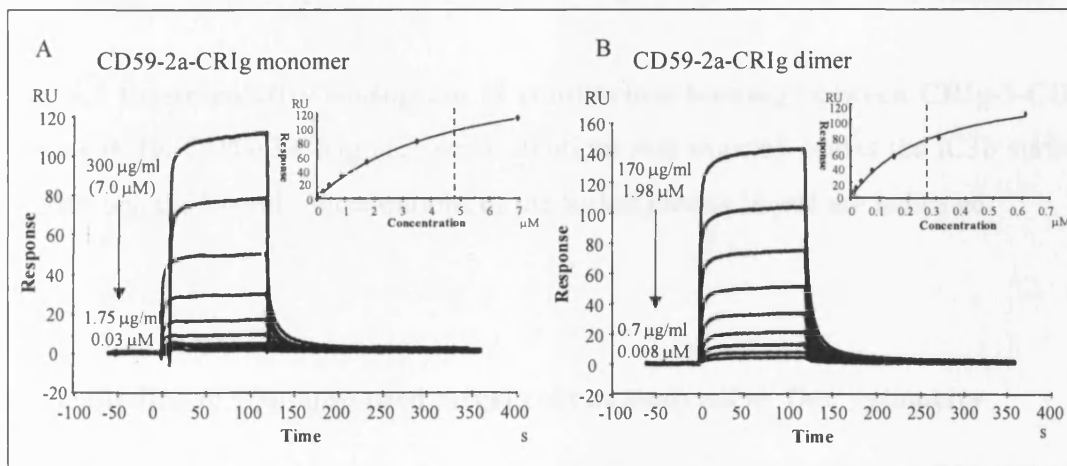


Fig.6.8 Equilibrium binding of monomeric and dimeric form of CD59-2a-CRIg with C3b. SPR sensograms of the interaction between C3b and (A) monomeric or (B) dimeric forms of CD59-2a-CRIg. Inset plots show steady-state affinity analysis for each reaction. The highest and the lowest concentration of fusion proteins flowed across the surface are indicated.

6.2.1.6. Interaction of CR1g-3-CD59 with iC3b

CR1g-3-CD59 protein was used to assess whether CR1g within fusion proteins was able to bind iC3b. Serial dilution of the fusion protein was flowed across the iC3b chip surface (Fig. 6.9). The analysis revealed that CR1g-3-CD59 bound iC3b. The affinity of CR1g-3-CD59 for iC3b could not be determined due to a heterogeneous binding interaction.

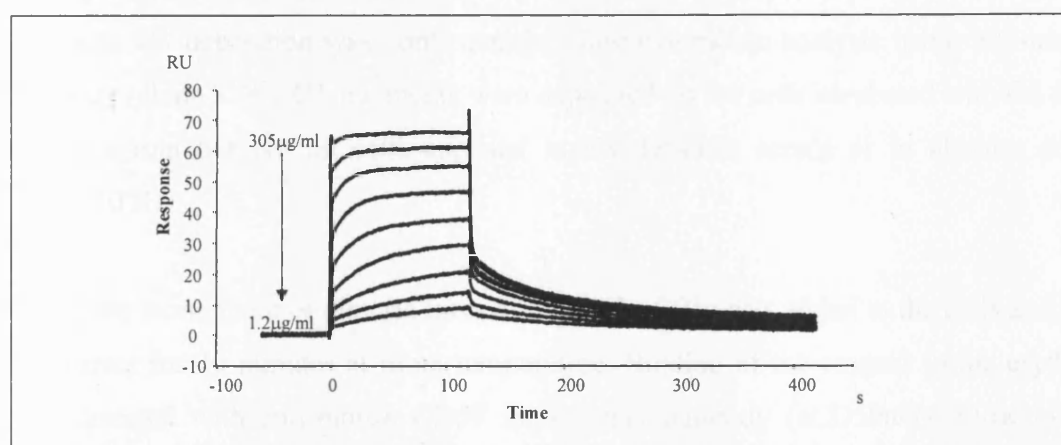


Fig. 6.9 Representative sensogram of equilibrium binding between CR1g-3-CD59 and mouse iC3b. CD59-3-CR1g (1:2 serial dilution) was injected across the iC3b surface. The highest and the lowest concentrations of the fusion protein in μM are indicated.

6.2.2. Binding to C3b-opsonised target cells as analysed by flow cytometry

The SPR analyses revealed that increased dimerisation of the reagents translated into improved targeting. Flow cytometry was next performed to confirm this observation. The ability of CD59-2a-CR1g monomer and dimer to target C3b-coated red blood cells was assessed.

CD59-2a-CR1g was selected for analysis because the dimeric form of the reagent demonstrated increased C3b binding affinity (Biacore analysis). Furthermore it became evident from functional analysis explained in section 6.2.2 that this orientation of CD59 was beneficial for complement inhibition (haemolytic assays). Prior to flow cytometric analysis,

the CD59-2a-CRIg was gel filtered using a Superdex 200 column to separate monomer and dimer.

The ability of CD59-2a-CRIg to target sites of complement activation (C3b/iC3b deposition) on the cell surface was assessed following method 2.7.8. Antibody-sensitised CD59-deficient erythrocytes were coated in C3b/iC3b via the classical pathway using 20% C6 deficient mouse serum to prevent MAC formation and cell lysis. CD59^{-/-} cells were chosen as target in order that anti-CD59 antibody could be used to detect CD59-2a-CRIg bound to the cells. C3 deposition was confirmed by flow cytometric analysis using anti-mouse C3 antibody (clone 3/26). C3 fragments were deposited on the cells incubated with C6 deficient mouse serum but not on cells exposed to C3 deficient serum or in absence of serum (Fig.6.10 A).

Either the monomeric or dimeric form of CD59-2a-CRIg was added to the cells and allowed to interact for 30 minutes at room temperature. Binding of the reagent to the erythrocytes was detected with anti-mouse CD59 monoclonal antibody (aCD59a-7). Flow cytometry plots illustrating representative examples of CD59-2a-CRIg interaction to C3b-positive and C3-negative control erythrocytes are shown in Fig.6.10 B and C. The dimeric CD59-2a-CRIg bound the C3b-coated red blood cells in a dose dependent manner. No binding was detected in absence of C3 or serum (Fig.6.10 B and D). In contrast to the dimer, the monomer showed binding to erythrocytes in presence and absence of C3 deposition (Fig.6.10 C). The binding to complement-coated cells was greater than to the “bare” cells. As seen from Fig.6.10 D, more binding to C3-opsonised cells was detected for the monomer compared to the dimer.

6.2.3. Complement Inhibition

The ability of CRIg-CD59 fusion proteins to inhibit complement and to protect erythrocytes from killing was assessed *in vitro* using variety of haemolysis assays.

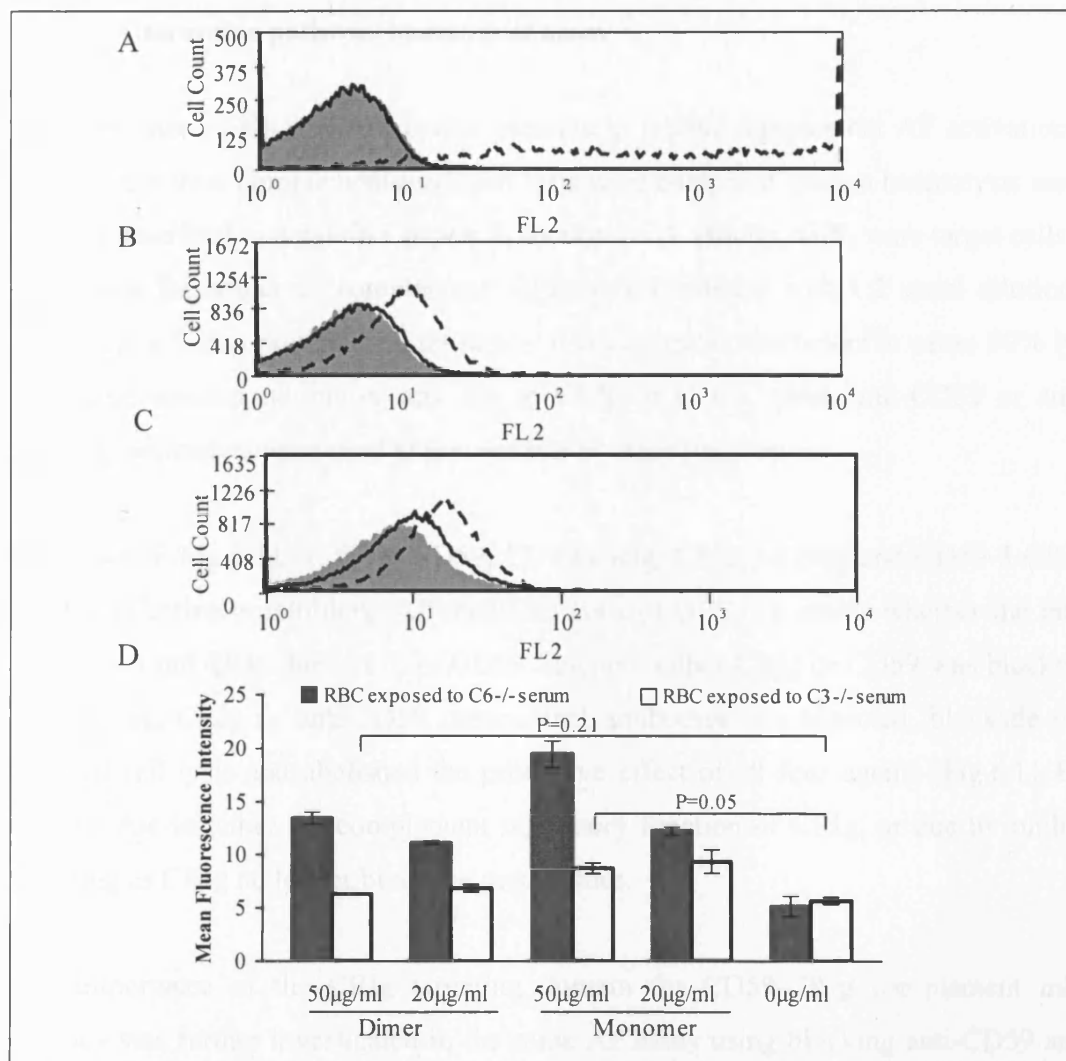


Fig.6.10 Targeting of CD59-2a-CRIg to C3-opsonised red blood cells. A. C3 deposition. Antibody-sensitised CD59^{-/-} mouse erythrocytes were incubated with C6^{-/-} (dotted line), C3^{-/-} (black line) mouse serum or buffer (filled area). Deposition of C3b was detected using rat-anti mouse C3 mAb. B. Representative binding profile of CD59-2a-CRIg dimer to C3b-coated cells. CD59-2a-CRIg dimer (40 µg/ml) was added to the C3b-opsonised or control cells. Binding of recombinant proteins was detected using anti-CD59 mAb, CD59-2a-CRIg dimer bound the C3b-coated cells (dotted line). No binding was detected to the cells treated with C3^{-/-} serum (black line) or with no serum (filled area). C. Representative binding profile of CD59-2a-CRIg monomer to C3b-coated cells. CD59-2a-CRIg monomer bound the C3b-opsonised red blood cells (dotted line). Less binding was observed to the cells treated with C3^{-/-} serum (black line) or with no serum (filled area). D. Analysis of CD59-2a-CRIg binding to red blood cells. Data are mean ±SD of two determinations.

6.2.3.1. Alternative pathway haemolysis assay

The capacities of CRIg-CD59 fusion proteins to inhibit complement AP activation and to protect cells from complement-mediated lysis were compared using a haemolysis assay. The assay is described in detail in Chapter 2, section 2.7.3. Briefly, GPE were target cells and rat serum was the source of complement. GPE were incubated with 1:2 serial dilution of the CD59-CRIg fusion proteins and rat serum at concentration sufficient to cause 90% lysis. To determine whether inhibition was due to CRIg or CD59, either anti-CD59 or anti-CRIg blocking antibodies were used to prevent one or other function.

As shown in Fig 6.11 A, CRIg-CD59, CD59-CRIg, CRIg-3-CD59 and CD59-3-CRIg were equally effective at inhibiting AP-mediated lysis of GPE. To assess whether the inhibition was due to the CRIg domain or to CD59 function, either CRIg or CD59 was blocked using specific anti-CRIg or anti-CD59 monoclonal antibodies. As expected, blockade of CRIg restored cell lysis and abolished the protective effect of all four agents (Fig.6.11 B). This may be due to either the complement regulatory function of CRIg, or due to inhibition of targeting as CRIg no longer binds the membranes.

The importance of the CRIg targeting domain for CD59-CRIg complement inhibitory efficacy was further investigated in the same AP assay using blocking anti-CD59 antibody. When the CD59-CRIg reagents were preincubated with anti-CD59 antibody the protective effect of the CD59-CRIg and CD59-2a-CRIg was abolished (Fig. 6.12 A and B). Blockade of the CD59 moiety in CD59-3-CRIg only partially reduced the capacity of the reagent to inhibit complement (Fig. 6.12 C). In contrast to the N-terminal CD59, the presence of the CD59 blocking antibody did not have any effect on inhibition when CD59 was located at the C-terminus of CRIg-CD59 or CRIg-3-CD59 (Fig. 6.12 D and E). This result suggests that CD59 at N-terminus inhibits complement with greater efficiency and thus provides better protection to the target cells.

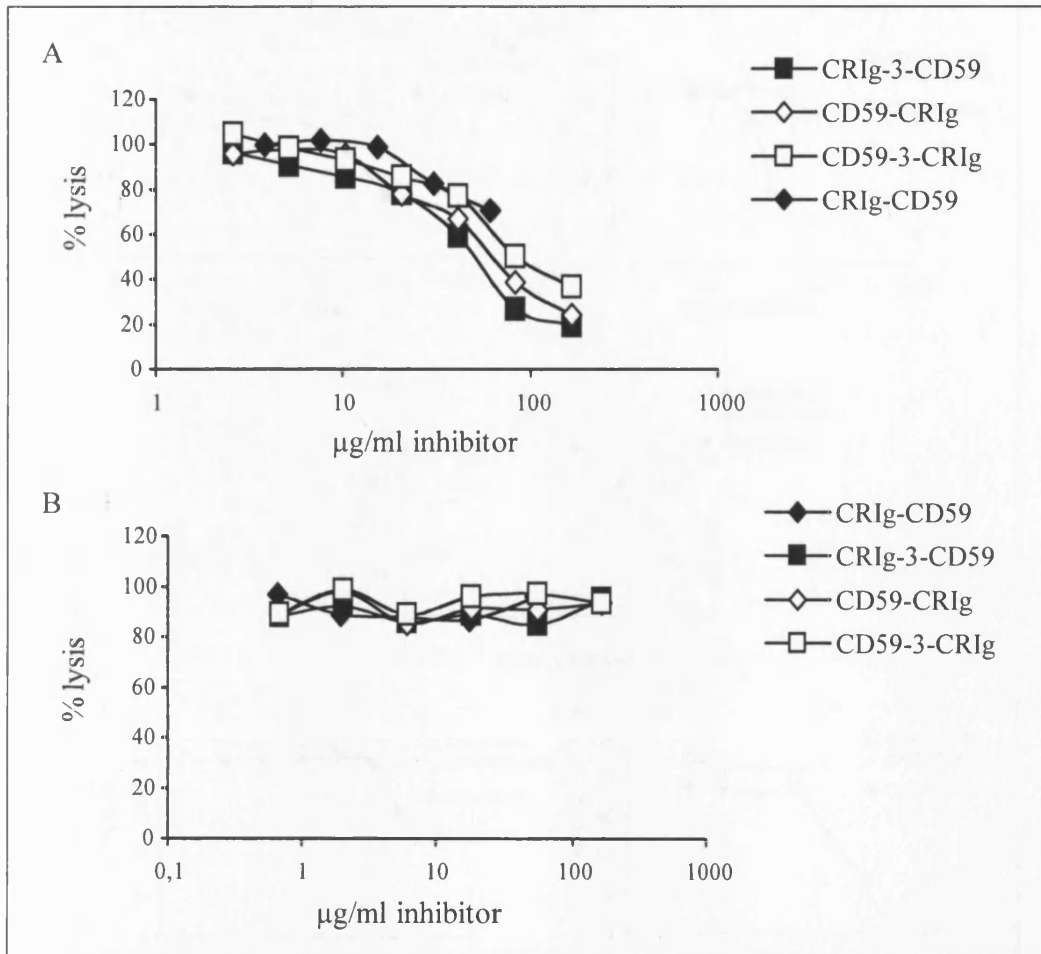


Fig. 6.11 CRIg effect on alternative pathway inhibition. GPE were incubated with rat serum and the ability of CD59-CRIg, CD59-3-CRIg, CRIg-CD59 and CRIg-3-CD59 to prevent alternative pathway-mediated haemolysis was determined. All four reagents were able to inhibit complement and to protect cells from complement mediated killing (A). To test whether this was a specific effect, CRIg was blocked using specific anti-CRIg monoclonal antibodies. Blockade of CRIg restored cell lysis and abolished the protective effect of all four agents (B).

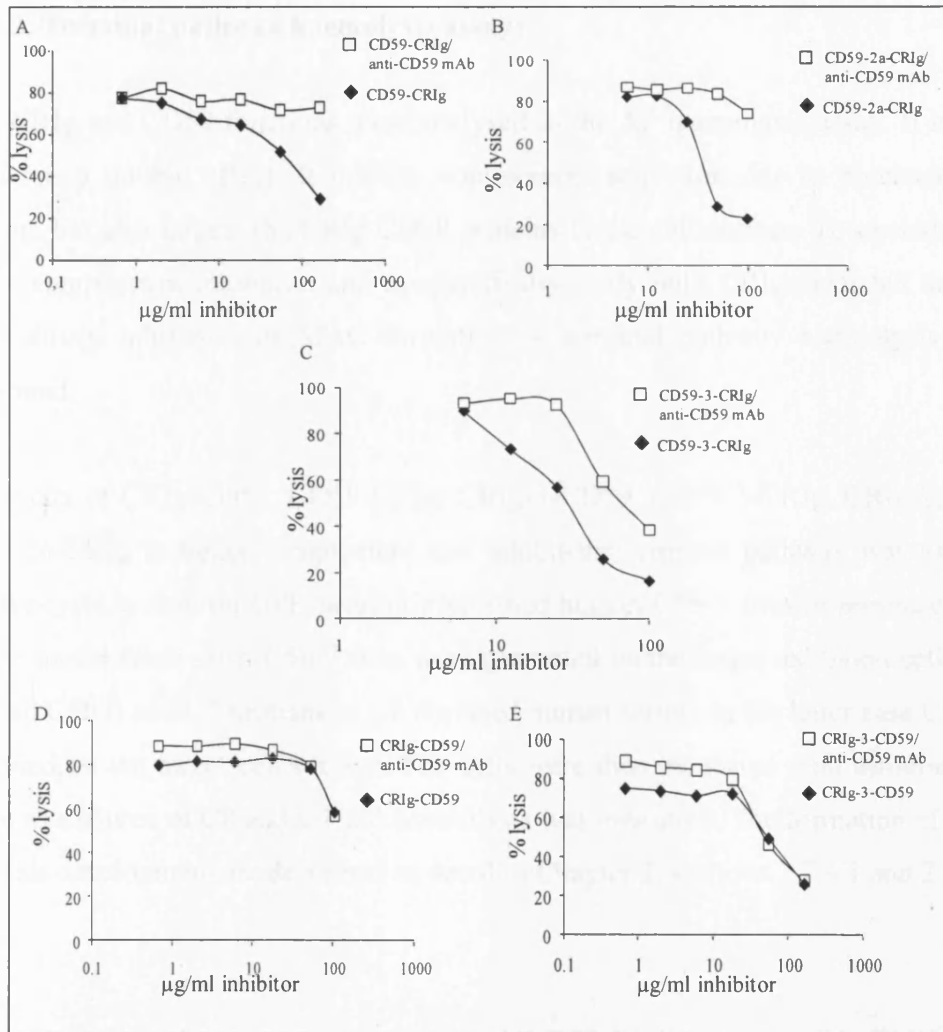


Fig. 6.12 CD59 effect on alternative pathway inhibition. GPE were incubated with rat serum and the ability of CD59-CRIg (A), CD59-2a-CRIg (B), CD59-3-CRIg (C), CRIG-CD59 (D) and CRIG-3-CD59 (E) in presence or absence of CD59 blocking antibody to prevent alternative pathway-mediated haemolysis was determined. All five reagents in absence of anti-CD59 mAb were able to inhibit complement and to protect cells from complement mediated killing. Blocking CD59 completely abolishes the protective effect of CD59-CRIg (A) and CD59-2a-CRIg (B) and only partially of CD59-3-CRIg (C). The antibody did not have a significant effect on CRIG-CD59 (D) and CRIG-3-CD59 (E) mediated inhibition

6.2.3.2. Terminal pathway haemolysis assays

Both CRIg and CD59 functions were analysed in the AP haemolysis assay. It is likely that CRIg has a double effect. It inhibits complement activation due to blockade of C3/C5 binding, but also targets the CRIg-CD59 proteins to the cell surface. To exclude the CRIg-driven complement inhibition and to specifically study only CRIg-mediated targeting and CD59-driven inhibition of MAC formation, a terminal pathway haemolysis assay was performed.

The ability of CRIg-CD59, CD59-CRIg, CRIg-3-CD59, CD59-3-CRIg, CRIg-2a-CD59 and CD59-2a-CRIg to target complement and inhibit the terminal pathway was assessed in a reactive-lysis system on GPE bearing preformed human C5b-7 sites in presence or absence of C3b on the same cells. C5b-7 sites were generated on the target red blood cells by adding purified C5b-6 and C7 proteins or C8 depleted human serum, in the latter case C3b was also deposited on the target cell surface. The cells were then incubated with dilutions of mouse serum as a source of C8 and C9 and haemolysis was measured. The formation of C5b-7 sites and lysis development are described in detail in Chapter 2, sections 2.7.4.1 and 2.7.4.2.

6.2.3.2.1. CD59-CRIg function on cells bearing C5b-7 sites in absence of C3b

The ability of CD59 within fusion proteins to inhibit the terminal pathway was analysed on GPE bearing C5b-7 sites generated by incubation with purified terminal pathway components (Chapter 2, section 2.7.4.2). The cells were pre-incubated with 1:3 serial dilutions of CRIg-CD59 fusion proteins, followed by addition of C3 deficient mouse serum to develop lysis at a predetermined concentration which causes 50-60% lysis in the absence of inhibition. To exclude any non-specific protein effects on cell lysis, a dilution series of CRIg-fH (generated in house) was used as a negative control. This protein contains CRIg but has no terminal pathway regulatory activity. Haemoglobin release from the cells was measured and percentage lysis was determined.

All CD59-CRIg fusion proteins inhibited the terminal complement pathway in a dose dependent manner. CD59-CRIg, CD59-3-CRIg and CD59-2a-CRIg had equal capacity to protect the target cells from complement-mediated lysis (Fig.6.13). In contrast, constructs

with CD59 at the C-terminus (CRIg-CD59, CRIg-3-CD59 and CRIg-2a-CD59) had decreased complement inhibitory function. This complement inhibitory capacity of the C-terminal CD59 was not observed in the AP haemolysis test. However the assay used here was specifically designed to study the terminal pathway and small changes in its activity could be detected. Nevertheless the data obtained by the two assays strongly suggests that the position and/or the orientation of CD59 within fusion proteins was important for its inhibitory function.

6.2.3.2.2. CRIg-CD59 function on cells bearing C5b-7 sites in presence of C3b

All tested CD59-CRIg fusion proteins demonstrated ability to block the terminal pathway. To investigate the capacity of reagents to target C3b deposition and then to inhibit MAC formation (i.e. in addition to working from the fluid phase), GPE were incubated with C8-depleted human serum to allowed C3b deposition and the generation of C5b-7 sites on the cell surface. Wash and non-wash haemolysis assays were used to assess the ability of the reagents to target C3 fragments and to physically bind to the cells to inhibit complement. In the first, non-wash assay, the reagents were present throughout, whilst they were washed out before subjecting the cells to complement attack in the second assay. Two proteins containing both CD59 and CRIg but not fused to each other were used as controls as they have no capacity for delivering CD59 to the cell surface. Generation of the control proteins was explained in Chapter 5, section 5.2.3.

For the non-wash assay the C5b-7 sites were generated on GPE using C8-depleted human serum. The cells were pre-incubated with 1:2 serial dilutions of CRIg-CD59 fusion proteins, followed by addition of C3 deficient mouse serum in a predetermined concentration causing 50-60% lysis. Percentage lysis was determined.

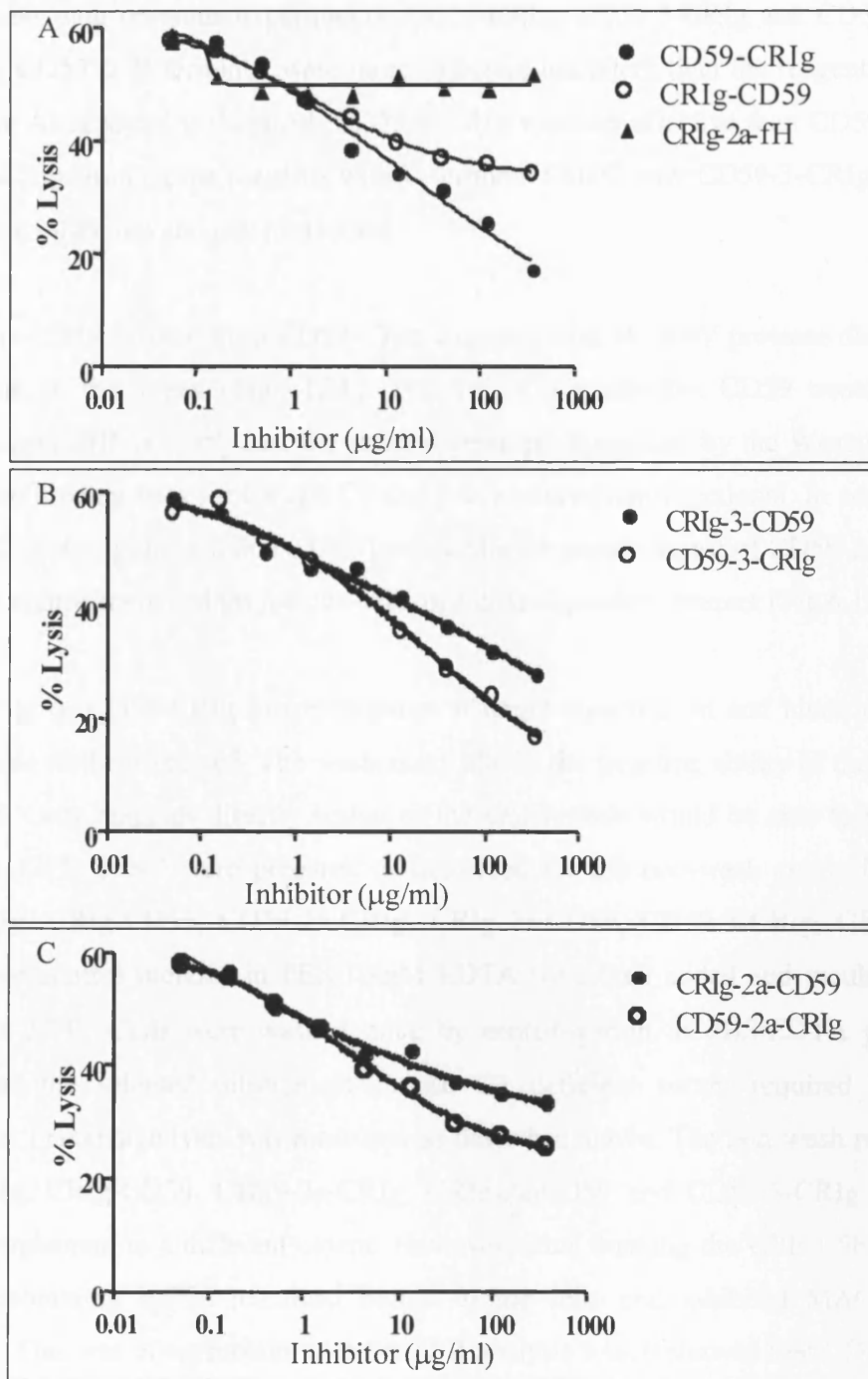


Fig.6.13 Terminal pathway regulatory function of CD59-CRIg fusion proteins. Guinea pig erythrocytes on which C5b-7 complex was preformed were attacked with C3 deficient mouse serum. The ability of C-terminal (closed circle) and N-terminal CD59 (open circle) within CRIg-CD59 and CD59-CRIg (A), CRIg-3-CD59 and CD59-3-CRIg (B) and CRIg-2a-CD59 and CD59-2a-CRIg (C) to inhibit MAC formation was assessed. CD59 located at the N-terminus of the protein was more effective complement inhibitor compared to the C-terminal CD59.

In agreement with previous experiments, CD59-CRIg, CD59-3-CRIg and CD59-2a-CRIg, containing CD59 at N-terminus were more effective inhibitors than the reagents in reverse orientation. As revealed in Fig.6.14, CD59-3-CRIg was less effective than CD59-CRIg and CD59-2a-CRIg. Among the reagents with C-terminal CD59, only CD59-3-CRIg showed no complement inhibition and cell protection.

The soluble CD59 derived from CD59-CRIg cleavage with 3C HRV protease did not inhibit complement in this assay (Fig.6.15A). This result suggests that CD59 treated with the reducing agent THP not only lost the antibody epitope (suggested by the Western blot), but also lost the binding sites for C8 and C9 and was rendered non-functional. In contrast to the cleaved CD59-CRIg, the soluble CD59 generated after papain digest of CD59-2a-CRIg was able to block complement and protect the cells in a dose dependent manner (Fig.6.15C).

The capacity of CD59-CRIg fusion proteins to target complement and block the terminal pathway was further explored. The wash assay allows the targeting ability of the reagents to be studied. Only reagents directly bound to the cell surface would be able to provide cell protection. GPE C5b-7 were prepared as described for the non-wash assay. Dilutions of CD59-CRIg, CRIg-CD59, CD59-2a-CRIg, CRIg-2a-CD59, CD59-3-CRIg, CRIg-3-CD59 and the two control proteins in PBS/10mM EDTA were then added and incubated for 30 minutes at 37°C. Cells were washed once by centrifugation in PBS/EDTA prior to the addition of the selected dilution of mouse C3 deficient serum required to develop haemolysis. Percentage lysis was measured as described above. The non-wash revealed that CD59-CRIg, CRIg-CD59, CD59-2a-CRIg, CRIg-2a-CD59 and CD59-3-CRIg are able to inhibit complement to a different extent. However, after washing the GPE C5b-7, only the reagents containing IgG2a remained bound to the cells and inhibited MAC-deposition (Fig.6.16). This was in agreement with the SPR analysis which showed that CD59-2a-CRIg had high affinity for a C3b-coated chip surface (section 6.2.1.1.3.3, table 6.3).

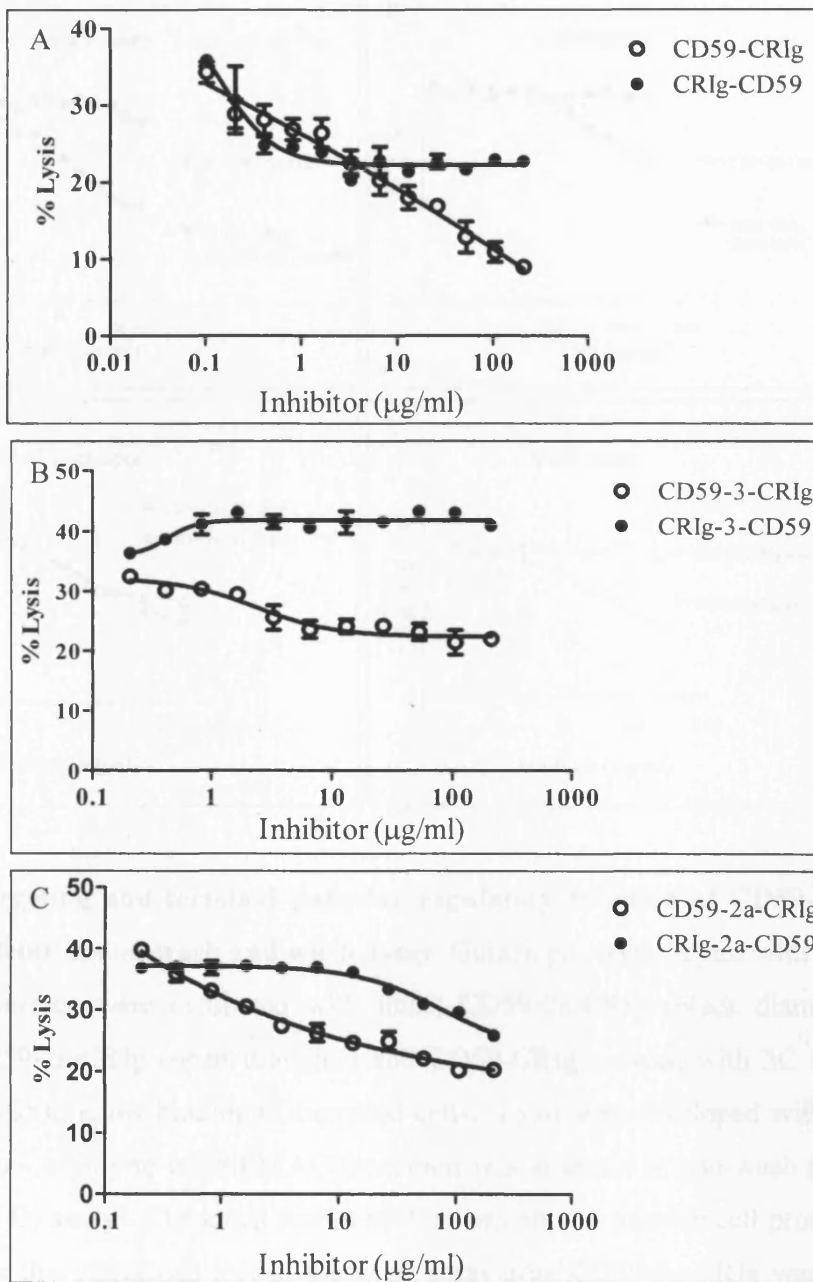


Fig.6.14 Targeting and terminal pathway regulatory function of CD59-CR1g fusion proteins in non-wash assay. GPE on which C3b and C5b-7 was deposited were generated using C8^{-/-} human serum; these were then incubated with C3 deficient mouse serum to develop MAC. The ability of C-terminal (closed circles) and N-terminal CD59 (open circles) within CR1g-CD59 and CD59-CR1g (A), CR1g-3-CD59 and CD59-3-CR1g (B) and CR1g-2a-CD59 and CD59-2a-CR1g (C) to target C3-coated cells and inhibit MAC formation was assessed. CD59 located at the N-terminus of the protein was more effective complement inhibitor compared to the C-terminal CD59.

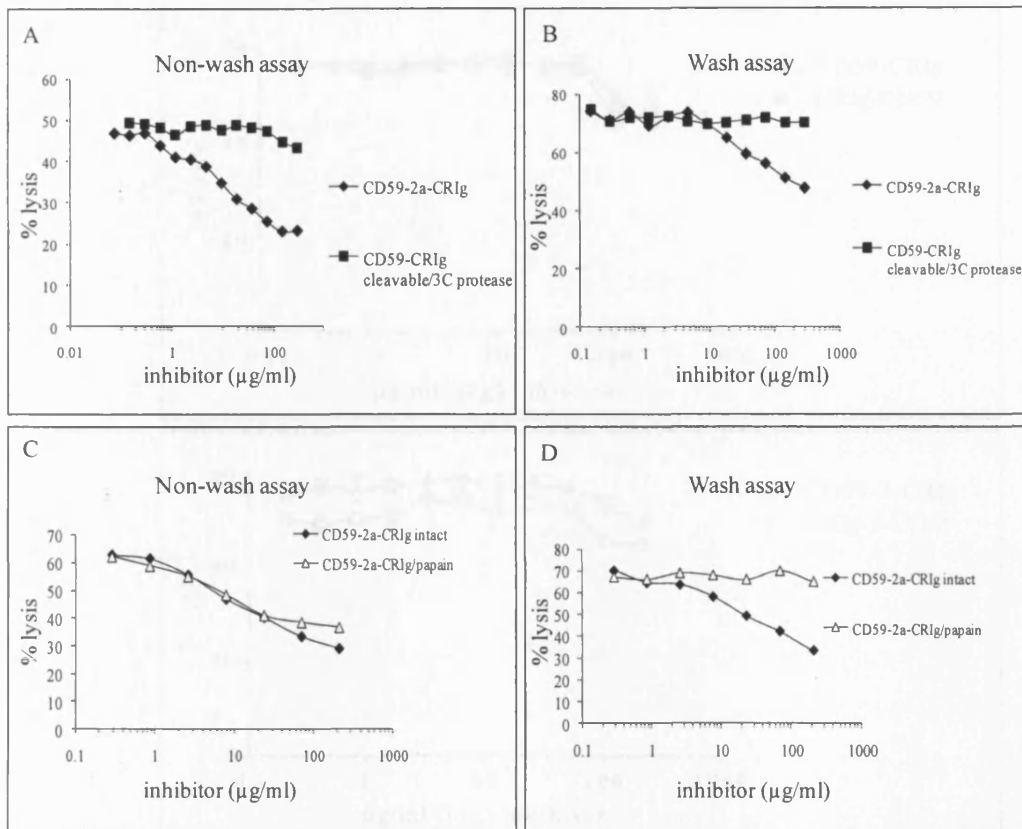


Fig.6.15 Targeting and terminal pathway regulatory function of CD59-2a-CRIg and control proteins in non-wash and wash assay. Guinea pig erythrocytes with C3b and C5b-7 on their surface were incubated with intact CD59-2a-CRIg (black diamonds), papain digested CD59-2a-CRIg (open triangles) and CD59-CRIg cleaved with 3C RHV protease (black squares) to allow binding C3b-coated cells. Lysis was developed with C3-deficient mouse serum. Ability to inhibit MAC formation was assessed in non-wash (A and C) and wash (B and D) assays. The intact fusion protein was able to provide cell protection in both assays, while this effect was lost in the wash assay after CD59-2a-CRIg was cleaved with papain (D). CD59-CRIg treated with 3C HRV protease did not inhibit complement in any of the assays (A and B).

Similarly to the result obtained from the non-wash assay, the cleaved CD59-CRIg (the cleavable reagent) did not inhibit the terminal pathway (Fig.6.15 B). However in contrast to the non-wash assay, the other control protein obtained from the papain cleavage of CD59-2a-CRIg lost its inhibitory activity in the wash assay indicating that CRIg was essential for targeting CD59 to the cells (Fig.6.15 D).

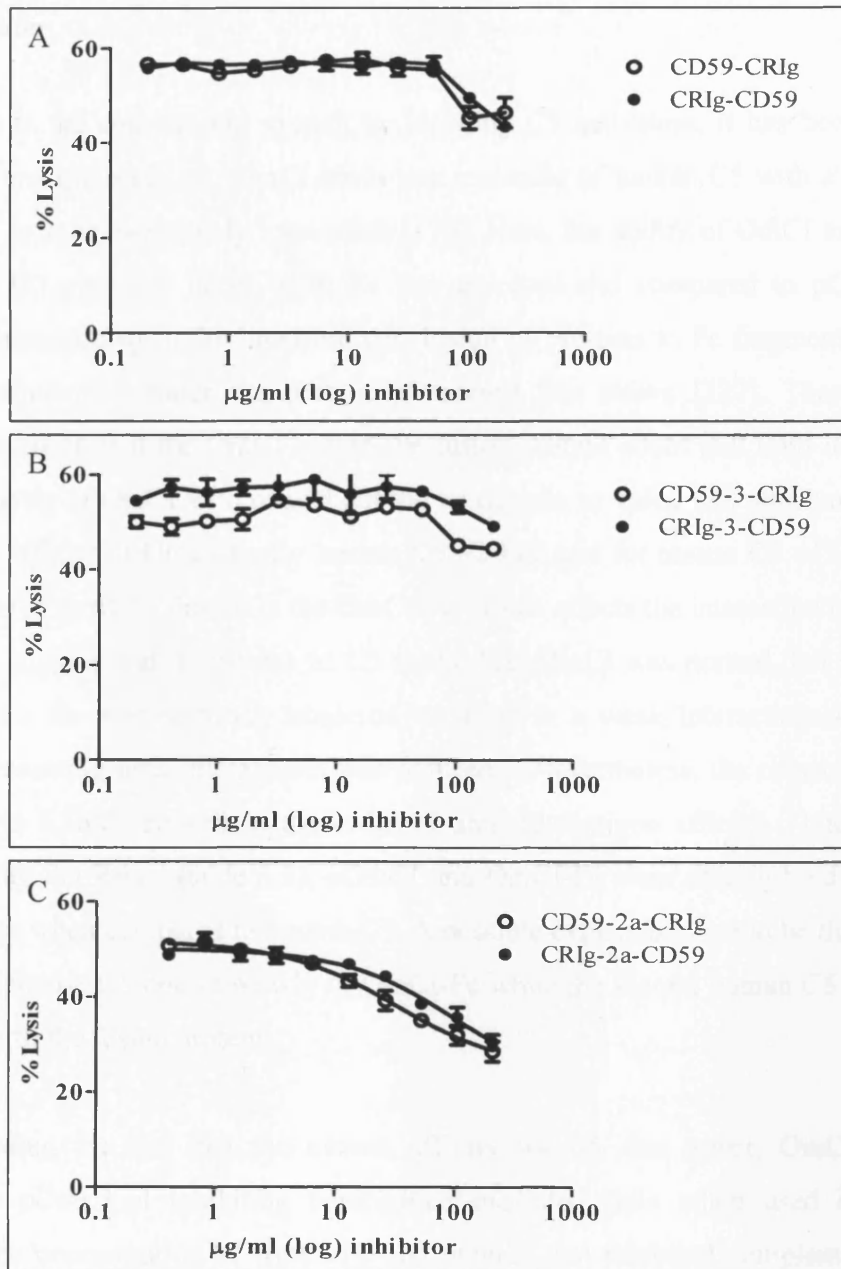


Fig.6.16 Targeting and terminal pathway regulatory function of CD59-CR1g fusion proteins in wash assays. C3b was deposited on Guinea pig erythrocytes and C5b-7 complex was preformed using C8^{-/-} human serum to activate complement. MAC was developed using C3 deficient mouse serum. The ability of C-terminal (closed circle) and N-terminal CD59 (open circle) within CR1g-CD59 and CD59-CR1g (A), CR1g-3-CD59 and CD59-3-CR1g (B) and CR1g-2a-CD59 and CD59-2a-CR1g (C) to target C3-tagged cells and inhibit MAC formation was assessed. After washing the target cells only CD59-2a-CR1g and CR1g-2a-CD59 remained bound to the surface and provided protection.

6.3. Discussion

OmCI inhibits the complement system by blocking C5 activation. It has been previously shown that one molecule of pOmCI binds one molecule of human C5 with a high affinity comparable to antigen-antibody interaction [176]. Here, the ability of OmCI to bind mouse and human C5 after the fusion with Fc was assessed and compared to pOmCI. It has previously been shown in the literature that fusion of proteins to Fc fragments can cause steric hindrance and render the protein of interest less active [327]. Therefore it was important to check that the OmCI within the fusion protein could still bind its ligand, C5. Biacore analysis of OmCI with or without the Fc domain revealed that attachment to the Fc reduced the affinity of OmCI-Fc for human C5 ~2-fold and for mouse C5 ~13-fold. This is probably due to steric hindrance in the OmCI-Fc, which affects the interaction of OmCI with its ligand. I suggest that the access of C5 to the first OmCI was normal, but access to the second OmCI site was sterically hindered resulting in a weak interaction so the overall affinity representing both interactions was reduced. Nevertheless, the respective affinities of 11nM and 5.3nM are still in the order of antibody/antigen affinity. Interestingly, as determined by the R_{max} (table 6.1), pOmCI and OmCI-Fc were able to bind more mouse C5 molecules when compared to human C5. A possible explanation could be that the second molecule of mouse C5 bound weakly to OmCI-Fc while the second human C5 was not able to interact with the fusion protein.

Notwithstanding the fact that the overall affinity for C5 was lower, OmCI-Fc was as effective as pOmCI at inhibiting complement-mediated lysis when used in equimolar amounts. The concentration of OmCI-Fc and pOmCI that inhibited complement-mediated lysis by 50% (IH_{50}) was calculated and compared. IH_{50} is the most widely used measure of drug inhibition. The analysis revealed that slightly less OmCI-Fc was needed to bring about 50% inhibition of cell lysis in all assays compared to pOmCI. However OmCI-Fc demonstrated different kinetics of complement inhibition compared to pOmCI with the two OmCI moieties binding C5 with different affinity (suggested by the SPR analysis) and therefore a direct comparison of OmCI-Fc and pOmCI activity using IH_{50} was inappropriate.

In addition to IH_{50} , other key factors, describing the effect of pOmCI and OmCI-Fc on complement, are the steepness of the dose response curve and the threshold dose level for inhibiting MAC formation. Increase in the concentration of the inhibitors resulted in a

decrease in the number of the C5 molecules able to form MAC. However, only a single C5 molecule is needed to form a MAC and even a very small amount of C5 was sufficient to cause cell lysis. For this reason a noticeable anti-complement effect was not observed until “the last” C5 molecule had been neutralised. pOmCI bound tightly to C5 and therefore a small increase in drug concentration resulted in a dramatic increase in complement inhibition and a steep dose response curve. In contrast to pOmCI, the inhibitory effect of OmCI-Fc increased much more slowly with increasing the drug concentration. This could be explained with the weaker OmCI-Fc-C5 interaction (with one OmCI-arm binding C5 with the expected affinity and second-binding with lower affinity). Therefore the OmCI-Fc response curve was less sharp with higher threshold dose level (the point at which complement inhibition first appear) when compared to pOmCI.

The inhibitory effects of pOmCI and OmCI-Fc on the complement system also differed in the threshold dose level of these two reagents. pOmCI had a lower threshold compared to OmCI-Fc. The difference in the threshold effect and the steepness of the dose response curve could be explained with the lower overall affinity of OmCI-Fc to C5 when compared to pOmCI. pOmCI bound more tightly to C5 leading to rapid complement inhibition (demonstrated by the steeper slope and the low threshold).

Targeted reagents comprised of the sole membrane regulator of MAC assembly, CD59, and the complement receptor, CR1g, were comprehensively characterised *in vitro* in order to select the optimal CD59-CR1g anti-complement reagent to take for further analysis *in vivo*.

The C3b/iC3b-targeting activity of the CR1g domain was assessed by SPR and flow cytometry. The SPR analysis revealed that CR1g within fusion proteins was able to bind C3b and iC3b. The dimeric proteins with CR1g located at the N-terminus showed higher C3b binding affinity than the proteins in reverse orientation. This implies that positioning of the receptor with regards to CD59 was of high importance for CR1g function. Even though the K_D of CR1g-3-CD59 interaction with C3b could not be calculated, the binding profile revealed that this reagent dissociated more slowly from the surface compared to CR1g-CD59. This was due either to the longer spacing domain between the CR1g and CD59 domains, providing greater conformational flexibility, or to the 5% dimerisation which occurred in the presence of the IgG3 hinge. Two strategies were tested to increase the dimerisation. First, CD59-3-CR1g and CR1g-3-CR1g were chemically cross-linked to

generate homodimers and secondly, the IgG3 hinge was replaced with the hinge from IgG2a. Although dimerisation was incomplete, replacing the hinge offered an advantage over chemical cross-linking and approximately 45% of the protein was assembled in a dimer. It was found that the C-terminal CRIg within CD59-2a-CRIg dimer bound C3b with high affinity similar to the N-terminal CRIg within CRIg-CD59 molecule. In other words, the low C3b affinity of the C-terminal CRIg was overcome by increasing the C3b binding avidity through dimerisation.

The targeting capacity of CD59-2a-CRIg reagent was verified by flow cytometry. The CD59-2a-CRIg dimer specifically bound C3b/iC3b deposited on the erythrocyte surface while the monomeric form interacted with the cell in the absence of C3 fragments. An enhanced binding of CD59-2a-CRIg monomer with C3b/iC3b coated cells was observed which could be an additive effect of CD59-2a-CRIg monomer binding to C3b and the unknown ligand simultaneously. The result suggests that CD59-2a-CRIg binds to a cell ligand different to C3b (or iC3b) and the epitope for this is sterically hindered in the dimeric reagent.

The ability of CD59-CRIg fusion proteins to target to a surface and/or to inhibit complement activation was explored using alternative and terminal pathway haemolysis assays. All proteins were effective at inhibiting the AP. This was not surprising since during my PhD it became evident that CRIg itself could inhibit the AP [167]. The observation was confirmed using anti-CRIg blocking antibody capable of abolishing the complement inhibitory effects of the reagents. However blocking CRIg binding to C3b/iC3b deposited on the cell surface did not only suppress its AP inhibitory activity but also prevented CRIg-mediated targeting of CD59 to the surface. The importance of CRIg-mediated targeting for complement inhibitory activity of the CD59-CRIg reagents was proved by blocking inhibitory function of CD59. It was demonstrated that CD59 at the N-terminus in particular, contributed to the complement inhibitory capacity of the whole protein. The conclusion from this experiment was that both CD59 and CRIg function better when located at the N-terminus of the fusion proteins. Interestingly, in contrast to other agents, CD59 at the N-terminus of CD59-3-CRIg reagent showed only minimal effect on complement. This could be due to restricted flexibility of the IgG3 hinge which prevented CD59 from free movement. In addition to that it was also possible the CRIg at C-terminus in this reagent functioned well compared to the other reagents with such orientation (CD59-CRIg and CD59-2a-CRIg). This could be due to

space between CR1g and CD59 provided by the IgG3 hinge. The hinge moved apart the two moieties of the chimeric molecule and thus prevented any steric hindrance within CR1g. The difference in function between N- and C-terminal CD59 was not unexpected. It was previously shown that positioning CD59 relative to CR2 within CR2-CD59 is important for its function. In contrast to results obtained in this study, C-terminal CD59 was found more active than N-terminal CD59 [330]. This difference could be due to the different complement receptor used for targeting.

The effect of CR1g-CD59 specifically on the terminal complement pathway was assessed. Firstly, the inhibitory effect of the CD59-CR1g reagents was studied in the absence of C3b on the target cell surface, then it was studied when C3b was present on the membrane, enabling targeting via CR1g. This enabled the dissection of CD59 inhibitory function and CR1g targeting.

A difference in function between proteins containing CD59 at N- or C-terminus, with N-terminal CD59 being more active, was also seen in terminal pathway assays in the absence of C3 (so only CD59, not CR1g was active on the target cells). While this assay studied only CD59 function, the combined effect of CR1g-mediated targeting and CD59 function was investigated in different terminal pathway specific haemolysis assays (non-wash and wash) in present of C3b. Using C8-depleted serum to deposit C3b/iC3b and C5b-7 and C3 deficient serum to finish off the assay, allowed to study CD59-driven complement inhibition and CR1g-mediated targeting in absence of CR1g complement suppression.

In a non-wash assay where the reagents were present throughout and C3b was deposited on the target cells, the complement inhibitory activity of the CD59-CR1g, CD59-3-CR1g and CD59-2a-CR1g was increased when compared to CR1g-CD59, CR1g-3-CD59 and CR1g-2a-CD59 respectively. The result further confirmed that CD59 at N-terminus of the protein was functionally more active than the C-terminal CD59. In contrast to the other terminal pathway assays, where the ligands for CR1g were not present on the cell surface, here CD59-3-CR1g and CR1g-3-CD59 reagents showed reduced or no functional activity respectively. This may be related to the rigid nature of the IgG3 hinge that prevents the simultaneous interactions of the C3 fragments and MAC components. It is very likely that upon binding of CR1g to C3b/iC3b on the cell surface, CD59 was held at distance from the cell membrane. The IgG3

hinge did not allow the cell surface-bound reagent to move freely in a more favourable orientation for interaction with C8 and C9.

In a wash assay, when the inhibitors not bound to the target cells were removed, the complement-blocking capacity of the untargeted CD59 (CD59-2a-CRIg cleaved with papain and CRIg-CD59 digested with 3C protease) was completely lost whereas CD59-2a-CRIg retained its complement inhibitory activity even after washing of the erythrocytes. This demonstrated that the increased avidity effect of CRIg targeting successfully delivered CD59 to the target cells. In contrast to the non-wash assay, the two dimer-containing reagents CRIg-2a-CD59 and CD59-2a-CRIg showed similar complement inhibitory activity. This suggests that the good targeting through the N-terminal CRIg compensated for the less effective complement inhibition via the C-terminal CD59 to achieve identical overall anti-complement effect of CRIg-2a-CD59 and CD59-2a-CRIg reagents.

The data in this Chapter demonstrate that CD59 at the N-terminus was more effective at protecting erythrocytes than C-terminal CD59, and that CRIg at the C-terminus had lower C3b-binding affinity. However the effect of the dimerisation balanced functional activities of C- and N-terminus CRIg and CD59, and CD59-2a-CRIg and CRIg-2a-CD59 demonstrated equal capacity to protect the target cells from complement attack. In contrast to the IgG2a hinge, the hinge of IgG3 restricted the flexibility of CD59-3CRIg and CRIg-3-CD59 molecules and thus reflected on the overall complement inhibitory activity of these reagents. The *in vitro* targeting analysis revealed CD59-2a-CRIg reagent as a promising therapeutic. This protein expressed as a dimer (45%) and provided efficient targeting through increased avidity to C3b/iC3b and good cell protection from complement-mediated killing. The project will therefore now focus upon CD59-2a-CRIg.

Chapter 7. *In vivo* and *ex vivo* functional analysis of OmCI-Fc and CD59-CRIg fusion proteins

The specific features of the OmCI-Fc and CD59-CRIg fusion proteins which are essential for therapy were explored *in vitro* (Chapter 6). The focus is now moved to analysis of the reagents *ex vivo* and *in vivo*. Chapter 7 opens with a section describing the pharmacokinetic parameters of OmCI-Fc and the establishment of a dosing regimen for anti-complement treatment. The Chapter continues with *in vivo* and *ex vivo* analysis of the most promising CD59-CRIg fusion protein characterised in Chapter 6, CD59-2a-CRIg. The capacity of CD59-2a-CRIg to target complement activation in tissues will be assessed.

7.1. OmCI-Fc

7.1.1. Clearance of OmCI-Fc in mice

It was previously shown that that pOmCI given to experimental animals bound C5 and circulated as a complex. However, free pOmCI was rapidly cleared from the circulation; consequently, it had a short half-life *in vivo*. Only a trace amount was detected in plasma 30 minutes post *iv* administration in C5 deficient mice [176]. The short half-life of pOmCI would limit its therapeutic use to acute disease and clinical conditions such as I/R. The purpose of generating OmCI-Fc was to create a soluble drug with extended circulating half-life for treatment of chronic disorders. To determine whether fusion to the Fc domain of antibody prolonged the circulating half-life of OmCI, OmCI-Fc was injected into C5 deficient or sufficient mice and its presence in the circulation and half-life were investigated by Western blot analysis and ELISA.

7.1.1.1. OmCI-Fc elimination in the absence of C5

To assess the affect of Fc fusion on clearance of OmCI, a mixture of OmCI-Fc (75µg) and pOmCI (150µg) was administered *iv* in C5 deficient mice. At specific times following

administration, plasma samples were harvested (Fig.7.1A) and analysed for the presence of OmCI-Fc and pOmCI by Western blot (Fig.7.1B).

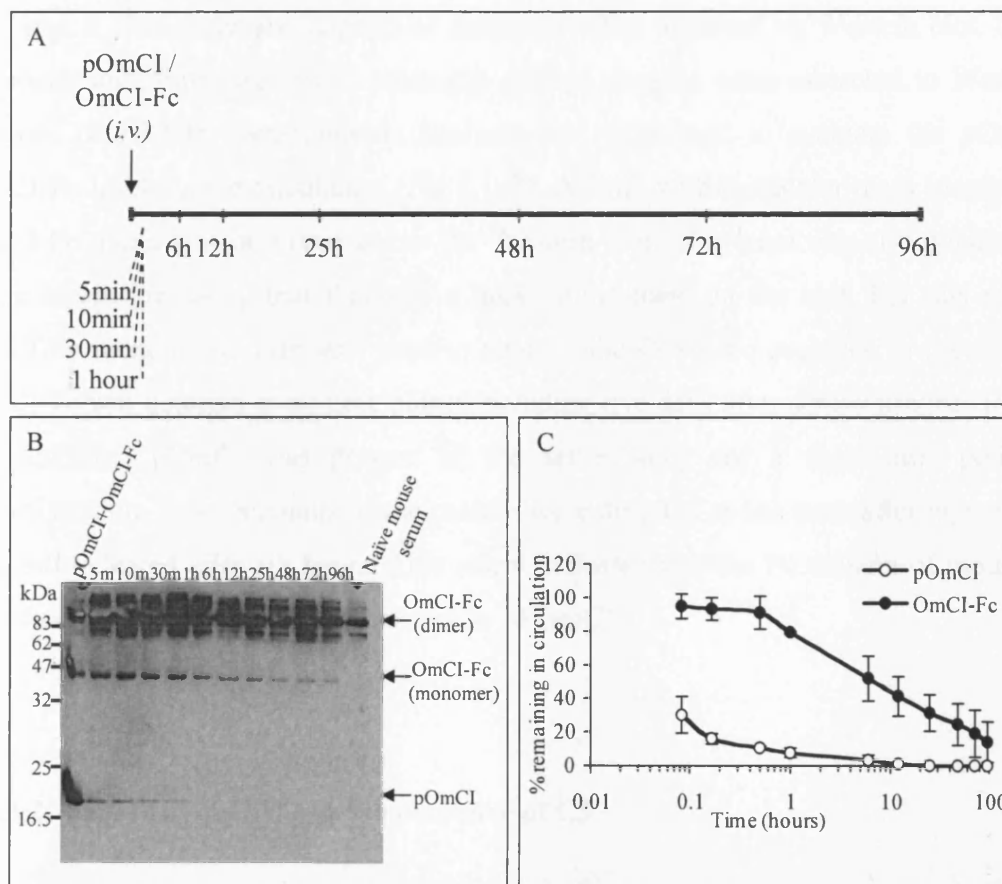


Fig.7.1 Clearance of OmCI-Fc and pOmCI in the absence of C5. A. Schematic representation of the experimental protocol. C5 deficient mice were given a mixture of 150 μ g pOmCI and 75 μ g OmCI-Fc *iv*. Plasma was collected at specific times post administration. B. Western blot analysis of pOmCI and OmCI-Fc illustrating clearance from the circulation. Plasma samples (1 μ l) from the experimental animals along with serum from a naive mouse and a mixture of purified pOmCI and OmCI-Fc were subjected to SDS-PAGE on a 15% gel. The proteins were transferred to a nitrocellulose membrane and detected with rabbit anti-OmCI polyclonal antibody. Arrows indicate the position of pOmCI, OmCI-Fc monomer and dimer. A background band (probably mouse Ig) with molecular weight similar to the mass of OmCI-Fc was present in the plasma. For this reason, the OmCI-Fc monomer (visible when the protein is denatured by SDS) was used as an indication of OmCI-Fc presence in the serum. The blot is representative of three animals. C. Densitometry analysis of western blot. Protein levels were evaluated by densitometric analysis of scanned autoradiographs using ImageJ software. The results are representative from three animals and are presented as percentage of proteins injected into the animals.

Fc fusion proteins are generally expressed as disulphide-linked dimers. However nondisulfide-linked dimers can also be formed [409] and due to the non-covalent nature of the bond it dissociates and appears as monomer when analysed by Western blot. OmCI-Fc monomer and dimer were seen when the plasma samples were subjected to Western blot analysis (Fig.7.1B). Densitometric analysis was performed to evaluate the pOmCI and OmCI-Fc levels in the circulation (Fig.7.1 C). A band with molecular mass identical to the OmCI-Fc dimer was observed across the Western blot. This band was also apparent in the naïve serum indicating that this was a background band on the blot. For this reason the OmCI-Fc monomeric form was used to analyse the OmCI-Fc presence in the circulation. OmCI-Fc was detected at all time points including five days after administration. In contrast to OmCI-Fc, pOmCI was present in the serum only for a short time period after administration. Trace amounts of the protein were detected at one hour after injection and it was fully cleared after six hours. This result indicated that the Fc domain of mouse IgG2a significantly decreased the elimination rate of OmCI.

7.1.1.2. Half-life OmCI-Fc in the presence of C5

Small molecules such as pOmCI are cleared by the kidneys and excreted in the urine. Higher molecular weight molecules, such as OmCI-Fc are cleared through the kidneys more slowly and liver clearance takes over as the molecular weight increases.

To measure the half-life, an important pharmacokinetic parameter, of OmCI-Fc and compare it to pOmCI, these proteins were injected into C57Bl/6 mice *iv*. The animals were divided into two groups (n=5) and received 500µg (6µMols) of OmCI-Fc or 200µg (12µMols) pOmCI intravenously. The presence of two OmCI molecules per fusion protein was taken into account when calculating the OmCI concentration in µMols. Blood samples were collected at various time points and plasma levels of OmCI-Fc and pOmCI quantified by ELISA (Chapter 2, section 2.4.6 and 2.8.4). The protein concentration was expressed as a percentage of initial dose injected and was plotted against time in hours (Fig.7.2).

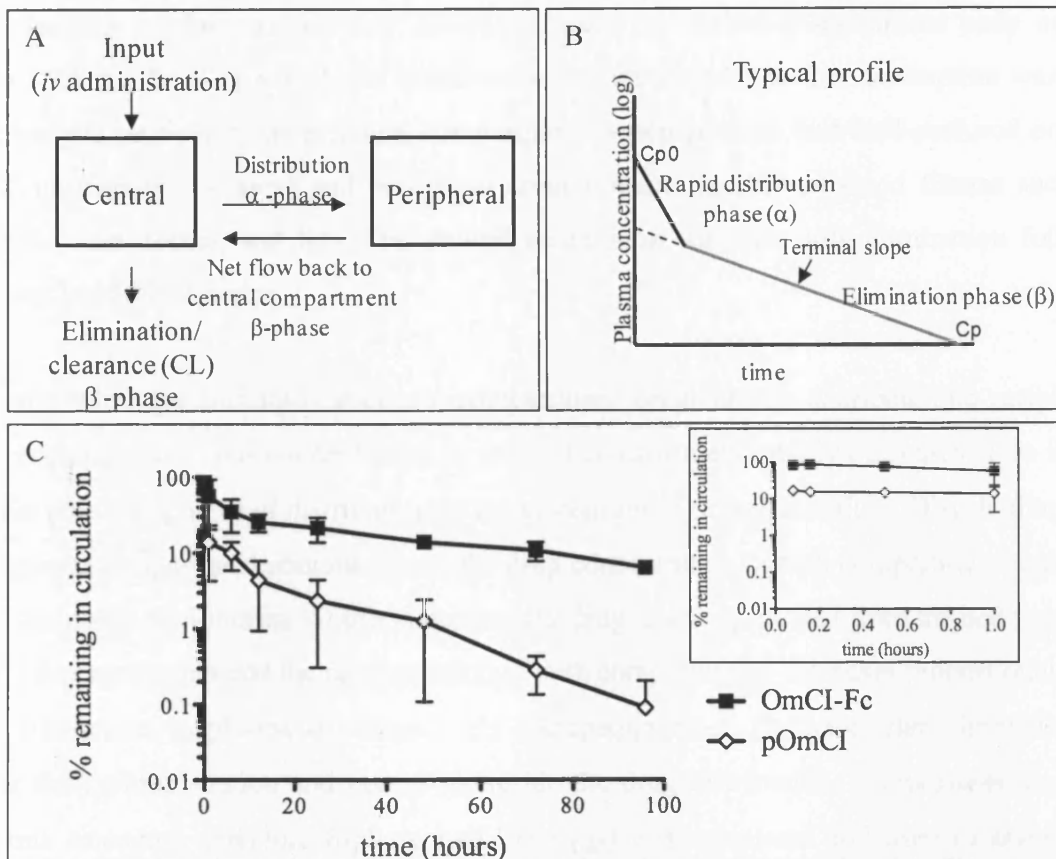


Fig.7.2 *In vivo* half-life of OmCI-Fc and pOmCI in C5-sufficient mice. A. Schematic diagram of the two-compartment model. The proteins enter the central compartment where they reach equilibrium before equilibrating with the peripheral compartment. B. Graph showing typical profile of the two-compartment model with plasma concentration plotted against time. The model is characterised by a rapid distribution (α -) phase followed by an elimination (β -) phase. The extrapolation of the elimination line back to the y axis, gives CP0, a theoretical point representing the concentration that would have existed at the start if the dose had been instantly distributed. The time needed for the concentration to drop by 50% can be calculated from this new straight line and the terminal slope; this is the elimination half life. Likewise, a similar procedure could be performed on the α phase: the distribution half life. C. β -phase (elimination) half-life of OmCI-Fc and pOmCI. Groups of five mice were injected *iv* with pOmCI or OmCI-Fc. The concentration of the OmCI proteins in mouse plasma was measured by ELISA. The log of the proteins remaining in the circulation was expressed as a percent of the injected dose against time (hours after injection). The inset shows percentage pOmCI and OmCI-Fc remaining in the circulation one hour after injection.

The half-life of the reagents was calculated based on the two-compartment body model (Fig.7.2A and B). The model was based on two assumptions. The first assumption was that the body is represented as a central compartment (vascular space and well-perfused organs such as liver and kidney) and peripheral compartments (poorly perfused tissues such as muscle, lean tissues, and fat). The second assumption was that drug elimination follows linear, first order kinetics.

Upon *iv* administration into the central compartment, drugs rapidly distribute into peripheral compartments and their concentration in the first compartment rapidly decreases. This is the initial phase (α -phase) of distribution of the protein into extracellular fluid. Distribution into peripheral compartment continues until the drug concentration in both compartments reaches and maintains equilibrium. At the same time the drug is slowly cleared from the body via the central compartment and the concentration in both compartments decreases proportionally as the elimination in plasma continues. This elimination phase (β -phase) starts immediately after drug administration and occurs alongside the drug distribution. It represents the true plasma clearance, therefore β -phase half-life ($t_{1/2\beta}$) was calculated and used to assess the clearance of OmCI-Fc and pOmCI. The half-life was determined using the terminal slope of the elimination (β -) phase using the following equations:

Integrated first-order rate law:

$$\ln[C_p] = -kt + \ln [C_{p0}] \text{ or } C_p = C_{p0}e^{-kt}$$

$$\ln [C_{p0}/2] = \ln C_{p0} - k \times t_{1/2}$$

$$\ln (C_{p0}/(2 \times C_{p0})) = -k \times t_{1/2}$$

$$\ln 2 = k \times t_{1/2}$$

$$t_{1/2} = \ln 2 / k$$

$$t_{1/2} = 0.693 / k$$

$t_{1/2}$ –half-time of elimination, the time taken for the plasma concentration to fall to half to its original value.

C_{p0} - start concentration

$C_{p0}/2$ -concentration at time when half of C_{p0} is cleared from circulation

k -the slope of the elimination phase

The maximum plasma concentration of pOmCI and OmCI-Fc was observed at 5 minutes (first bleeding time point) after *iv* administration and remained almost unchanged over the

next 10 minutes (Fig.7.2.C). Clearance of OmCI-Fc from the plasma was significantly slower than that of the pOmCI ($P=0.001$). The half-life of OmCI-Fc was 96 hours whereas pOmCI was cleared much more rapidly and demonstrated a half-life of 38 hours, presumably due to its complex with C5 [176].

7.1.2. *In vivo* inhibitory activity

To assess OmCI-Fc functional activity *in vivo*, the fusion protein was given to mice and its impact on systemic complement activity was studied. A comparison with pOmCI was made to investigate how the fusion to Fc of antibody modified the complement inhibitory capacity of the reagent *in vivo*. The combine effect of pOmCI and OmCI-Fc on complement was also studied to establish a strategy for effective complement inhibition.

7.1.2.1. pOmCI and OmCI-Fc- individual effect on complement inhibition

To assess the ability of OmCI-Fc to block C5 *in vivo* and to investigate whether the prolonged half-life translated in to extended complement inhibition, OmCI-Fc (300 μ g) and pOmCI (200 μ g) were injected into C57bl/6 ($n=5$ in each group) mice through the tail vein. Higher dose of OmCI-Fc was used because the OmCI moieties contribute only one third of the molecular mass of the protein. The animals were tail bled before being given any reagents, and also at different time points post-injection. A schematic representation of the experimental plan is shown in Fig.7.3.A. Complement activity was assessed by haemolysis assay and quantified by the amount of the test serum necessary to kill 50% of antibody-sensitised rabbit erythrocytes (CH50). The serum complement activity was expressed as percent of the activity prior to pOmCI or OmCI-Fc administration (Fig.7.3B).

A single injection of pOmCI and OmCI-Fc was able to completely block the complement system at the first hour after injection when no complement activity was detected. An increase in the serum haemolytic activity (66%) was measured over the next 12 hours in the mice injected with pOmCI while the complement activity remained very low (15%) in mice injected with OmCI-Fc. The pOmCI treated animals had restored their haemolytic activity

48 hours after the drug administration while only 57% activity was measured at the same time point in OmCI-Fc injected mice.

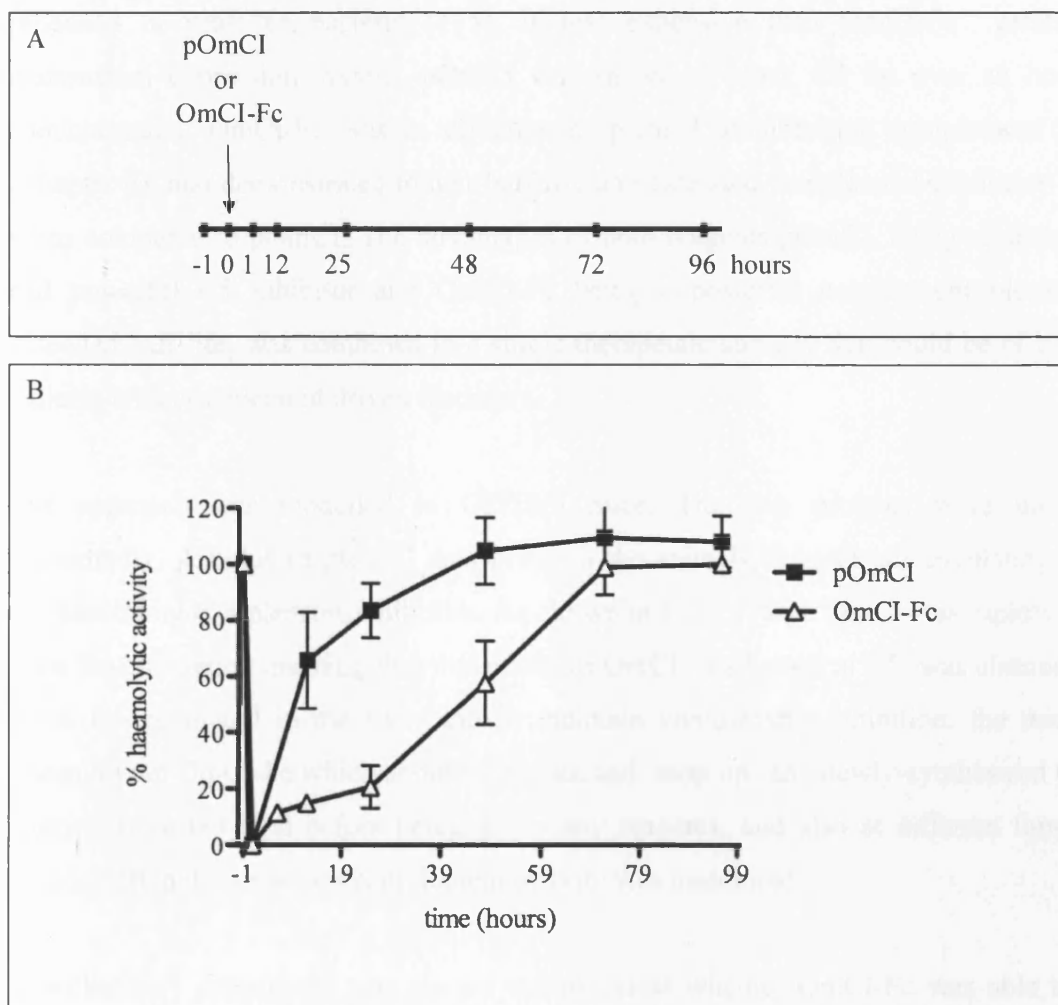


Fig.7.3 Effect of OmCI-Fc and pOmCI on complement haemolytic activity *in vivo*. A. Schematic representation of the experimental protocol. C57Bl6 mice were injected with pOmCI 200 μ g or OmCI-Fc (300 μ g) through the tail vein. Blood was collected at specific time point post administration (indicated with tick marks). A pre-injection serum sample (time -1) was also harvested. B. Serum haemolytic activity. CH50 was determined by haemolysis assay. The results are expressed as percent complement activity compared with the activity pre-administration. Results are means of determinations from five animals, and vertical bars represent standard deviations.

7.1.2.2. pOmCI and OmCI-Fc-cooperative effect on complement inhibition

To establish an effective and potentially less expensive strategy to therapeutically inhibit complement, the cooperative effect of pOmCI and OmCI-Fc was studied *in vivo*. pOmCI, produced in yeast or bacteria [175], is less expensive than OmCI-Fc produced in mammalian expression system. pOmCI was shown to block C5 for over an hour after administration. OmCI-Fc was as effective as pOmCI at inhibiting complement *in vitro* (Chapter 6), and demonstrated longer half-life and extended complement inhibitory activity when compared to pOmCI. The advantages of both reagents pOmCI, being an inexpensive and powerful C5 inhibitor and OmCI-Fc being a powerful complement blocker with extended half-life, was combined in a single therapeutic strategy that could be of benefit to patients with complement driven disorders.

The approach was modelled in C57Bl/6 mice. The two proteins were injected *iv* sequentially. A bolus of pOmCI was given to the animals to block all circulating C5 and provide initial complement inhibition. As shown in Fig.7.1, free OmCI was rapidly cleared from the circulation meaning that the excess of OmCI (not bound to C5) was eliminated. To block C5 generated in the liver and to maintain complement inhibition, the mice were injected with OmCI-Fc which should circulate and 'mop up' any newly-synthesised C5. The animals were tail bled before being given any reagents, and also at different time points post-injection. C5 or serum complement activity was monitored.

A preliminary experiment was carried out to assess whether OmCI-Fc was able to block complement *in vivo* in a dose-dependent manner and to establish the dose range of OmCI-Fc required for effective complement inhibition. Two mice were injected with OmCI (200 μ g) to achieve rapid systemic C5 inhibition [176] followed by *iv* injection of OmCI-Fc at concentrations of 50 μ g or 150 μ g one hour later to determine the optimal dose sufficient to maintain good complement inhibition. A schematic representation of the experimental plan is shown in Fig.7.4.A.

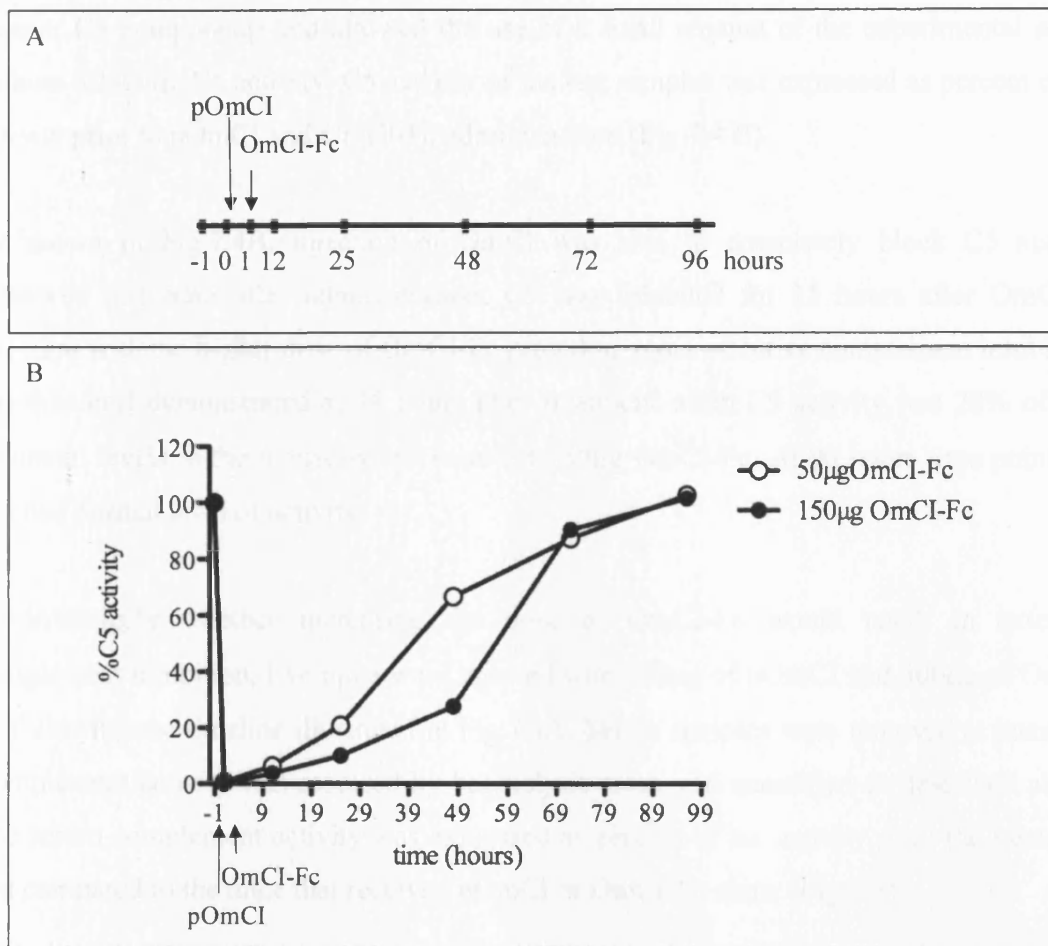


Fig.7.4 Effect of pOmCI and OmCI-Fc on C5 activity in mice. A. Schematic representation of the experimental protocol. C57Bl/6 mice were given 200µg OmCI intravenously at time 0. One hour later the mice were injected with 50µg (n=1) or 150µg (n=1) OmCI-Fc through the tail vein. Blood was collected at specific time point post administration (indicated with tick marks). Test serum sample at 1h was harvested immediately before OmCI-Fc administration. A pre-injection serum sample (time 0) was also harvested. B. C5 activity was determined by haemolysis assay. Haemolytic activity in the test mouse serum was assessed using antibody sensitised rabbit erythrocytes in presence of C5-/-mouse serum. Results are expressed as percentage C5 activity compared with pre-injection levels.

C5 activity was assessed by haemolysis assay in presence of 8% C5 deficient mouse serum and quantified by the amount of the test serum necessary to kill 50% of antibody-sensitised rabbit erythrocytes (CH50). The C5-deficient serum provided a source of complement

(except C5 component) and allowed the use of a small amount of the experimental serum without affecting C5 activity. C5 activity of the test samples was expressed as percent of C5 activity prior to pOmCI and OmCI-Fc administration (Fig.7.4 B).

As shown in Fig.7.4B, injection of OmCI was able to completely block C5 activity measured one hour after administration. C5 was inhibited for 11 hours after OmCI-Fc injection with the higher dose of OmCI-Fc providing more effective complement inhibition; this was best demonstrated at 48 hours after treatment when C5 activity was 28% of pre-treatment levels in the mouse which received 150 μ g OmCI-Fc. At 96 hours time point, C5 reached normal level of activity.

To investigate whether increasing the dose of OmCI-Fc would result in extended complement inhibition, five mice were injected with 200 μ g of pOmCI and 300 μ g of OmCI-Fc following the timeline illustrated in Fig.7.4A. Serum samples were removed at intervals. Complement activity was assessed by haemolysis assay and quantified as described above. The serum complement activity was expressed as percent of the activity prior the treatment and compared to the mice that received pOmCI or OmCI-Fc alone (Fig.7.5).

The mice that received the combined pOmCI and OmCI-Fc treatment showed complete complement inhibition at the first hour after OmCI injection. Very low complement activity (<27%) was detected over the first 24 hours after OmCI-Fc was given to the mice. As seen in Fig. 7.5 there was a dramatic reduction of complement function in these animals compared to the mice that received pOmCI alone. However no difference was observed between the groups that received pOmCI-OmCI-Fc and OmCI-Fc alone over the first 48 hours of the experiment.

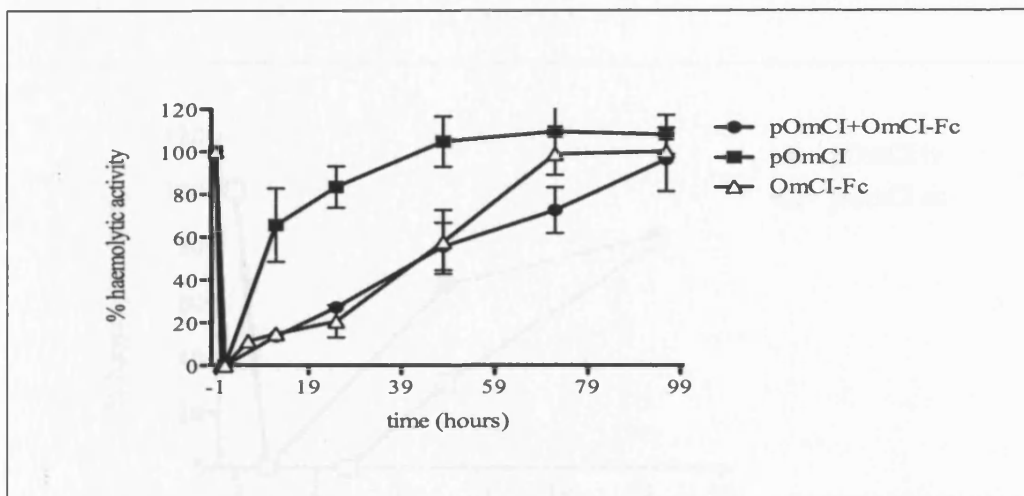


Fig.7.5 Effect of OmCI treatment on complement haemolytic activity *in vivo*. Two groups of mice were injected intravenously with 200 μ g of pOmCI (black squares) or 300 μ g OmC-Fc (open triangles) at time 0. A third group of animals received a combined treatment with pOmCI and OmCI-Fc (black circles) according to schematic illustrated in fig. 7.4. CH50 was determined by haemolysis assay. The results are expressed as percent complement activity compared with activity pre-administration. Results are means of determinations from five animals, and vertical bars represent standard deviations.

7.1.2.3. Routes of administration: subcutaneous versus intravenous

The biological activity of a protein drug and duration of its effect may depend on the route of administration. It is important that during the preclinical study, several routes of administration are tested.

To explore whether the route of administration affected inhibitory activity, pOmCI and OmCI-Fc were injected *sc* in C57Bl/6 mice (two mice in each group). The animals were tail bled before reagent administration and then at different time points post-injection. Complement activity was quantified by CH50, expressed as percent lysis obtained before treatment as described before and compared to those values obtained from the previous experiment when the reagents were given *iv*. As seen in Fig.7.6A, single *sc* or *iv* injection of pOmCI provided complete complement inhibition one hour post administration.

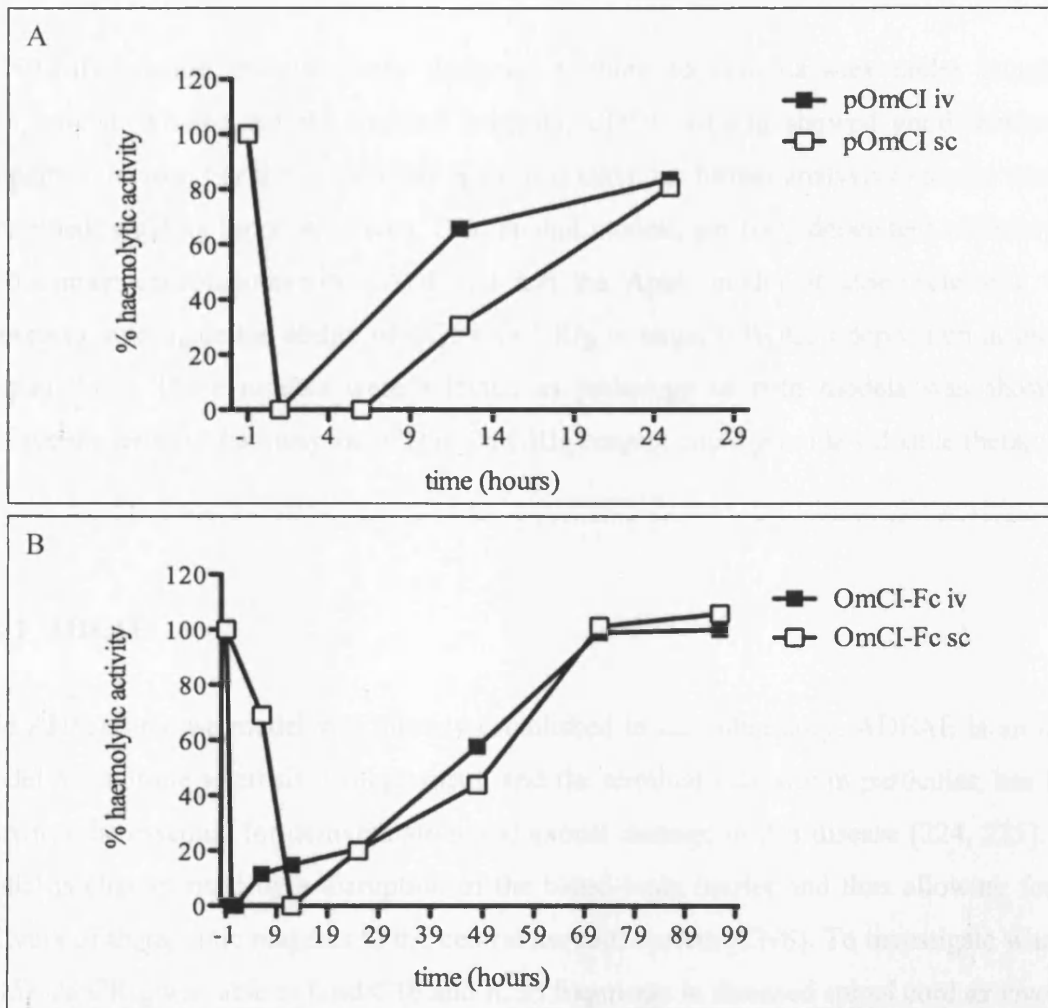


Fig.7.6 Comparison of *sc* and *iv* routes of administration of pOmCI and OmCI-Fc. Mice (two mice in each group) were given with OmCI reagents *sc*. Inhibition data are plotted alongside those when the reagents were administered *iv* (obtained from previous experiment, fig.7.5). CH50 was determined by haemolysis assay. The results are expressed as percent complement activity compared with the pre-administration levels.

However inhibition lasted longer when the reagent was administered *sc*. No measurement was taken at 6 hours post *iv* injection of pOmCI (Fig.7.6 A). Serum complement 12 hours after *sc* administration of pOmCI showed lower haemolytic activity than when pOmCI was given *iv*. The mice that received OmCI-Fc *iv* showed no detectable complement activity at 1 hour after the drug administration while the same effect was achieved 12 hours after *sc* injection of this reagent.

7.2. Targeting of CD59-CRIg *in vivo* and *ex vivo*

CD59-CRIg fusion proteins were designed to bind to cell surfaces under attack by complement. Among the six targeted reagents, CD59-2a-CRIg showed good therapeutic properties *in vitro*. For this reason this agent was taken for further analysis to assess whether it retained targeting function *in vivo*. Two animal models, antibody dependent experimental autoimmune encephalomyelitis (ADEAE) and the ApoE model of atherosclerosis, were chosen to investigate the ability of CD59-2a-CRIg to target C3b/iC3b deposition at the site of pathology. These models were selected as pathology in both models was shown to involve the terminal pathway and CD59-2a-CRIg reagent could provide valuable therapy.

7.2.1. ADEAE

The ADEAE mouse model was already established in our laboratory. ADEAE is an acute model of multiple sclerosis. Complement, and the terminal pathway in particular, has been shown to be essential for demyelination and axonal damage in this disease [224, 225]. The model is characterised by a disruption of the blood-brain barrier and thus allowing for the delivery of therapeutic reagents to the central nervous system (CNS). To investigate whether CD59-2a-CRIg was able to bind C3b and iC3b fragments in diseased spinal cord *ex vivo* and *in vivo*, ADEAE was induced in six CD59a deficient male mice as described (Chapter 2, section 2.8.6). A schematic of disease induction is illustrated in Fig 7.7. CD59a^{-/-} animals were chosen in order that anti-CD59 antibody could be used for detection of CD59-2a-CRIg. Briefly, mice were immunised with emulsion containing rMOG in CFA supplemented with *Mycobacterium tuberculosis*. Before onset of disease (day 8), mice received anti-mouse MOG mAb (clone Z12, mouse IgG2a with high complement fixing capacity) [223]. The mice were monitored daily for development of disease symptoms which were scored as follows: 0, no disease; 2, hind limb weakness; 3, hind limb paralysis; 4, moribund and 5, dead. Disease signs were first apparent on day 10 and 100% of mice developed clinical disease. When the disease severity reached a clinical score of 2 (on day 11), four of the mice were injected with 100µg CD59-2a-CRIg and the remaining two received PBS *iv*. The animals that received CD59-2a-CRIg were randomly divided in two groups, which were

sacrificed at one or three hours after the drug administration. Spinal cord was harvested and frozen sections prepared.

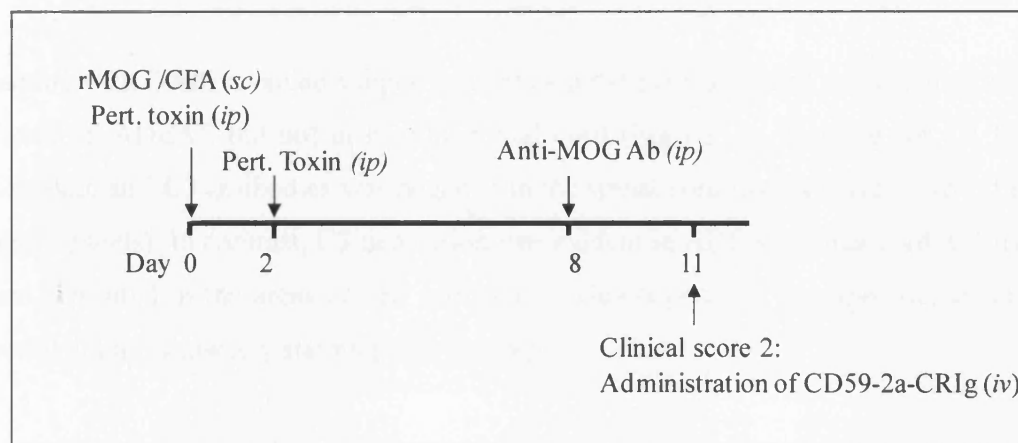


Fig.7.7 Induction of ADEAE. On day 0, mice (7 weeks old males) were immunised with 200µl of 1:1 emulsion of rMOG (50µg) and CFA containing 2.5mg/ml *Mycobacterium tuberculosis* H37 Ra. Mice also received 200ng of pertussis toxin *ip* in PBS on days 0 and 2. Anti-MOG antibody (Z12) was injected *ip* at day 8. The animals were weighed and monitored daily for signs of clinical disease. 0, no clinical signs; 1, tail atony; 2, hind-limb weakness; 3, hind-limb paralysis; 4, moribund; 5, dead. Animals that had a clinical score of 2 (day 11) at monitoring were injected with 200µl of 100µg of CD59-2a-CRIg or PBS intravenously. The mice were sacrificed while under terminal anaesthesia and spinal cord was harvested one or three hours after CD59-2a-CRIg administration. The spinal cord was immediately frozen in OCT on dry ice.

7.2.1.1. Identification of ligands for CRIg, C3b and iC3b, in diseased tissue

Deposition of C3b and iC3b in spinal cord was assessed in ADEAE and in naïve mice by immunohistochemical analysis. Two different rat anti-mouse C3 monoclonal antibodies, clones 11H9 and 2/11, were used to identify the site of complement activation (Fig.7.8). Initially, anti-C3 mAb clone 11H9 was used to detect C3 fragment deposition. It specifically recognises C3 and its break down products C3b, iC3b and C3d. To prove that the staining observed with 11H9 was due to the presence of the ligands for CRIg, C3b and/or iC3b, and

not the further cleavage fragment C3d, anti-C3 mAb clone 2/11 was also used. This antibody does not bind C3d. Nuclei were visualised with the DNA counterstain DAPI (diamidino-2-phenylindole).

Staining with DAPI revealed subpial (underneath the pia mater) and perivascular infiltration of cells in ADEAE but not in healthy spinal cord (Fig.7.8 A). Staining for C3 fragments using both anti-C3 antibodies was negative in the spinal cord from a naïve mouse (Fig.7.8 B, bottom panels). In contrast, C3 deposition was evident in ADEAE spinal cord. C3 fragments were deposited in the areas of cell infiltration. This deposition was specific, as an isotype control did not show any staining (not shown).

7.2.1.2. *Ex vivo* and *in vivo* targeting of reagents to demyelinating lesion

Having demonstrated deposition of CRIg ligands, C3b and iC3b, the ability of CD59-2a-CRIg to target the site of pathology was investigated *ex vivo*. Spinal cord cryosections from the mice with ADEAE and treated with PBS were incubated with CD59-2a-CRIg/488. Nuclei were stained with DAPI.

As seen from the merged images in Fig.7.8 C, CD59-2a-CRIg was clearly localised in areas of cell infiltration. This region correlated with C3b and iC3b deposition illustrated in Fig. 7.8 B. No CD59-2a-CRIg staining was detected in spinal cord from a naïve mouse indicating that CD59-2a-CRIg targeted specifically to C3 activation fragments.

To assess the capacity of CD59-2a-CRIg to target complement activation *in vivo*, spinal cord sections from ADEAE mice injected with CD59-2a-CRIg and from naïve mice were probed with anti-CD59 mAb. No CD59-2a-CRIg was detected in the spinal cord at any of the time-points (data not shown). The directly conjugated CD59-2a-CRIg/488 reagent was not tested *in vivo*.

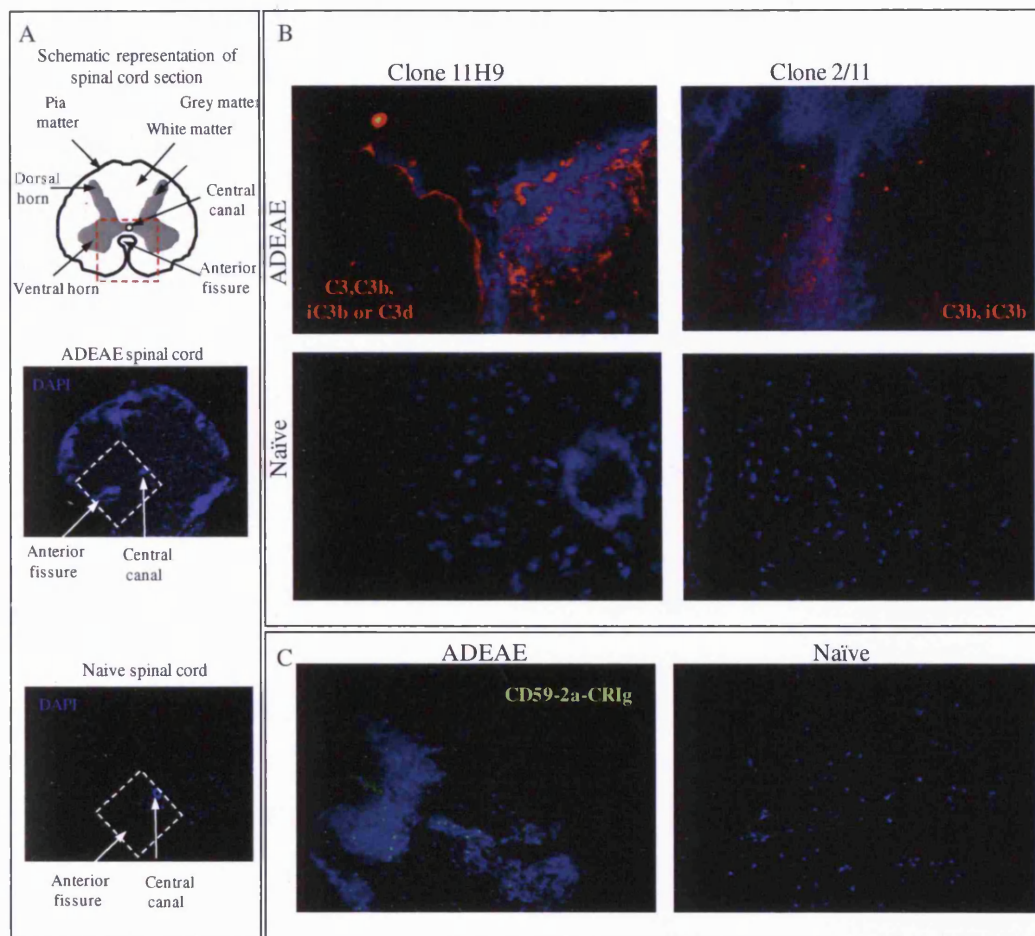


Fig.7.8. Immunohistochemical analysis of spinal cord from mouse with ADEAE and naïve mouse and *ex vivo* targeting of CD59-2a-CRIg. ADEAE was induced in CD59^{-/-} mice. Spinal cord was isolated when the disease reached clinical score of 2. Schematic representation and DAPI staining (ADEAE and naïve spinal cord section) with the area used for analysis indicated in dotted square (A). Representative lumbar cryosections were analysed for deposition of C3 fragments (B) and CD59-2a-CRIg localisation (C). C3b and iC3b deposition was assessed using two rat anti-mouse C3 mAbs, clone 11H9 binds C3 and its breakdown fragments and clone 2/11 interacts with C3b and iC3b. CD59-2a-CRIg *ex vivo* targeting was assessed using CD59-2a-CRIg conjugated with Ana Tag Hilyte fluor 488. Sections were counterstained with DAPI (blue) to reveal cell nuclei and provide a means of imaging the negative sections. Staining is shown as merged images. Images are taken x40 objective and are representative of n=2.

7.2.2. Atherosclerosis

The ApoE mouse model of atherosclerosis was already established in our laboratory. To investigate whether CD59-2a-CRIg was capable of targeting C3 activation in atherosclerotic plaques, ApoE^{-/-}/CD59^{-/-} double knockout mice on a high-fat diet received 200µg of CD59-2a-CRIg (three mice) or PBS (two mice) intravenously. The body weight was measured and the mice were sacrificed 30 minutes or 1 hour post- administration. Serum sample and brachiocephalic artery were harvested. Feeding a high fat, cholesterol-enriched diet for 8 weeks to male ApoE^{-/-} mice results in innominate/brachiocephalic plaque rupture with mural thrombosis and intra-plaque haemorrhage [410]. The innominate/ brachiocephalic trunk is a small segment of artery situated between the ascending aortic arch and the bifurcation of the right subclavian artery from the right carotid artery (Fig.7.9A).

Frozen sections of brachiocephalic artery with plaques from mice injected with CD59-2a-CRIg and PBS were analysed for deposition of C3 fragments. Sections were also incubated with CD59-2a-CRIg/488 to study *ex vivo* targeting. *In vivo* targeting was assessed by staining of brachiocephalic artery sections obtained from mice injected with CD59-2a-CRIg with anti-CD59 mAb.

7.2.2.1. Identification of ligands for CRIg, C3b and iC3b, in diseased tissue

Deposition of C3 activation products in atherosclerotic plaques of ApoE^{-/-}/CD59a^{-/-} mice has already been demonstrated [242]. To confirm the presence of CRIg ligands, C3b and iC3b, in atherosclerotic brachiocephalic arteries in this experiment, frozen sections were stained with anti-C3 mAb clone 2/11.

The immunohistochemical analysis revealed that C3b or/and iC3b was deposited in the atherosclerotic plaques (Fig 7.9B). The control staining with an irrelevant isotype-matched monoclonal rat antibody instead of the specific antibody was negative. Comparison with a naïve (non-diseased) vessel was not appropriate as no plaque would be formed for analysis.

7.2.2.2. *Ex vivo* targeting of reagents to atherosclerotic plaques

To investigate whether CD59-2a-CRIg was able to bind to the C3b and iC3b detected in the tissue, brachiocephalic sections were incubated with CD59-2a-CRIg/488 *ex vivo*. The analysis revealed that the fusion protein bound to the tissue section within the plaque area (Fig.7.9 C). Moreover, the CD59-2a-CRIg staining pattern resembled that obtained with the anti-C3 mAb. This suggests that CD59-2a-CRIg interacts with C3b and iC3b deposited in the disease tissue.

To investigate whether CD59-2a-CRIg binding co-localised with the C3b and iC3b fragments, cryosections were double-stained. The brachiocephalic artery was incubated with anti-C3 mAb and with CD59-2a-CRIg/488 simultaneously. The anti-C3 antibody bound the C3 fragments deposited in the plaques, but CD59-2a-CRIg protein could not be detected. It is possible that CRIg and the antibody competed for the same C3b/iC3b epitope, thus CD59-2a-CRIg was not able to interact with iC3b and C3b in presence of the anti-C3 antibody.

7.2.2.3. Plasma levels of CD59-2a-CRIg in treated atherosclerotic mice and *in vivo* targeting of reagent to atherosclerotic plaques

To study whether CD59-2a-CRIg could target C3 activation *in vivo*, mice were injected with the CRIg reagent or PBS and were sacrificed 30 minutes or 1 hour post administration. The presence of CD59-2a-CRIg in the circulation of experimental animals at the time of tissue harvest was assessed by ELISA. A dilution series of the serum samples collected from the experimental mice was prepared and incubated on ELISA plates coated with mouse anti-mouse CD59 mAb. The CD59-2a-CRIg was detected with a non-competitive rat anti-mouse CD59 mAb. The serum concentration of CD59-2a-CRIg was calculated from a standard curve generated using pure CD59-2a-CRIg protein. As seen in Fig.7.10, CD59-2a-CRIg was present in the circulation at the two time points chosen in this experiment (30 minutes and 1 hour after administration). The serum concentration of the reagent was between 28 and 78µg/ml (Fig.7.10). No CD59-2a-CRIg was detected in the mouse injected with PBS.

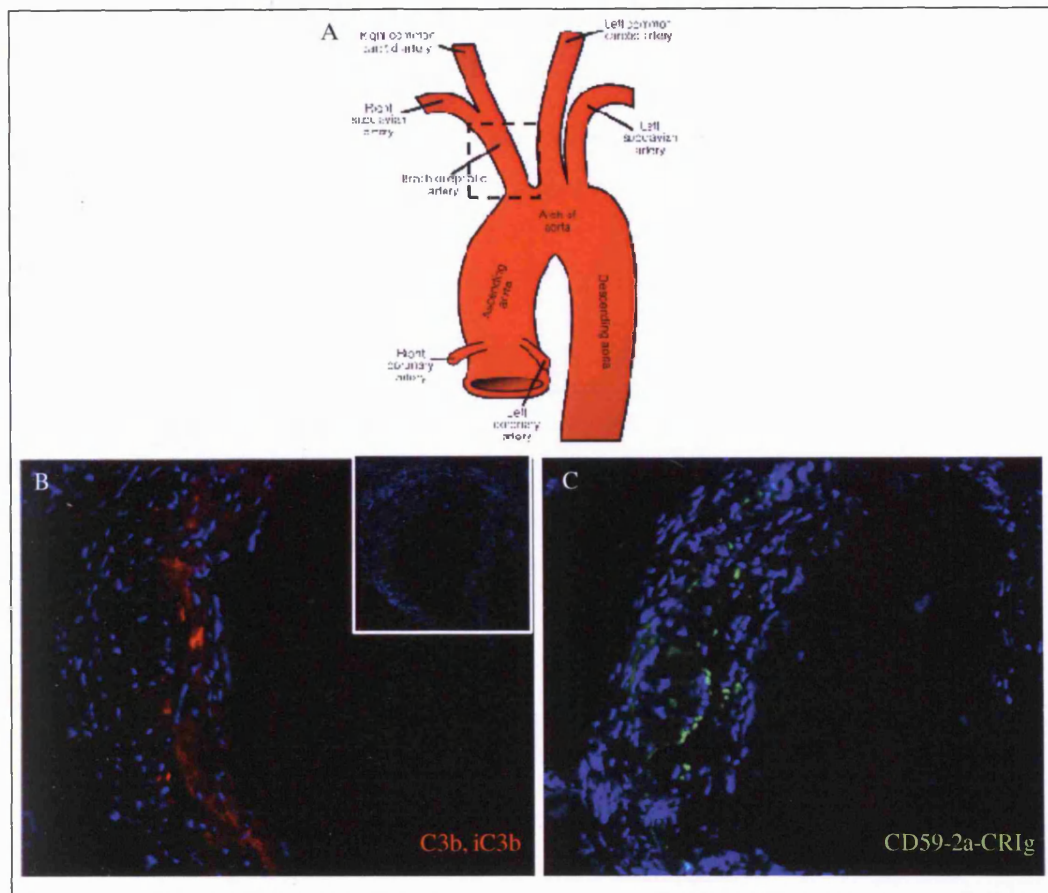


Fig.7.9 Deposition of C3b and iC3b and localisation of CD59-2a-CRIg in atherosclerotic brachiocephalic arteries *ex vivo*. The brachiocephalic artery, the third branch of the aorta and the first branch from the arch of the aorta, is indicated with a dotted square on the diagram of the proximal aorta (A) from diseased ApoE^{-/-}/CD59a^{-/-} mice (A). Frozen sections were stained with rat anti-mouse C3 mAb specific for C3b and iC3b (red) (B) and with CD59-2a-CRIg/488 (green) (C). Nuclei were stained with DAPI (blue). Inset image shows isotype antibody (rat IgG1) control staining. Merged images are presented.

To assess whether CD59-2a-CRIg reagent was able to target C3b/iC3b fragments, brachiocephalic artery sections from mice injected with this reagent were incubated with rat anti-CD59 mAb followed by incubation with anti-rat IgG conjugated with alexa 488. CD59-2a-CRIg could not be localised and no immunoreactivity was observed in any of the time-points (data not shown).

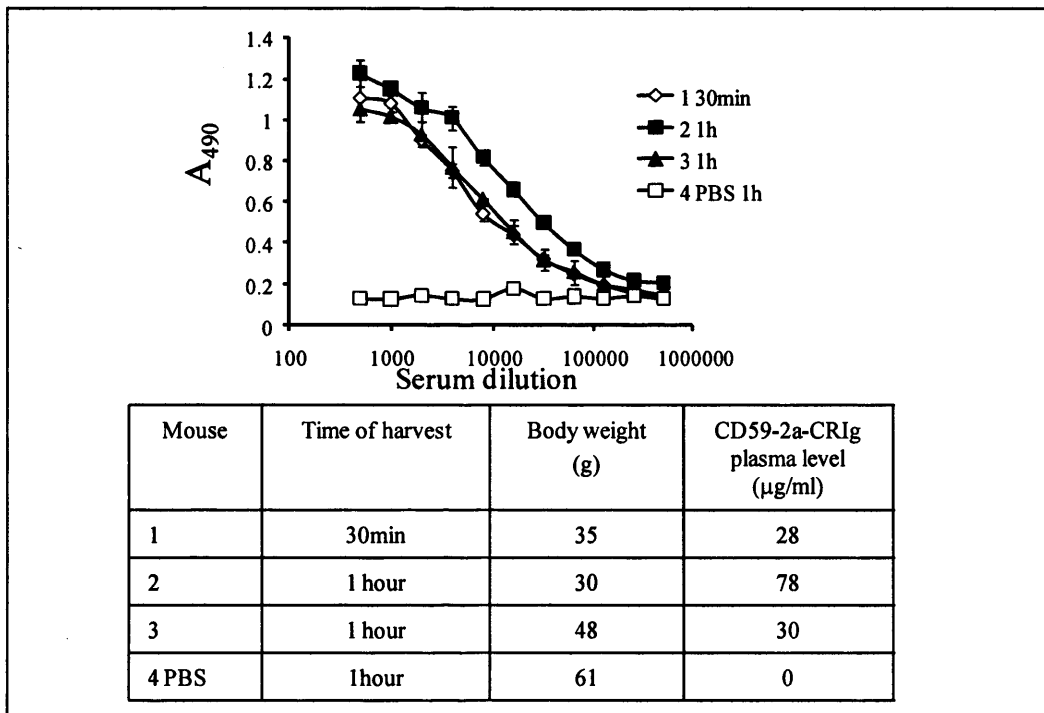


Fig.7.10 Identification of CD59-2a-CRIg in plasma of mice with atherosclerosis. Atherosclerosis was induced in CD59^{-/-}-ApoE^{-/-} mice. Animals 1, 2 and 3 received CD59-2a-CRIg and mouse 4 was injected with PBS. Body weight was measured and mouse 1 was sacrificed 30 minutes after the administration and mice 2, 3 and 4 were sacrificed one hour after injection. Serum samples were collected and subjected to ELISA. Dilution series (1:2) were prepared from the test serum and added to 96-well plate coated with mouse anti-mouse CD59 mAb. The assay was developed with rat mCD59a-7. Serum CD59-2a-CRIg concentration was determined from a standard curve. The calculated CD59-2a-CRIg levels along with the body weights are listed.

7.3 Discussion

Understanding the behaviour of drugs in a biological system is of high importance in treatment of disease. Pharmacokinetic parameters for protein drugs include measurement of circulatory half-lives, volumes of distribution, clearance rates and total bioavailability. One of these parameters (the *in vivo* half-life) was characterised for OmCI-Fc.

Clearance of protein drugs from the systemic circulation begins with passage through the capillary endothelia. Drugs are eliminated from the body through proteolytic, renal, hepatic, and receptor-mediated mechanisms. Small proteins (<30kDa) such as pOmCI and peptides are efficiently filtered by the glomerulus and then excreted. The liver also plays an important role in the removal of proteins from the systemic circulation. There are several strategies to reduce the clearance rates of proteins from peripheral blood circulation, such as covalent attachment of polyethylene glycol (PEG, PEGylation) [411], fusion to serum albumin or serum albumin binding receptor or fusion to the Fc portion of antibody.

Attachment of PEG increases the molecular weight of the protein and hence prolongs its circulating life. PEG is hydrophilic long chain molecule capable of forming a protective shield around the therapeutic reagent in aqueous solution, thus diminishing the immunogenicity of the drug [412]. However, the use of PEGylation is limited by the number and distribution of polyethylene glycol attachment sites such as lysyl ϵ -amino groups (epsilon amino groups of lysine residues) and the high cost of PEGylation agents. PEGylation can also mask the effector function of the drug [413].

An alternative method to extend circulating half-life of a drug is fusion of the therapeutic to a protein with a long half-life or to a receptor which binds such a protein. Serum albumin with its half-life of up to 19 hours (in human blood) and its abundance is a suitable candidate as a carrier protein. Fusion of therapeutic reagents to serum albumin, or serum albumin binding receptor from Streptococcal protein G, extends circulating half-life when compared to the non-fused drugs (from two to four fold increase) [309, 414-416].

Here, I extended the half-life of OmCI by fusion to the Fc of mouse IgG2a antibody. The Fc region is the part of the antibody important for the half-life and the distribution of the molecule in the body. Fc binds to receptors on cells and modulates the serum half-life of the

antibody. FcRn interacts with the Fc portion of IgG and other Fc molecules that are otherwise destined for degradation, and thereby selectively extends their half-lives in the circulation (Fig.7.11).

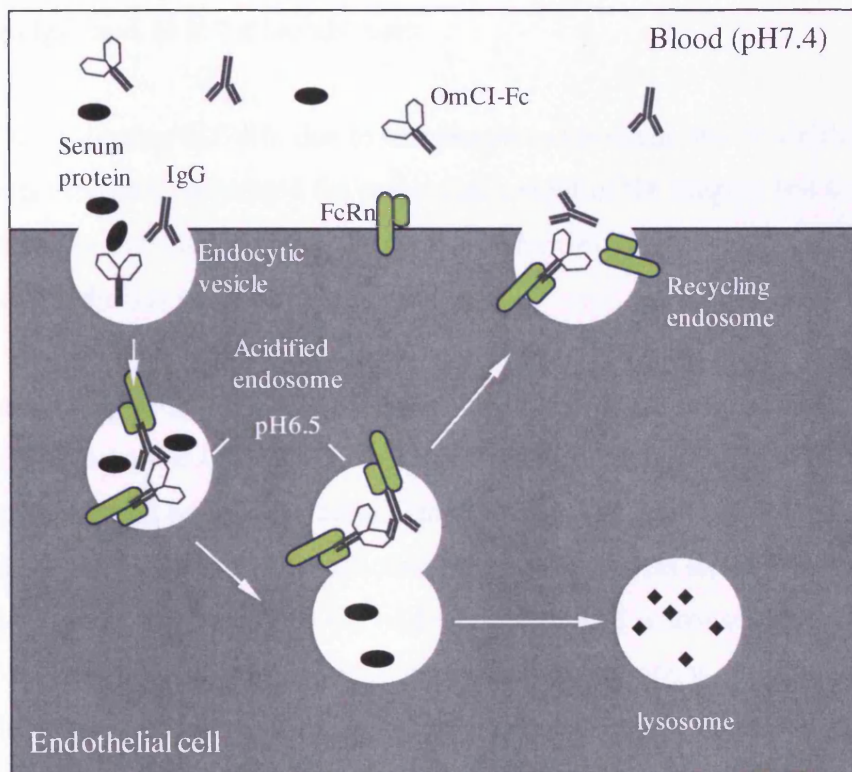


Fig. 7.11 Schematic diagram showing FcRn recycling of OmCI-Fc and IgG. Endothelial cells internalize serum OmCI-Fc and IgG, which bind to FcRn in an acidic endosomal compartment. FcRn (in green) is a heterodimer consisting of a non-classical MHC-I-related glycoprotein noncovalently bound to β 2-microglobulin. The Fc portion of OmCI-Fc and IgG bind with high affinity to FcRn at acidic pH (<6.5) but not at physiological pH (7.4). FcRn then recycles OmCI-Fc and IgG back into circulation, thus extending their serum half-life. Serum proteins without a recycling receptor are destined for lysosomal degradation. The figure is adapted from *Roopenian and Ahreeram. Nature Reviews Immunology. 2007.*

The proteins in the bloodstream enter the endothelial cells and endosomes via fluid-phase endocytosis as cells sample their environment. Fc containing molecules are able to bind FcRn expressed within the endosomes. Fc has a greater binding affinity for FcRn in the endosome (pH6.0-6.5) than at the cell surface (pH7.4) because a favourable interaction

between Fc and FcRn is induced by the protonation of certain histidines ($pK_a=6.4$) within the Fc domain at the lower pH [417, 418]. The binding to FcRn to Fc enhances the recycling of IgG back to the cell surface. This recycling mechanism decreases the amount of IgG that is degraded in the lysosomes. Dissociation of the Fc fragment from FcRn at the cell surface then releases IgG back in to the bloodstream.

In addition to increasing half-life due to the receptor-dependent rate of clearance, attaching an Fc fragment to OmCI increased the molecular weight of the reagent and thus reduced its clearance through the kidney. It is likely that the primary route of OmCI-Fc clearance (similar to antibodies) is via proteolytic catabolism.

The presence of pOmCI and OmCI-Fc was analysed in C5 deficient and C5 sufficient animals. In the absence of C5, pOmCI was rapidly cleared (within an hour) whereas, OmCI-Fc was apparent at 96 hours after administration (Fig.7.1). The half-life of OmCI-Fc and pOmCI was also determined in C5 sufficient mice. The reagents injected *iv* bind C5 and the complex circulates in the body thus the half-life determined is that of the complex, not free OmCI [176]. The plasma concentration-time profiles following *iv* administration were described by a two-compartment model with linear elimination where the drug half-life is independent of the concentration and the clearance is independent of the dose and dosing intervals. Small molecules such as pOmCI follow linear clearance (characterised by first-order kinetic). The half-life of an antibody is determined by the Fc portion. It is likely that the OmCI-Fc has a pharmacokinetic profile similar to an antibody molecule. It has been shown that many antibodies directed against cell-surface antigens exhibit non-linear (dose-dependent) pharmacokinetic behaviour whereas antibody specific to soluble antigens often exhibit linear behaviour (dose-independent) [419, 420]. OmCI-Fc binds plasma C5 and therefore it was assumed that it exhibited linear clearance because the primary route of clearance would be limited to catabolism.

Using the linear model of elimination, pOmCI had a half-life of 38 hours, while the half-life of OmCI-Fc was 96 hours, demonstrating that the fusion to Fc prolonged the half-life of OmCI/C5 complex 2.5-fold. The short-lived pOmCI would require frequent administration, while the longer circulating half-life *in vivo* of OmCI-Fc would reduce the frequency of injections to achieve comparable complement-inhibitory effects. This rapid decline in plasma concentration of pOmCI is indicative of rapid distribution of the drug into highly

perfused organs such as liver, lung, spleen and kidney. It is important to note that the ELISA used here to quantify pOmCI and OmCI-Fc in plasma did not distinguish free molecules from those in complex with C5. As described earlier, OmCI-C5 is a long-lived complex and this explains the higher half-life values obtained here compared to other Fc fusion proteins.

Having established that OmCI-Fc had a long circulating half-life, the capacity of OmCI-Fc to inhibit complement *in vivo* in mice, and the optimum dose and route of administration was investigated and compared to pOmCI. The experiments revealed that the short-lived pOmCI (200µg) had a capacity to inhibit complement for approximately an hour, while the reagent with extended half-life, OmCI-Fc (300µg) demonstrated longer lasting complement inhibitory effect *in vivo*. Based on these data, a strategy using both pOmCI and OmCI-Fc was developed to effectively inhibit complement long-term. The *iv* injection of 200µg of pOmCI was chosen to block circulating C5 and to achieve rapid systemic C5 inhibition for an hour. A preliminary experiment measuring serum C5 activity in serum from mice treated with pOmCI followed by *iv* injection of 50µg or 150µg OmCI-Fc to wipe out the newly synthesised C5, demonstrated the ability of OmCI-Fc to block complement *in vivo* in a dose dependent manner. C5 activity of 70% was measured in the mouse treated with 50µg OmCI-Fc while only 28% was detected in the mouse that received the higher dose after 48 hours of the treatment. The percentage of C5 activity determined in this experiment did not necessarily directly translate to an equivalent percentage of circulating C5 level. This is due to the fact that only a single C5 molecule is needed to form a MAC and to observe any complement inhibition at this level, majority of the C5 molecules should be neutralised. For example 28% of C5 activity (measured here) was likely to correspond to lower (than 28%) protein level.

A separate experiment measuring total serum complement activity after *iv* administration of a combined pOmCI (200µg)/OmCI-Fc (300µg) dose revealed very low (27%) complement activity after the first 24 hours. However, a similar level of complement activity was detected in the mice that received OmCI-Fc alone. It is likely that the effect of OmCI-Fc in the combined staggered dose masked the pOmCI-mediated complement inhibition. This suggests that the pOmCI and/or OmCI-Fc concentration could be decreased. The lowest dose and optimal duration of the treatment remain to be determined. However if the maximum C5 concentration in plasma is 80µg/ml (C5 concentration range 50-80µg/ml [421,

422]) and plasma volume of a mouse is 3.5% of the body weight (3.5ml/100g) then the C5 pool in a 25g mouse is 70 μ g. The molecular weight of C5 is 190kDa and the molecular mass of pOmCI is 17kDa, therefore 6.4 μ g of pOmCI would be needed to neutralise 70 μ g C5. The binding interaction pOmCI-C5 is very tight (as shown from the SPR analysis in Chapter 6; K_D of 0.4nM) meaning that this dose of pOmCI (approximately 0.4 μ M) should be sufficient to bind all C5 and ablate complement lytic activity in a mouse. Therefore the optimal strategy would be to inject mice with 6.5 μ g of pOmCI (30-fold less than the dose used in here) followed by OmCI-Fc given one hour later. The minimum effective dose of OmCI-Fc needs to be determined experimentally by titrating the reagent *in vivo*.

Differing routes of administration of OmCI were also investigated. The *iv* and *sc* routes are the most frequently used routes of therapeutic administration. Because of gastrointestinal enzymatic degradation of the protein molecules, the oral route was not feasible. pOmCI and OmCI-Fc were given *iv* or *sc* to mice and their effect on complement activity was monitored. The analysis revealed that the reagents were efficiently delivered to the circulation and effectively blocked C5 after *iv* and *sc* injection. However pOmCI and OmCI-Fc absorption from the *sc* route was slow, with peak functional activity occurring approximately 1-6 hours after pOmCI administration and 12 hours post OmCI-Fc injection. Subcutaneous injection of pOmCI resulted in longer lasting complement inhibition when compared to *iv* administration. In contrast to pOmCI injected *iv*, pOmCI given to the animals *sc* gradually entered the circulation and provided extended complement inhibition. OmCI-Fc injected *sc* blocked C5 and showed level of complement activity similar to OmCI-Fc when given *iv* however there was an initial delay of an approximately 12 hours in this effect. OmCI-Fc took a longer time to reach the circulation and block C5 compared to the small pOmCI. Protein-based therapeutics given *sc* enter systemic circulation via the blood capillaries or lymphatic system depending on their molecular weight [423]. Proteins with molecular weights larger than 16kDa are predominantly absorbed by the lymphatic system, while smaller proteins are absorbed by blood capillaries. Proteins that enter systemic circulation via the lymphatic system require a longer time to reach maximum concentration (t_{max}) than protein drug absorbed via the blood capillaries [424]. In other words t_{max} is increased with increasing molecular mass of the therapeutic [423]. For example the absorption of antibody administered *sc* proceeds slowly and t_{max} ranges from 2 to 8 days

[425]. Although additional experiments are required, the results suggested that *sc* administration might be advantageous in OmCI based anti-complement treatment.

Two animal models were chosen to study the ability of CD59-2a-CRIg to target to sites of complement activation, and localisation to C3b/iC3b in particular, was investigated. Mouse models of multiple sclerosis (ADEAE) and atherosclerosis (ApoE model) were selected because of the well-defined role of the complement and the terminal pathway in the disease pathology. Deposition of C3 fragments and binding of CD59-2a-CRIg to disease tissues were investigated by immunofluorescence microscopy.

ADEAE is an acute demyelinating model of MS. The disease was induced in CD59^{-/-} mice on C57Bl/6 background. C57Bl/6 is one of the commonly used mouse strain in neuroimmunological disease including MS and CD59 deficiency was required because anti-CD59 mAb was used for CD59-2a-CRIg detection. ADEAE is characterised with severe pathology. This model was selected because the disruption of the BBB which allowed transport and localisation of CD59-2a-CRIg to the CNS. CD59-2a-CRIg targeting was analysed *ex vivo* and *in vivo*.

For the *ex vivo* analysis, CD59-2a-CRIg was labelled with a green fluorophor. This allowed direct detection without using antibody and thus reduced the washing steps and preserved CRIg-C3b/iC3b interaction. When diseased spinal cord sections were incubated with a directly labelled reagent, it was found that the CD59-2a-CRIg localisation pattern resembled those for C3b/iC3 deposition. The C3b and iC3b staining co-localised with cell infiltrates shown in the spinal cord from ADEAE mice but not from healthy animals. An additional experiment using a control protein is required to confirm that CD59-2a-CRIg specifically targets complement activation *ex vivo*.

For the *in vivo* targeting, CD59-2a-CRIg reagent was injected in ADEAE mice at day 11. The reagent could not be detected in the spinal cord one or three hours post administration. A possible reason for this could be that the time chosen to harvest tissue sample was not appropriate and more time was required for CD59-2a-CRIg to reach the site of pathology (spinal cord). Additional time points could be also included in order to determine the time frame in which the reagent reached the target. In addition to time, a physical obstacle could also account for negative *in vivo* targeting. The passage of compounds from the blood to the

CNS is controlled by the brain capillary endothelial cells forming BBB. The restriction of brain penetration is due to the tight junctions between adjacent cells. However the integrity of the BBB is lost in animal models of multiple sclerosis [426, 427]. Furthermore, the anti-MOG antibody injected at day 8 amplifies the disease pathology through binding to MOG of the myelin sheath and triggering complement activation [223]. This means that the antibody needs to cross the BBB barrier in order to cause exacerbation of CNS inflammation and demyelination suggesting that the BBB was disrupted at the time of CD59-2a-CRIg injection at day 11. Another explanation for this result could be that the high number of washes during the staining had a detrimental effect on CD59-2a-CRIg binding to C3b and iC3b. This could be possibly avoided if CD59-2a-CRIg/488 was used for *in vivo* targeting.

The second model tested here was ApoE model of atherosclerosis. The disease was induced in ApoE^{-/-} CD59^{-/-} double knockout mice. ApoE, a glycoprotein synthesised mainly in the liver and brain, is a constituent of most of the lipoprotein. It functions as receptors that clear chylomicrons and very low-density lipoprotein remnants. ApoE is also synthesised by monocytes and macrophages in vessels and it plays a role in clearing cholesterol-rich lipoproteins from plasma to maintain cholesterol homeostasis [428, 429]. Targeted deletion of the gene for ApoE leads to impaired clearing of plasma lipoproteins and atherosclerosis. The pathogenesis of atherosclerotic lesions in these mice resembled that found in humans. The terminal complement pathway was found to contribute to the development of this disorder. The lack of CD59 in mice worsened disease pathology and increased the plaque area [242].

Similarly to ADEAE, deposition of CRIg ligands, C3b and iC3b, was shown in the diseased tissue (brachiocephalic artery) isolated from mice with atherosclerosis. The analysed C3 fragments were found in the atherosclerotic plaques. Directly labelled CD59-2a-CRIg/488 effectively target complement activation fragments when added to diseased tissue *ex vivo*. Double C3b/iC3b and CD59-2a-CRIg was also tested. It is very likely that the reagent competed with the anti-C3 antibody for the same C3b/iC3b epitope and therefore CD59-2a-CRIg was not able to interact with its ligands. This finding supported the observation that the anti-complement agent specifically targeted complement activation fragments deposited at the site of pathology.

For *in vivo* analysis, CD59-2a-CRIg was administered *iv* into diseased mice and the high plasma levels (28-78 μ g/ml) of CD59-2a-CRIg detected at the time of sacrifice in the circulation confirmed the efficacy of injection. Similarly to the ADEAE model, CD59-2a-CRIg could not be detected at the site of pathology after intravenous injection. This could not be explained by the lack of the CRIg ligands within the atherosclerotic vessel. C3b and iC3b were found within the plaque beneath the endothelial wall as demonstrated by immunohistochemistry. It is highly likely that the intact vessel wall was an obstacle preventing CD59-2a-CRIg from reaching the target. The result obtained here could also be due to the high number of washes during the staining procedure as explained earlier for ADEAE model. This could be investigated by using directly labelled CD59-2a-CRIg/488 reagent.

The analysis performed in this Chapter clearly demonstrated that CD59-2a-CRIg was able to target complement activation at the site of pathology. The reagent effectively targeted C3b/iC3b complement fragments *ex vivo*. Additional analysis is required to demonstrate that CD59-2a-CRIg is capable of targeting complement activation *in vivo*.

Chapter 8. Final Discussion

The overall aim of the proposed study was to design and develop effective novel anti-complement biologicals. Long-lived OmCI-Fc and targeted CRIg-CD59 reagents were generated and comprehensive characterisation was carried out *in vitro*, *ex vivo* and *in vivo*.

Complement is a central element of innate immunity, defending the host against pathogens, synchronising various events during inflammation, and linking innate and adaptive immune responses. However disturbance in complement regulatory mechanisms can turn complement from a defensive to an attacking system contributing to the pathology of many diseases. The potential therapeutic value of inhibiting complement was illustrated in Chapter 1. Anti-complement therapy began with CVF in 1971 [430], a reagent used as a proof-of-concept that complement inhibition could reduce disease severity in many experimental models of complement-mediated pathologies. However, the strong antibody response and the uncontrolled complement activation occurring during CVF decompensation restricted its *in vivo* use. Since then, many different anti-complement reagents ranging from small natural complement inhibitors (K-76COOH), synthetic serine protease inhibitors (FUT-175), antibody inhibitors of complement activation and recombinant soluble forms of complement regulators (sCR1) were developed. Despite the success of many of the anti-complement therapeutics their uses *in vivo* have been limited. Developing anti-complement therapeutic agents is a challenging task and various factors including rapid clearance of small reagents *in vivo*, broad-spectrum activities and low-specificity (FUT-175), side effects of systemic complement inhibition in long-term treatment and the point at which to inhibit complement should be taken into account. These aspects were considered when designing OmCI-Fc and CD59-CRIg reagents.

8.1. OmCI therapy

8.1.1. pOmCI: a powerful C5 inhibitor for treatment of acute disease and conditions

Several research advances, including knock-out animals lacking terminal pathway complement proteins (C5 and C6) or C5a receptor, C5-neutralising antibodies, and

recombinant C5a receptor antagonists have provided strong evidence for the involvement of C5 and the terminal pathway in various disorders such as RA [210] and retinal disorders [431, 432]. The anti-C5 reagents, pOmCI and OmCI-Fc, described in this project represent promising therapeutics for such disorders. The small molecule, pOmCI (17kDa) is a powerful complement inhibitor and the therapeutic potential of small molecules inhibiting at the C5 level has been already proven. C5aR antagonist (ADC-1004) is a small molecule (9.5kDa) that was highly effective in preclinical studies and is now a candidate for clinical treatment in situations where IR injury is a risk, including acute myocardial infarction, stroke and transplantation. ADC-1004 prevented neutrophil activation thereby reducing inflammation and reducing the myocardial infarction in a porcine IR model [433]. Similarly to ADC-1004, the therapeutic potential of pOmCI was also shown in an acute model of rat myasthenia gravis, where a single injection of pOmCI was able to protect rats from disease development [324]. The ability of this reagent to bind tightly to C5 (also demonstrated in this project) effectively prevented MAC formation and C5a generation. Blocking C5a, a powerful chemoattractant, decreased the cellular infiltration and inhibited MAC, preventing direct tissue damage. pOmCI given to experimental animals rapidly formed a complex with C5 and thus turned off the destructive power of complement instantaneously. However, excess reagent which did not bind C5 was rapidly cleared from the circulation so that when C5 was resynthesised, complement activity was quickly restored. The high synthesis rate of C5, 70-134 μ g/kg per hour (in human) [434] and the short half-life of free pOmCI increased the frequency of administration required to achieve effective therapy in chronic disease. Therefore, reagents with a molecular size below the renal clearance threshold, such as pOmCI (17kDa) and ADC-1004 (9.5kDa), show good therapeutic effect only in acute diseases and conditions [435].

8.1.2. OmCI-Fc: an excellent long-lived reagent for treatment of chronic disease

The ability of OmCI to prevent C5a formation and inhibit the terminal pathway is an attractive proposition in therapy, as physical damage and proinflammatory effects caused by MAC and C5a-activated neutrophils would be prevented whilst key physiological functions of the complement system, such as protection from infection and immune complex solubilisation, would be sustained. Preserving the upstream events of the complement

activation such as an opsonisation would diminish side effects in treatment of chronic disease when long-term anti-complement therapy is required. Many disorders with complement-driven pathology, (including MS, RA and SLE) are chronic and as such, require lifelong medication following diagnosis. To generate a long-acting mouse OmCI therapeutic suitable for chronic disorders, OmCI was fused to the Fc portion of mouse IgG2a and a long-lived OmCI-Fc fusion protein was created. Fusion of proteins to the Fc domain of antibody has been widely used to increase half-life of many therapeutic proteins, including CTLA-4 (Abatacept) and TNF- α receptor (Etanercept). Abatacept and Etanercept are now in the clinic for treatment of various inflammatory diseases such as severe RA, moderate to severe polyarticular-course juvenile RA, psoriatic arthritis, ankylosing spondylitis, moderate to severe plaque psoriasis, MS and SLE [436-440]. The Fc-fusion strategy was previously used in our laboratory to decrease the plasma elimination rate of recombinant complement regulators (the functional domains) such as DAF and CD59. The OmCI-Fc protein developed in this project was designed for therapy of mouse models of chronic disease. Unlike other therapeutics, including Soliris (anti-C5 mAb), the OmCI functional activity is not species-restricted and prevents complement activation in human, mice, rats and guinea pigs. One of the limitations of anti-complement therapeutics is the fact that many reagents created are based on human regulators so the capacity to test them in chronic animal models of disease is limited because of their immunogenicity and species selectivity [441]. For example, treatment of rat CIA with human sCR1 could not continue beyond five days because of the immunogenicity of this human reagent in animals [304]. It is highly likely that pOmCI, as with most other salivary components of *O. moubata*, is poorly immunogenic, thus avoiding this issue. The lack of immunogenicity is useful to the tick as it evades the host immune system during blood feeding [442] and thus avoids generating a host immune response -especially in larger hosts, such as cattle, where thousands of ticks can infest a single animal. Moreover no anti-pOmCI IgM response was detected in rats after receiving this reagent [435]. The choice of mouse Fc used in this project will allow the reagent to be tested in mouse models of complement-driven diseases without generating an antibody response. The low immunogenicity and the capacity to bind C5 from different species will enable OmCI-Fc to be tested, and dose and frequency of administration to be established in a variety of preclinical models before applying it to the clinic.

The comprehensive *in vitro* analysis undertaken in this research project revealed that the novel reagent OmCI-Fc is a hybrid molecule which retains good anti-complement activity. OmCI-Fc displayed a slower plasma clearance rate and achieved longer lasting complement inhibition in mice compared to pOmCI. OmCI-Fc when bound to C5 demonstrated 2.5-fold longer β -phase half-life compared to pOmCI-C5 complex. However, the true clearance rate of free OmCI-Fc and pOmCI was obtained in the absence of C5. While the majority (70%) of the free pOmCI was cleared within the first 5 minutes after drug administration, high levels (52%) of OmCI-Fc were measured 6 hours post administration. Circulating fusion protein was detected even on day five of the experiment (Fig.7.1) suggesting that OmCI-Fc was suitable for long-term therapy in chronic complement-mediated diseases. The extended plasma half-life of OmCI-Fc translated into longer lasting C5 inhibition and thus decreased the frequency of injections required to effectively block complement. Sometimes biological activity of a fusion protein can be significantly reduced relative to the nonfused protein due to steric hindrance or misfolding [327, 443]. The fusion of Fc to OmCI slightly reduced the C5 binding affinity, so I hypothesised that C5 bound with normal affinity to one OmCI moiety in the fusion protein, and following occupation of the first site, with a lower affinity to the second site. By binding to C5, both OmCI arms of the dimeric molecule were able to provide cell protection from complement attack. These unique features, high C5-binding affinity of pOmCI and the long lasting functional activity of OmCI-Fc, were combined to design a strategy to achieve long-term complement inhibition. C5 would be removed with a bolus of OmCI, which can be readily synthesised in high quantity, and second injection of the long-acting OmCI-Fc would be given to neutralise “newly” synthesised C5 thereafter for 24 hours. The strategy was modelled in mice, however the high dose of OmCI-Fc used masked the effect that pOmCI had on complement (pOmCI-OmCI-Fc treatment and OmCI-Fc alone had similar effect on complement; fig.7.5), further experiments to titrate the dose of pOmCI and OmCI-Fc are required to determine the minimal effective concentration of the reagents. Establishing the minimal dose of pOmCI and OmCI-Fc which will deliver effective anti-complement therapy will diminish the cost of medication of chronic disease.

Testing different routes of administration is of high importance for delivering effective therapy especially when using drugs with short half-life such as pOmCI. pOmCI, injected *iv* bound C5 immediately and the excess was rapidly cleared from the circulation whereas a *sc* injection allowed the reagent to be gradually released into the circulation and neutralised C5

for hours longer compared to the *iv* administration. Both, the *sc* and *iv* injections of OmCI-Fc resulted in complete C5 blockade. The route of administration did not affect the functional capacity of OmCI-Fc to block complement (duration of complement inhibition) but only had an impact on the time needed for the blocking effect to develop. OmCI-Fc delivered *sc* took longer to enter the circulation and to neutralize complement. Because *sc* injections are more convenient for repeated treatment and are able to maintain efficient complement inhibition, this route of administration could be considered for OmCI therapy of chronic disease. Other Fc fusion proteins, including Etanercept, have proved to be effective treatment for chronic diseases (for example RA) when administered *sc*.

8.1.3. OmCI: Prospects for therapy

I have successfully generated the long-lived anti-complement therapeutic, OmCI-Fc, and have established an OmCI-inhibition strategy. An optimal tactic for treating specific complement-mediated disease must be designed. Possible approaches to further increase the *in vivo* half-life and delivery strategies will be discussed.

I have shown that OmCI-Fc demonstrated a markedly increased half-life compared to pOmCI in C5 sufficient mice. Attaching Fc to other complement regulators has also been shown to prolong their circulating half-life; that of DAF was increased from 20 minutes to 33 hours and Crry from 7 minutes to 53 hours [324, 327]. The half-life of free (uncomplexed with C5) pOmCI and OmCI-Fc was not determined in this study and direct comparison with DAF and Crry Fc fusion proteins could not be made. However free pOmCI was observed for only one hour after the administration in C5 deficient mice while OmCI-Fc was detected even at day five of the experiment (at 96 hours) suggesting that attachment of Fc greatly decreased the clearance rate of OmCI. As a long-term goal, the half-life of OmCI-Fc could be further extended which may result in increased therapeutic capacity. Certain modifications, such as substitution of amino acid residues located near the Fc-FcRn interface within in the Fc portion, have been shown to additionally extend the half-life of antibodies and Fc fusion proteins. It has been demonstrated in the mouse that mutations in the Fc which resulted in stronger binding to FcRn at pH6 whilst maintaining similar or weaker binding at pH7.4, translated into longer lived molecules [444]. Human IgG1, IgG2 and IgG3 Fc double

mutants within the FcRn-binding domain (Thr250Gln and Met428Leu) also demonstrated increased binding affinity to human and rhesus monkey FcRn at pH 6 and increased half-lives *in vivo* (in rhesus monkeys) compared to the wild type forms [445]. A similar approach could be employed to further increase the half-life of OmCI-Fc. The Fc of mouse OmCI-Fc (generated in this study) can be easily modified, especially as the interaction site for FcRn on mouse IgG2a has been already mapped [446], and tested in animal models of complement mediated disease prior to developing an optimal human OmCI-Fc (with human Fc) reagent.

In addition to FcRn, Fc of IgG antibodies interact with Fc γ Rs on various cell types. A correlation between the affinity of the Fc-Fc γ R interaction and the half-life of Fc coupled molecules has been observed [447]. Fc molecules with higher affinity for Fc γ R were cleared rapidly from circulation compared to those with reduced binding affinity. This has been illustrated with IL-2 fused to the Fc of human IgG4 [447]. This reagent had a longer serum half-life compared to the high affinity IL-2-Fc proteins derived from IgG1 or IgG3 which were cleared from the circulation faster through enhanced interaction with FcR-expressing cells. The same effect on half-life was achieved by site-directed mutagenesis of the Fc γ R binding site in IgG1, reducing the affinity for the receptor. This approach could be utilised to additionally prolong the serum half-life of OmCI-Fc. It is important to note that the sites for FcRn and Fc γ R interactions on Fc of IgG are distinct, thus mutations that impact FcRn binding would not affect the interaction with Fc γ R [383, 384, 448-450].

OmCI-Fc has been designed for treatment of chronic disease. The administration route is critical for patients suffering from chronic disorders requiring long-term therapy; less invasive routes of delivery such as *sc* and intranasal (*i.n.*) would be preferential in such disorders. Although they have not yet been employed in routine clinical use, there is an interest in the development of Fc-fusion proteins for non-invasive pulmonary delivery. Pulmonary epithelial cells (upper and central airways) are known to express FcRn, which may facilitate efficient systemic absorption of Fc fusion proteins delivered to the lung (Fig. 8.1). Whether FcRn is expressed in mouse lung is still not clear [451, 452] however high molecular weight Fc fusion proteins, such as Epo-Fc (120kDa) and follicle stimulating hormone-Fc (128kDa), have been successfully delivered at high concentration from the air space across the epithelial cells into the interstitium and to the circulation in neonatal rats,

monkeys and human volunteers after oral or *i.n.* administration [453]. It is very likely that the pulmonary route would deliver OmCI-Fc (83kDa) to the systemic circulation.

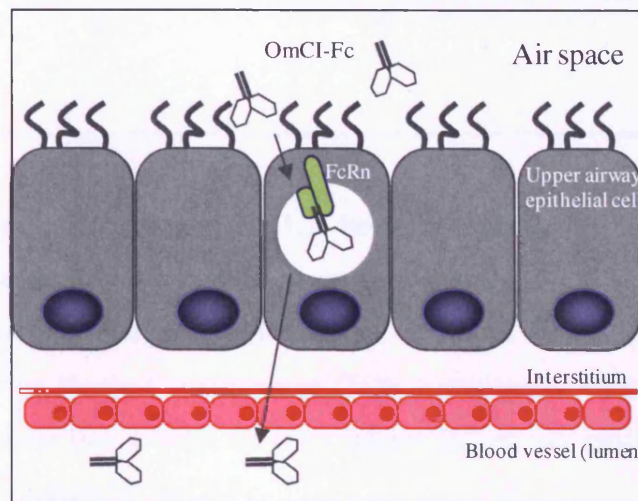


Fig 8.1 A schematic representation of OmCI-Fc pulmonary delivery. OmCI-Fc in the air space is captured by FcRn on the airway epithelial cells. The transport vesicles containing OmCI-Fc bound to FcRn do not fuse with the degradative lysosomes, but pass through the epithelial cell in the apical to basolateral direction and release the OmCI-Fc to the interstitial space (neutral to slightly alkaline pH) and the circulation. The figure is adapted from *Roopenian and Ahreeram. Nature Reviews Immunology. 2007.*

It has been hypothesised that steric hindrance between the effector and Fc moieties within Fc-fusion proteins may alter the Fc-FcRn interaction and hampers protein transcytosis through the epithelial cells [454, 455]. Monomeric Epo-Fc and Factor IX- Fc (monomeric in respect to the therapeutic protein and dimeric in respect to Fc) delivered *i.n.* have shown improved therapeutic efficiency (2-10-fold) compared to the dimeric forms. Monomeric Factor IX- Fc is currently in phase II clinical trial for treatment of Hemophilia B [454, 455]. If needed monomeric OmCI-Fc could be generated to improve its delivery. In the light of this, the combined OmCI strategy explained in this project could be modified. OmCI would be injected *sc* while OmCI-Fc would be given *i.n.* to achieve less invasive and sustained treatment of complement-mediated disease (Fig.8.2).

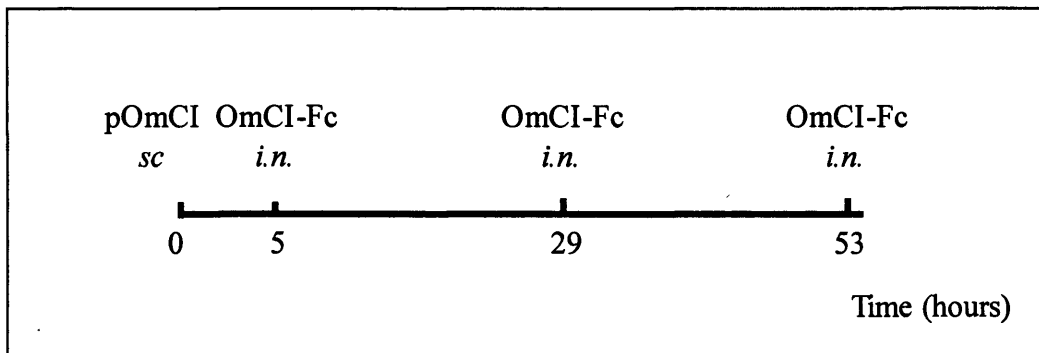


Fig.8.2 OmCI therapeutic strategy for less invasive treatment of complement-mediated disease. pOmCI will be injected *sc* at time 0 to neutralize C5 in circulation. This will provide 6-hours complete complement inhibition. OmCI-Fc will be given *i.n.* at intervals. *Iv* injection of OmCI-Fc blocked complement (80% complement inhibition) for 24 hours. It could be hypothesized that similar or even longer lasting C5 blockade will be achieved through *i.n.* administration of OmCI-Fc.

As described in Chapter 1, the complement system has been implicated in diseases and conditions with organ specific pathology including organ specific IR injury, glomerulonephritis, RA and CNS disorders. Therefore local delivery of therapeutics could be beneficial in such illness. The delivery of therapeutic proteins to the CNS to treat neurological disease and conditions, such as demyelination, Alzheimer's disease and brain tumors, is a challenging goal. The BBB is formed from tight junctions between the capillary endothelial cells in the brain microvasculature, which prevents free diffusion of molecules across the membrane and prevent most molecules from reaching the CNS from the blood stream. Thus the BBB blocks drug entry to the CNS and therefore is the main obstacle for developing effective therapy [456]. Therapeutics can be introduced directly into the CNS by intracerebroventricular or intraparenchymal injections, however for multiple dosing regimens both delivery methods are invasive, risky and expensive techniques. A strategy for OmCI could be developed for effective complement inhibition specifically in the CNS. An increasing numbers of studies suggested that *i.n.* delivery provides a method for bypassing the BBB and directly delivering therapeutic drugs to the CNS. The exact mechanism of drug delivery has not been entirely understood and it is likely that a combination of pathways involving nerves (olfactory and trigeminal nerves) connecting the nasal passages to the brain and spinal cord and pathways involving the vasculature, cerebrospinal fluid and lymphatic system convey the therapeutics from the nasal cavity to the CNS through either intra- or

extraneuronal routes [457]. It has been shown that Il-10 delivered *i.n.* suppressed neurologic symptoms in a rat model of MS while *sc* administration did not [458]. Similarly, the anticancer drug methotrexate administered *i.n.* was shown to be directly delivered to the cerebrospinal fluid (CSF) and more effectively reduced brain tumours in rats when compared to systemic administration [459]. Fig. 8.3 illustrates the route by which *i.n.* administered drugs could reach the CNS.

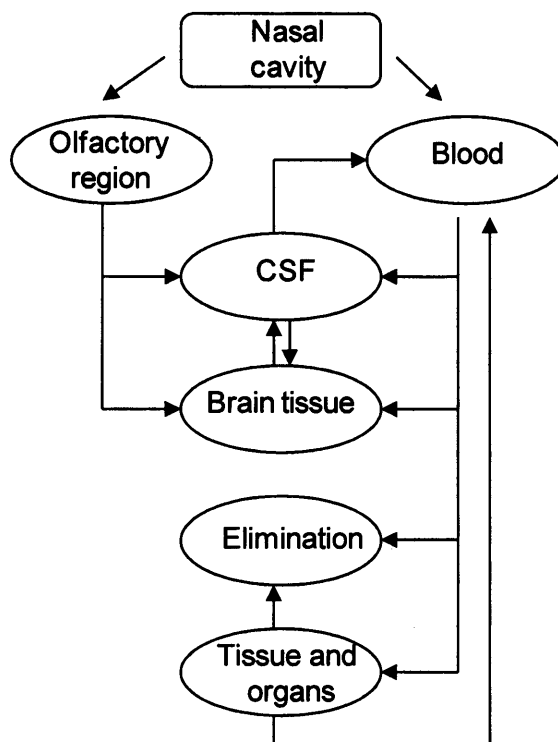


Fig.8.3 Pathways of drug distribution from the nasal cavity to CNS. Following *i.n.* administration, drugs come into contact with the nasal mucosa, which is innervated by olfactory and trigeminal nerves. Drugs can be transported through the nasal mucosa to the CNS by entering perivascular channels in the lamina propria (connective tissue which lies beneath the epithelium) or via extracellular or intracellular mechanisms involving olfactory and trigeminal nerves. After reaching the lamina propria, drugs can enter channels created by olfactory ensheathing cells surrounding the olfactory nerves, where they can access the CSF and olfactory bulb. From the CSF, drugs can be distributed via bulk flow mechanisms and mix with brain interstitial fluid throughout the brain. Drugs can also enter perivascular spaces after reaching the brain to be rapidly distributed throughout the CNS. Drugs that entered perivascular spaces from the nasal mucosa can also exit these spaces in the brain. These same pathways in the reverse direction are involved in the clearance of the drug from the CNS to the periphery.

Comparative analysis of *i.n.* and *iv* delivery of IFN- β (~18kDa) demonstrated that *i.n.* administration produced much higher concentration in the CNS with minimal systemic exposure, and achieved much higher degree of delivery of intact protein to CNS than did *iv* administration [460]. Drug uptake in the CSF and brain depends on its molecular weight; pOmCI (17kDa) has molecular weight similar to IFN- β and therefore it is possible that pOmCI administered *i.n.* could reach the CNS to provide local complement inhibition. Compared with traditional drug-delivery strategies, *i.n.* pOmCI delivery has advantages. This noninvasive route of administration causes less pain and it is easily conducted by the patients themselves. Potential side effects of the drugs on the peripheral system could be minimised and also smaller amounts of drugs are required to produce the desired concentrations of drugs in the CNS and thus reduce the treatment cost.

Another possible way to deliver OmCI therapy across the BBB and to the CNS is through receptor-mediated transport. In many neurological diseases and models, including EAE, the BBB is disrupted enabling therapeutic reagents to enter the CNS. However the BBB and capillary endothelium in particular express FcRn [461]. This receptor mediates reverse transcytosis of Fc containing molecules from the brain to the blood [462]. For this reason it is possible that OmCI-attached to Fc would not provide optimal therapy for CNS diseases (Fig 8.4). While FcRn only transports Fc molecules to the bloodstream, other receptors such as the insulin receptor (IR) and transferrin receptor 1 (TfR1) are also expressed in the BBB (on luminal and abluminal endothelial membranes), resulting in transport of their ligands in both blood-brain and brain-blood directions [463]. The ability of these receptors to transport their ligands across the BBB to the CNS has proved beneficial for drug delivery. Highly selective antibodies against human insulin receptor and mouse and rat TfR1 have been generated and used as a “Trojan horse” to transport attached drugs across the BBB [464, 465]. The human brain-derived neutrophilic factor fused to mouse anti-human insulin receptor mAb was specifically delivered to the brain after *iv* injection into rhesus monkeys. Antibodies that bound TfR at sites distinct from the transferrin binding site enabled the transcytosis of avidin (64kDa) and nerve growth factor (26kDa) to the CNS [466, 467]. This delivery strategy could be used for delivering OmCI therapy to treat complement driven neurological disease such as MS. When administered *iv*, the bifunctional OmCI-Anti-TfR protein would selectively bind TfR1, expressed at high levels on brain capillaries (TfR1 expression in rat is restricted to brain capillaries) [468, 469], which are part of the BBB, thus

enabling transport of the drug via endogenous transport systems for Tf across the BBB. Following penetration of OmCI into the brain, OmCI would initiate its pharmacological effect. Intranasal pOmCI delivery combined with *iv* administration of OmCI-anti-TfR could provide an effective and less invasive way protection to the CNS from complement mediated damage in the context of disease.

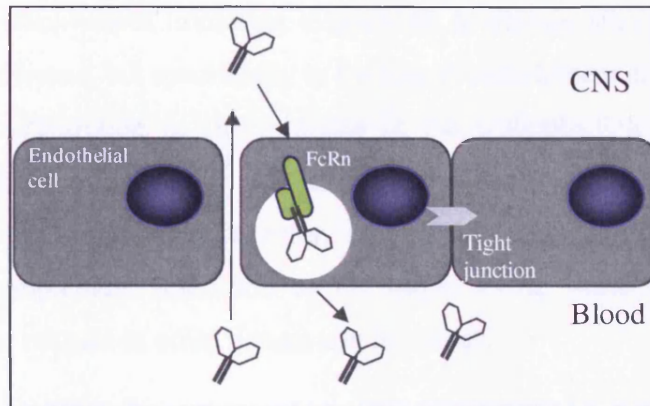


Fig. 8.4 Schematic diagram of FcRn-mediated reverse transport. The cerebral vascular endothelial cells are joined by tight junctions that prevent the passive diffusion of macromolecules across the BBB in the absence of specific transporters. In some neurological disorders such as MS, the BBB is disrupted and therefore protein drugs such as OmCI-Fc are able to reach the CNS. However, the FcRn expressed in BBB mediates reverse transcytosis of OmCI-Fc from the CNS back into the circulation. The figure is adapted from *Roopenian and Ahreeram. Nature Reviews Immunology. 2007*

8.2. CD59-CRIg therapy

8.2.1. CD59-2a-CRIg: a unique targeted anti-complement drug

Recombinant sCD59 (non-targeted) has been previously generated, however its therapeutic capacity has never been tested *in vivo* because of its low specific activity in the presence of serum and small size (12kDa) leading to rapid elimination [376, 470, 471]. Due to its short half-life, sCD59 would require frequent administration or continual infusion to control

complement. sCD59 has been further engineered to improve its therapeutic efficacy. Attempts have been made to generate more active forms of sCD59 by designing chimeras or fusion proteins [327, 337]. sCD59, linked to a membrane “tag”, a chemically engineered lipid targeting peptide, (sCD59-APT542), significantly inhibited disease progression when delivered to the cell surface in a rat model of AIA [365]. This proved that targeting terminal pathway inhibition to the cell surface was a promising anti-complement strategy for *in vivo* therapy. Novel anti-complement therapeutics, based on CD59-CRIg, were generated in this project to deliver complement inhibition exclusively to disease sites. Targeting CD59 not just to any cell membrane, but specifically to the site of complement activation, will result in increased local concentration of the inhibitor at the pathophysiologically relevant sites relative to other parts of the body. My strategy was that linking the terminal pathway inhibitor, CD59, to the complement receptor, CRIg, would allow delivery and localisation of CD59-mediated complement inhibition to the target tissue while reducing the relative concentration of the reagent in other tissues and in blood.

The choice of ligand used for targeting, CRIg, was driven by the fact that C3 is a central molecule of the complement system and its activation fragments are abundant opsonins deposited at sites of complement activation. Upon activation, C3 is cleaved by C3 convertase to a small C3a peptide and a large C3b fragment, which covalently attaches to the cell surface before degradation to iC3b and C3dg. C3 fragments are present at sites of pathology in various complement driven diseases and conditions such as RA [52, 53], MS [54] and atherosclerosis [55, 56]. These fragments can be targeted through C3 complement receptors such as CRIg and CR2. The use of a complement receptor to deliver targeted complement inhibition has already been shown to be an effective strategy to protect host tissue from complement attack. Several targeted anti-complement reagents have been generated and their efficacy tested in various animal models of disease with complement driven pathology. CR2-CD59, CR2-DAF, CR2-fH and CR2-Crry were discussed in Chapter 1. These fusion proteins utilised the ability of the first four N-terminal SCRs of complement receptor CR2 to bind C3 fragments C3dg and, with lower affinity, to iC3b. A macrophage receptor CRIg was used here to target CD59 to the site of complement activation. CRIg binds iC3b as demonstrated by ELISA and flow cytometry [57]. However it also interacts with the first fragment generated upon the C3 activation, C3b. CD59-CRIg (generated in this project) and CR2-CD59 fusion proteins are design to bind to C3 activation fragments at the

cell surface and to prevent MAC formation. The interaction with the first C3 activation product, C3b, enables CR1g-CD59 to come into action before CR2-CD59 and thus provides cell protection as soon as complement attack starts. C3b deposited on surfaces is regulated further by conversion to iC3b, if this regulation does not occur, complement activation continues and amplifies C3 deposition. Anti-complement therapy would therefore benefit from targeting the two earliest fragments of C3 activation; this will effectively localise more CD59-CR1g molecules to the site of complement activation and thus provide immediate and powerful protection.

In the presence of membrane bound complement regulators (CR1 or Crry), iC3b deposited on cell is further degraded to C3dg. The agents (based on CR2 or CR1g) given to patients or experimental animals will be circulating in the blood stream. Because of the expression of the complement inhibitor CR1 on human red blood cells, I believe that most of the C3b in the blood (on neighbouring blood cells and endothelial tissues) would be converted to C3dg [58-61], therefore it is likely that CR2-CD59 reagent will be mopped up to a greater extent than CR1g-CD59, which does not bind C3dg. For this reason CR1g-mediated targeting might be advantageous over CR2 targeting and provide more effective therapy as it will survive longer in the circulation. Whilst studies are limited, the *in vivo* therapeutic effect of CR2-CD59 (generated by others) was described only in one animal model a model of liver resection [472]. This reagent has shown to be protective against IR injury and induced enhanced liver regeneration; the reagent has not yet been tested in other models.

By binding its target, C3b, CR1g also turns off further activity in the AP. It selectively blocks the AP C3 and C5 convertases while leaving the CP and LP intact to mount host response to pathogens [166]. Thus the CR1g-CD59 agents provide a double-hit on the complement system, delivering both MAC inhibition and convertase blockade, this makes CD59-CR1g a potential treatment for disorders known to involve both the AP and the terminal pathway such as aHUS [253, 255, 473, 474], RA [197, 198, 201, 202, 205, 208, 210, 211], AMD [328, 336, 475] and MS [218, 219, 221, 224, 225, 476]. For example, complement inhibition with CD59-CR1g may provide effective therapy and become the treatment of choice for aHUS associated with factor I mutations. Factor I cleaves C3b to generate iC3b and C3dg. Factor I mutations (10% of the aHUS cases) result either in quantitative or functional deficiency of factor I [477, 478]. A hypothesis could be made that reduced levels of iC3b and C3dg would be deposited in the kidney (the site of pathology) in

such patients. Although C3 fragments deposition has not been investigated in such patients, animal studies revealed that the only C3 fragment found on the glomerular basement membrane of factor I deficient mice was C3b [479, 480]. In cases like this CR2 targeting would not be effective while CRIg would target C3b and deliver CD59 to the site of complement activation.

I generated monomeric CD59-CRIg reagents with different orientations of CD59 either at the N- or C-terminus. The functional analysis revealed that the CD59-CRIg reagent (with CD59 at N-terminus) had higher capacity to inhibit the terminal pathway while CRIg-CD59 (with CD59 at the C-terminus) demonstrated better targeting. This suggested that the N-terminal position within the fusion molecule was favourable in terms of functional activity for both CD59 and CRIg domains. The monomeric CRIg-CD59 proteins (CRIg-CD59 and CRIg-3-CD59) had a structure similar to that of CR2-CD59, both reagents contained a CD59 molecule linked to a single complement receptor molecule. CD59 was either directly linked to CRIg to create CD59-CRIg, or the hinge of IgG3 was used to join the two molecules. CR2-CD59 was generated using the Gly-Ser sequence, (GGGS)₂, to link the two moieties in one hybrid molecule [330]. In contrast to CD59-CRIg, CD59 at the C-terminus within CR2-CD59 reagent blocked complement more effectively than the reagent in the reverse orientation. The difference in the CD59 functional activity could be possibly explained by the different linking sequences used within the fusion proteins. This hypothesis is illustrated in Fig.8.5.

When CD59 was linked to the C-terminus of CRIg via the hinge of IgG3, the CD59 functional site could not be easily accessed due to steric constraints and rendered CRIg-3-CD59 less functional. Similarly, the CD59 active site within CRIg-CD59 (two moieties linked directly without linker sequence), was likely to be partially hidden because of the very short distance between the two parts of the molecule. The Ser-Gly linker used in CR2-CD59 distances CR2 and CD59 without restraining their flexibility and thus allowed CD59 to function well when located at the C-terminus of the molecule. Despite the long upper hinge (an indication of flexibility), the mouse IgG3 hinge has been shown to be fairly rigid resulting in reduced segmental flexibility of the IgG3 antibody [378]. Segmental flexibility facilitates bivalent antigen binding. Similarly to antibodies, the lack of segmental flexibility was likely to cause steric hindrance of CD59 and CRIg. For this reason, the more flexible

hinge of IgG2a was also used in this project. In addition to less restricted motion, the presence of IgG2a hinge caused a better dimersisation of the hybrid molecule.

Using this novel strategy to assemble two CD59-CRIg proteins, a unique anti-complement therapeutic reagent was generated. The presence of two CRIg moieties in a single dimeric molecule dramatically increased the C3b binding avidity of this reagent. To the best of my knowledge this is the first dimeric targeted reagent developed for anti-complement therapy. The increased targeting capacity of CD59-2a-CRIg will translate into improved therapy for disease.

8.2.2. CD59-2a-CRIg: Prospects for therapy

The encouraging *in vitro* and *ex vivo* data presented in this study using the dimeric CD59-2a-CRIg agent, will be extended to analysis of its *in vivo* therapeutical potential. Diseases with organ specific damage in which pathology is mediated in part by the terminal and/or the alternative pathway such as glomerulonephritis, MS and RA will benefit from local (injected directly into tissue of question) CD59-2a-CRIg application. Here I propose a strategy for treatment of RA in experimental models. Recombinant CD59 and CRIg reagents have already been shown to have a therapeutic effect in models of RA. Soluble CRIg (CRIg-Fc) injected *sc* demonstrated protective effect in animal models of RA [325]. Similarly, the membrane-targeted CD59-APT542 agent at concentration of 250µg given intra-articularly markedly inhibited disease progression in a mouse model of AIA [365]. Combining the function of the two molecules in one therapeutic would have an additive or synergistic effect. As explain earlier in this chapter, the delivery approach is of a high importance when designing a therapeutic approach. It has been demonstrated that local drug delivery into the knee (intra-articular) was more efficient than systemic administration [481]. Local delivery into the joint could be used for CD59-2a-CRIg. Such delivery would be advantageous over systemic administration. The diseased joint is a significant source of complement, local synthesis of complement components C3, C1q, C1r/s and complement activation have been demonstrated [482-484] and therefore an intra-articular administration would be an appropriate delivery strategy to achieve instant local complement inhibition.

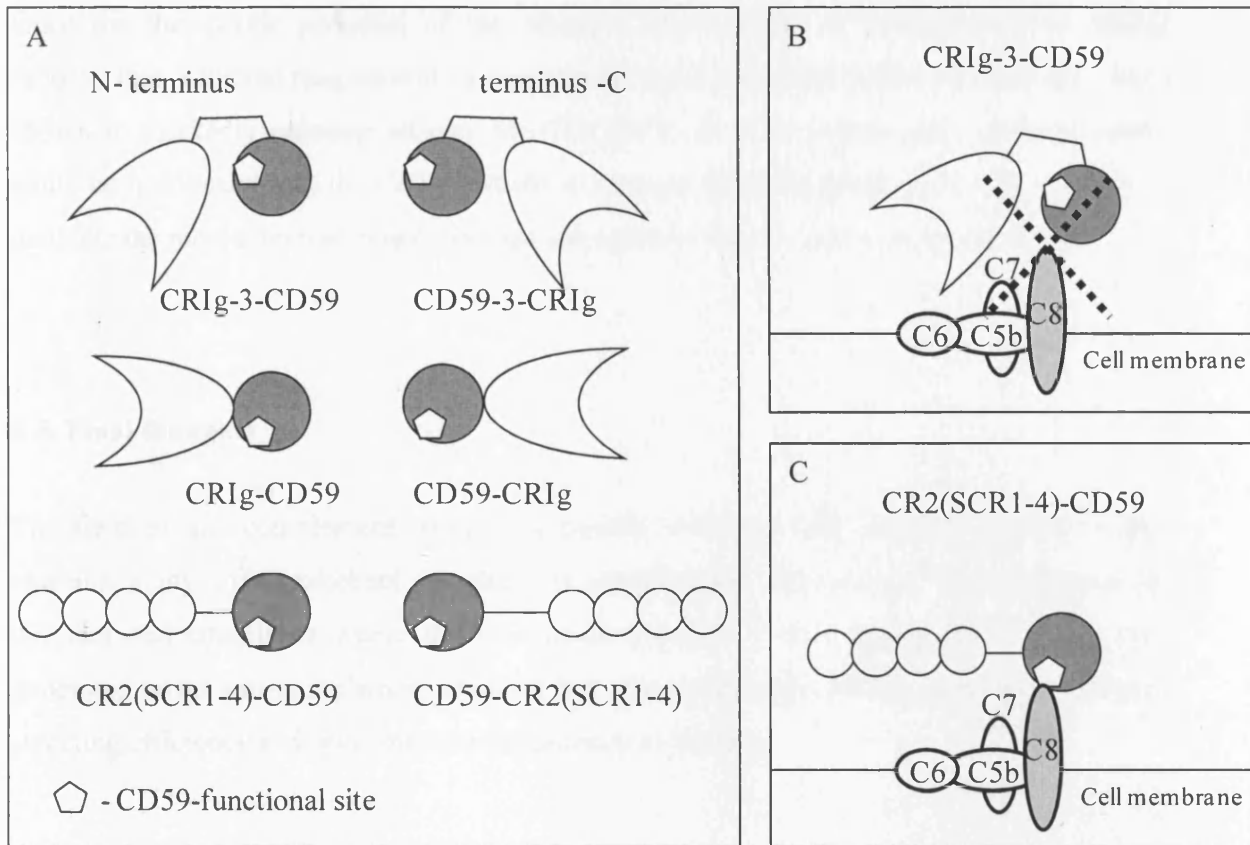


Fig. 8.5 Schematic representation of CRIg-CD59 and CR2-CD59 fusion proteins and binding to C8. A. In this project, CD59 was linked to the C- or N-terminus of CRIg directly or via the hinge of mouse IgG3 antibody; and previously others have fused CR2 (SCR1-4) to the N- or C-terminus of CD59 through linker sequences, (GGGS)₂ or SS(GGGGS)₃. In this hypothesis, the CD59-functional active site, shown in white, within fusion proteins containing CD59 at the N-terminus is not sterically hindered and is available for binding to C8. B. Because of steric restriction (due to the nature of the hinge and orientation of the proteins with respect to each other), the CD59 active site within CRIg-3-CD59 cannot be accessed easily. This may explain the lower complement inhibitory capacity of CRIg-3-CD59 reagent compared to CD59-3-CRIg. C. In contrast to the C-terminal CD59 within CD59-3-CRIg, the C-terminal CD59 in CR2-CD59 protein has its active site available for binding to C8. This is likely due to the Ser-Gly sequence linking the two moieties. This linker moves apart CD59 and CR2 without causing any steric constraints (seen with the antibody hinge linker) allowing CD59 to function.

Once the therapeutic potential of the mouse CD59-2a-CRIg is demonstrated in animal models, then a human reagent will be engineered. Point mutations in human CRIg have been shown to markedly enhance affinity for C3b [325]. As a long-term goal, such mutations could be introduced into the CRIg domain to increase targeting potential further still and to generate the most effective human therapeutic agent by improving targeting efficiency.

8.3. Final thoughts

The field of anti-complement therapy is rapidly evolving. The reagents created in this research study offer excellent prospect of specific and safe control of complement in diseases and conditions where the complement system is the driving force. I not only generated novel anti-complement reagents but also developed a unique strategy to enhance targeting efficiency and thus improve the potency of the drug.

References

1. Reid, K., *Activation and control of the complement system*. Essays Biochem, 1986. **22**: p. 27-68.
2. Fujita, T., *Evolution of the lectin-complement pathway and its role in innate immunity*. Nat Rev Immunol, 2002. **2**(5): p. 346-53.
3. Dodds, A., *Which came first, the lectin/classical pathway or the alternative pathway of complement?* Immunobiology, 2002. **205**(4-5): p. 340-54.
4. Weis, W., K. Drickamer, and W. Hendrickson, *Structure of a C-type mannose-binding protein complexed with an oligosaccharide*. Nature, 1992. **360**(6400): p. 127-34.
5. Schwaeble, W., et al., *The mannan-binding lectin-associated serine proteases (MASPs) and MASP19: four components of the lectin pathway activation complex encoded by two genes*. Immunobiology, 2002. **205**(4-5): p. 455-66.
6. Fearon, D. and K. Austen, *Properdin: binding to C3b and stabilization of the C3b-dependent C3 convertase*. J Exp Med, 1975. **142**(4): p. 856-63.
7. Fearon, D., *Activation of the alternative complement pathway*. CRC Crit Rev Immunol, 1979. **1**(1): p. 1-32.
8. Spitzer, D., et al., *Properdin can initiate complement activation by binding specific target surfaces and providing a platform for de novo convertase assembly*. J Immunol, 2007. **179**(4): p. 2600-8.
9. Brouwer, N., et al., *Mannan-binding lectin (MBL)-mediated opsonization is enhanced by the alternative pathway amplification loop*. Mol Immunol, 2006. **43**(13): p. 2051-60.
10. Harboe, M., et al., *The quantitative role of alternative pathway amplification in classical pathway induced terminal complement activation*. Clin Exp Immunol, 2004. **138**(3): p. 439-46.
11. Wetsel, R., *Structure, function and cellular expression of complement anaphylatoxin receptors*. Curr Opin Immunol, 1995. **7**(1): p. 48-53.
12. Gee, A., M. Boyle, and T. Borsos, *Distinction between C8-mediated and C8/C9-mediated hemolysis on the basis of independent 86Rb and hemoglobin release*. J Immunol, 1980. **124**(4): p. 1905-10.
13. Dalmaso, A. and B. Benson, *Lesions of different functional size produced by human and guinea pig complement in sheep red cell membranes*. J Immunol, 1981. **127**(6): p. 2214-8.
14. Ramm, L., M. Whitlow, and M. Mayer, *The relationship between channel size and the number of C9 molecules in the C5b-9 complex*. J Immunol, 1985. **134**(4): p. 2594-9.
15. Papadimitriou, J., et al., *Quantitative analysis of adenine nucleotides during the prelytic phase of cell death mediated by C5b-9*. J Immunol, 1991. **147**(1): p. 212-7.
16. Niculescu, F., T. Badea, and H. Rus, *Sublytic C5b-9 induces proliferation of human aortic smooth muscle cells: role of mitogen activated protein kinase and phosphatidylinositol 3-kinase*. Atherosclerosis, 1999. **142**(1): p. 47-56.
17. Rus, H., F. Niculescu, and M. Shin, *Sublytic complement attack induces cell cycle in oligodendrocytes*. J Immunol, 1996. **156**(12): p. 4892-900.
18. Fosbrink, M., et al., *C5b-9-induced endothelial cell proliferation and migration are dependent on Akt inactivation of forkhead transcription factor FOXO1*. J Biol Chem, 2006. **281**(28): p. 19009-18.

19. Dashiell, S., H. Rus, and C. Koski, *Terminal complement complexes concomitantly stimulate proliferation and rescue of Schwann cells from apoptosis*. *Glia*, 2000. **30**(2): p. 187-98.
20. Ross, G. and M. Medof, *Membrane complement receptors specific for bound fragments of C3*. *Adv Immunol*, 1985. **37**: p. 217-67.
21. Gasque, P., *Complement: a unique innate immune sensor for danger signals*. *Mol Immunol*, 2004. **41**(11): p. 1089-98.
22. Ross, G. and V. Větvička, *CR3 (CD11b, CD18): a phagocyte and NK cell membrane receptor with multiple ligand specificities and functions*. *Clin Exp Immunol*, 1993. **92**(2): p. 181-4.
23. Crawford, M., et al., *Complement and neutrophil activation in the pathogenesis of ischemic myocardial injury*. *Circulation*, 1988. **78**(6): p. 1449-58.
24. Petty, H. and R.r. Todd, *Receptor-receptor interactions of complement receptor type 3 in neutrophil membranes*. *J Leukoc Biol*, 1993. **54**(5): p. 492-4.
25. Springer, T., *Traffic signals for lymphocyte recirculation and leukocyte emigration: the multistep paradigm*. *Cell*, 1994. **76**(2): p. 301-14.
26. Sugimori, T., D. Griffith, and M. Arnaout, *Emerging paradigms of integrin ligand binding and activation*. *Kidney Int*, 1997. **51**(5): p. 1454-62.
27. Gregory, S., et al., *Complementary adhesion molecules promote neutrophil-Kupffer cell interaction and the elimination of bacteria taken up by the liver*. *J Immunol*, 2002. **168**(1): p. 308-15.
28. Haas, P. and J. van Strijp, *Anaphylatoxins: their role in bacterial infection and inflammation*. *Immunol Res*, 2007. **37**(3): p. 161-75.
29. Ember, J. and T. Hugli, *Complement factors and their receptors*. *Immunopharmacology*, 1997. **38**(1-2): p. 3-15.
30. Ramm, L., M. Whitlow, and M. Mayer, *Transmembrane channel formation by complement: functional analysis of the number of C5b6, C7, C8, and C9 molecules required for a single channel*. *Proc Natl Acad Sci U S A*, 1982. **79**(15): p. 4751-5.
31. Kay, A., H. Shin, and K. Austen, *Selective attraction of eosinophils and synergism between eosinophil chemotactic factor of anaphylaxis (ECF-A) and a fragment cleaved from the fifth component of complement (C5a)*. *Immunology*, 1973. **24**(6): p. 969-76.
32. Hook, W., R. Siraganian, and S. Wahl, *Complement-induced histamine release from human basophils. I. Generation of activity in human serum*. *J Immunol*, 1975. **114**(4): p. 1185-90.
33. Falk, W. and E. Leonard, *Human monocyte chemotaxis: migrating cells are a subpopulation with multiple chemotaxin specificities on each cell*. *Infect Immun*, 1980. **29**(3): p. 953-9.
34. McCarthy, K. and P. Henson, *Induction of lysosomal enzyme secretion by alveolar macrophages in response to the purified complement fragments C5a and C5a des-arg*. *J Immunol*, 1979. **123**(6): p. 2511-7.
35. Yao, J., et al., *Chemotaxis by a CNS macrophage, the microglia*. *J Neurosci Res*, 1990. **27**(1): p. 36-42.
36. Mollnes, T., et al., *Essential role of the C5a receptor in E coli-induced oxidative burst and phagocytosis revealed by a novel lepirudin-based human whole blood model of inflammation*. *Blood*, 2002. **100**(5): p. 1869-77.
37. Sacks, T., et al., *Oxygen radicals mediate endothelial cell damage by complement-stimulated granulocytes. An in vitro model of immune vascular damage*. *J Clin Invest*, 1978. **61**(5): p. 1161-7.

38. Joiner, K., et al., *Studies on the mechanism of bacterial resistance to complement-mediated killing. III. C5b-9 deposits stably on rough and type 7 S. pneumoniae without causing bacterial killing.* J Immunol, 1983. **130**(2): p. 845-9.
39. Fearon, D., *Identification of the membrane glycoprotein that is the C3b receptor of the human erythrocyte, polymorphonuclear leukocyte, B lymphocyte, and monocyte.* J Exp Med, 1980. **152**(1): p. 20-30.
40. Chevalier, J. and M. Kazatchkine, *Distribution in clusters of complement receptor type one (CRI) on human erythrocytes.* J Immunol, 1989. **142**(6): p. 2031-6.
41. Cohen, J., et al., *Peripheral catabolism of CRI (the C3b receptor, CD35) on erythrocytes from healthy individuals and patients with systemic lupus erythematosus (SLE).* Clin Exp Immunol, 1992. **87**(3): p. 422-8.
42. Taylor, R., et al., *Decreased complement mediated binding of antibody/3H-dsDNA immune complexes to the red blood cells of patients with systemic lupus erythematosus, rheumatoid arthritis, and hematologic malignancies.* Arthritis Rheum, 1983. **26**(6): p. 736-44.
43. Verbovetski, I., et al., *Opsonization of apoptotic cells by autologous iC3b facilitates clearance by immature dendritic cells, down-regulates DR and CD86, and up-regulates CC chemokine receptor 7.* J Exp Med, 2002. **196**(12): p. 1553-61.
44. Korb, L. and J. Ahearn, *C1q binds directly and specifically to surface blebs of apoptotic human keratinocytes: complement deficiency and systemic lupus erythematosus revisited.* J Immunol, 1997. **158**(10): p. 4525-8.
45. Taylor, P., et al., *A hierarchical role for classical pathway complement proteins in the clearance of apoptotic cells in vivo.* J Exp Med, 2000. **192**(3): p. 359-66.
46. Nauta, A., et al., *Direct binding of C1q to apoptotic cells and cell blebs induces complement activation.* Eur J Immunol, 2002. **32**(6): p. 1726-36.
47. Chang, M., et al., *C-reactive protein binds to both oxidized LDL and apoptotic cells through recognition of a common ligand: Phosphorylcholine of oxidized phospholipids.* Proc Natl Acad Sci U S A, 2002. **99**(20): p. 13043-8.
48. Pozdnyakova, O., et al., *Impaired antibody response to group B streptococcal type III capsular polysaccharide in C3- and complement receptor 2-deficient mice.* J Immunol, 2003. **170**(1): p. 84-90.
49. Ochsenbein, A., et al., *Protective T cell-independent antiviral antibody responses are dependent on complement.* J Exp Med, 1999. **190**(8): p. 1165-74.
50. Fischer, M., et al., *Regulation of the B cell response to T-dependent antigens by classical pathway complement.* J Immunol, 1996. **157**(2): p. 549-56.
51. Cherukuri, A., P. Cheng, and S. Pierce, *The role of the CD19/CD21 complex in B cell processing and presentation of complement-tagged antigens.* J Immunol, 2001. **167**(1): p. 163-72.
52. Dempsey, P., et al., *C3d of complement as a molecular adjuvant: bridging innate and acquired immunity.* Science, 1996. **271**(5247): p. 348-50.
53. Carter, R. and D. Fearon, *CD19: lowering the threshold for antigen receptor stimulation of B lymphocytes.* Science, 1992. **256**(5053): p. 105-7.
54. Matsumoto, A., et al., *Intersection of the complement and immune systems: a signal transduction complex of the B lymphocyte-containing complement receptor type 2 and CD19.* J Exp Med, 1991. **173**(1): p. 55-64.
55. Bradbury, L., et al., *The CD19/CD21 signal transducing complex of human B lymphocytes includes the target of antiproliferative antibody-1 and Leu-13 molecules.* J Immunol, 1992. **149**(9): p. 2841-50.
56. Liu, Y., et al., *Follicular dendritic cells and germinal centers.* Int Rev Cytol, 1996. **166**: p. 139-79.

57. Reynes, M., et al., *Human follicular dendritic cells express CR1, CR2, and CR3 complement receptor antigens*. J Immunol, 1985. **135**(4): p. 2687-94.
58. Papamichail, M., et al., *Complement dependence of localisation of aggregated IgG in germinal centres*. Scand J Immunol, 1975. **4**(4): p. 343-47.
59. Yoshida, K., T. van den Berg, and C. Dijkstra, *Two functionally different follicular dendritic cells in secondary lymphoid follicles of mouse spleen, as revealed by CR1/2 and FcR gamma II-mediated immune-complex trapping*. Immunology, 1993. **80**(1): p. 34-9.
60. Vora, K., J. Ravetch, and T. Manser, *Amplified follicular immune complex deposition in mice lacking the Fc receptor gamma-chain does not alter maturation of the B cell response*. J Immunol, 1997. **159**(5): p. 2116-24.
61. Cutler, A., et al., *T cell-dependent immune response in C1q-deficient mice: defective interferon gamma production by antigen-specific T cells*. J Exp Med, 1998. **187**(11): p. 1789-97.
62. Snapper, C., et al., *Induction of IgG3 secretion by interferon gamma: a model for T cell-independent class switching in response to T cell-independent type 2 antigens*. J Exp Med, 1992. **175**(5): p. 1367-71.
63. Kopf, M., et al., *Complement component C3 promotes T-cell priming and lung migration to control acute influenza virus infection*. Nat Med, 2002. **8**(4): p. 373-8.
64. Kemper, C., et al., *Activation of human CD4+ cells with CD3 and CD46 induces a T-regulatory cell 1 phenotype*. Nature, 2003. **421**(6921): p. 388-92.
65. Tsiftoglou, S., et al., *The catalytically active serine protease domain of human complement factor I*. Biochemistry, 2005. **44**(16): p. 6239-49.
66. Harrison, R. and P. Lachmann, *Novel cleavage products of the third component of human complement*. Mol Immunol, 1980. **17**(2): p. 219-28.
67. Ross, G., et al., *Generation of three different fragments of bound C3 with purified factor I or serum. I. Requirements for factor H vs CR1 cofactor activity*. J Immunol, 1982. **129**(5): p. 2051-60.
68. Shiraishi, S. and R. Stroud, *Cleavage products of C4b produced by enzymes in human serum*. Immunochemistry, 1975. **12**(12): p. 935-9.
69. Nagasawa, S., C. Ichihara, and R. Stroud, *Cleavage of C4b by C3b inactivator: production of a nicked form of C4b, C4b', as an intermediate cleavage product of C4b by C3b inactivator*. J Immunol, 1980. **125**(2): p. 578-82.
70. Weis, J., et al., *A complement receptor locus: genes encoding C3b/C4b receptor and C3d/Epstein-Barr virus receptor map to 1q32*. J Immunol, 1987. **138**(1): p. 312-5.
71. Heine-Suñer, D., et al., *A high-resolution map of the regulator of the complement activation gene cluster on 1q32 that integrates new genes and markers*. Immunogenetics, 1997. **45**(6): p. 422-7.
72. Barlow, P., et al., *Secondary structure of a complement control protein module by two-dimensional 1H NMR*. Biochemistry, 1991. **30**(4): p. 997-1004.
73. Chou, K. and R. Heinrikson, *Prediction of the tertiary structure of the complement control protein module*. J Protein Chem, 1997. **16**(8): p. 765-73.
74. Pangburn, M., R. Schreiber, and H. Müller-Eberhard, *Human complement C3b inactivator: isolation, characterization, and demonstration of an absolute requirement for the serum protein beta1H for cleavage of C3b and C4b in solution*. J Exp Med, 1977. **146**(1): p. 257-70.
75. Weiler, J., et al., *Control of the amplification convertase of complement by the plasma protein beta1H*. Proc Natl Acad Sci U S A, 1976. **73**(9): p. 3268-72.

76. Pangburn, M., R. Schreiber, and H. Müller-Eberhard, *C3b deposition during activation of the alternative complement pathway and the effect of deposition on the activating surface*. J Immunol, 1983. **131**(4): p. 1930-5.
77. Kazatchkine, M., D. Fearon, and K. Austen, *Human alternative complement pathway: membrane-associated sialic acid regulates the competition between B and beta1 H for cell-bound C3b*. J Immunol, 1979. **122**(1): p. 75-81.
78. Fearon, D., *Regulation by membrane sialic acid of beta1H-dependent decay-dissociation of amplification C3 convertase of the alternative complement pathway*. Proc Natl Acad Sci U S A, 1978. **75**(4): p. 1971-5.
79. Ripoche, J., et al., *The complete amino acid sequence of human complement factor H*. Biochem J, 1988. **249**(2): p. 593-602.
80. Kühn, S., C. Skerka, and P. Zipfel, *Mapping of the complement regulatory domains in the human factor H-like protein 1 and in factor H1*. J Immunol, 1995. **155**(12): p. 5663-70.
81. Alsenz, J., et al., *Structural and functional analysis of the complement component factor H with the use of different enzymes and monoclonal antibodies to factor H*. Biochem J, 1985. **232**(3): p. 841-50.
82. Gordon, D., et al., *Identification of complement regulatory domains in human factor H*. J Immunol, 1995. **155**(1): p. 348-56.
83. Jokiranta, T., et al., *Analysis of the recognition mechanism of the alternative pathway of complement by monoclonal anti-factor H antibodies: evidence for multiple interactions between H and surface bound C3b*. FEBS Lett, 1996. **393**(2-3): p. 297-302.
84. Zipfel, P. and C. Skerka, *FHL-1/reconnectin: a human complement and immune regulator with cell-adhesive function*. Immunol Today, 1999. **20**(3): p. 135-40.
85. Hellwege, J., et al., *Functional properties of complement factor H-related proteins FHR-3 and FHR-4: binding to the C3d region of C3b and differential regulation by heparin*. FEBS Lett, 1999. **462**(3): p. 345-52.
86. Murphy, B., et al., *Factor H-related protein-5: a novel component of human glomerular immune deposits*. Am J Kidney Dis, 2002. **39**(1): p. 24-7.
87. McRae, J.L., et al., *Human factor H-related protein 5 has cofactor activity, inhibits C3 convertase activity, binds heparin and C-reactive protein, and associates with lipoprotein*. J Immunol, 2005. **174**(10): p. 6250-6.
88. Barilla-LaBarca, M., et al., *Role of membrane cofactor protein (CD46) in regulation of C4b and C3b deposited on cells*. J Immunol, 2002. **168**(12): p. 6298-304.
89. Liszewski, M.K., I. Tedja, and J.P. Atkinson, *Membrane cofactor protein (CD46) of complement. Processing differences related to alternatively spliced cytoplasmic domains*. J Biol Chem, 1994. **269**(14): p. 10776-9.
90. Devaux, P., et al., *Control of C3b and C5b deposition by CD46 (membrane cofactor protein) after alternative but not classical complement activation*. Eur J Immunol, 1999. **29**(3): p. 815-22.
91. Nanche, D., et al., *Human membrane cofactor protein (CD46) acts as a cellular receptor for measles virus*. J Virol, 1993. **67**(10): p. 6025-32.
92. Dörig, R., et al., *The human CD46 molecule is a receptor for measles virus (Edmonston strain)*. Cell, 1993. **75**(2): p. 295-305.
93. Santoro, F., et al., *CD46 is a cellular receptor for human herpesvirus 6*. Cell, 1999. **99**(7): p. 817-27.
94. Giannakis, E., et al., *Identification of the streptococcal M protein binding site on membrane cofactor protein (CD46)*. J Immunol, 2002. **168**(9): p. 4585-92.

95. Johansson, L., et al., *CD46 in meningococcal disease*. *Science*, 2003. **301**(5631): p. 373-5.
96. Segerman, A., et al., *Adenovirus type 11 uses CD46 as a cellular receptor*. *J Virol*, 2003. **77**(17): p. 9183-91.
97. Schnorr, J., et al., *Measles virus-induced down-regulation of CD46 is associated with enhanced sensitivity to complement-mediated lysis of infected cells*. *Eur J Immunol*, 1995. **25**(4): p. 976-84.
98. Rivaller, P., et al., *Enhanced MHC class II-restricted presentation of measles virus (MV) hemagglutinin in transgenic mice expressing human MV receptor CD46*. *Eur J Immunol*, 1998. **28**(4): p. 1301-14.
99. Cardoso, A., et al., *Formaldehyde inactivation of measles virus abolishes CD46-dependent presentation of nucleoprotein to murine class I-restricted CTLs but not to class II-restricted helper T cells*. *Virology*, 1995. **212**(1): p. 255-8.
100. Karp, C., et al., *Mechanism of suppression of cell-mediated immunity by measles virus*. *Science*, 1996. **273**(5272): p. 228-31.
101. Katayama, Y., A. Hirano, and T. Wong, *Human receptor for measles virus (CD46) enhances nitric oxide production and restricts virus replication in mouse macrophages by modulating production of alpha/beta interferon*. *J Virol*, 2000. **74**(3): p. 1252-7.
102. Gerlier, D., et al., *Efficient MHC class II-restricted presentation of measles virus to T cells relies on its targeting to its cellular receptor human CD46 and involves an endosomal pathway*. *Cell Biol Int*, 1994. **18**(5): p. 315-20.
103. Nicholson-Weller, A. and C. Wang, *Structure and function of decay accelerating factor CD55*. *J Lab Clin Med*, 1994. **123**(4): p. 485-91.
104. Caras, I., et al., *Cloning of decay-accelerating factor suggests novel use of splicing to generate two proteins*. *Nature*, 1987. **325**(6104): p. 545-9.
105. Medof, M., et al., *Cloning and characterization of cDNAs encoding the complete sequence of decay-accelerating factor of human complement*. *Proc Natl Acad Sci U S A*, 1987. **84**(7): p. 2007-11.
106. Brodbeck, W., et al., *Cooperation between decay-accelerating factor and membrane cofactor protein in protecting cells from autologous complement attack*. *J Immunol*, 2000. **165**(7): p. 3999-4006.
107. Morgan, B. and S. Meri, *Membrane proteins that protect against complement lysis*. *Springer Semin Immunopathol*, 1994. **15**(4): p. 369-96.
108. Kinoshita, T., et al., *Distribution of decay-accelerating factor in the peripheral blood of normal individuals and patients with paroxysmal nocturnal hemoglobinuria*. *J Exp Med*, 1985. **162**(1): p. 75-92.
109. Moore, J., et al., *Decay-accelerating factor is present on paroxysmal nocturnal hemoglobinuria erythroid progenitors and lost during erythropoiesis in vitro*. *J Exp Med*, 1985. **162**(4): p. 1182-92.
110. Nicholson-Weller, A., et al., *Surface membrane expression by human blood leukocytes and platelets of decay-accelerating factor, a regulatory protein of the complement system*. *Blood*, 1985. **65**(5): p. 1237-44.
111. Medof, M., et al., *Identification of the complement decay-accelerating factor (DAF) on epithelium and glandular cells and in body fluids*. *J Exp Med*, 1987. **165**(3): p. 848-64.
112. Song, W., et al., *Mouse decay-accelerating factor: selective and tissue-specific induction by estrogen of the gene encoding the glycosylphosphatidylinositol-anchored form*. *J Immunol*, 1996. **157**(9): p. 4166-72.

113. Spicer, A., M. Seldin, and S. Gendler, *Molecular cloning and chromosomal localization of the mouse decay-accelerating factor genes. Duplicated genes encode glycosylphosphatidylinositol-anchored and transmembrane forms.* J Immunol, 1995. **155**(6): p. 3079-91.
114. Harris, C., N. Rushmere, and B. Morgan, *Molecular and functional analysis of mouse decay accelerating factor (CD55).* Biochem J, 1999. **341** (Pt 3): p. 821-9.
115. Shafren, D., et al., *Coxsackievirus A21 binds to decay-accelerating factor but requires intercellular adhesion molecule 1 for cell entry.* J Virol, 1997. **71**(6): p. 4736-43.
116. Hafenstein, S., et al., *Interaction of decay-accelerating factor with coxsackievirus B3.* J Virol, 2007. **81**(23): p. 12927-35.
117. Scharfstein, J., et al., *Human C4-binding protein. I. Isolation and characterization.* J Exp Med, 1978. **148**(1): p. 207-22.
118. Dahlbäck, B. and H. Müller-Eberhard, *Ultrastructure of C4b-binding protein fragments formed by limited proteolysis using chymotrypsin.* J Biol Chem, 1984. **259**(19): p. 11631-4.
119. Gigli, I., T. Fujita, and V. Nussenzweig, *Modulation of the classical pathway C3 convertase by plasma proteins C4 binding protein and C3b inactivator.* Proc Natl Acad Sci U S A, 1979. **76**(12): p. 6596-600.
120. Helsing, M., et al., *The localization of heparin-binding fragments on human C4b-binding protein.* J Immunol, 1990. **144**(1): p. 204-8.
121. Dahlbäck, B. and J. Stenflo, *High molecular weight complex in human plasma between vitamin K-dependent protein S and complement component C4b-binding protein.* Proc Natl Acad Sci U S A, 1981. **78**(4): p. 2512-6.
122. Schwalbe, R., et al., *Assembly of protein S and C4b-binding protein on membranes.* J Biol Chem, 1990. **265**(27): p. 16074-81.
123. Foley, S., et al., *Mouse Crry/p65 is a regulator of the alternative pathway of complement activation.* Eur J Immunol, 1993. **23**(6): p. 1381-4.
124. Kim, Y.U., et al., *Mouse complement regulatory protein Crry/p65 uses the specific mechanisms of both human decay-accelerating factor and membrane cofactor protein.* J Exp Med, 1995. **181**(1): p. 151-9.
125. Gettins, P., *Serpin structure, mechanism, and function.* Chem Rev, 2002. **102**(12): p. 4751-804.
126. Ziccardi, R., *Activation of the early components of the classical complement pathway under physiologic conditions.* J Immunol, 1981. **126**(5): p. 1769-73.
127. Ambrus, G., et al., *Natural substrates and inhibitors of mannan-binding lectin-associated serine protease-1 and -2: a study on recombinant catalytic fragments.* J Immunol, 2003. **170**(3): p. 1374-82.
128. Matsushita, M., Y. Endo, and T. Fujita, *Cutting edge: complement-activating complex of ficolin and mannose-binding lectin-associated serine protease.* J Immunol, 2000. **164**(5): p. 2281-4.
129. Matsushita, M., et al., *Proteolytic activities of two types of mannose-binding lectin-associated serine protease.* J Immunol, 2000. **165**(5): p. 2637-42.
130. Gigli, I., et al., *Interaction of plasma kallikrein with the C1 inhibitor.* J Immunol, 1970. **104**(3): p. 574-81.
131. Rollins, S. and P. Sims, *The complement-inhibitory activity of CD59 resides in its capacity to block incorporation of C9 into membrane C5b-9.* J Immunol, 1990. **144**(9): p. 3478-83.

132. Farkas, I., et al., *CD59 blocks not only the insertion of C9 into MAC but inhibits ion channel formation by homologous C5b-8 as well as C5b-9*. J Physiol, 2002. **539**(Pt 2): p. 537-45.
133. Sugita, Y., et al., *Determination of carboxyl-terminal residue and disulfide bonds of MACIF (CD59), a glycosyl-phosphatidylinositol-anchored membrane protein*. J Biochem, 1993. **114**(4): p. 473-7.
134. Meri, S., H. Waldmann, and P. Lachmann, *Distribution of protectin (CD59), a complement membrane attack inhibitor, in normal human tissues*. Lab Invest, 1991. **65**(5): p. 532-7.
135. Qian, Y., et al., *Identification and functional characterization of a new gene encoding the mouse terminal complement inhibitor CD59*. J Immunol, 2000. **165**(5): p. 2528-34.
136. Baalalabramanian, S., et al., *CD59a is the primary regulator of membrane attack complex assembly in the mouse*. J Immunol, 2004. **173**(6): p. 3684-92.
137. Cooper, N., *Immune adherence by the fourth component of complement*. Science, 1969. **165**(891): p. 396-8.
138. Yoon, S. and D. Fearon, *Characterization of a soluble form of the C3b/C4b receptor (CR1) in human plasma*. J Immunol, 1985. **134**(5): p. 3332-8.
139. Pascual, M., et al., *Circulating soluble CR1 (CD35). Serum levels in diseases and evidence for its release by human leukocytes*. J Immunol, 1993. **151**(3): p. 1702-11.
140. Hamer, I., et al., *Soluble form of complement C3b/C4b receptor (CR1) results from a proteolytic cleavage in the C-terminal region of CR1 transmembrane domain*. Biochem J, 1998. **329** (Pt 1): p. 183-90.
141. Klickstein, L., et al., *Identification of distinct C3b and C4b recognition sites in the human C3b/C4b receptor (CR1, CD35) by deletion mutagenesis*. J Exp Med, 1988. **168**(5): p. 1699-717.
142. Hourcade, D., et al., *Identification of an alternative polyadenylation site in the human C3b/C4b receptor (complement receptor type 1) transcriptional unit and prediction of a secreted form of complement receptor type 1*. J Exp Med, 1988. **168**(4): p. 1255-70.
143. Krych, M., D. Hourcade, and J. Atkinson, *Sites within the complement C3b/C4b receptor important for the specificity of ligand binding*. Proc Natl Acad Sci U S A, 1991. **88**(10): p. 4353-7.
144. Krych, M., R. Hauhart, and J. Atkinson, *Structure-function analysis of the active sites of complement receptor type 1*. J Biol Chem, 1998. **273**(15): p. 8623-9.
145. Krych, M., et al., *Analysis of the functional domains of complement receptor type 1 (C3b/C4b receptor; CD35) by substitution mutagenesis*. J Biol Chem, 1994. **269**(18): p. 13273-8.
146. Lindorfer, M., et al., *Heteropolymer-mediated clearance of immune complexes via erythrocyte CR1: mechanisms and applications*. Immunol Rev, 2001. **183**: p. 10-24.
147. Hess, C. and J. Schifferli, *Immune adherence revisited: novel players in an old game*. News Physiol Sci, 2003. **18**: p. 104-8.
148. Cornacoff, J., et al., *Primate erythrocyte-immune complex-clearing mechanism*. J Clin Invest, 1983. **71**(2): p. 236-47.
149. Iida, K., L. Nadler, and V. Nussenzweig, *Identification of the membrane receptor for the complement fragment C3d by means of a monoclonal antibody*. J Exp Med, 1983. **158**(4): p. 1021-33.
150. Weis, J., T. Tedder, and D. Fearon, *Identification of a 145,000 Mr membrane protein as the C3d receptor (CR2) of human B lymphocytes*. Proc Natl Acad Sci U S A, 1984. **81**(3): p. 881-5.

151. Lowell, C., et al., *Mapping of the Epstein-Barr virus and C3dg binding sites to a common domain on complement receptor type 2*. J Exp Med, 1989. **170**(6): p. 1931-46.
152. Szakonyi, G., et al., *Structure of complement receptor 2 in complex with its C3d ligand*. Science, 2001. **292**(5522): p. 1725-8.
153. Moore, M., et al., *Inhibition of Epstein-Barr virus infection in vitro and in vivo by soluble CR2 (CD21) containing two short consensus repeats*. J Virol, 1991. **65**(7): p. 3559-65.
154. Pramoonjago, P., et al., *Ligand specificities of mouse complement receptor types 1 (CR1) and 2 (CR2) purified from spleen cells*. Int Immunol, 1993. **5**(4): p. 337-43.
155. Molina, H., et al., *Analysis of C3b/C3d binding sites and factor I cofactor regions within mouse complement receptors 1 and 2*. J Immunol, 1994. **153**(2): p. 789-95.
156. Hu, H., et al., *Expression of the murine CD21 gene is regulated by promoter and intronic sequences*. J Immunol, 1997. **158**(10): p. 4758-68.
157. Erdei, A., et al., *Role of C3b receptors in the enhancement of interleukin-2-dependent T-cell proliferation*. Mol Immunol, 1984. **21**(12): p. 1215-21.
158. Dupuy, A. and E. Caron, *Integrin-dependent phagocytosis: spreading from microadhesion to new concepts*. J Cell Sci, 2008. **121**(Pt 11): p. 1773-83.
159. Myones, B., et al., *Neutrophil and monocyte cell surface p150,95 has iC3b-receptor (CR4) activity resembling CR3*. J Clin Invest, 1988. **82**(2): p. 640-51.
160. Larson, R. and T. Springer, *Structure and function of leukocyte integrins*. Immunol Rev, 1990. **114**: p. 181-217.
161. Helmy, K., et al., *CR1g: a macrophage complement receptor required for phagocytosis of circulating pathogens*. Cell, 2006. **124**(5): p. 915-27.
162. Lee, M., et al., *Z39Ig is expressed on macrophages and may mediate inflammatory reactions in arthritis and atherosclerosis*. J Leukoc Biol, 2006. **80**(4): p. 922-8.
163. Vogt, L., et al., *VSIG4, a B7 family-related protein, is a negative regulator of T cell activation*. J Clin Invest, 2006. **116**(10): p. 2817-26.
164. Gorgani, N., et al., *Complement receptor of the Ig superfamily enhances complement-mediated phagocytosis in a subpopulation of tissue resident macrophages*. J Immunol, 2008. **181**(11): p. 7902-8.
165. Kim, D., et al., *Deficiency of decay-accelerating factor and complement receptor 1-related gene/protein y on murine platelets leads to complement-dependent clearance by the macrophage phagocytic receptor CR1g*. Blood, 2008. **112**(4): p. 1109-19.
166. Wiesmann, C., et al., *Structure of C3b in complex with CR1g gives insights into regulation of complement activation*. Nature, 2006. **444**(7116): p. 217-20.
167. Katschke, K.J., et al., *A novel inhibitor of the alternative pathway of complement reverses inflammation and bone destruction in experimental arthritis*. J Exp Med, 2007. **204**(6): p. 1319-25.
168. Frank, M., *Complement deficiencies*. Pediatr Clin North Am, 2000. **47**(6): p. 1339-54.
169. Rooijackers, S. and J. van Strijp, *Bacterial complement evasion*. Mol Immunol, 2007. **44**(1-3): p. 23-32.
170. Kraiczy, P. and R. Würzner, *Complement escape of human pathogenic bacteria by acquisition of complement regulators*. Mol Immunol, 2006. **43**(1-2): p. 31-44.
171. Bernet, J., et al., *Viral mimicry of the complement system*. J Biosci, 2003. **28**(3): p. 249-64.
172. Meri, T., et al., *The hyphal and yeast forms of Candida albicans bind the complement regulator C4b-binding protein*. Infect Immun, 2004. **72**(11): p. 6633-41.

173. Rooijackers, S., et al., *Immune evasion by a staphylococcal complement inhibitor that acts on C3 convertases*. *Nat Immunol*, 2005. **6**(9): p. 920-7.
174. Skerra, A., *Lipocalins as a scaffold*. *Biochim Biophys Acta*, 2000. **1482**(1-2): p. 337-50.
175. Nunn, M., et al., *Complement inhibitor of C5 activation from the soft tick *Ornithodoros moubata**. *J Immunol*, 2005. **174**(4): p. 2084-91.
176. Hepburn, N., et al., *In vivo characterization and therapeutic efficacy of a C5-specific inhibitor from the soft tick *Ornithodoros moubata**. *J Biol Chem*, 2007. **282**(11): p. 8292-9.
177. Fredslund, F., et al., *Structure of and influence of a tick complement inhibitor on human complement component 5*. *Nat Immunol*, 2008. **9**(7): p. 753-60.
178. Zhang, M., et al., *Activation of the lectin pathway by natural IgM in a model of ischemia/reperfusion injury*. *J Immunol*, 2006. **177**(7): p. 4727-34.
179. Austen, W.J., et al., *The role of complement and natural antibody in intestinal ischemia-reperfusion injury*. *Int J Immunopathol Pharmacol*, 2003. **16**(1): p. 1-8.
180. Collard, C., et al., *Complement activation following oxidative stress*. *Mol Immunol*. **36**(13-14): p. 941-8.
181. Thurman, J., et al., *Lack of a functional alternative complement pathway ameliorates ischemic acute renal failure in mice*. *J Immunol*, 2003. **170**(3): p. 1517-23.
182. Kyriakides, C., et al., *Skeletal muscle reperfusion injury is mediated by neutrophils and the complement membrane attack complex*. *Am J Physiol*, 1999. **277**(6 Pt 1): p. C1263-8.
183. Spain, D., et al., *Complement activation mediates intestinal injury after resuscitation from hemorrhagic shock*. *J Trauma*, 1999. **46**(2): p. 224-33.
184. Jordan, J., M. Montalto, and G. Stahl, *Inhibition of mannose-binding lectin reduces postischemic myocardial reperfusion injury*. *Circulation*, 2001. **104**(12): p. 1413-8.
185. Weisman, H., et al., *Soluble human complement receptor type 1: in vivo inhibitor of complement suppressing post-ischemic myocardial inflammation and necrosis*. *Science*, 1990. **249**(4965): p. 146-51.
186. Woodcock, S., et al., *Soluble P-selectin moderates complement dependent injury*. *Shock*, 2000. **14**(6): p. 610-5.
187. Stahl, G., et al., *Role for the alternative complement pathway in ischemia/reperfusion injury*. *Am J Pathol*, 2003. **162**(2): p. 449-55.
188. Dreyer, W., et al., *Neutrophil accumulation in ischemic canine myocardium. Insights into time course, distribution, and mechanism of localization during early reperfusion*. *Circulation*, 1991. **84**(1): p. 400-11.
189. Nicholson-Weller, A. and J. Halperin, *Membrane signaling by complement C5b-9, the membrane attack complex*. *Immunol Res*, 1993. **12**(3): p. 244-57.
190. Zhou, W., et al., *Predominant role for C5b-9 in renal ischemia/reperfusion injury*. *J Clin Invest*, 2000. **105**(10): p. 1363-71.
191. Gardai, S., et al., *Recognition ligands on apoptotic cells: a perspective*. *J Leukoc Biol*, 2006. **79**(5): p. 896-903.
192. Minami, K., et al., *C4d deposition and clearance in cardiac transplants correlates with alloantibody levels and rejection in rats*. *Am J Transplant*, 2006. **6**(5 Pt 1): p. 923-32.
193. Wehner, J., et al., *Antibody and complement in transplant vasculopathy*. *Circ Res*, 2007. **100**(2): p. 191-203.
194. Smith, R., et al., *Chronic antibody mediated rejection of renal allografts: pathological, serological and immunologic features in nonhuman primates*. *Am J Transplant*, 2006. **6**(8): p. 1790-8.

195. Davies, K., J. Schifferli, and M. Walport, *Complement deficiency and immune complex disease*. Springer Semin Immunopathol, 1994. **15**(4): p. 397-416.
196. Botto, M., et al., *Homozygous C1q deficiency causes glomerulonephritis associated with multiple apoptotic bodies*. Nat Genet, 1998. **19**(1): p. 56-9.
197. Brodeur, J., et al., *Synovial fluid levels of complement SC5b-9 and fragment Bb are elevated in patients with rheumatoid arthritis*. Arthritis Rheum, 1991. **34**(12): p. 1531-7.
198. Banda, N., et al., *Alternative complement pathway activation is essential for inflammation and joint destruction in the passive transfer model of collagen-induced arthritis*. J Immunol, 2006. **177**(3): p. 1904-12.
199. Jarvis, J., et al., *Complement activation and immune complexes in children with polyarticular juvenile rheumatoid arthritis: a longitudinal study*. J Rheumatol, 1994. **21**(6): p. 1124-7.
200. Mewar, D. and A. Wilson, *Autoantibodies in rheumatoid arthritis: a review*. Biomed Pharmacother, 2006. **60**(10): p. 648-55.
201. Hanauske-Abel, H., B. Pontz, and H. Schorlemmer, *Cartilage specific collagen activates macrophages and the alternative pathway of complement: evidence for an immunopathogenic concept of rheumatoid arthritis*. Ann Rheum Dis, 1982. **41**(2): p. 168-76.
202. Schaapherder, A., et al., *Human complement activation via the alternative pathway on porcine endothelium initiated by IgA antibodies*. Transplantation, 1995. **60**(3): p. 287-91.
203. Banda, N., et al., *Pathogenic complement activation in collagen antibody-induced arthritis in mice requires amplification by the alternative pathway*. J Immunol, 2007. **179**(6): p. 4101-9.
204. Swaak, A., et al., *An analysis of the levels of complement components in the synovial fluid in rheumatic diseases*. Clin Rheumatol, 1987. **6**(3): p. 350-7.
205. Morgan, B., R. Daniels, and B. Williams, *Measurement of terminal complement complexes in rheumatoid arthritis*. Clin Exp Immunol, 1988. **73**(3): p. 473-8.
206. Anthony, D. and T. Haqqi, *Collagen-induced arthritis in mice: an animal model to study the pathogenesis of rheumatoid arthritis*. Clin Exp Rheumatol, 1999. **17**(2): p. 240-4.
207. Hietala, M., et al., *Complement deficiency ameliorates collagen-induced arthritis in mice*. J Immunol, 2002. **169**(1): p. 454-9.
208. Hietala, M., et al., *Complement activation by both classical and alternative pathways is critical for the effector phase of arthritis*. Eur J Immunol, 2004. **34**(4): p. 1208-16.
209. Wang, Y., et al., *A role for complement in antibody-mediated inflammation: C5-deficient DBA/1 mice are resistant to collagen-induced arthritis*. J Immunol, 2000. **164**(8): p. 4340-7.
210. Wang, Y., et al., *Anti-C5 monoclonal antibody therapy prevents collagen-induced arthritis and ameliorates established disease*. Proc Natl Acad Sci U S A, 1995. **92**(19): p. 8955-9.
211. Williams, A., et al., *Deletion of the gene encoding CD59a in mice increases disease severity in a murine model of rheumatoid arthritis*. Arthritis Rheum, 2004. **50**(9): p. 3035-44.
212. Storch, M., et al., *Multiple sclerosis: in situ evidence for antibody- and complement-mediated demyelination*. Ann Neurol, 1998. **43**(4): p. 465-71.
213. Rus, H., C. Cudrici, and F. Niculescu, *C5b-9 complement complex in autoimmune demyelination and multiple sclerosis: dual role in neuroinflammation and neuroprotection*. Ann Med, 2005. **37**(2): p. 97-104.

214. Lumsden, C., *The immunogenesis of the multiple sclerosis plaque*. Brain Res, 1971. **28(3)**: p. 365-90.
215. Reindl, M., et al., *Antibodies against the myelin oligodendrocyte glycoprotein and the myelin basic protein in multiple sclerosis and other neurological diseases: a comparative study*. Brain, 1999. **122 (Pt 11)**: p. 2047-56.
216. Vanguri, P., et al., *Complement activation by isolated myelin: activation of the classical pathway in the absence of myelin-specific antibodies*. Proc Natl Acad Sci U S A, 1982. **79(10)**: p. 3290-4.
217. Wren, D. and M. Noble, *Oligodendrocytes and oligodendrocyte/type-2 astrocyte progenitor cells of adult rats are specifically susceptible to the lytic effects of complement in absence of antibody*. Proc Natl Acad Sci U S A, 1989. **86(22)**: p. 9025-9.
218. Compston, D., et al., *Cerebrospinal fluid C9 in demyelinating disease*. Neurology, 1986. **36(11)**: p. 1503-6.
219. Morgan, B., A. Campbell, and D. Compston, *Terminal component of complement (C9) in cerebrospinal fluid of patients with multiple sclerosis*. Lancet, 1984. **2(8397)**: p. 251-4.
220. Sanders, M., et al., *Terminal complement complexes (SC5b-9) in cerebrospinal fluid in autoimmune nervous system diseases*. Ann N Y Acad Sci, 1988. **540**: p. 387-8.
221. Wing, M., et al., *Oligodendrocytes lack glycolipid anchored proteins which protect them against complement lysis. Restoration of resistance to lysis by incorporation of CD59*. Immunology, 1992. **76(1)**: p. 140-5.
222. Gold, R., C. Lington, and H. Lassmann, *Understanding pathogenesis and therapy of multiple sclerosis via animal models: 70 years of merits and culprits in experimental autoimmune encephalomyelitis research*. Brain, 2006. **129(Pt 8)**: p. 1953-71.
223. Piddlesden, S., et al., *The demyelinating potential of antibodies to myelin oligodendrocyte glycoprotein is related to their ability to fix complement*. Am J Pathol, 1993. **143(2)**: p. 555-64.
224. Mead, R., et al., *Deficiency of the complement regulator CD59a enhances disease severity, demyelination and axonal injury in murine acute experimental allergic encephalomyelitis*. Lab Invest, 2004. **84(1)**: p. 21-8.
225. Mead, R., et al., *The membrane attack complex of complement causes severe demyelination associated with acute axonal injury*. J Immunol, 2002. **168(1)**: p. 458-65.
226. Soane, L., et al., *Inhibition of oligodendrocyte apoptosis by sublytic C5b-9 is associated with enhanced synthesis of bcl-2 and mediated by inhibition of caspase-3 activation*. J Immunol, 1999. **163(11)**: p. 6132-8.
227. Soane, L., et al., *C5b-9 terminal complement complex protects oligodendrocytes from death by regulating Bad through phosphatidylinositol 3-kinase/Akt pathway*. J Immunol, 2001. **167(4)**: p. 2305-11.
228. Esposti, M., *The roles of Bid*. Apoptosis, 2002. **7(5)**: p. 433-40.
229. Kostner, K., *Activation of the complement system: a crucial link between inflammation and atherosclerosis?* Eur J Clin Invest, 2004. **34(12)**: p. 800-2.
230. Niculescu, F. and H. Rus, *Complement activation and atherosclerosis*. Mol Immunol, 1999. **36(13-14)**: p. 949-55.
231. Niculescu, F. and H. Rus, *Mechanisms of signal transduction activated by sublytic assembly of terminal complement complexes on nucleated cells*. Immunol Res, 2001. **24(2)**: p. 191-9.

232. Stary, H., et al., *A definition of advanced types of atherosclerotic lesions and a histological classification of atherosclerosis. A report from the Committee on Vascular Lesions of the Council on Arteriosclerosis, American Heart Association.* *Circulation*, 1995. **92**(5): p. 1355-74.
233. Niculescu, F., T. Niculescu, and H. Rus, *C5b-9 terminal complement complex assembly on apoptotic cells in human arterial wall with atherosclerosis.* *Exp Mol Pathol*, 2004. **76**(1): p. 17-23.
234. Seifert, P., et al., *Isolation and characterization of a complement-activating lipid extracted from human atherosclerotic lesions.* *J Exp Med*, 1990. **172**(2): p. 547-57.
235. Bhakdi, S., et al., *On the pathogenesis of atherosclerosis: enzymatic transformation of human low density lipoprotein to an atherogenic moiety.* *J Exp Med*, 1995. **182**(6): p. 1959-71.
236. Bhakdi, S., et al., *Complement and atherogenesis: binding of CRP to degraded, nonoxidized LDL enhances complement activation.* *Arterioscler Thromb Vasc Biol*, 1999. **19**(10): p. 2348-54.
237. Vlaicu, R., et al., *Immunoglobulins and complement components in human aortic atherosclerotic intima.* *Atherosclerosis*, 1985. **55**(1): p. 35-50.
238. Seifert, P. and G. Hansson, *Complement receptors and regulatory proteins in human atherosclerotic lesions.* *Arteriosclerosis*, 1989. **9**(6): p. 802-11.
239. Vlaicu, R., et al., *Immunohistochemical localization of the terminal C5b-9 complement complex in human aortic fibrous plaque.* *Atherosclerosis*, 1985. **57**(2-3): p. 163-77.
240. Oksjoki, R., et al., *Function and regulation of the complement system in cardiovascular diseases.* *Front Biosci*, 2007. **12**: p. 4696-708.
241. Schmiedt, W., et al., *Complement C6 deficiency protects against diet-induced atherosclerosis in rabbits.* *Arterioscler Thromb Vasc Biol*, 1998. **18**(11): p. 1790-5.
242. Lewis, R., et al., *The membrane attack complex of complement drives the progression of atherosclerosis in apolipoprotein E knockout mice.* *Mol Immunol*, 2010. **47**(5): p. 1098-105.
243. Patel, S., et al., *ApoE(-/-) mice develop atherosclerosis in the absence of complement component C5.* *Biochem Biophys Res Commun*, 2001. **286**(1): p. 164-70.
244. Appel, G., et al., *Membranoproliferative glomerulonephritis type II (dense deposit disease): an update.* *J Am Soc Nephrol*, 2005. **16**(5): p. 1392-403.
245. Zipfel, P., et al., *Complement and diseases: defective alternative pathway control results in kidney and eye diseases.* *Mol Immunol*, 2006. **43**(1-2): p. 97-106.
246. Ault, B., et al., *Human factor H deficiency. Mutations in framework cysteine residues and block in H protein secretion and intracellular catabolism.* *J Biol Chem*, 1997. **272**(40): p. 25168-75.
247. Dragon-Durey, M., et al., *Heterozygous and homozygous factor h deficiencies associated with hemolytic uremic syndrome or membranoproliferative glomerulonephritis: report and genetic analysis of 16 cases.* *J Am Soc Nephrol*, 2004. **15**(3): p. 787-95.
248. Licht, C., et al., *Deletion of Lys224 in regulatory domain 4 of Factor H reveals a novel pathomechanism for dense deposit disease (MPGN II).* *Kidney Int*, 2006. **70**(1): p. 42-50.
249. Pérez-Caballero, D., et al., *Clustering of missense mutations in the C-terminal region of factor H in atypical hemolytic uremic syndrome.* *Am J Hum Genet*, 2001. **68**(2): p. 478-84.
250. Fremaux-Bacchi, V., et al., *Complement factor I: a susceptibility gene for atypical haemolytic uraemic syndrome.* *J Med Genet*, 2004. **41**(6): p. e84.

251. Fremeaux-Bacchi, V., et al., *Genetic and functional analyses of membrane cofactor protein (CD46) mutations in atypical hemolytic uremic syndrome*. J Am Soc Nephrol, 2006. **17**(7): p. 2017-25.
252. Fremeaux-Bacchi, V., et al., *Unusual clinical severity of complement membrane cofactor protein-associated hemolytic-uremic syndrome and uniparental isodisomy*. Am J Kidney Dis, 2007. **49**(2): p. 323-9.
253. Manuelian, T., et al., *Mutations in factor H reduce binding affinity to C3b and heparin and surface attachment to endothelial cells in hemolytic uremic syndrome*. J Clin Invest, 2003. **111**(8): p. 1181-90.
254. Noris, M., et al., *Familial haemolytic uraemic syndrome and an MCP mutation*. Lancet, 2003. **362**(9395): p. 1542-7.
255. Goicoechea de Jorge, E., et al., *Gain-of-function mutations in complement factor B are associated with atypical hemolytic uremic syndrome*. Proc Natl Acad Sci U S A, 2007. **104**(1): p. 240-5.
256. Sánchez-Corral, P., et al., *Structural and functional characterization of factor H mutations associated with atypical hemolytic uremic syndrome*. Am J Hum Genet, 2002. **71**(6): p. 1285-95.
257. Sánchez-Corral, P., et al., *Functional analysis in serum from atypical Hemolytic Uremic Syndrome patients reveals impaired protection of host cells associated with mutations in factor H*. Mol Immunol, 2004. **41**(1): p. 81-4.
258. Takahashi, M., et al., *Deficient biosynthesis of N-acetylglucosaminyl-phosphatidylinositol, the first intermediate of glycosyl phosphatidylinositol anchor biosynthesis, in cell lines established from patients with paroxysmal nocturnal hemoglobinuria*. J Exp Med, 1993. **177**(2): p. 517-21.
259. Wiedmer, T., et al., *Complement-induced vesiculation and exposure of membrane prothrombinase sites in platelets of paroxysmal nocturnal hemoglobinuria*. Blood, 1993. **82**(4): p. 1192-6.
260. Bessler, M., et al., *Paroxysmal nocturnal haemoglobinuria (PNH) is caused by somatic mutations in the PIG-A gene*. EMBO J, 1994. **13**(1): p. 110-7.
261. Vogel, C., et al., *Structure and function of cobra venom factor, the complement-activating protein in cobra venom*. Adv Exp Med Biol, 1996. **391**: p. 97-114.
262. Kölln, J., et al., *Complement inactivation by recombinant human C3 derivatives*. J Immunol, 2004. **173**(9): p. 5540-5.
263. Kölln, J., R. Bredehorst, and E. Spillner, *Engineering of human complement component C3 for catalytic inhibition of complement*. Immunol Lett, 2005. **98**(1): p. 49-56.
264. Gorsuch, W., et al., *Humanized cobra venom factor decreases myocardial ischemia-reperfusion injury*. Mol Immunol, 2009. **47**(2-3): p. 506-10.
265. Vogel, C. and D. Fritzinger, *Humanized cobra venom factor: experimental therapeutics for targeted complement activation and complement depletion*. Curr Pharm Des, 2007. **13**(28): p. 2916-26.
266. Asghar, S., *Pharmacological manipulation of complement system*. Pharmacol Rev, 1984. **36**(4): p. 223-44.
267. Almeda, S., R. Rosenberg, and D. Bing, *The binding properties of human complement component C1q. Interaction with mucopolysaccharides*. J Biol Chem, 1983. **258**(2): p. 785-91.
268. Calabrese, G., et al., *An active fraction of unfractionated heparin from a natural source is recognized by the first component of the complement system*. Cell Mol Biol (Noisy-le-grand), 2001. **47 Online Pub**: p. OL119-23.

269. Oberkersch, R., A. Attorresi, and G. Calabrese, *Low-molecular-weight heparin inhibition in classical complement activation pathway during pregnancy*. *Thromb Res*, 2010. **125**(5): p. e240-5.
270. Baker, P., et al., *Studies on the inhibition of C56-induced lysis (reactive lysis). VI. Modulation of C56-induced lysis polyanions and polycations*. *J Immunol*, 1975. **114**(2 Pt 1): p. 554-8.
271. Hughes-Jones, N. and B. Gardner, *The reaction between the complement subcomponent C1q, IgG complexes and polyionic molecules*. *Immunology*, 1978. **34**(3): p. 459-63.
272. Weiler, J., et al., *Modulation of the formation of the amplification convertase of complement, C3b, Bb, by native and commercial heparin*. *J Exp Med*, 1978. **147**(2): p. 409-21.
273. Ovrum, E., et al., *High and low heparin dose with heparin-coated cardiopulmonary bypass: activation of complement and granulocytes*. *Ann Thorac Surg*, 1995. **60**(6): p. 1755-61.
274. Heyer, E., et al., *Heparin-bonded cardiopulmonary bypass circuits reduce cognitive dysfunction*. *J Cardiothorac Vasc Anesth*, 2002. **16**(1): p. 37-42.
275. Miyazaki, W., et al., *Effects of K-76 monocarboxylic acid, an anticomplementary agent, on various in vivo immunological reactions and on experimental glomerulonephritis*. *Complement*, 1984. **1**(3): p. 134-46.
276. Inagi, R., et al., *FUT-175 as a potent inhibitor of C5/C3 convertase activity for production of C5a and C3a*. *Immunol Lett*, 1991. **27**(1): p. 49-52.
277. Ino, Y., et al., *Effects of FUT-175, a novel synthetic protease inhibitor, on the development of adjuvant arthritis in rats and some biological reactions dependent on complement activation*. *Gen Pharmacol*, 1987. **18**(5): p. 513-6.
278. Miyagawa, S., et al., *Prolonging discordant xenograft survival with anticomplement reagents K76COOH and FUT175*. *Transplantation*, 1993. **55**(4): p. 709-13.
279. Kozlov, L., et al., *[Inhibition of the binding and activation of the first component of human complement. The effect of synthetic peptides, immunoglobulin fragments and various proteins]*. *Biokhimiia*, 1986. **51**(5): p. 707-18.
280. Sahu, A., B. Kay, and J. Lambris, *Inhibition of human complement by a C3-binding peptide isolated from a phage-displayed random peptide library*. *J Immunol*, 1996. **157**(2): p. 884-91.
281. Furlong, S., et al., *C3 activation is inhibited by analogs of compstatin but not by serine protease inhibitors or peptidyl alpha-ketoheterocycles*. *Immunopharmacology*, 2000. **48**(2): p. 199-212.
282. Sahu, A., D. Morikis, and J. Lambris, *Compstatin, a peptide inhibitor of complement, exhibits species-specific binding to complement component C3*. *Mol Immunol*, 2003. **39**(10): p. 557-66.
283. Fiane, A., et al., *Compstatin, a peptide inhibitor of C3, prolongs survival of ex vivo perfused pig xenografts*. *Xenotransplantation*, 1999. **6**(1): p. 52-65.
284. Fiane, A., et al., *Prolongation of ex vivo-perfused pig xenograft survival by the complement inhibitor Compstatin*. *Transplant Proc*, 1999. **31**(1-2): p. 934-5.
285. Finch, A., et al., *Low-molecular-weight peptidic and cyclic antagonists of the receptor for the complement factor C5a*. *J Med Chem*, 1999. **42**(11): p. 1965-74.
286. Short, A., et al., *Effects of a new C5a receptor antagonist on C5a- and endotoxin-induced neutropenia in the rat*. *Br J Pharmacol*, 1999. **126**(3): p. 551-4.
287. Haynes, D., et al., *Inhibition of C5a-induced neutrophil chemotaxis and macrophage cytokine production in vitro by a new C5a receptor antagonist*. *Biochem Pharmacol*, 2000. **60**(5): p. 729-33.

288. Strachan, A., et al., *Inhibition of immune-complex mediated dermal inflammation in rats following either oral or topical administration of a small molecule C5a receptor antagonist*. Br J Pharmacol, 2001. **134**(8): p. 1778-86.
289. Strachan, A., et al., *A new small molecule C5a receptor antagonist inhibits the reverse-passive Arthus reaction and endotoxic shock in rats*. J Immunol, 2000. **164**(12): p. 6560-5.
290. Arumugam, T., et al., *Protective effect of a new C5a receptor antagonist against ischemia-reperfusion injury in the rat small intestine*. J Surg Res, 2002. **103**(2): p. 260-7.
291. Jacob, A., et al., *Inhibition of C5a receptor alleviates experimental CNS lupus*. J Neuroimmunol, 2010. **221**(1-2): p. 46-52.
292. Smith, E.r., et al., *Reduction of myocardial reperfusion injury with human soluble complement receptor type 1 (BRL 55730)*. Eur J Pharmacol, 1993. **236**(3): p. 477-81.
293. Pemberton, M., et al., *Microvascular effects of complement blockade with soluble recombinant CR1 on ischemia/reperfusion injury of skeletal muscle*. J Immunol, 1993. **150**(11): p. 5104-13.
294. Hill, J., et al., *Soluble complement receptor type 1 ameliorates the local and remote organ injury after intestinal ischemia-reperfusion in the rat*. J Immunol, 1992. **149**(5): p. 1723-8.
295. Eror, A., et al., *Antiinflammatory effects of soluble complement receptor type 1 promote rapid recovery of ischemia/reperfusion injury in rat small intestine*. Clin Immunol, 1999. **90**(2): p. 266-75.
296. Pruitt, S. and R. Bollinger, *The effect of soluble complement receptor type 1 on hyperacute allograft rejection*. J Surg Res, 1991. **50**(4): p. 350-5.
297. Pruitt, S., et al., *The effect of soluble complement receptor type 1 on hyperacute xenograft rejection*. Transplantation, 1991. **52**(5): p. 868-73.
298. Pruitt, S., et al., *The effect of soluble complement receptor type 1 on hyperacute rejection of porcine xenografts*. Transplantation, 1994. **57**(3): p. 363-70.
299. Pruitt, S., et al., *Continuous complement (C) inhibition using soluble C receptor type 1 (sCR1): effect on hyperacute rejection (HAR) of pig-to-primate cardiac xenografts*. Transplant Proc, 1996. **28**(2): p. 756.
300. Piddlesden, S., et al., *Soluble recombinant complement receptor 1 inhibits inflammation and demyelination in antibody-mediated demyelinating experimental allergic encephalomyelitis*. J Immunol, 1994. **152**(11): p. 5477-84.
301. Piddlesden, S., et al., *Soluble complement receptor 1 (sCR1) protects against experimental autoimmune myasthenia gravis*. J Neuroimmunol, 1996. **71**(1-2): p. 173-7.
302. Couser, W., et al., *The effects of soluble recombinant complement receptor 1 on complement-mediated experimental glomerulonephritis*. J Am Soc Nephrol, 1995. **5**(11): p. 1888-94.
303. Goodfellow, R., et al., *Local therapy with soluble complement receptor 1 (sCR1) suppresses inflammation in rat mono-articular arthritis*. Clin Exp Immunol, 1997. **110**(1): p. 45-52.
304. Goodfellow, R., et al., *Soluble complement receptor one (sCR1) inhibits the development and progression of rat collagen-induced arthritis*. Clin Exp Immunol, 2000. **119**(1): p. 210-6.
305. Zimmerman, J., et al., *Phase I trial of the recombinant soluble complement receptor 1 in acute lung injury and acute respiratory distress syndrome*. Crit Care Med, 2000. **28**(9): p. 3149-54.

306. Lazar, H., et al., *Soluble human complement receptor 1 limits ischemic damage in cardiac surgery patients at high risk requiring cardiopulmonary bypass*. *Circulation*, 2004. **110**(11 Suppl 1): p. II274-9.
307. Lazar, H., et al., *Beneficial effects of complement inhibition with soluble complement receptor 1 (TP10) during cardiac surgery: is there a gender difference?* *Circulation*, 2007. **116**(11 Suppl): p. I83-8.
308. Keshavjee, S., et al., *A randomized, placebo-controlled trial of complement inhibition in ischemia-reperfusion injury after lung transplantation in human beings*. *J Thorac Cardiovasc Surg*, 2005. **129**(2): p. 423-8.
309. Makrides, S., et al., *Extended in vivo half-life of human soluble complement receptor type 1 fused to a serum albumin-binding receptor*. *J Pharmacol Exp Ther*, 1996. **277**(1): p. 534-42.
310. Mulligan, M., et al., *Endothelial targeting and enhanced antiinflammatory effects of complement inhibitors possessing sialyl Lewisx moieties*. *J Immunol*, 1999. **162**(8): p. 4952-9.
311. Rittershaus, C., et al., *Recombinant glycoproteins that inhibit complement activation and also bind the selectin adhesion molecules*. *J Biol Chem*, 1999. **274**(16): p. 11237-44.
312. Dodd, I., et al., *Overexpression in Escherichia coli, folding, purification, and characterization of the first three short consensus repeat modules of human complement receptor type 1*. *Protein Expr Purif*, 1995. **6**(6): p. 727-36.
313. Dong, J., et al., *Strategies for targeting complement inhibitors in ischaemia/reperfusion injury*. *Mol Immunol*, 1999. **36**(13-14): p. 957-63.
314. Linton, S., et al., *Therapeutic efficacy of a novel membrane-targeted complement regulator in antigen-induced arthritis in the rat*. *Arthritis Rheum*, 2000. **43**(11): p. 2590-7.
315. Halstead, S., et al., *Complement inhibition abrogates nerve terminal injury in Miller Fisher syndrome*. *Ann Neurol*, 2005. **58**(2): p. 203-10.
316. Mahmood, I. and M. Green, *Pharmacokinetic and pharmacodynamic considerations in the development of therapeutic proteins*. *Clin Pharmacokinet*, 2005. **44**(4): p. 331-47.
317. Ward, E. and R. Ober, *Chapter 4: Multitasking by exploitation of intracellular transport functions the many faces of FcRn*. *Adv Immunol*, 2009. **103**: p. 77-115.
318. Gillies, S., et al., *Improved circulating half-life and efficacy of an antibody-interleukin 2 immunocytokine based on reduced intracellular proteolysis*. *Clin Cancer Res*, 2002. **8**(1): p. 210-6.
319. Quigg, R., et al., *Blockade of antibody-induced glomerulonephritis with Crry-Ig, a soluble murine complement inhibitor*. *J Immunol*, 1998. **160**(9): p. 4553-60.
320. Rehrig, S., et al., *Complement inhibitor, complement receptor 1-related gene/protein γ -Ig attenuates intestinal damage after the onset of mesenteric ischemia/reperfusion injury in mice*. *J Immunol*, 2001. **167**(10): p. 5921-7.
321. Holers, V., et al., *Complement C3 activation is required for antiphospholipid antibody-induced fetal loss*. *J Exp Med*, 2002. **195**(2): p. 211-20.
322. Bao, L., et al., *Administration of a soluble recombinant complement C3 inhibitor protects against renal disease in MRL/lpr mice*. *J Am Soc Nephrol*, 2003. **14**(3): p. 670-9.
323. Leinhase, I., et al., *Pharmacological complement inhibition at the C3 convertase level promotes neuronal survival, neuroprotective intracerebral gene expression, and neurological outcome after traumatic brain injury*. *Exp Neurol*, 2006. **199**(2): p. 454-64.

324. Hepburn, N.J., et al., *Prevention of experimental autoimmune myasthenia gravis by rat Crry-Ig: A model agent for long-term complement inhibition in vivo*. *Mol Immunol*, 2008. **45**(2): p. 395-405.
325. Li, B., et al., *Improving therapeutic efficacy of a complement receptor by structure-based affinity maturation*. *J Biol Chem*, 2009. **284**(51): p. 35605-11.
326. Chen, J., et al., *A Novel Inhibitor of the Alternative Pathway of Complement Attenuates Intestinal Ischemia/Reperfusion-Induced Injury*. *J Surg Res*, 2009. DOI: 10.1016/j.jss.2009.05.041 (ahead of print).
327. Harris, C., et al., *Coupling complement regulators to immunoglobulin domains generates effective anti-complement reagents with extended half-life in vivo*. *Clin Exp Immunol*, 2002. **129**(2): p. 198-207.
328. Bora, N., et al., *CD59, a complement regulatory protein, controls choroidal neovascularization in a mouse model of wet-type age-related macular degeneration*. *J Immunol*, 2007. **178**(3): p. 1783-90.
329. Smith, R., *Targeting anticomplement agents*. *Biochem Soc Trans*, 2002. **30**(Pt 6): p. 1037-41.
330. Song, H., et al., *Complement receptor 2-mediated targeting of complement inhibitors to sites of complement activation*. *J Clin Invest*, 2003. **111**(12): p. 1875-85.
331. Atkinson, C., et al., *Targeted complement inhibition by C3d recognition ameliorates tissue injury without apparent increase in susceptibility to infection*. *J Clin Invest*, 2005. **115**(9): p. 2444-53.
332. Huang, Y., et al., *A novel targeted inhibitor of the alternative pathway of complement and its therapeutic application in ischemia/reperfusion injury*. *J Immunol*, 2008. **181**(11): p. 8068-76.
333. Qiao, F., et al., *Complement plays an important role in spinal cord injury and represents a therapeutic target for improving recovery following trauma*. *Am J Pathol*, 2006. **169**(3): p. 1039-47.
334. He, S., et al., *A complement-dependent balance between hepatic ischemia/reperfusion injury and liver regeneration in mice*. *J Clin Invest*, 2009. **119**(8): p. 2304-16.
335. Banda, N., et al., *Targeted inhibition of the complement alternative pathway with complement receptor 2 and factor H attenuates collagen antibody-induced arthritis in mice*. *J Immunol*, 2009. **183**(9): p. 5928-37.
336. Rohrer, B., et al., *A targeted inhibitor of the alternative complement pathway reduces angiogenesis in a mouse model of age-related macular degeneration*. *Invest Ophthalmol Vis Sci*, 2009. **50**(7): p. 3056-64.
337. Zhang, H., et al., *Targeting of functional antibody-CD59 fusion proteins to a cell surface*. *J Clin Invest*, 1999. **103**(1): p. 55-61.
338. Zhang, H., et al., *Targeting of functional antibody-decay-accelerating factor fusion proteins to a cell surface*. *J Biol Chem*, 2001. **276**(29): p. 27290-5.
339. Spitzer, D., et al., *ScFv-mediated in vivo targeting of DAF to erythrocytes inhibits lysis by complement*. *Mol Immunol*, 2004. **40**(13): p. 911-9.
340. He, C., et al., *Complement inhibitors targeted to the proximal tubule prevent injury in experimental nephrotic syndrome and demonstrate a key role for C5b-9*. *J Immunol*, 2005. **174**(9): p. 5750-7.
341. Kung, P., et al., *Monoclonal antibodies defining distinctive human T cell surface antigens*. *Science*, 1979. **206**(4416): p. 347-9.
342. Morrison, S., et al., *Chimeric human antibody molecules: mouse antigen-binding domains with human constant region domains*. *Proc Natl Acad Sci U S A*, 1984. **81**(21): p. 6851-5.

343. Boulianne, G., N. Hozumi, and M. Shulman, *Production of functional chimaeric mouse/human antibody*. *Nature*, 1984. **312**(5995): p. 643-6.
344. Riechmann, L., et al., *Reshaping human antibodies for therapy*. *Nature*, 1988. **332**(6162): p. 323-7.
345. Winter, G., et al., *Making antibodies by phage display technology*. *Annu Rev Immunol*, 1994. **12**: p. 433-55.
346. Brüggemann, M., et al., *Human antibody production in transgenic mice: expression from 100 kb of the human IgH locus*. *Eur J Immunol*, 1991. **21**(5): p. 1323-6.
347. Frei, Y., J.D. Lambris, and B. Stockinger, *Generation of a monoclonal antibody to mouse C5 application in an ELISA assay for detection of anti-C5 antibodies*. *Mol Cell Probes*, 1987. **1**(2): p. 141-9.
348. Würzner, R., et al., *Inhibition of terminal complement complex formation and cell lysis by monoclonal antibodies*. *Complement Inflamm*, 1991. **8**(5-6): p. 328-40.
349. Girardi, G., et al., *Complement C5a receptors and neutrophils mediate fetal injury in the antiphospholipid syndrome*. *J Clin Invest*, 2003. **112**(11): p. 1644-54.
350. Peng, T., et al., *Role of C5 in the development of airway inflammation, airway hyperresponsiveness, and ongoing airway response*. *J Clin Invest*, 2005. **115**(6): p. 1590-600.
351. Evans, M., et al., *In vitro and in vivo inhibition of complement activity by a single-chain Fv fragment recognizing human C5*. *Mol Immunol*, 1995. **32**(16): p. 1183-95.
352. Marzari, R., et al., *The cleavage site of C5 from man and animals as a common target for neutralizing human monoclonal antibodies: in vitro and in vivo studies*. *Eur J Immunol*, 2002. **32**(10): p. 2773-82.
353. Fischetti, F., et al., *Selective therapeutic control of C5a and the terminal complement complex by anti-C5 single-chain Fv in an experimental model of antigen-induced arthritis in rats*. *Arthritis Rheum*, 2007. **56**(4): p. 1187-97.
354. Thomas, T., et al., *Inhibition of complement activity by humanized anti-C5 antibody and single-chain Fv*. *Mol Immunol*, 1996. **33**(17-18): p. 1389-401.
355. Mahaffey, K., et al., *Effect of pexelizumab on mortality in patients with acute myocardial infarction or undergoing coronary artery bypass surgery: a systematic overview*. *Am Heart J*, 2006. **152**(2): p. 291-6.
356. Fitch, J., et al., *Pharmacology and biological efficacy of a recombinant, humanized, single-chain antibody C5 complement inhibitor in patients undergoing coronary artery bypass graft surgery with cardiopulmonary bypass*. *Circulation*, 1999. **100**(25): p. 2499-506.
357. Sherman, S., et al., *Impact of pexelizumab, an anti-C5 complement antibody, on total mortality and adverse cardiovascular outcomes in cardiac surgical patients undergoing cardiopulmonary bypass*. *Ann Thorac Surg*, 2004. **77**(3): p. 942-9; discussion 949-50.
358. Sellke, F. and M. Boodhwani, *Inhibition of complement activation in cardiac surgery*. *J Thorac Cardiovasc Surg*, 2006. **131**(2): p. 266-7.
359. Carrier, M., et al., *Inhibition of complement activation by pexelizumab reduces death in patients undergoing combined aortic valve replacement and coronary artery bypass surgery*. *J Thorac Cardiovasc Surg*, 2006. **131**(2): p. 352-6.
360. Smith, P., et al., *Effect of pexelizumab in coronary artery bypass graft surgery with extended aortic cross-clamp time*. *Ann Thorac Surg*, 2006. **82**(3): p. 781-8; discussion 788-9.
361. Hillmen, P., et al., *Effect of eculizumab on hemolysis and transfusion requirements in patients with paroxysmal nocturnal hemoglobinuria*. *N Engl J Med*, 2004. **350**(6): p. 552-9.

362. Hill, A., et al., *Sustained response and long-term safety of eculizumab in paroxysmal nocturnal hemoglobinuria*. *Blood*, 2005. **106**(7): p. 2559-65.
363. Hillmen, P., et al., *The complement inhibitor eculizumab in paroxysmal nocturnal hemoglobinuria*. *N Engl J Med*, 2006. **355**(12): p. 1233-43.
364. Hillmen, P., et al., *Effect of the complement inhibitor eculizumab on thromboembolism in patients with paroxysmal nocturnal hemoglobinuria*. *Blood*, 2007. **110**(12): p. 4123-8.
365. Fraser, D., et al., *Generation of a recombinant, membrane-targeted form of the complement regulator CD59: activity in vitro and in vivo*. *J Biol Chem*, 2003. **278**(49): p. 48921-7.
366. Hill, A., et al., *Protection of erythrocytes from human complement-mediated lysis by membrane-targeted recombinant soluble CD59: a new approach to PNH therapy*. *Blood*, 2006. **107**(5): p. 2131-7.
367. Soltys, J., et al., *Novel complement inhibitor limits severity of experimentally myasthenia gravis*. *Ann Neurol*, 2009. **65**(1): p. 67-75.
368. Quigg, R., et al., *Immune complex glomerulonephritis in C4- and C3-deficient mice*. *Kidney Int*, 1998. **53**(2): p. 320-30.
369. Botto, M., *C1q knock-out mice for the study of complement deficiency in autoimmune disease*. *Exp Clin Immunogenet*, 1998. **15**(4): p. 231-4.
370. Fodor, W., et al., *A novel bifunctional chimeric complement inhibitor that regulates C3 convertase and formation of the membrane attack complex*. *J Immunol*, 1995. **155**(9): p. 4135-8.
371. Dvorak, A. and H. Dvorak, *Structure of Freund's complete and incomplete adjuvants. Relation of adjuvanticity to structure*. *Immunology*, 1974. **27**(1): p. 99-114.
372. Stenberg, E., et al., *Quantitative determination of surface concentration of protein with surface plasmon resonance using radiolabeled proteins*. 1991. **143**(2): p. 513-526.
373. Holt, D.S., et al., *Targeted deletion of the CD59 gene causes spontaneous intravascular hemolysis and hemoglobinuria*. *Blood*, 2001. **98**(2): p. 442-9.
374. Mayer, M. and E. Kabat, *Complement and complement fixation*. *Experimental immunochemistry*, ed. M. M1961: Springfield Ill: Charles C. Thomas. 133-240.
375. *Complement methods and protocols*, ed. B.P. Morgan. Vol. 150. 2000: Humana press.
376. Väkevä, A., et al., *High-density lipoproteins can act as carriers of glycoposphoinositol lipid-anchored CD59 in human plasma*. *Immunology*, 1994. **82**(1): p. 28-33.
377. Quigg, R., et al., *Production and functional analysis of rat CD59 and chimeric CD59-Crry as active soluble proteins in Pichia pastoris*. *Immunology*, 2000. **99**(1): p. 46-53.
378. Dangl, J., et al., *Segmental flexibility and complement fixation of genetically engineered chimeric human, rabbit and mouse antibodies*. *EMBO J*, 1988. **7**(7): p. 1989-94.
379. Harris, L., et al., *Refined structure of an intact IgG2a monoclonal antibody*. *Biochemistry*, 1997. **36**(7): p. 1581-97.
380. Baneyx and Francois, *Protein Expression Technologies: Current Status and Future Trends2004*: Horizon Bioscience.
381. Jefferis, R., *Glycosylation of natural and recombinant antibody molecules*. *Adv Exp Med Biol*, 2005. **564**: p. 143-8.

382. Jefferis, R., *Glycosylation of recombinant antibody therapeutics*. Biotechnol Prog, 2005. **21**(1): p. 11-6.
383. Jefferis, R., J. Lund, and J. Pound, *IgG-Fc-mediated effector functions: molecular definition of interaction sites for effector ligands and the role of glycosylation*. Immunol Rev, 1998. **163**: p. 59-76.
384. Jefferis, R. and J. Lund, *Interaction sites on human IgG-Fc for Fcγ₃R: current models*. Immunol Lett, 2002. **82**(1-2): p. 57-65.
385. Capon, D., et al., *Designing CD4 immunoadhesins for AIDS therapy*. Nature, 1989. **337**(6207): p. 525-31.
386. Day, J., A. Murdoch, and T. Hardingham, *The folded protein modules of the C-terminal G3 domain of aggrecan can each facilitate the translocation and secretion of the extended chondroitin sulfate attachment sequence*. J Biol Chem, 1999. **274**(53): p. 38107-11.
387. Morgan, B.P., et al., *The membrane attack pathway of complement drives pathology in passively induced experimental autoimmune myasthenia gravis in mice*. Clin Exp Immunol, 2006. **146**(2): p. 294-302.
388. Chamberlain-Banou, J., et al., *Complement membrane attack is required for endplate damage and clinical disease in passive experimental myasthenia gravis in Lewis rats*. Clin Exp Immunol, 2006. **146**(2): p. 278-86.
389. Ramo, K., S. Cashman, and R. Kumar-Singh, *Evaluation of adenovirus-delivered human CD59 as a potential therapy for AMD in a model of human membrane attack complex formation on murine RPE*. Invest Ophthalmol Vis Sci, 2008. **49**(9): p. 4126-36.
390. Andersen, D. and L. Krummen, *Recombinant protein expression for therapeutic applications*. Curr Opin Biotechnol, 2002. **13**(2): p. 117-23.
391. Baldi, L., et al., *Recombinant protein production by large-scale transient gene expression in mammalian cells: state of the art and future perspectives*. Biotechnol Lett, 2007. **29**(5): p. 677-84.
392. Ye, J., et al., *High-level protein expression in scalable CHO transient transfection*. Biotechnol Bioeng, 2009. **103**(3): p. 542-51.
393. Durocher, Y., S. Perret, and A. Kamen, *High-level and high-throughput recombinant protein production by transient transfection of suspension-growing human 293-EBNA1 cells*. Nucleic Acids Res, 2002. **30**(2): p. E9.
394. Pham, P., A. Kamen, and Y. Durocher, *Large-scale transfection of mammalian cells for the fast production of recombinant protein*. Mol Biotechnol, 2006. **34**(2): p. 225-37.
395. Xia, W., et al., *High levels of protein expression using different mammalian CMV promoters in several cell lines*. Protein Expr Purif, 2006. **45**(1): p. 115-24.
396. Running Deer, J. and D. Allison, *High-level expression of proteins in mammalian cells using transcription regulatory sequences from the Chinese hamster EF-1α gene*. Biotechnol Prog, 2004. **20**(3): p. 880-9.
397. Kim, H., et al., *Dynamical structure of the hinge region of immunoglobulin G as studied by ¹³C nuclear magnetic resonance spectroscopy*. J Mol Biol, 1994. **236**(1): p. 300-9.
398. Köhler, G. and C. Milstein, *Continuous cultures of fused cells secreting antibody of predefined specificity*. Nature, 1975. **256**(5517): p. 495-7.
399. Schwarz, A., F. Kohen, and M. Wilchek, *Novel heterocyclic ligands for the thiophilic purification of antibodies*. J Chromatogr B Biomed Appl, 1995. **664**(1): p. 83-8.

400. Hollander, Z. and E. Katchalski-Katzir, *Use of monoclonal antibodies to detect conformational alterations in lactate dehydrogenase isoenzyme 5 on heat denaturation and on adsorption to polystyrene plates*. Mol Immunol, 1986. **23**(9): p. 927-33.
401. Shields, M., et al., *An appraisal of polystyrene-(ELISA) and nitrocellulose-based (ELIFA) enzyme immunoassay systems using monoclonal antibodies reactive toward antigenically distinct forms of human C-reactive protein*. J Immunol Methods, 1991. **141**(2): p. 253-61.
402. Schwab, C. and H. Bosshard, *Caveats for the use of surface-adsorbed protein antigen to test the specificity of antibodies*. J Immunol Methods, 1992. **147**(1): p. 125-34.
403. Aston, W., A. Mhatre, and J. Macrae, *Isolation of the fifth component of the bovine complement system*. Vet Immunol Immunopathol, 1990. **24**(4): p. 301-12.
404. Petranka, J., et al., *Structure-function relationships of the complement regulatory protein, CD59*. Blood Cells Mol Dis, 1996. **22**(3): p. 281-96.
405. Yamaguchi, Y., et al., *Proteolytic fragmentation with high specificity of mouse immunoglobulin G. Mapping of proteolytic cleavage sites in the hinge region*. J Immunol Methods, 1995. **181**(2): p. 259-67.
406. Adamczyk, M., J. Gebler, and J. Wu, *Papain digestion of different mouse IgG subclasses as studied by electrospray mass spectrometry*. J Immunol Methods, 2000. **237**(1-2): p. 95-104.
407. Ghose, S., B. Hubbard, and S. Cramer, *Binding capacity differences for antibodies and Fc-fusion proteins on protein A chromatographic materials*. Biotechnol Bioeng, 2007. **96**(4): p. 768-79.
408. Wilson, I., Y. Gavel, and G. von Heijne, *Amino acid distributions around O-linked glycosylation sites*. Biochem J, 1991. **275** (Pt 2): p. 529-34.
409. Cox, G., et al., *Enhanced circulating half-life and hematopoietic properties of a human granulocyte colony-stimulating factor/immunoglobulin fusion protein*. Exp Hematol, 2004. **32**(5): p. 441-9.
410. Rosenfeld, M., et al., *Animal models of spontaneous plaque rupture: the holy grail of experimental atherosclerosis research*. Curr Atheroscler Rep, 2002. **4**(3): p. 238-42.
411. Hershfield, M., et al., *Use of site-directed mutagenesis to enhance the epitope-shielding effect of covalent modification of proteins with polyethylene glycol*. Proc Natl Acad Sci U S A, 1991. **88**(16): p. 7185-9.
412. Kozlowski, A., S. Charles, and J. Harris, *Development of pegylated interferons for the treatment of chronic hepatitis C*. BioDrugs, 2001. **15**(7): p. 419-29.
413. Chapman, A., *PEGylated antibodies and antibody fragments for improved therapy: a review*. Adv Drug Deliv Rev, 2002. **54**(4): p. 531-45.
414. Huang, Y., et al., *Substantially improved pharmacokinetics of recombinant human butyrylcholinesterase by fusion to human serum albumin*. BMC Biotechnol, 2008. **8**: p. 50.
415. Halpern, W., et al., *Albugranin, a recombinant human granulocyte colony stimulating factor (G-CSF) genetically fused to recombinant human albumin induces prolonged myelopoietic effects in mice and monkeys*. Pharm Res, 2002. **19**(11): p. 1720-9.
416. Osborn, B., et al., *Albutropin: a growth hormone-albumin fusion with improved pharmacokinetics and pharmacodynamics in rats and monkeys*. Eur J Pharmacol, 2002. **456**(1-3): p. 149-58.
417. Martin, W., et al., *Crystal structure at 2.8 Å of an FcRn/heterodimeric Fc complex: mechanism of pH-dependent binding*. Mol Cell, 2001. **7**(4): p. 867-77.

418. Ghetie, V. and E. Ward, *Multiple roles for the major histocompatibility complex class I-related receptor FcRn*. *Annu Rev Immunol*, 2000. **18**: p. 739-66.
419. Mould, D. and K. Sweeney, *The pharmacokinetics and pharmacodynamics of monoclonal antibodies--mechanistic modeling applied to drug development*. *Curr Opin Drug Discov Devel*, 2007. **10**(1): p. 84-96.
420. Tabrizi, M., C. Tseng, and L. Roskos, *Elimination mechanisms of therapeutic monoclonal antibodies*. *Drug Discov Today*, 2006. **11**(1-2): p. 81-8.
421. Nilsson, U.R. and H.J. Müller-Eberhard, *Deficiency of the fifth component of complement in mice with an inherited complement defect*. *J Exp Med*, 1967. **125**(1): p. 1-16.
422. Lin, R.H. and B. Stockinger, *Purification of the fifth component of murine complement from ascites fluid*. *J Immunol Methods*, 1988. **115**(1): p. 127-31.
423. Supersaxo, A., W. Hein, and H. Steffen, *Effect of molecular weight on the lymphatic absorption of water-soluble compounds following subcutaneous administration*. *Pharm Res*, 1990. **7**(2): p. 167-9.
424. Toon, S., *The relevance of pharmacokinetics in the development of biotechnology products*. *Eur J Drug Metab Pharmacokinet*, 1996. **21**(2): p. 93-103.
425. Wang, W., E. Wang, and J. Balthasar, *Monoclonal antibody pharmacokinetics and pharmacodynamics*. *Clin Pharmacol Ther*, 2008. **84**(5): p. 548-58.
426. Fabis, M., et al., *Loss of blood-brain barrier integrity in the spinal cord is common to experimental allergic encephalomyelitis in knockout mouse models*. *Proc Natl Acad Sci U S A*, 2007. **104**(13): p. 5656-61.
427. Paul, C. and C. Bolton, *Modulation of blood-brain barrier dysfunction and neurological deficits during acute experimental allergic encephalomyelitis by the N-methyl-D-aspartate receptor antagonist memantine*. *J Pharmacol Exp Ther*, 2002. **302**(1): p. 50-7.
428. Mahley, R. and Y. Huang, *Apolipoprotein E: from atherosclerosis to Alzheimer's disease and beyond*. *Curr Opin Lipidol*, 1999. **10**(3): p. 207-17.
429. Curtiss, L. and W. Boisvert, *Apolipoprotein E and atherosclerosis*. *Curr Opin Lipidol*, 2000. **11**(3): p. 243-51.
430. Pabst, H., et al., *Prevention of experimental allergic encephalomyelitis with cobra venom factor*. *Proc Soc Exp Biol Med*, 1971. **136**(2): p. 555-60.
431. Nozaki, M., et al., *Drusen complement components C3a and C5a promote choroidal neovascularization*. *Proc Natl Acad Sci U S A*, 2006. **103**(7): p. 2328-33.
432. Copland, D., et al., *Systemic and local anti-C5 therapy reduces the disease severity in experimental autoimmune uveoretinitis*. *Clin Exp Immunol*, 2010. **159**(3): p. 303-14.
433. van der Pals, J., et al., *Treatment with the C5a receptor antagonist ADC-1004 reduces myocardial infarction in a porcine ischemia-reperfusion model*. *BMC Cardiovasc Disord*, 2010. **10**(1): p. 45.
434. Sissons, J., et al., *Metabolism of the fifth component of complement, and its relation to metabolism of the third component, in patients with complement activation*. *J Clin Invest*, 1977. **59**(4): p. 704-15.
435. Hepburn, N., et al., *In vivo characterization and therapeutic efficacy of a C5-specific inhibitor from the soft tick *Ornithodoros moubata**. *J Biol Chem*, 2007(11): p. 8292-9.
436. Linsley, P., et al., *CTLA-4 is a second receptor for the B cell activation antigen B7*. *J Exp Med*, 1991. **174**(3): p. 561-9.
437. Linsley, P., et al., *Immunosuppression in vivo by a soluble form of the CTLA-4 T cell activation molecule*. *Science*, 1992. **257**(5071): p. 792-5.

438. Linsley, P. and S. Nadler, *The clinical utility of inhibiting CD28-mediated costimulation*. Immunol Rev, 2009. **229**(1): p. 307-21.
439. Pugsley, M., *Etanercept*. Immunex. Curr Opin Investig Drugs, 2001. **2**(12): p. 1725-31.
440. Tyring, S., et al., *Long-term safety and efficacy of 50 mg of etanercept twice weekly in patients with psoriasis*. Arch Dermatol, 2007. **143**(6): p. 719-26.
441. Harris, C.L., O.B. Spiller, and B.P. Morgan, *Human and rodent decay-accelerating factors (CD55) are not species restricted in their complement-inhibiting activities*. Immunology, 2000. **100**(4): p. 462-70.
442. Oleaga, A., et al., *A proteomic approach to the identification of salivary proteins from the argasid ticks Ornithodoros moubata and Ornithodoros erraticus*. Insect Biochem Mol Biol, 2007. **37**(11): p. 1149-59.
443. Dikov, M., et al., *A functional fibroblast growth factor-1 immunoglobulin fusion protein*. J Biol Chem, 1998. **273**(25): p. 15811-7.
444. Ghetie, V., et al., *Increasing the serum persistence of an IgG fragment by random mutagenesis*. Nat Biotechnol, 1997. **15**(7): p. 637-40.
445. Hinton, P., et al., *An engineered human IgG1 antibody with longer serum half-life*. J Immunol, 2006. **176**(1): p. 346-56.
446. Zhou, J., et al., *Generation of mutated variants of the human form of the MHC class I-related receptor, FcRn, with increased affinity for mouse immunoglobulin G*. J Mol Biol, 2003. **332**(4): p. 901-13.
447. Gillies, S., et al., *Improving the efficacy of antibody-interleukin 2 fusion proteins by reducing their interaction with Fc receptors*. Cancer Res, 1999. **59**(9): p. 2159-66.
448. Duncan, A., et al., *Localization of the binding site for the human high-affinity Fc receptor on IgG*. Nature, 1988. **332**(6164): p. 563-4.
449. Kim, J., et al., *Localization of the site of the murine IgG1 molecule that is involved in binding to the murine intestinal Fc receptor*. Eur J Immunol, 1994. **24**(10): p. 2429-34.
450. Shields, R., et al., *High resolution mapping of the binding site on human IgG1 for Fc gamma RI, Fc gamma RII, Fc gamma RIII, and FcRn and design of IgG1 variants with improved binding to the Fc gamma R*. J Biol Chem, 2001. **276**(9): p. 6591-604.
451. Spiekermann, G., et al., *Receptor-mediated immunoglobulin G transport across mucosal barriers in adult life: functional expression of FcRn in the mammalian lung*. J Exp Med, 2002. **196**(3): p. 303-10.
452. Akilesh, S., et al., *Neonatal FcR expression in bone marrow-derived cells functions to protect serum IgG from catabolism*. J Immunol, 2007. **179**(7): p. 4580-8.
453. Low, S., et al., *Oral and pulmonary delivery of FSH-Fc fusion proteins via neonatal Fc receptor-mediated transcytosis*. Hum Reprod, 2005. **20**(7): p. 1805-13.
454. Bitonti, A., et al., *Pulmonary delivery of an erythropoietin Fc fusion protein in non-human primates through an immunoglobulin transport pathway*. Proc Natl Acad Sci U S A, 2004. **101**(26): p. 9763-8.
455. Dumont, J., et al., *Monomeric Fc fusions: impact on pharmacokinetic and biological activity of protein therapeutics*. BioDrugs, 2006. **20**(3): p. 151-60.
456. Pardridge, W., *The blood-brain barrier: bottleneck in brain drug development*. NeuroRx, 2005. **2**(1): p. 3-14.
457. Dhuria, S., L. Hanson, and W.n. Frey, *Intranasal delivery to the central nervous system: mechanisms and experimental considerations*. J Pharm Sci, 2010. **99**(4): p. 1654-73.

458. Xiao, B., et al., *Suppression of acute and protracted-relapsing experimental allergic encephalomyelitis by nasal administration of low-dose IL-10 in rats.* J Neuroimmunol, 1998. **84**(2): p. 230-7.
459. Wang, F., X. Jiang, and W. Lu, *Profiles of methotrexate in blood and CSF following intranasal and intravenous administration to rats.* Int J Pharm, 2003. **263**(1-2): p. 1-7.
460. Ross, T., et al., *Intranasal administration of interferon beta bypasses the blood-brain barrier to target the central nervous system and cervical lymph nodes: a non-invasive treatment strategy for multiple sclerosis.* J Neuroimmunol, 2004. **151**(1-2): p. 66-77.
461. Schlachetzki, F., C. Zhu, and W. Pardridge, *Expression of the neonatal Fc receptor (FcRn) at the blood-brain barrier.* J Neurochem, 2002. **81**(1): p. 203-6.
462. Zhang, Y. and W. Pardridge, *Mediated efflux of IgG molecules from brain to blood across the blood-brain barrier.* J Neuroimmunol, 2001. **114**(1-2): p. 168-72.
463. Zhang, Y. and W. Pardridge, *Rapid transferrin efflux from brain to blood across the blood-brain barrier.* J Neurochem, 2001. **76**(5): p. 1597-600.
464. Lee, H., et al., *Targeting rat anti-mouse transferrin receptor monoclonal antibodies through blood-brain barrier in mouse.* J Pharmacol Exp Ther, 2000. **292**(3): p. 1048-52.
465. Fu, A., et al., *Intravenous treatment of experimental Parkinson's disease in the mouse with an IgG-GDNF fusion protein that penetrates the blood-brain barrier.* Brain Res, 2010.
466. Yoshikawa, T. and W. Pardridge, *Biotin delivery to brain with a covalent conjugate of avidin and a monoclonal antibody to the transferrin receptor.* J Pharmacol Exp Ther, 1992. **263**(2): p. 897-903.
467. Bäckman, C., et al., *Systemic administration of a nerve growth factor conjugate reverses age-related cognitive dysfunction and prevents cholinergic neuron atrophy.* J Neurosci, 1996. **16**(17): p. 5437-42.
468. Li, J., R. Boado, and W. Pardridge, *Blood-brain barrier genomics.* J Cereb Blood Flow Metab, 2001. **21**(1): p. 61-8.
469. Jefferies, W., et al., *Transferrin receptor on endothelium of brain capillaries.* Nature, 1984. **312**(5990): p. 162-3.
470. Sugita, Y., et al., *Recombinant soluble CD59 inhibits reactive haemolysis with complement.* Immunology, 1994. **82**(1): p. 34-41.
471. Rushmere, N., C. Van Den Berg, and B. Morgan, *Production and functional characterization of a soluble recombinant form of mouse CD59.* Immunology, 2000. **99**(2): p. 326-32.
472. Morris, K., et al., *The terminal pathway of complement in hepatic ischemia/reperfusion injury and regeneration.* XXIII International Complement Workshop, August 1-5, 2010, New York, 2010. **47**(13): p. 2209-2209.
473. Józsi, M., et al., *Anti factor H autoantibodies block C-terminal recognition function of factor H in hemolytic uremic syndrome.* Blood, 2007. **110**(5): p. 1516-8.
474. Waters, A. and C. Licht, *aHUS caused by complement dysregulation: new therapies on the horizon.* Pediatr Nephrol, 2010.
475. Klein, R., et al., *Complement factor H polymorphism in age-related macular degeneration.* Science, 2005. **308**(5720): p. 385-9.
476. Nataf, S., et al., *Attenuation of experimental autoimmune demyelination in complement-deficient mice.* J Immunol, 2000. **165**(10): p. 5867-73.

477. Bienaime, F., et al., *Mutations in components of complement influence the outcome of Factor I-associated atypical hemolytic uremic syndrome*. *Kidney Int*, 2010. **77**(4): p. 339-49.
478. Nilsson, S., et al., *Mutations in complement factor I as found in atypical hemolytic uremic syndrome lead to either altered secretion or altered function of factor I*. *Eur J Immunol*, 2010. **40**(1): p. 172-85.
479. Rose, K., et al., *Factor I is required for the development of membranoproliferative glomerulonephritis in factor H-deficient mice*. *J Clin Invest*, 2008. **118**(2): p. 608-18.
480. Paixão-Cavalcante, D., et al., *Factor H facilitates the clearance of GBM bound iC3b by controlling C3 activation in fluid phase*. *Mol Immunol*, 2009. **46**(10): p. 1942-50.
481. Konai, M., et al., *Monoarticular corticosteroid injection versus systemic administration in the treatment of rheumatoid arthritis patients: a randomized double-blind controlled study*. *Clin Exp Rheumatol*, 2009. **27**(2): p. 214-21.
482. Ruddy, S. and H. Colten, *Rheumatoid arthritis. Biosynthesis of complement proteins by synovial tissues*. *N Engl J Med*, 1974. **290**(23): p. 1284-8.
483. Firestein, G., M. Paine, and B. Littman, *Gene expression (collagenase, tissue inhibitor of metalloproteinases, complement, and HLA-DR) in rheumatoid arthritis and osteoarthritis synovium. Quantitative analysis and effect of intraarticular corticosteroids*. *Arthritis Rheum*, 1991. **34**(9): p. 1094-105.
484. Breitner, S., et al., *Complement components C1q, C1r/C1s, and C1INH in rheumatoid arthritis. Correlation of in situ hybridization and northern blot results with function and protein concentration in synovium and primary cell cultures*. *Arthritis Rheum*, 1995. **38**(4): p. 492-8.